

T-2133

THE USE OF HELIUM  
IN URANIUM EXPLORATION

by

Richard H. Mead

ProQuest Number: 11016679

All rights reserved

INFORMATION TO ALL USERS

The quality of this reproduction is dependent upon the quality of the copy submitted.

In the unlikely event that the author did not send a complete manuscript and there are missing pages, these will be noted. Also, if material had to be removed, a note will indicate the deletion.



ProQuest 11016679

Published by ProQuest LLC (2019). Copyright of the Dissertation is held by the Author.

All rights reserved.

This work is protected against unauthorized copying under Title 17, United States Code  
Microform Edition © ProQuest LLC.

ProQuest LLC.  
789 East Eisenhower Parkway  
P.O. Box 1346  
Ann Arbor, MI 48106 – 1346

A thesis submitted to the Faculty and the Board of Trustees  
of the Colorado School of Mines in partial fulfillment of the require-  
ments for the degree of Doctor of Philosophy (Geology).

Golden, Colorado

Date April 2, 1980

Signed: Richard H. Mead  
Student  
Richard H. Mead

Approved: Richard H. DeVoto  
Thesis Advisor  
Dr. Richard H. DeVoto

Golden, Colorado

Date 4/10, 1980

J. Finney  
Head of Department  
Dr. J. Finney

## ABSTRACT

The constant generation of inert helium gas from the radioactive decay of uranium and its daughter products provides a potentially useful exploration tool for the detection of buried uranium deposits. A program to test this idea was initiated at four uranium districts. These included the Pumpkin Buttes, Wyoming, the southern Powder River Basin, Wyoming, the Grants-Ambrosia Lake area, New Mexico, and the Schwartzwaldler mine, Golden, Colorado. Helium-in-soil-gas concentrations were determined in the field by means of a portable mass spectrometer. Other exploration techniques were used concurrently on a limited basis for comparison purposes. These included electronic radon alpha counting in the field, gamma-ray spectrometric measurements of soil, helium dissolved in ground water, laboratory mass spectrometer measurements of  $^4\text{He}/^{36}\text{Ar}$  and  $^4\text{He}/^{22}\text{Ne}$  in soil gas samples, and fluorometric analysis for uranium in ground water samples. A total of 4574 soil gas and atmosphere samples and 81 water samples were analyzed in the field for helium concentration.

The Powder River Basin results, in a region of unfaulted Lower Tertiary mudstones and sandstones, showed that helium-in-soil-gas surveys conducted in a grid sampling pattern could indicate the presence of subsurface uranium mineralization when all samples were collected in a short period of time (<4 hours). Interpretation of results was hampered by random and meteorological variations in the measurements. Anomalies related to mineralization were of the order of 40 to 80 ppb greater than the atmospheric helium concentration. Helium concentrations in ground water were potentially of greater significance although more difficult to interpret in terms of their



source. Helium concentrations in ground water were up to 11 ppm greater than the atmospheric helium concentration.

The results in the Grants-Ambrosia Lake area, a faulted region with uranium mineralization at depths of 240-915 meters which is overlain by thick Cretaceous shales, sandstones, and siltstones, indicated a more limited applicability of the method due to the large size of the targets. The larger deposits necessitated increasing the survey size which introduced environmental changes into the data. The concentration of helium in ground water was up to 44.7 ppm in the main trend of ore deposits.

Measurements of helium at the Schwartzwald mine revealed the highest concentrations in soil gas of any test site ranging up to 7.38 ppm. The greater helium concentration is related to the increased fracture density of the Precambrian schists and gneisses.

The other exploration methods in general gave results of limited significance because of their low sampling density at any particular test site. However, it was found that the electronic radon alpha counters could be an effective substitute for Track Etch cups. Alpha counters were able to delineate the distribution of subsurface uranium mineralization in at least one site. The  $^4\text{He}/^{22}\text{Ne}$  and  $^4\text{He}/^{36}\text{Ar}$  measurements indicated a fairly good correlation with the uranium mineralization, but due to the low sample density and low precision, these also must be considered tentative.

## TABLE OF CONTENTS

	<u>Page</u>
ABSTRACT	iii
LIST OF FIGURES	x
LIST OF TABLES	xix
ACKNOWLEDGEMENTS	xxi
INTRODUCTION	1
Summary of Previous Work in Helium Measurements and Behavior in Geologic Environments	4
Helium Flux and Concentration Calculations	8
Helium Flux	9
Concentration of Helium in Soil Gas	11
INSTRUMENTATION	13
Helium Field Measurements	13
Field Mass Spectrometer System	13
Soil Gas Sampling Probes	19
Water Bottles for Dissolved Helium Measurements	21
Data Reduction	23
Miniature Electronic Radon Alpha Counters (MERAC)	23
Soil Gas and Water Sample Analyses in the Laboratory	25
Stainless Steel Gas Sample Containers	25
Quadrupole Mass Spectrometer System	25
Gamma-Ray Analysis of Soil Samples	27
PRELIMINARY INSTRUMENT PERFORMANCE TESTS	30
Idaho Springs Geothermal Test	30

Turkey Creek Uranium Test	30
POWDER RIVER BASIN, WYOMING	34
General Geology	34
Test Site A - Irigaray Ranch	38
Geology and Hydrology	38
Measurements of Helium-4 in the Atmosphere and Soil Gas	38
Syringe Leak Test	45
Helium Variations in a Local Area	50
Twenty-Four Hour Variations	50
Instantaneous Traverses	58
Detailed 24-Hour Test	64
Helium Isotope Ratios	68
Basis of Helium Isotope Differences	68
$^3\text{He}/^4\text{He}$ Measurements in the Vicinity of the Ore Body	70
Analysis of Near Surface Soils	75
Gamma-Ray Scintillation and KUT Profiles	75
Gamma-Ray Spectrometric Analysis of Canned Soil Samples	85
Chemical Analysis of Soil Samples	89
In-Situ Radon Detection with Alpha Detectors	89
Miniature Electronic Radon Alpha Counters	89
Track-etch Cups	92
Test Site B	96
Geology and Hydrology	96
Helium Soil-Gas and Atmosphere Measurements	97

Average Values of Helium in Soil Gas	113
Test Site C	115
Geology and Hydrology	115
Helium Soil Gas and Atmosphere Measurements	117
Helium Dissolved in Well Water	123
Test Site D	123
Geology and Hydrology	123
Helium Soil Gas and Atmosphere Measurements	126
Diurnal Test of Helium Concentration as Related to Moisture Content	130
Syringe Diffusion Leak Test	132
Radon Counting Rates Measured with MERAC's	134
Gamma-Ray Analyses of Soil Samples	134
Laboratory Analyses of Soil Gas Samples	142
Test Site E	142
Geology and Hydrology	142
Helium Soil-Gas Measurements	144
Radon Counting Rates Measured with MERAC's	144
Gamma-Ray Spectrometric Analysis of Soil Samples	149
Regional Surveys	149
Helium in Ground Water	149
Uranium in Ground Water	156
Helium in Soil Gas Along Basin-Wide Traverse	158
GRANTS-AMBROSIA LAKE REGION, NEW MEXICO	161
Introduction	161
General Geology	161
Test Site F	164
Geology and Hydrology	164

Helium Soil-Gas Measurements	166
Radon Counting Rates Measured with MERAC's	177
Gamma-Ray Spectrometric Analysis of Soil Samples	181
Micro-Environment Test	181
$^4\text{He}/^{36}\text{Ar}$ and $^4\text{He}/^{22}\text{Ne}$ Ratios in Soil Gas	186
Test Site G	191
Geology and Hydrology	191
Helium Measurements in Soil Gas	193
Regional Surveys	196
Uranium in Ground Water	198
Helium in Ground Water	202
Helium in Soil Gas Along Four Regional Traverses	204
FRONT RANGE, COLORADO	209
Schwartzwalder Mine Area, Colorado	209
Geology and Uranium Deposits	209
Helium-in-Soil-Gas Surveys	211
SUMMARY AND CONCLUSIONS	220
Collection and Measurement Techniques	220
Field Mass Spectrometer System	220
Soil-Gas Collection	220
Electronic Radon Alpha Counters (MERAC)	221
Helium Dissolved in Ground Water	221
Gamma-Ray Analysis of Soil Samples	222
Grid Survey Results	222
Helium in the Atmosphere	222
Helium, Radon, Uranium, and Thorium in Soil	223

Short-Term Surveys	223
Long-Term Surveys	226
Summary of Grid Survey Conclusions	228
Regional Profiles	229
Helium-in-Soil-Gas	229
Helium and Uranium in Ground Water	230
RECOMMENDATIONS	235
LITERATURE CITED	236

## LIST OF FIGURES

	<u>Page</u>
1. Schematic diagram of $^4\text{He}$ field sampling mass spectrometer system.	15
2. Helium survey instrumentation in the truck cab, showing the hypodermic syringe inserted in the syringe inlet septum.	17
3. Instrument sequencer and electronics.	18
4. Soil-gas sampling probe.	20
5. Soil-gas sampling probe with syringe inserted.	22
6. Details of 1-liter gas sample containers.	26
7. Schematic diagram of mass spectrometer system for noble gas measurements.	28
8. Solubility of helium in water versus temperature.	31
9. Reproducibility test of helium concentration measurements, Turkey Creek roadcut, Jefferson County.	32
10. Distribution of facies within the Wasatch Formation in the Powder River Basin.	35
11. Isometric map of the Upper Irigaray Sandstone, Powder River Basin, Wyoming. The location of northern and southern traverses is shown on Figure 15.	39
12. Map of the Irigaray Ranch test site A, showing the uranium roll fronts and the three principal traverses.	41
13. Helium concentration measured in syringe samples taken from 60 cm deep probes on the first run of the northern traverse of the Irigaray Ranch, June 17-29, 1976.	42
14. Meteorological data collected simultaneously with the first run on the northern traverse of the Irigaray Ranch, June 17-29, 1976.	43

15. Continuous flow helium measurements from the soil probe and the atmosphere and syringe atmosphere measurements on the first run across the northern traverse of the Irigaray Ranch, June 17-29, 1976. 44
16. Helium concentration measured in syringe samples taken from 60 cm deep probes on the second run of the northern traverse of the Irigaray Ranch, June 29 - July 2, 1976. 46
17. Meteorological data collected simultaneously with the second run on the northern traverse of the Irigaray Ranch. 47
18. Leak rate measured from 18 syringes filled with  $R_7$  calibration gas. 49
19. Measurements of helium concentration as a function of time and height above ground surface, July 7, 1976. 51
20. Hourly samples from six probes spaced 60 cm apart at PR-37, July 7, 1976. 52
21. Helium concentration in soil-gas and atmosphere collected over a 24-hour period from northern traverse locations NT-1, -5, -11, -17, -23 and -29 on July 8 and July 9, 1976. 54
22. Helium concentration in soil-gas and atmosphere collected over a 24-hour period from northern traverse locations NT-35, -41, -47, -49, -51 and -55 on July 8 and July 9, 1976. 55
23. Twenty-four-hour run, July 8-9, 1976 across NT, average over locations NT-41, -47, -49, -51 and -55 over the "ore" deposit and over locations NT-1, -5, -11, -17, -23, -29 and -35 over the background region. 57
24. Helium concentration on northern traverse on early morning runs, Irigaray Ranch. 59
25. Helium concentration on northern traverse on mid-morning runs, Irigaray Ranch. 61



26.	Helium concentration in soil-gas on northern traverse on afternoon run and averaged values of helium in soil-gas and atmosphere for all six NT "instantaneous traverses", Irigaray Ranch.	62
27.	Helium concentrations in soil-gas and atmosphere, southern traverse, Irigaray Ranch, July 13, 1976.	65
28.	Helium concentrations in soil-gas and atmosphere collected over a 24-hour period from Wyoming Minerals' drill holes, 101, 102, 103, 104, 105 and 106, July 22-23, 1976, Irigaray Ranch.	66
29.	Helium concentrations in soil-gas and atmosphere collected over a 24-hour period from NT-17, -23, -35 and Wyoming Minerals' drill holes 107, 108 and 109, July 22-23, 1976, Irigaray Ranch.	67
30.	Averages of helium in soil gas and atmosphere locations across known mineralization, Irigaray Ranch.	69
31.	Averages of helium in soil gas and atmosphere locations over background regions, Northern Traverse, Irigaray Ranch.	69
32.	Air temperature and relative humidity during Northern Traverse, Irigaray Ranch.	69
33.	$^3\text{He}/^4\text{He}$ ratio measurements from samples collected during a 24-hour period at location 104, July 22-23, 1976.	74
34.	$^3\text{He}/^4\text{He}$ ratio measurements from samples collected along the northern traverse.	77
35.	Gamma-ray scintillometer counting rates along the northern traverse of the Irigaray Ranch.	78
36.	Map of the Irigaray Ranch exploration site showing the locations and mile markers for the five traverses in the KUT truck survey.	79
37a.	KUT traverse No. 1, Irigaray Ranch.	80
37b.	KUT traverse No. 2, Irigaray Ranch.	81
37c.	KUT traverse No. 3, Irigaray Ranch.	82
37d.	KUT traverse No. 4, Irigaray Ranch.	83

37e.	KUT traverse No. 5, Irigaray Ranch.	84
38.	Uranium and thorium content by gamma-ray spectrometer analysis of soil samples collected from 60 cm deep drill holes on the southern traverse of the Irigaray Ranch.	86
39.	Uranium and thorium content by gamma-ray spectrometer analysis of soil samples collected from 60 cm deep drill holes on the northern traverse of the Irigaray Ranch.	87
40.	Uranium and thorium contents by gamma-ray spectrometer analysis of soil samples collected from 60 cm deep drill holes on the parallel traverse of the Irigaray Ranch.	88
41.	Chemical analyses by BFEC of soil samples collected from 60 cm deep drill holes on the northern traverse of the Irigaray Ranch.	90
42.	MERAC counting rates averaged over eight days along the northern traverse, Irigaray Ranch.	93
43.	MERAC counting rates averaged over 10 days along the southern traverse, Irigaray Ranch.	94
44.	Location map for Terradex cup locations.	95
45.	Generalized north-south geologic cross section of test site B.	98
46.	Generalized east-west geologic cross section of test site B.	99
47.	Location map showing soil gas sampling station numbers for all helium soil gas data collected at test site B.	100
48.	Comparison of morning and afternoon runs at test site B showing helium concentration anomaly-in-soil-gas over ore in the afternoon runs.	103
49.	Helium concentration in soil gas at test site B on July 30, 1976.	104
50.	Helium concentration in soil gas at test site B on August 5, 1976.	105

51. Helium concentration in soil gas at test site B on August 5, 1976.	106
52. Helium concentration in soil gas at test site B on August 7, 1976.	107
53. Helium concentration in soil gas at test site B on August 7, 1976.	108
54. Helium concentration in soil gas at test site B on August 12, 1976.	109
55. Helium concentration in atmosphere at test site B on August 5, 1976.	110
56. Helium concentration in atmosphere at test site B on August 7, 1976.	111
57. Helium concentration in soil gas. Average of all soil gas measurements at test site B.	114
58. Generalized cross section of the Wasatch and Fort Union formations in the southern Powder River Basin.	116
59. Uranium deposits and helium sampling stations, test site C.	118
60. Helium concentration in soil gas measured five times on east-west traverse of test site C.	119
61. Helium concentration in soil gas for samples collected on August 13, 1976 at test site C.	120
62. Helium concentration in soil gas for samples collected on August 21, 1976 at test site C.	122
63. Helium concentration in ground water collected on October 26, 1976 from wells in test site C.	125
64. Uranium ore deposits and helium sampling stations for the August 27, 1976 survey, test site D.	127
65. Helium concentration in soil gas collected on August 27, 1976, test site D.	128
66. Helium concentration for atmosphere samples collected at test site D on August 27, 1976.	129

67. Helium concentration in soil gas collected on October 17, 1976, test site D.	131
68. Helium concentration in soil gas collected from probes at six locations across test site D on October 23-24, 1976, with undried and dried samples.	133
69. Syringe leak test over a 24-hour period with 24 capped B-D syringes all loaded with R <sub>7</sub> reference gas at the start of the period.	135
70. Radon counting rates measured with MERAC's buried 60 cm deep at the locations where average counts/min. are indicated, test site D.	136
71. Equivalent uranium (eU) concentration in soil samples collected from test site D.	139
72. Comparisons of Teledyne gamma-ray spectrometry data for 21 soil samples collected from test site D.	141
73. Helium concentration in soil gas collected on November 11, 1976, showing mineralization buried at a depth of 244 m, test site E.	145
74. Helium concentration in soil gas collected on November 13, 1976, test site E.	146
75. Contours of helium concentration in soil gas derived from averages of data accumulated on November 11, 1976 and November 13, 1976, test site E.	147
76. Radon counting rates measured with MERAC's averaged over seven days, buried 60 cm deep at the locations indicated, test site E.	148
77. Equivalent uranium (eU) measurements from soil samples collected from MERAC holes at test site E.	151
78. Equivalent thorium(eTh) measurements from soil samples collected from MERAC holes at test site E.	152

79. Helium concentration in ground water collected from water wells in the southern Powder River Basin.	154
80. Generalized diagram showing the chemical facies of the ground water flow system in the southern Powder River Basin and its relationship to the Highland uranium deposits.	155
81. Uranium concentration in ground water samples collected from the southern Powder River Basin.	157
82. Helium in soil gas, basin-wide traverse, Powder River Basin, Wyoming.	159
83. Schematic diagram of stratigraphic relations of Cretaceous and Jurassic rocks, Ambrosia Lake area.	162
84. Generalized geologic cross section of test site F in the Grants-Ambrosia Lake region.	165
85. Map of test site F showing areas of known mineralization, soil gas sampling stations, and faults.	167
86. Helium concentrations in atmosphere and soil gas at reference stations from February 5 to February 13, 1977 at test site F.	169
87. Composite data, helium concentrations in atmosphere and soil gas at reference stations, from February 5 to February 13, 1977, averaged over one-hour intervals.	170
88. Contours of helium concentrations in soil gas measured at test site F from samples collected during the period from February 5 to February 13, 1977.	171
89. Helium concentrations in atmosphere and soil gas at reference stations from February 15 to February 20, 1977 at test site F (survey 2).	173
90. Helium concentration in soil gas, February 15 to February 20, 1977, test site F.	175

91. Average helium concentrations in soil gas, February 5 to February 20, 1977, test site F.	176
92. MERAC data, February 4 to February 13, 1977 at test site F.	178
93. MERAC data, February 16 to February 21, 1977 at test site F.	179
94. Equivalent uranium and thorium data from soil samples from MERAC holes at test site F.	182
95. Micro-environment tests and time of day variations of helium in soil gas at reference station 40 at test site F.	183
96. Percentage deviations from assumed constant atmospheric ratios in $^4\text{He}/^{36}\text{Ar}$ and $^4\text{He}/^{22}\text{Ne}$ measured from soil gas collected from test site F.	187
97. Regional map of the Grants-Ambrosia Lake Uranium District showing the location of test site G.	192
98. Geologic cross section of test site G.	194
99. Helium concentration in soil gas on February 23, 1977, at test site G.	195
100. Helium concentration in soil gas on February 24, 1977, at test site G.	197
101. Helium and uranium concentrations in ground water in the Grants-Gallup-Ambrosia Lake region. The geologic formations in the region are shown also.	200
102. Helium concentration in soil gas collected at 1.6 kilometer (1 mile) intervals along roads in the Grants-Gallup-Ambrosia Lake region from December 14 to December 16, 1976.	205
103. Helium concentration in soil gas collected at 1.6 kilometer (1 mile) intervals along roads in the Grants-Gallup-Ambrosia Lake region on December 21, 1976.	206

104. Helium in soil gas for samples collected on May 6 and May 9, 1977, Schwartzwalder mine area.	210
105. Schematic geologic cross section of the Schwartzwalder mine.	212
106. Helium-in-soil-gas collected during the detailed survey of May 24, 1977, Schwartzwalder mine.	214
107. Helium-in-soil-gas collected during the second detailed survey (June 16, 1977), Schwartzwalder mine.	215
108. Summary of all helium in soil gas data, Schwartzwalder mine.	217
109. Schematic cross section and helium in soil gas data, in the vicinity of the Schwartzwalder mine.	218

## LIST OF TABLES

	<u>Page</u>
1. Reference Gas Calibration	16
2. ( $H_{sg} - H_{atm}$ ) Differential from July 16, 1976 Survey, Irigaray Ranch	60
3. Average Helium Concentrations, Irigaray Ranch	63
4. Soil-Gas and Atmosphere Samples Collected for $^3He/^4He$ , Irigaray Ranch	72
5. $^3He/^4He$ Measurements in Soil-Gas Samples Collected by Teledyne Isotopes, Irigaray Ranch	73
6. $^3He/^4He$ Measurements in Soil-Gas Samples Collected by Martin Marietta, Irigaray Ranch	76
7. Ratios of Chemical to Gamma-Ray Spectrometer Determinations of Uranium and Thorium in Soil Samples, Irigaray Ranch	91
8. Times and Dates of Surveys, Test Site B	97
9. Helium-in-Soil-Gas Anomalies, Test Site B	102
10. Helium-in-Soil-Gas Anomalies, Test Site C	124
11. Uranium and Thorium Concentrations in Soil Samples from Test Site D Determined by Gamma-Ray Analysis by Geolabs	138
12. Gamma-Ray Activities Recorded in Soil Samples from Test Site D by Gamma Spectrometry by Teledyne Isotopes	140
13. Laboratory Soil Gas Analyses from Test Site D	143
14. Uranium and Thorium Concentrations in Soil Samples from Test Site E Determined by Gamma-Ray Analysis by Geolabs.	150
15. MERAC Data at Test Site F	180
16. Helium in Soil Gas Concentrations for the Microenvironment Test, Test Site F	184



17. $^4\text{He}/^{36}\text{Ar}$ and $^4\text{He}/^{22}\text{Ne}$ Data, Test Site F	188
18. Helium Data Comparison, Test Site F	190
19. Helium and Uranium Concentrations in Ground Water Samples in the Grants-Gallup-Ambrosia Lake Region.	199

## ACKNOWLEDGEMENTS

I would like to thank my committee members, Dr. R. H. De Voto, chairman, Dr. S. B. Romberger, Dr. K. W. Edwards, Professor H. Bloom, and Dr. E. D. Sloan, for their guidance and assistance throughout the program. I am grateful to Mr. Robert Rodriguez of Wyoming Minerals Corporation for guidance and financial assistance throughout my stay at the Colorado School of Mines.

Thanks also go to the Electric Power Research Institute, particularly Jeremy Platt, Wyoming Minerals Corporation, and the Bendix Field Engineering Corporation for financial assistance in conducting this research program and for providing gamma-ray spectrometric analyses. I would also like to acknowledge the support of Geolabs and GX Lab for providing chemical uranium analyses. The financial assistance of Rocky Mountain Energy Company in the preparation of this document is greatly appreciated.

The technical assistance of Dr. Joe Martin and Mr. L. E. Bergquist of Martin Marietta is gratefully acknowledged.

Special thanks go to the company geologists who allowed access to their properties. Without their geologic assistance this program would have been much less meaningful. Finally, I would like to thank my parents, Hubert and Dorothy Mead, for moral support throughout my college career.

## INTRODUCTION

Uranium ore deposits are generally extremely difficult to locate, causing the need for the development of multiple methods and techniques of uranium prospecting and integration of these prospecting techniques into a comprehensive geologic analysis. Among these techniques are:

1. Geologic analysis and evaluation which helps determine which types of formations are most likely to contain uranium deposits (Bowie, 1972; Childers, 1974; Davis, 1970).
2. Gamma-ray surveys (Miller and Lasemore, 1972) by geiger counter or scintillometer, including total gamma radioactivity (Puibaraud, 1972) and potassium-uranium-thorium (KUT) spectrometry (Lovbord, 1972). These data are collected by truck, foot, aircraft, or in borehole logging.
3. Direct geochemical techniques (Bowie, et al., 1971) involving detection of uranium in soil samples, ground water, or stream sediments by x-ray fluorescence, neutron activation (Ostle, et al., 1972), or ultraviolet fluorometry (Grimbert, 1972).
4. Indirect geochemical techniques (Bowie, et al., 1971) such as testing soil samples, water or stream sediments for radioactive daughter products such as radon-222 by its alpha-emission, or bismuth-214 by its gamma-emission, or other elements which are geochemical associates of uranium ore deposits, such as iron, copper, selenium, and

molybdenum.

5. Emanometry (Adkisson and Reimer, 1976) measuring the gaseous emissions from the radioactive decay of uranium and its daughter products in soil gases, viz, helium-4 by mass spectrometry (Grammakov, et al., 1965 and Dyck, 1976) and radon-222 (Dyck, 1969) by Track-etch (Gingrich, 1975) or electronic alpha counter.
6. Geobotanical methods in which indicator elements, such as selenium, stimulate growth of certain botanical species or biogeochemical methods where chemical analysis of leaves of plants reveals concentration variations of uranium or indicator elements (Bowie, 1972).
7. Exploration drilling.

These techniques cover a range of sensitivity to the ore and of specificity for uranium. No single prospecting technique can be regarded as a panacea, rather, each of the methods is regarded as having specific applications in particular geologic circumstances.

The objective of the research program was to evaluate helium emanometry techniques which have a potential for sensing remote uranium deposits and to compare these with other exploration techniques. The two gaseous emissions from uranium-series decay are radon-222 and helium-4 (Adkisson and Reimer, 1976). Because of its complete nuclear stability and chemical inertness, helium is potentially an ideal indicator of the remote presence of uranium ore (Grammakov, et al., 1965). On the other hand, the detection of radon-222 gas and its daughter products serves more as a near-proximity indicator because

its short half life of 3.8 days restricts the distance that it can be transported from its source before it decays to solid daughter elements (Dyck, 1972). Therefore, as the distance from the uranium deposit becomes greater, one would expect the potential of using radon as an indicator of a buried uranium deposit to decrease relative to helium.

For a more detailed description of the instrumentation used in this program, one is referred to two previous reports (Martin and Bergquist, 1977 and Martin, et al., 1975). The previous reports also contain a summary of the preliminary results concerning the applicability of helium as a pathfinder for uranium. This report will elaborate on the geological and hydrological evaluation of the data with recommendations for future programs.

The program reported here is part of a more comprehensive program of evaluating the use of helium in exploring for uranium deposits, a cooperative effort among the U.S. Department of Energy (D. O. E.)/Bendix Field Engineering Corp. (BFEC), Electric Power Research Institute (EPRI), Westinghouse Corporation - Wyoming Minerals Division (WM), Colorado School of Mines, Earth Sciences Inc., and Martin Marietta Corporation. Helium-gas research at the Irigaray Ranch in the Pumpkin Buttes District of the Powder River Basin was conducted by Martin Marietta in cooperation with the Colorado School of Mines. The Irigaray work was begun under the auspices of Wyoming Minerals and then completed with D. O. E. support. The Martin Marietta effort and attendant field exploration, instrumentation, and laboratory measurements program was supported by a D. O. E. /BFEC contract (Martin and Bergquist, 1977). The Colorado School of Mines participation, including field exploration,

geological direction, and data analysis was supported by a contract with Westinghouse Corporation (Wyoming Minerals Division). Finally, the work reported here in the southern Powder River Basin in Wyoming, in the Grants region of New Mexico, and at the Schwartzwalder mine in Colorado was performed under contract to EPRI (Martin, et al., 1978) by Martin Marietta with Earth Sciences as principal subcontractor.

#### Summary of Previous Work in Helium Measurements and Behavior in Geologic Environments

In the radioactive decay of the most common isotope of uranium (uranium-238) to its final stable daughter, Pb-206, eight alpha particles are produced. These alpha particles, being positively charged, readily pick up electrons to become inert, gaseous, helium-4 atoms. The constant generation of inert helium gas from uranium and its daughter products provides a potentially useful means of detecting buried uranium accumulations.

In addition to the uranium-238 series, helium-4 is also generated in the decay series of uranium-235 and thorium-232. Other natural alpha emitters such as samarium-147 and platinum-190 contribute helium but in negligible quantities.

The rocks which generate helium-4 have many differing degrees of helium retention (Morrison and Pine, 1955) and therefore, differing rates of release for migration to the ground surface and the atmosphere. Therefore, the background levels of helium content will differ from one geologic environment to another.

The mechanisms of helium migration to the ground surface include diffusion and transport in ground water. The coefficient of molecular diffusion of helium through water is  $5 \times 10^{-9} \text{ m}^2/\text{sec}$  (Hurley, 1954) whereas the coefficient of convective diffusion of helium in water is estimated to be  $10^{-2} \text{ m}^2/\text{sec}$ , a rate about six and one half orders of magnitude higher (Golubev, et al., 1974). It is also assumed that most fracture zones below the water table are saturated with water (Golubev, et al., 1974). Therefore, the migration of helium upward from a uranium deposit to the ground surface is dominated by transport in the ground water system and convective diffusion in water. Its concentration in the near-surface soil zone will depend on the molecular diffusion rate through the upper layer of the soil when it is not saturated with water.

Analyses of the geology of the known helium accumulations of the United States show that most of the significant helium accumulations occur in Paleozoic reservoir rocks, some of which are spatially associated with slightly uraniferous Paleozoic black shales. Helium accumulations are rarely found in association with the major uranium deposits or districts in Mesozoic and Cenozoic host rocks of the Western United States. This suggests that Paleozoic reservoir rocks are generally less permeable to helium migration than are Mesozoic and Cenozoic shales and mudstones. Thus, helium generated continuously from uranium deposits in Mesozoic and Cenozoic rocks is probably migrating upward toward the atmosphere through the overlying rocks where it is potentially detectable and is not being trapped and accumulated as it is in Paleozoic reservoir rocks.

Previous research in utilizing helium for uranium exploration has been conducted in Canada by Goldak (1973), Dyck (1976) and

Clark et al. (1973, 1977). Goldak's work at the Gunnar Mine in Saskatchewan showed helium in soil gas concentrations as high as 65 ppm in the vicinity of the deposit. The samples were collected from a 2.5 cm diameter hollow probe driven approximately one meter into the ground.

Clark, et al. (1977), in a region in central Labrador, made measurements of dissolved helium,  $^3\text{He}/^4\text{He}$ , and neon in 60 water samples collected from 56 lakes and ponds in the Kaipokok region in Labrador. They also measured tritium in eight water samples. The purpose of the survey was to search for excess helium-4 from the decay of uranium and its daughter products. The purpose of the neon measurements was to estimate the amount of atmospheric contamination during the sample collection and to make appropriate corrections.

Clark (1973) measured the  $^3\text{He}/^4\text{He}$  ratio to determine if measurements of excess helium-4 were from uranium deposits or long residence time accumulations from granitic basement rocks. According to Morrison and Pine (1955), if the excess helium-4 was due to accumulations from the basement rock, the ratio should approach  $10^{-7}$  whereas an accumulation from a one percent uranium ore deposit should approach  $10^{-9}$ . The results of hydrogen bomb testing in the atmosphere in the 1950's complicated this matter since tritium picked up from the atmosphere by precipitation eventually decayed (half life = 12.26 years) to helium-3, adding to the helium-3 content of the ground water. This turned out to be beneficial, however. By measuring the tritium content, an estimate could be made of the residence time of the water in the ground water system. This was done by relating the measured tritium concentration in ground water samples to independent measurements made from precipitation in the same region. These showed



levels of two TU (one TU = 1 tritium/ $10^{18}$  hydrogen) before 1950 to a peak of 2,959 TU in 1963 and then decreasing to 258 TU in 1968.

Clark (1977) postulated that the residence time estimates coupled with the excess helium-4 measurement gave a method for determining the rate of helium generation in the region of the ground water system and thus a measure of the amount of uranium in a uranium deposit.

Excess helium-4 varied from zero percent to 65 percent relative to the equilibrium solubility concentration at the temperature of the sample (Clark, et al., 1977).  $\delta(^3\text{He})$ , the anomaly in  $^3\text{He}/^4\text{He}$  measured in the water samples relative to atmospheric helium, varied from +11 to -25 percent. There was a good correlation between the lakes which have  $\delta(^3\text{He})$  less than or equal to two percent and lakes with excess radiogenic  $^4\text{He}$  greater than or equal to four percent. The anomalous helium data show a remarkable coincidence with the locations of known uranium mineralization.

The U.S. Geological Survey in Denver has made measurements of helium in soil gas and in water samples using a truck-mounted helium leak detector (Reimer, 1976). Two test sites were visited; a geothermal spring in the vicinity of Idaho Springs, Colorado (Auberts, et al., 1975), where anomalous helium concentrations in soil gas were observed, and a uranium deposit in Weld County, Colorado (Reimer and Otton, 1976), where anomalous helium concentrations in soil gas of 0.04 ppm above the atmospheric value of 5.24 ppm were recorded. Helium concentrations measured in ground waters were as great as 8.46 ppm and as low as 5.28 ppm.

Several conclusions concerning the research to date can be made at this time.

1. Helium-in-soil gas can be very useful in the exploration for uranium deposits and geothermal sites although the methodology is not yet well defined.
2. Helium-in-ground water exhibits larger variations from the atmospheric concentration than did helium-in-soil gas.
3. Variations in atmospheric helium concentration do not exist.

#### Helium Flux and Concentration Calculations

The detectability of a uranium deposit by measurement of helium in soil gas depends on the diffusivity of helium in the overlying strata (Grammakov, et al., 1965; Golubev, et al., 1974). A low diffusivity medium, i. e. siltstone-claystone, allows helium to concentrate in the soil zone. When the strata has a high diffusivity rate, i. e. sand, it allows the upward-migrating helium to pass through quickly without building up an appreciable concentration. Ground water or soil moisture, however, can act as a concentrator, trapping helium as it migrates upward from the uranium body. Therefore, the greatest use of helium in exploration for buried uranium deposits may be in the measurement of the helium contained in ground water or soil moisture.

To estimate the expected helium concentration in soil gas above a buried uranium deposit, it is first necessary to estimate the flux (Naughton, et al., 1973) of helium which migrates upward from the ore body (J. Martin, personal communication). Then the diffusion coefficient for the movement of helium through the soil is used to estimate

the concentration difference between the atmospheric helium and soil gas helium.

### Helium Flux

It is assumed for these calculations that  $^{238}\text{U}$  is in secular equilibrium with its daughters and that all the helium generated in the radioactive decay of uranium and its daughter products will migrate vertically to the ground surface. The first step is to estimate the amount of helium generated in a uranium deposit in terms of  $q$ , the rate of helium generated per cubic meter of ore (Naughton, et al., 1973). The rate of decay of uranium is given by the radioactive decay law:

$$-\frac{dN_{\text{U}}}{dT} = \lambda N_{\text{U}} \quad 1$$

where  $N_{\text{U}}$  = number of  $^{238}\text{U}$  atoms per cubic meter

$\lambda$  = radioactive decay constant for  $^{238}\text{U}$

$\lambda = 4.85 \times 10^{-18} \text{ sec}^{-1}$  (Fleming, et al., 1952)

After a uranium-238 atom emits an alpha particle, the remaining thorium-234 atom undergoes a sequence of 13 radioactive disintegrations before ending up as an atom of stable lead-206. In this decay chain a total of eight alpha-particles are emitted. All of the subsequent disintegrations have much shorter half lives than the parent uranium-238 and, therefore, the uranium decay rate defines all the subsequent disintegration rates. Thus, for each uranium atom that disintegrates, eight helium atoms are formed. The rate of formation of helium can be written as (Naughton, et al., 1973):

$$q = \frac{dN_{\text{He}}}{dT} = 8 \frac{-dN_{\text{U}}}{dT} = 8\lambda N_{\text{U}} \quad 2$$

where  $N_{\text{He}}$  = the number of helium atoms per cubic meter

Ore grades are usually quoted in terms of  $\text{U}_3\text{O}_8$ . The number of uranium atoms per cubic meter can be expressed as (Naughton, et al., 1973):

$$N_{\text{U}} = 3 p g N_{\text{O}} / M \quad 3$$

where  $p$  = the ore density in  $\text{kg/m}^3$

$g$  = ore grade in percent

$N_{\text{O}}$  = Avogadro's number in molecules/K mole

$M$  = the molecular weight = 842 kg for  $\text{U}_3\text{O}_8$

Therefore  $q = 24 \lambda p g N_{\text{O}} / M$ , in  ${}^4\text{He}$  atoms  $\text{m}^{-3} \text{sec}^{-1}$  4

Finally the flux,  $F$ , would be the generation rate times the thickness,  $H$ , of the ore deposit (Naughton, et al., 1973).

$$F = qH = 24 \lambda p g H N_{\text{O}} / M \text{ in } {}^4\text{He atoms } \text{m}^{-2} \text{sec}^{-1} \quad 5$$

For a typical uranium deposit in sandstone, an ore grade of 0.15 percent is assumed; and with an ore density,  $p = 2 \times 10^3 \text{ kg/m}^3$ , and a thickness,  $H = 5\text{m}$ , the flux is determined to be:

$$F = 1.25 \times 10^9 {}^4\text{He atoms in } \text{m}^{-2} \text{sec}^{-1}$$

Naughton, et al. (1973) calculated, on the basis of measurements of helium in Hawaiian fumarolic degassing, that the global average of helium flux from the earth's mantle is about  $10^9$  helium-4 atoms in  $\text{m}^{-2} \text{sec}^{-1}$ . This is similar to an estimate of  $1.4 \times 10^9$  helium-4 atoms  $\text{m}^{-2} \text{sec}^{-1}$  by Turekian (1964). These estimates are not much different

than the flux just calculated, so an enhancement of helium concentration in the atmosphere over an ore body is not to be expected.

### Concentration of Helium in Soil Gas

Using the equation for the rate of formation of helium derived in the last section, it is possible to calculate an estimate of the enhancement of helium in soil gas as a result of a subsurface uranium deposit (Naughton, et al., 1973). Adapting the equation derived by Grammakov, et al. (1965) for the increase in concentration produced by helium emanating from a subsurface uranium deposit with an overburden of relatively inert rock, yields:

$$\Delta C = \frac{V_o}{DN_o C_o} Y \left[ q_o \left( H_o - \frac{Y}{2} \right) + qH \right] \quad 6$$

where  $\Delta C$  = the fractional difference in helium concentration in the soil compared to the nominal atmospheric concentration.

$C_o$  = nominal atmospheric concentration of helium =  
5.24 ppm =  $5.24 \times 10^{-6}$

$V_o$  = molar volume of ideal gas at standard temperature  
and pressure =  $22.4 \text{ m}^3/\text{k mole}$

$N_o$  = Avogadro's number =  $6.023 \times 10^{26}$  molecules/k mole

$D$  = diffusion coefficient of helium through top soil above  
the sampling point ( $\text{m}^2\text{sec}^{-1}$ )

$Y$  = depth in the soil at which concentration is measured  
(m).

$q_o$  = helium production rate due to uranium and thorium  
in the rock overburden (eq. 4)

$H_o$  = depth of overburden (m)

$q$  = helium production rate in the uranium deposit  
(eq. 4)

$H$  = thickness of the uranium deposit (m)

Rewriting equation 6 with equation 4 substituted for  $q$  and  $q_o$ , using  $g$  = equivalent concentration of  $U_3O_8$  in the ore body and  $g_o$  = equivalent concentration of  $U_3O_8$  in the rock overburden, gives:

$$\Delta C = \frac{24\lambda p V_o}{DMC_o} Y \left[ g_o \left( H_o - \frac{Y}{2} \right) + gH \right] \quad 7$$

Assuming an average density  $p = 2 \times 10^3 \text{ kg/m}^3$  for the ore and the rock overburden, this becomes the dimensionless quantity (Naughton, et al., 1973):

$$\Delta C = 1.18 \times 10^{-9} \frac{Y}{D} \left[ g_o \left( H_o - \frac{Y}{2} \right) + gH \right] \quad 8$$

In the overburden as well as in the ore, the thorium decay series generates helium as well as the uranium series. The generation rate of helium from the thorium series is lower by a factor of 0.75 (for equal concentrations) since the thorium decay series yields only six alpha emissions compared to the eight from the uranium series (Naughton, et al., 1973). The rate is lower by a factor of 0.329 because of the longer half life of thorium (Naughton, et al., 1973). Thus, the helium production rate of a weight fraction of thorium will be 0.247 times that for an equal weight fraction of uranium.

To estimate the approximate helium enrichment in soil gas due to a typical buried uranium deposit of economic significance, values of four ppm and 12 ppm are used for the assumed average concentrations of uranium and thorium in the overburden. The 12 ppm of thorium is equivalent to about three ppm of uranium in the rate of helium

generation. For simplification, the total relative concentration,  $g_o = 7 \text{ ppm} = 0.007 \text{ percent}$ . An overburden thickness of 200 meters ( $H_o$ ), an ore deposit thickness (H) of 3 meters, an ore grade (g) of 0.15 percent  $U_3O_8$ , and a sampling depth (Y) of 0.6 meters are assumed for calculation purposes. If the soil is water saturated, a diffusion coefficient,  $D = 5 \times 10^{-9} \text{ m}^2/\text{sec}$ , of helium can be used to calculate  $\Delta C$ . The calculation indicates that the helium content in soil gas, using the above assumptions, should be 4.4 ppb greater than the atmospheric concentration, or a percentage difference of 0.08%. Such an anomaly is slightly less than the detection limit of the instrumentation.

The largest uncertainty in this estimate of  $\Delta C$  comes from the variability in the diffusion coefficient. It is the diffusion coefficient above the sampling depth which determines the helium concentration measured. The diffusion coefficient can vary widely depending on the amount of clay, sand, rock, soil moisture and other constituents. A heavy dry clay soil could have a smaller diffusion coefficient yielding higher anomalies while a dry sandy soil would have a much larger diffusion coefficient yielding lower anomalies. In the example given above, 76 percent of the increase over atmospheric concentration is due to the uranium deposit and 24 percent from the overburden.

## INSTRUMENTATION

### Helium Field Measurements

#### Field Mass Spectrometer System

The field instrumentation system used in this research consisted of a modified Consolidated Electrodynamics Corporation (CEC) helium leak detector mass spectrometer installed in the cab of a four-wheel drive crew cab pickup truck. The truck was equipped with a roof-top air conditioner and a cover shell for the bed. Gas bottles, a five kilovolt motor generator, and miscellaneous equipment were kept in the rear of the truck. The CEC mass spectrometer was modified for batch sampling and increased sensitivity by installing an automated shut-off valve between the mass spectrometer and its evacuation pump and by including a chemical getter pump to remove active gases from the gas samples and to keep the system pressure down during the measurement period. A block diagram of the system is shown in figure 1.

Two reference gases were provided for frequent calibration of the instrument. The reference gases were K-bottles filled with dry air, calibrated at the U.S. Bureau of Mines as shown in table 1. One ( $R_5$ ) was mixed with nearly atmospheric helium concentration, whereas the other ( $R_7$ ) was enriched 46 per cent higher than atmospheric concentration.



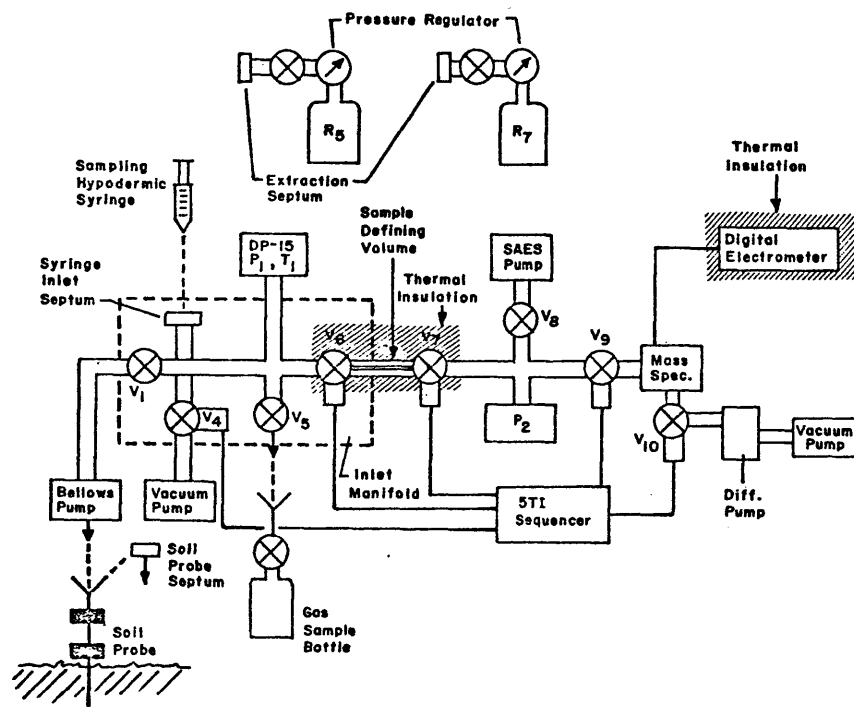


Figure 1. Schematic diagram of  $^4\text{He}$  field sampling mass spectrometer system.

Table 1. Reference Gas Calibration

Reference Gas	He, ppm	N <sub>2</sub> , %	O <sub>2</sub> , %	Ar, %	CO <sub>2</sub> , %
R <sub>5</sub>	5.27 ± 0.02	78.9	20.2	0.9	0.05
R <sub>7</sub>	7.65 ± 0.06	78.7	20.4	0.9	0.05

All measurements of helium concentration in soil gas, atmosphere, water, or reference gas were made by filling a 20 cm<sup>3</sup> hypodermic syringe with the desired gas sample and then injecting this sample into the inlet manifold.

The measurement is made by inserting the hypodermic needle into the syringe inlet septum on the inlet manifold, as illustrated in figure 2. During injection of the gas into the manifold, the pressure ( $P_1$ ) is monitored to determine when to stop injecting the gas. Thus, the gas is always injected at the same manifold pressure, viz., 90,000 pascals (675 torr), to normalize the sample size.

The remaining operating sequences for making a measurement are controlled by the Texas Instrument (Model 5TI) sequencer (figures 1 and 3). After the pressure,  $P_1$ , and temperature,  $T_1$ , have equalized, the 5TI sequencer system is initiated to provide an automatic series of valve operations to accomplish the measurement.

The temperature ( $T_1$ ) and pressure ( $P_1$ ) were measured with a Western Systems Model DP-15 digital pressure-temperature indicator with an accuracy better than 0.5 per cent. The mass spectrometer output was measured by a Keithley Model 616 digital electrometer amplifier which has a rated accuracy of 0.2 per cent.

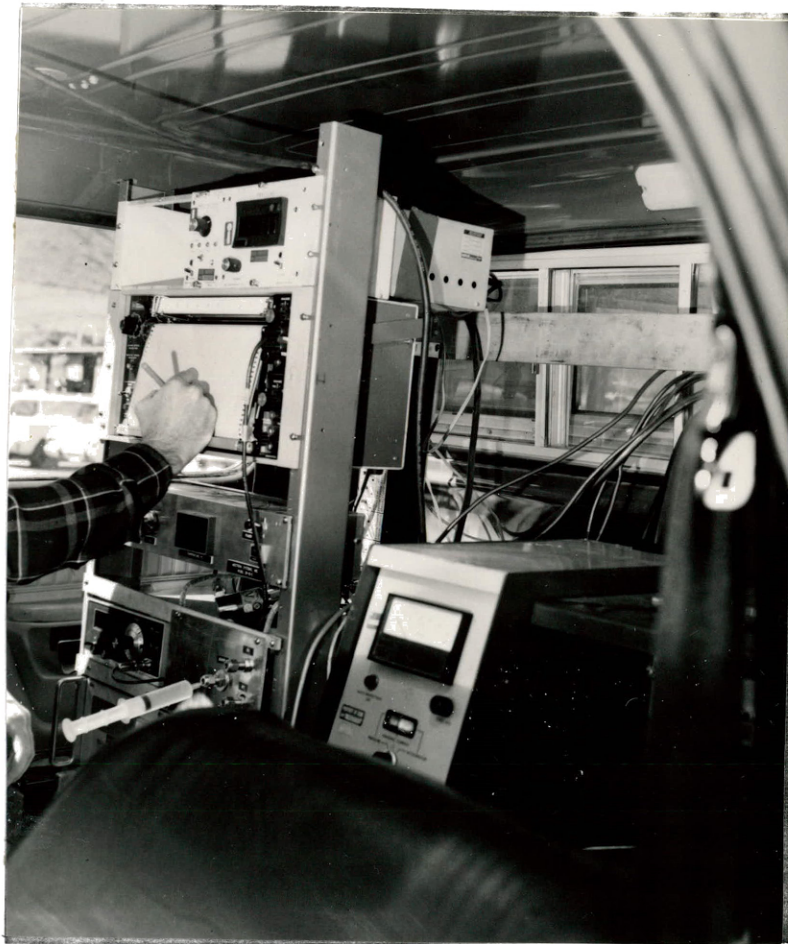


Figure 2. Helium survey instrumentation in the truck cab, showing the hypodermic syringe inserted in the syringe inlet septum.

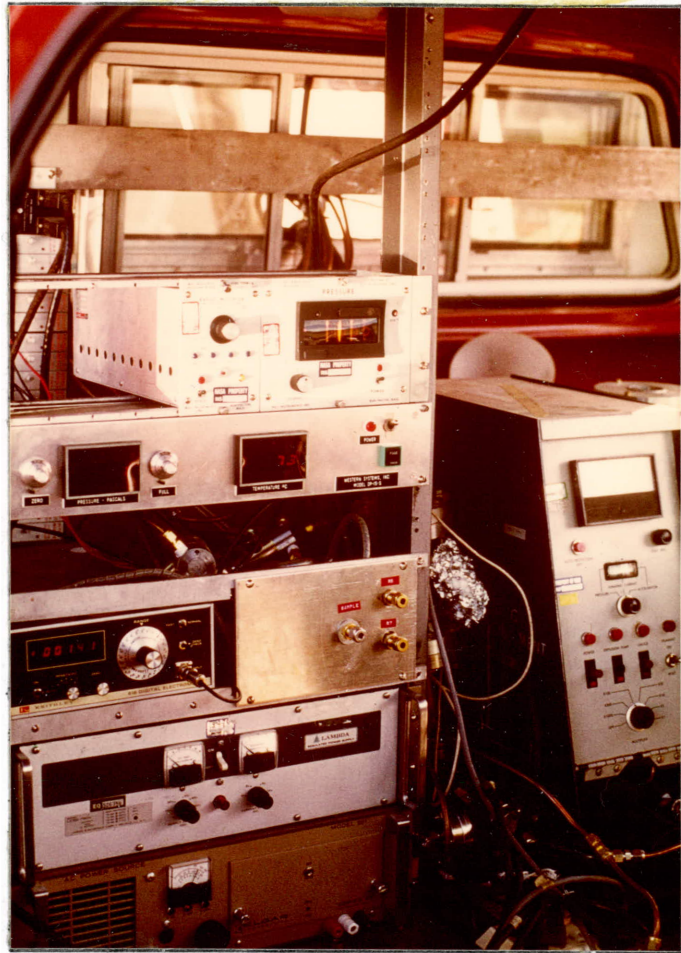


Figure 3. Instrument sequencer (on the right) and electronics.

Each measurement of soil gas or atmosphere was interspersed with a  $R_5$  reference-gas measurement in order to reduce the effects of long term instrument variations caused by temperature variations or system sensitivity changes. Therefore, the sample-defining volume was not measured accurately since its only accuracy requirement for the purposes of the helium measurements was in remaining constant from sample to reference measurement.

Syringe measurements of the atmosphere were made by filling a syringe directly from the air (usually right at the soil surface), and injecting it into the manifold as described above. The calibration reference gas,  $R_5$  or  $R_7$ , was admitted to the manifold by drawing a syringe of the gas out of the respective calibration septum and then injecting it into the manifold in exactly the same way as a field sample syringe was injected for measurement. The time required for one measurement was approximately 45 seconds.

The system was improved during the course of the program by reducing the volume of the inlet manifold enough to allow making three measurements from each  $20 \text{ cm}^3$  syringe instead of just one. A further improvement consisted of adding thermal insulation around both the sample-defining volume and the digital electrometer. This improved the instrument accuracy from  $\pm 25$  ppb to  $\pm 10$  ppb.

### Soil Gas Sampling Probes

Syringe measurements of soil-gas were made by pushing a probe about 60 cm into the ground (figure 4). The probes were constructed from 0.25 in (6.4 mm) outside-diameter, 0.093 in (2.4 mm) inside-diameter stainless tubing. The lower end was welded shut, tapered to

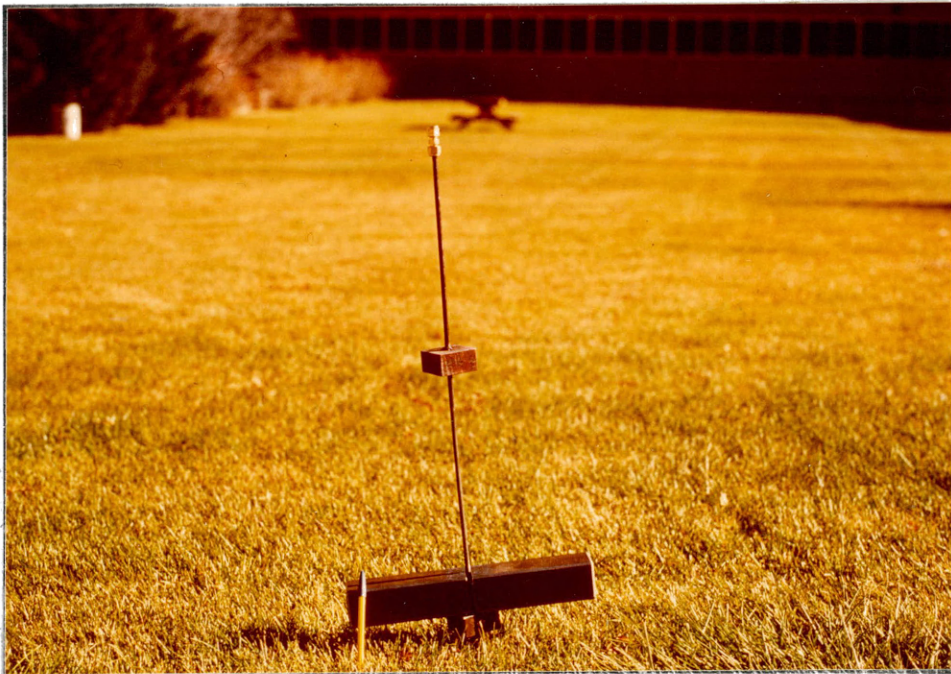


Figure 4. Soil-gas sampling probe.

a point, and three air inlet holes were drilled through the tube several centimeters up from the tip. The top end was equipped with a Swagelok fitting containing a thick surgical rubber septum. Blocks were welded at two points along the length of the probe for hammering into or out of the ground with a slotted steel bar. Soil gas samples were then collected by inserting the hypodermic syringe needle into the septum and withdrawing the air in the probe (figure 5). The first syringe (usually less than the full  $20 \text{ cm}^3$ ) was discarded to evacuate the probe (total internal volume =  $5.6 \text{ cm}^3$ ). The second syringe (a full  $20 \text{ cm}^3$ ) was used for the measurements.

#### Water Bottles for Dissolved Helium Measurements

In order to compare the amount of helium dissolved in water recovered from various underground sources, Nalgene bottles were used to collect water from water wells and windmills. The water was loaded into the 1-quart (0.946 l) Nalgene bottle to a standard fill level of 0.85 liter and closed immediately with an air-tight cap equipped with a septum identical to the one used on the mass spectrometer inlet manifold. The bottle was stored two to three hours until time of measurement. It was then shaken vigorously for 30 seconds to establish an equilibrium between the helium concentration in the water and in the air space above the water. After shaking, it was allowed to settle for two minutes, whereupon a syringe needle was inserted in the septum to withdraw an air sample which was immediately introduced into the mass spectrometer for helium measurement. If the concentration of helium in the water was greater than the equilibrium concentration equivalent to the helium concentration in the ambient air, the shaking released helium into the head space. If the helium concentration in





Figure 5. Soil-gas sampling probe with syringe inserted.



the water was lower, then the shaking caused some of the helium in the head space to dissolve into the water. Diffusion of helium through the container did occur; however, the level of concentration still allowed detection of anomalous samples.

#### Data Reduction

The method used for converting digital electrometer count readings into ppm of helium was as follows: Each set of three measurements from a single sample syringe was bracketed by measurements of the R<sub>5</sub> reference gas. The average of four such R<sub>5</sub> readings was divided into 5.270 ppm (the R<sub>5</sub> calibration value) to obtain the instrument sensitivity in ppm/electrometer count. This sensitivity was averaged with a similarly obtained sensitivity from the R<sub>7</sub> reference gas. The resultant sensitivity was multiplied by the three sample readings and averaged to obtain a measurement of the helium concentration in the sample in ppm.

#### Miniature Electronic Radon Alpha Counter (MERAC)

A miniature instrument for detecting and counting electronically the alpha particles emitted in the radioactive decay of radon gas had been developed by Martin Marietta in a preliminary form before the start of this program. For the purposes of the measurements desired in this program, a set of 50 of these MERAC's were fabricated and used in the field. Due to the preliminary nature of the design when the 50 MERAC's were fabricated, there were a number of field operational

problems which resulted in fewer than 30 of the MERAC's being fully operational at any one time. Therefore, data were collected only from those which were operational.

The entire MERAC unit is contained in the 3.8 cm diameter by 29.2 cm long aluminum tube which weighs 0.29 Kg (0.65 lb). The detector is a silicon surface barrier type with a 100  $\mu$ m thick depletion layer.

The silicon detector, which is protected from moisture and light by a 63.5  $\mu$ m thick aluminized mylar film is recessed from the end of the tube and in operational use is maintained far enough from any surrounding soil to exceed the range of alpha particles from any radioactive elements in the soil. It is further protected from damage by a wire screen. Thus, the only alpha particles detected are those emitted by radon gas nuclei which undergo radioactive decay within a distance from the detector defined as that travelled in air by a radon alpha particle before its energy has been reduced to the 2 Mev threshold of the instrument with its aluminized mylar film. At an atmospheric pressure of 620 torr, this distance is 4.1 cm for radon-222 (from the uranium-238 decay series) and 5.3 cm for radon-220 (from the thorium-232 decay series) (Joe Martin, personal communication).

Typical field operations resulted in 1000 to 10,000 counts per day when placed at the site of a uranium deposit. The method of installation involved drilling a 60 cm deep hole with a 7.6 cm (3 in) auger, inserting a 60 cm long piece of 6.4 cm ( $2\frac{1}{2}$  in) plastic pipe in the hole and simply lowering the MERAC into the pipe and screwing a cap on the pipe. The pipes were constructed with a constriction about 10 cm from the bottom to prevent the detector from coming within range

of alpha particles emitted by solid radioactive elements in the soil, thus making it sensitive only to radon gas. Then at periodic intervals, readings of alpha counts from the entire set of MERAC's could be obtained by visiting each pipe, uncapping it, lowering a magnet stick alongside the MERAC to activate the LED display, and observing the displayed accumulated counts.

### Soil Gas and Water Sample Analyses in the Laboratory

#### Stainless Steel Gas Sample Containers

The measurements of helium-4 to argon-36 and of helium-4 to neon-22 ratios were made by collecting one-liter samples of soil gas and returning these to the laboratory for measurement with a Finnegan Spectrascan Quad 750 mass spectrometer. The sample collecting containers, shown in figure 6, were all welded stainless steel cylinders to essentially eliminate leakage. The internal volume of the cylinders was actually 1.02 liter. A set of five similar cylinders with the same diameter but long enough to contain about four liters were fabricated for collecting samples for radon-222 measurements by Teledyne Isotopes. These samples were also analyzed by Teledyne for the helium-4 to argon-36 ratio.

#### Quadrupole Mass Spectrometer System

The Finnegan Quad 750 mass spectrometer is a quadrupole system with an electron multiplier and a Keithley electrometer for amplifying the ion current sufficiently for recording on a strip chart recorder. The electronic stability combined with ion current stability

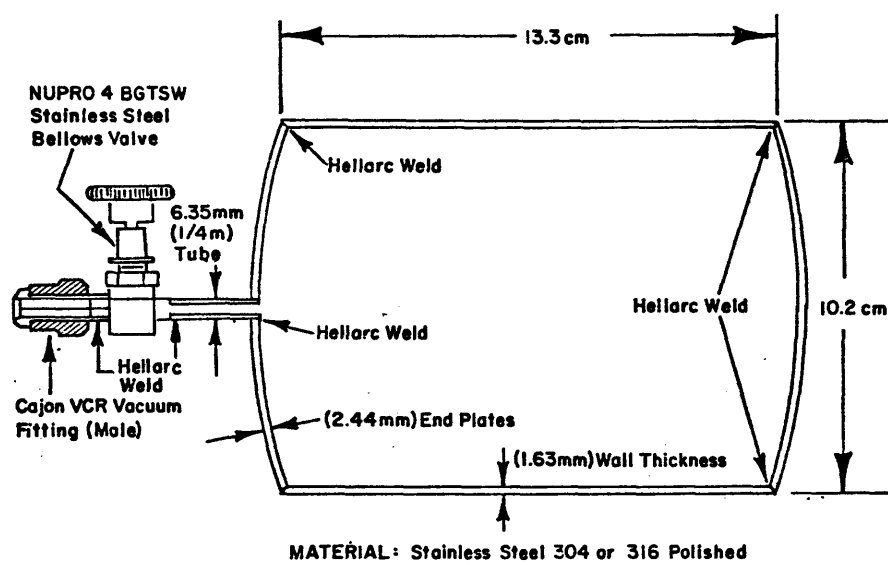


Figure 6. Details of 1-liter gas sample containers.

is such that peak heights are reproducible to better than plus or minus three per cent. It was discovered subsequent to the completion of the measurements that noble gas retention in the system limited the ultimate reproducibility of results with this system to plus or minus 10 per cent.

The mass spectrometer sampling system for the laboratory measurements is very similar in concept to that used for the field measurements as shown in figure 1. It is shown in figure 7.

#### Gamma Ray Analysis of Soil Samples

Soil samples were collected by bagging and labeling approximately one kilogram of soil removed by the 7.6 cm power auger in the process of drilling holes for planting the MERAC's. These samples were sealed in cans containing 130-150 gms, measuring 7.6 cm diameter by 2.5 cm thick. The sealing in cans and the subsequent gamma-ray analyses were performed by Geolabs division of Natural Resources Laboratory of Golden, Colorado.

The gamma-ray analysis is performed about 20 days after sealing the soil in the can. This allows the radon gas generated by radium-226 in the soil to come to secular equilibrium with its parent radium since this corresponds to about five half-lives of the radon-222. The specific gamma rays used to identify the uranium-238 series are emitted by bismuth-214, one of the products in the rapid radioactive decay chain following the radon decay. Therefore, this method, in effect, measures the radium in the soil from which the uranium is inferred on the assumption that the radium with its 1620 year half-life has remained associated with the uranium and is, therefore, in secular equilibrium with it.

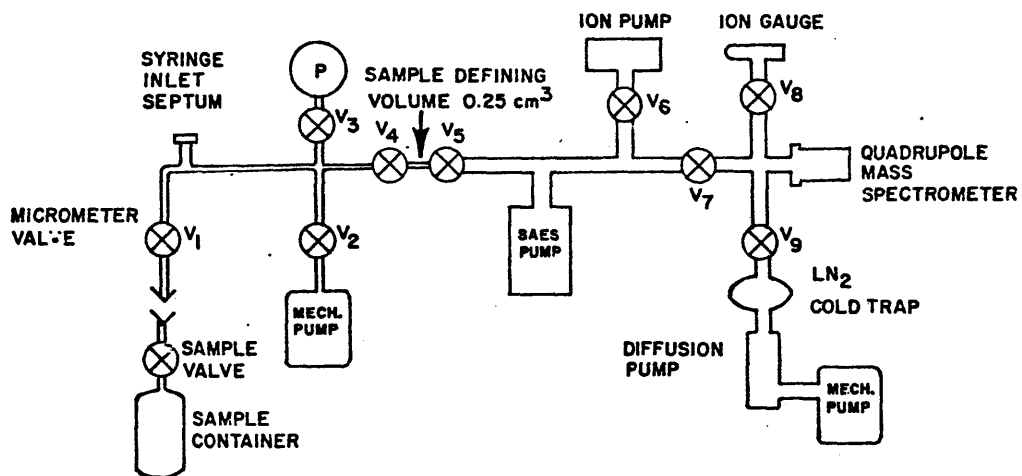


Figure 7. Schematic diagram of mass spectrometer system for noble gas measurements.

The concentration of thorium is deduced from a measurement of the gamma activity of thallium-208 which is in the thorium decay series. This series also has a gaseous link in the series (thoron or radon-220) which requires establishment of secular equilibrium after the can is sealed. However, the thoron half-life is only 56 seconds and therefore, the determining half-life for establishment of secular equilibrium in this case is the longest lived intermediary product in the decay chain between radon-220 and thallium-208. This is the 10.6 hour half-life of lead-212. This is still short compared to the 3.83 day half-life of radon-222 and therefore, the 20 day waiting period for allowing secular equilibrium in the uranium decay series is more than adequate for establishment of secular equilibrium in the radium-224 decay series.

The gamma-ray spectrometer system uses a 7.6 cm x 7.6 cm NaI (Tl) scintillation counter in four-inch thick lead shielding. The total background counting rate in the uranium channels is five counts per minute. The measurements were made in 10-minute runs for a precision of plus or minus two parts per million. A calculator program was used to correct for background, thorium interference in uranium analysis, and uranium interference in thorium analysis, and uranium and thorium interference in potassium analysis, mass of sample, geometry of sample, and counting time to give the results in ppm of uranium and thorium. A primary sample calibrated at New Brunswick laboratory was used for reference.

## PRELIMINARY INSTRUMENT PERFORMANCE TESTS

### Idaho Springs Geothermal Test

Initial instrument performance tests were conducted at the site of a hot springs area at Idaho Springs, Colorado. A total of 45 soil-gas samples were collected from three sites, a hot spring (40°C), a warm water seep (26°C) and near Soda Creek. The 60 cm probe samples showed helium-4 concentrations in soil gas ranging from five to seven parts per million at the warm seep, 5.3 parts per million in the vicinity of Soda Creek and up to eight parts per million at the hot spring. Figure 8 shows the decrease in solubility of helium-4 up to 60 degrees Celsius (Cook, 1961). This does not explain the increased helium-4 concentration in the warm and hot springs. This increase is probably related to the depth of the source for the warm and hot water which would encourage supersaturation. Instantaneous syringe probe samples collected at each site showed a reproducibility within plus or minus five per cent. The variation was probably due to depletion of helium relative to the other soil gases with each successive sample. This is accomplished by preferential migration of helium into the probe and subsequent depletion of the surrounding soil.

### Turkey Creek Uranium Test

A brief orientation traverse was conducted across the small secondary uranium deposit (approximately seven meters across) in the Dakota Sandstone at the Turkey Creek roadcut south of Morrison,



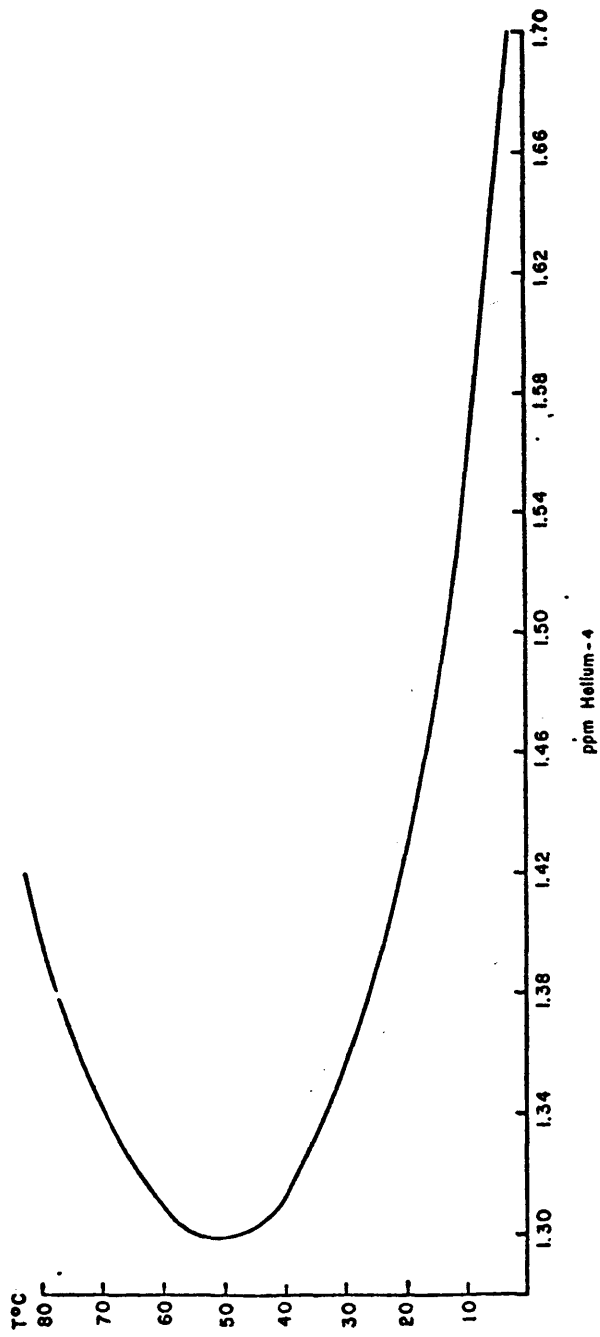


Figure 8. Solubility of helium in water versus temperature (after Cook, 1961).

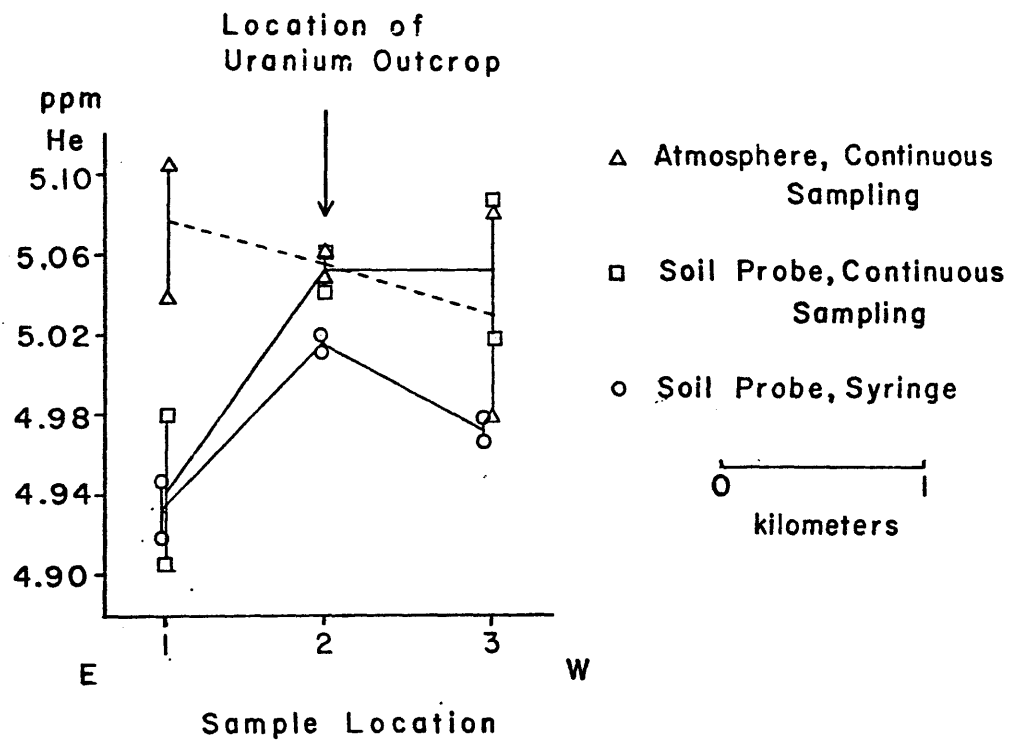


Figure 9. Reproducibility test of helium concentration measurements, Turkey Creek roadcut, Jefferson County.

Colorado. This traverse (figure 9) conducted during daylight hours, showed that the helium-4 concentration in the soil gas measured by the syringe sampling method (4.92 to 5.02 ppm) was everywhere lower than in the atmosphere measured by continuous sampling (4.98 to 5.10 ppm). These data also showed that repeat soil gas measurements using the syringe sampling method were more reproducible than the continuous sampling data. An increase in soil gas helium concentration was detected along the growth fault in the area of uranium mineralization exposed in the south roadcut at Turkey Creek. This increase is attributed to helium migration along the fault rather than as a result of the surficial uranium deposit.

## POWDER RIVER BASIN, WYOMING

General Geology

Extensive test work was conducted in the Powder River Basin, Wyoming from June 29 to September 4, 1976. This area was chosen primarily for its simple geologic structure with no known faulting in the area and an overburden of primarily mudstone and arkosic sandstone. There were no known stratigraphic factors either above or below these uranium deposits which would adversely affect the helium-4 concentration.

The Fort Union Formation of Paleocene Age overlies, generally conformably, the Lance Formation of late Cretaceous Age. The Fort Union ranges in thickness from 900 to 1,160 meters (Hagmaier, 1971). The Fort Union is composed principally of non-marine carbonaceous mudstones and thin lenticular sandstones and lignite beds. Locally, however, several thick sandstones occur in the Fort Union in the Southern Powder River Basin. The sediments are considered to be derived from the Mesozoic and Paleozoic rocks that covered the basin (figure 10).

The Fort Union Formation locally contains three distinct sedimentary facies: a sandstone facies, a siltstone-claystone facies, and a lignite-claystone facies. All of these intertongue with one another (Hagmaier, 1971).

The sandstone facies consists of medium to fine-grained, well-rounded sand. Subangular sand occurs locally in the uppermost part of the formation in the southern end of the basin. This facies is

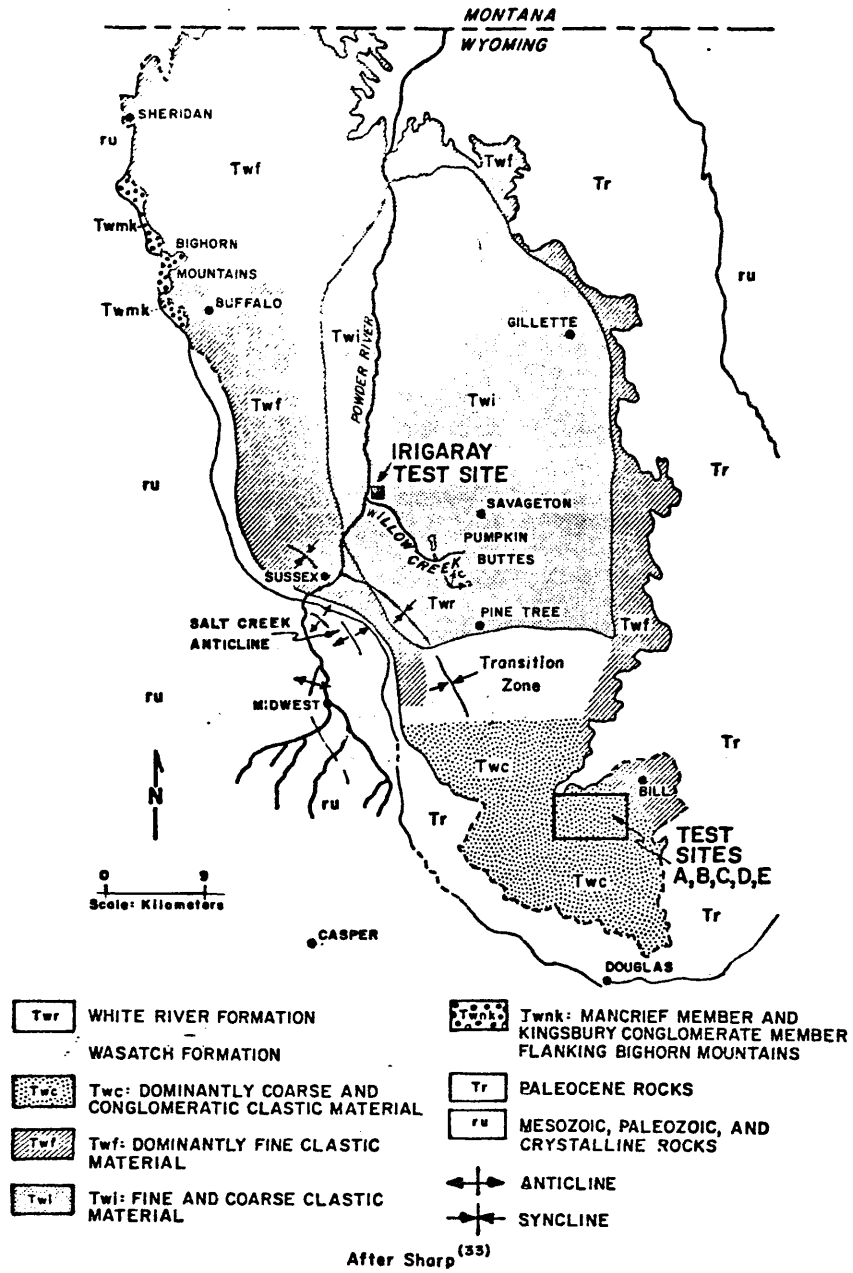


Figure 10. Distribution of facies within the Wasatch Formation in the Powder River Basin.

interpreted (Hagmaier, 1971) to be the fluvial channel deposit of high-discharge perennial rivers. Most of the sediment was transported as bed load and deposited in point bars and channel bars.

The siltstone-claystone facies consists of clayey silt with minor amounts of sandy silt and in some places silty sand. Poorly preserved organic material is commonly found within this unit. This facies is interpreted (Hagmaier, 1971) to be sediments deposited on river levees and flood plains.

The lignite-claystone facies consists of lignite, carbonaceous and variegated claystone. It is interpreted to be flood basin sediments deposited between the meander belts of the major rivers draining the area.

Throughout most of the Powder River Basin the Wasatch Formation, of Eocene Age, unconformably overlies the Fort Union Formation (figure 10). The Wasatch ranges in thickness from 90 to 300 meters, thickening toward the center of the basin. The Wasatch Formation is thought to be derived primarily from the igneous rocks exposed around the margins of the basin that were uplifted as a result of the Laramide Orogeny (Hagmaier, 1971).

The sediments of the Wasatch may be divided into three sedimentary facies (Hagmaier, 1971; Sharp, 1964). All of these facies intertongue with one another locally and on a regional scale. Montmorillonite clay is common in all of the facies and is probably derived from alteration and devitrification of volcanic ash.

The sandstone facies consists (Hagmaier, 1971) of angular to subangular coarse-grained arkoses in the Southern Powder River Basin and become gradually finer and more rounded in the northern part of

the basin. The sandstones are generally concentrated in a north-south band coincident with an early Eocene depositional low area and synclinal axis of the basin, so that regionally the sandstones change facies to mudstones laterally to the east and west from the basin center. This regional pattern of facies change within the Wasatch is illustrated in figure 10. Plant fragments and organic material are abundant in the sandstone facies. This facies is interpreted (Hagmaier, 1971) as being composed of fluvial channel deposits of perennial meandering rivers. Most of the sandstones accumulated as channel and point bar deposits.

The siltstone-claystone facies consist of sandy silt and to a lesser extent clayey silt and silty sand. This facies is interpreted (Hagmaier, 1971) as being overbank deposits, i. e., silt and clay accumulated during flooding of the flood plain.

The lignite-claystone facies consists of lignite, carbonaceous claystone, and grey silty claystone. The lignite increases in abundance in the northern part of the basin. It is interpreted (Hagmaier, 1971) as being flood plain and swamp deposits in the lowland areas of the basin.

The Wasatch consists of (Hagmaier, 1971) approximately 45 per cent siltstone and claystone, 45 per cent sandstone, and 10 per cent lignite and claystone in the northern part of the basin. In the southern part, the Wasatch consists of approximately 25 per cent siltstone and claystone, 70 per cent arkosic sandstone, and five per cent lignite and claystone.

The White River Formation of Oligocene Age, unconformably overlies the Wasatch Formation on the Pumpkin Buttes in the center of the basin. The formation consists of coarse-grained stream deposits with significant amounts of devitrified volcanic ash (Hagmaier, 1971).

Based on isolated occurrences of the White River Formation on the margins of the basin, it is thought that the formation once covered the entire basin and was eroded as a result of Late Tertiary uplift.

### Test Site A - Irigaray Ranch

#### Geology and Hydrology

Uranium mineralization at the Irigaray Ranch, locality of Test Site A, occurs in two distinct fluvial channel sequences within the Wasatch Formation. The upper and lower mineralized sandstone sequences occur at a depth of 100 and 120 meters respectively. The siltstone-claystone facies predominates above the ore horizons. Lignite and clayey sandstone zones occur to a limited extent. Faulting was not recognized either on the surface or in drill holes. Figure 11 is a fence diagram of the Upper Irigaray Sandstone of Test Site A.

Soil development is minimal and vegetation consists of sagebrush and sparse grasses.

The regional groundwater direction in the Powder River Basin is to the northeast. The local groundwater flow at Test Site A is controlled by the Powder River which causes the groundwater to flow to the west.

#### Measurements of Helium-4 in the Atmosphere and Soil Gas

##### Continuous Profiling

Figure 12 shows the station and traverse locations with respect to the two mineralized rollfronts and the Powder River. The initial





measurements at each location included; (1) helium analysis of a syringe sample taken from a probe inserted 60 cm into the ground, (2) a continuous-pumping sample taken from the same probe as the syringe sample, and (3) a sample (taken by continuous pumping) of the atmosphere at the ground surface.

The northern traverse (figure 12) consisted of 83 stations on a line approximately 15 kilometers long with stations located at 160 meter intervals. During the seven-day period it took to complete the traverse, the air temperature, relative humidity and soil moisture underwent significant variations. The helium in soil gas syringe data collected during this traverse are shown in figure 13. The ends of the error bars represent two syringe measurements at the same location. The point is the average of the two measurements. The syringe helium soil-gas measurements ranged from 4.95 to 5.31 ppm, and the syringe atmosphere samples ranged from 5.04 to 5.30 ppm helium. There was no recognizable increase of helium concentration over the uranium mineralization. Meteorological data (figure 14) were collected simultaneously with the helium samples. There is a slight correlation between relative humidity and helium concentration (as seen by the superposition of the relative humidity data in figure 14). This suggests that meteorological changes occurring during the course of sampling could cause variations in helium-4 concentration which could mask any effect due to the uranium deposit.

The continuous-sampling data collected on this traverse from both the soil probe and the atmosphere (figure 15) show no correlation with the uranium mineralization. The data also show greater fluctuations than recorded with the syringe collection methods.

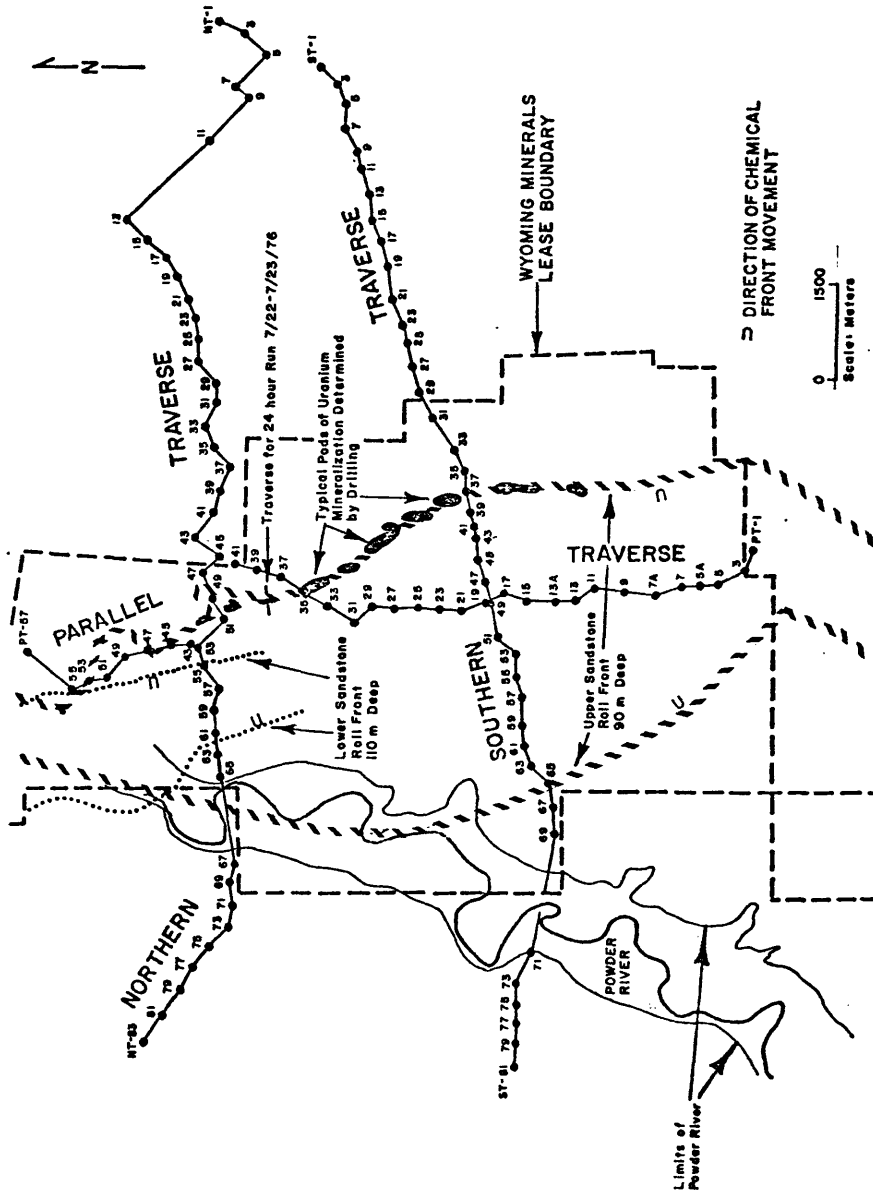


Figure 12. Map of the Irigaray Ranch test site A, showing the uranium roll fronts and the three principal traverses.

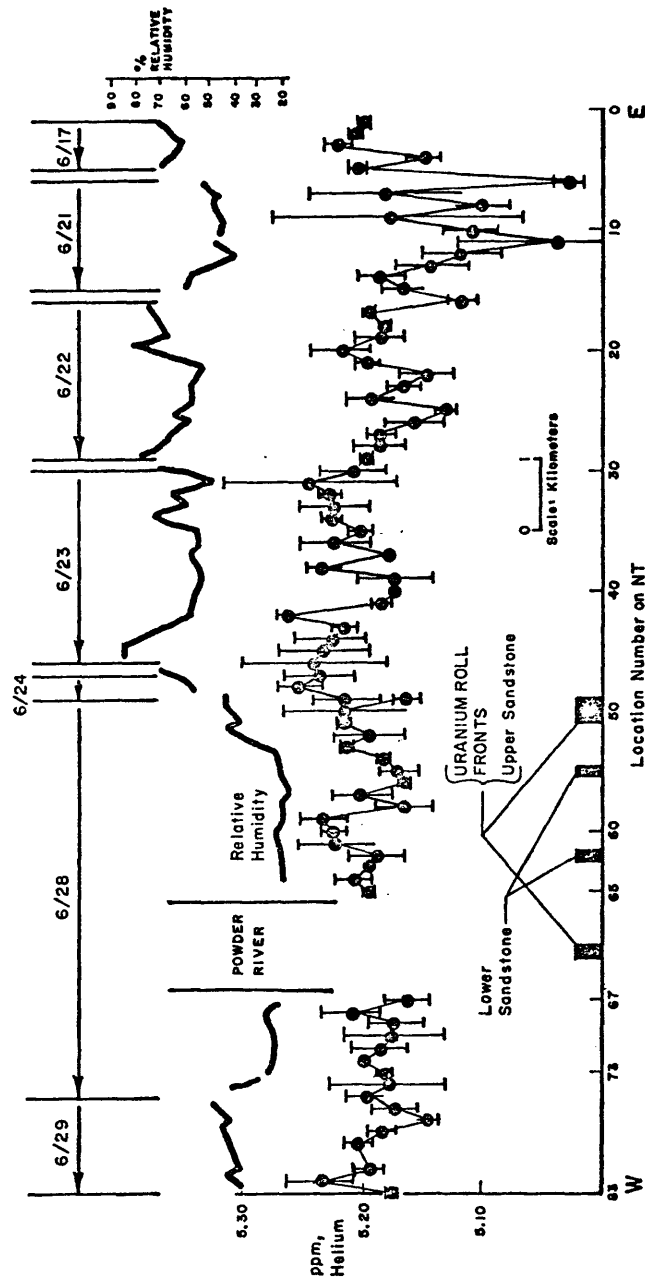


Figure 13. Helium concentration measured in syringe samples taken from 60 cm deep probes on the first run of the northern traverse of the Irigaray Ranch, June 17-29, 1976. Each point is the average of the two measurements. The separate measurements are shown as the ends of the error bars.

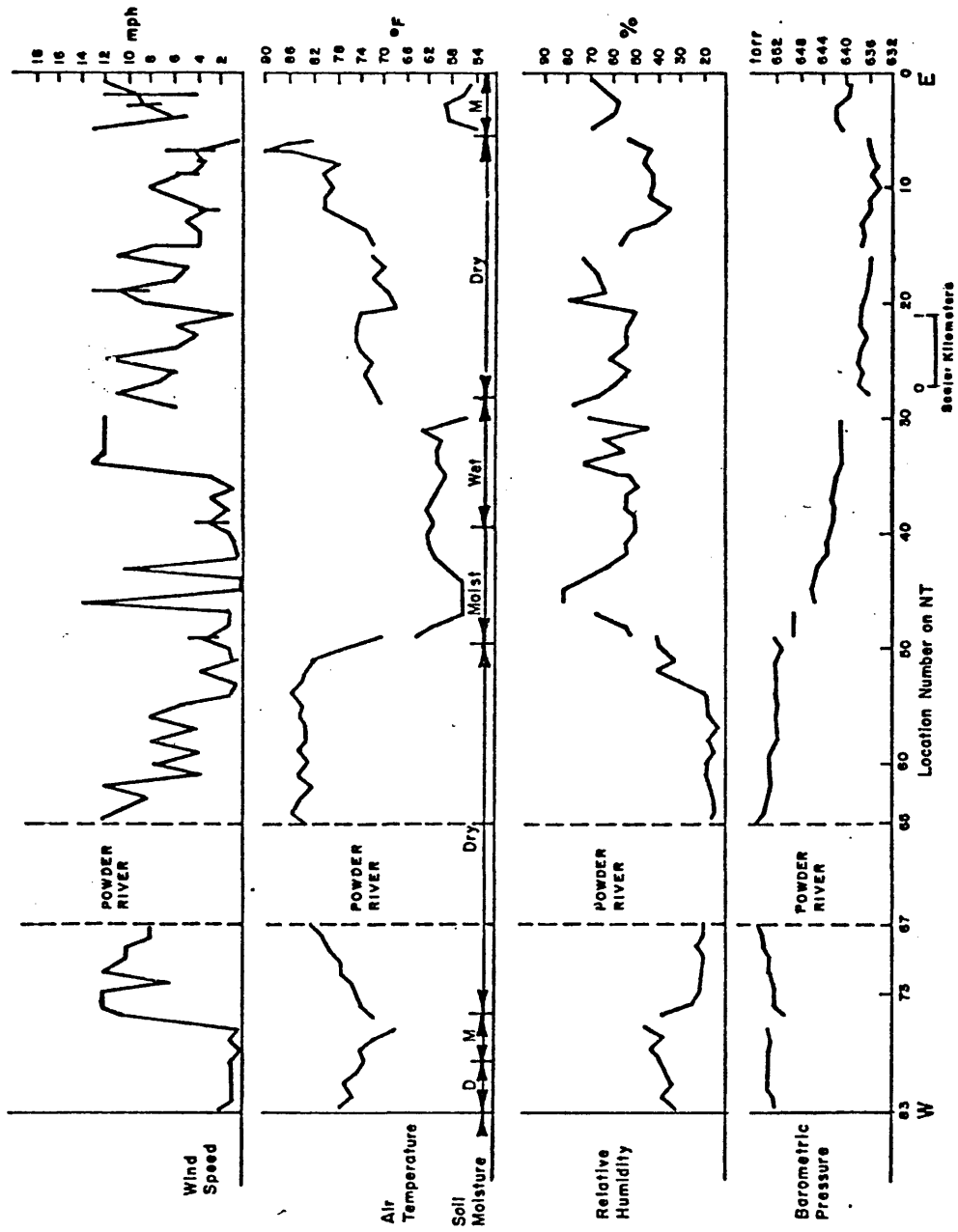


Figure 14. Meteorological data collected simultaneously with the first run on the northern traverse of the Irigaray Ranch, June 17-29, 1976.

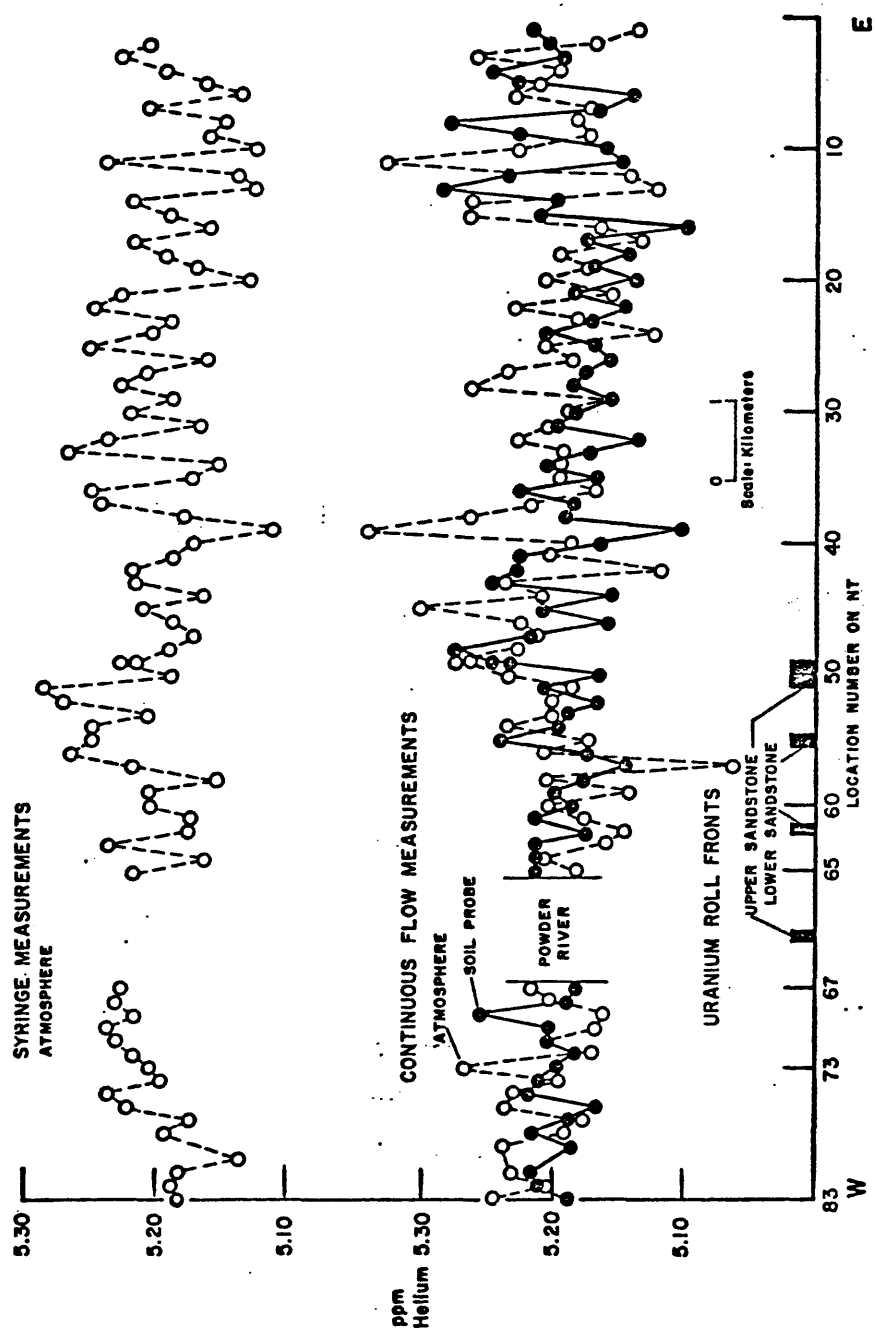


Figure 15. Continuous flow helium measurements from the soil probe and the atmosphere and syringe atmosphere measurements on the first run across the northern traverse of the Irigaray Ranch, June 17-29, 1976.

A second four-day test (6/29 to 7/2/76) across the northern traverse showed helium in soil-gas (syringe samples) values ranging from 5.05 to 5.31 ppm. There was no correlation of the high and low helium-soil-gas concentrations from the first run (6/17 to 6/29/76) on the northern traverse to the second run (6/29 to 7/2/76). The meteorological data collected during this second traverse repeated the minor correlation of the helium content in soil gas with relative humidity that was observed in the earlier test. This is seen by comparing the data on figures 16 and 17.

Meteorological factors have an effect on the helium data that is not easily interpretable. The continuous-pumping method of soil-gas sampling produced measurements which were more erratic and less reproducible than the syringe samples. The continuous-pumping sampling also had the disadvantage of being more time consuming. This resulted in environmental changes on the sample traverse over the duration of collection time. As a result, the continuous-pumping sampling of soil-gas and atmospheric gas was abandoned after the first two runs of the northern traverse.

As a result of the data from the first two runs of the northern traverse, it was decided to sample the traverse again with all samples collected within a few hours to minimize the meteorological variations. Additionally, it became necessary to test the diurnal dependence of the helium concentration of the soil-gas and atmosphere.

#### Syringe Leak Test

Syringe samples were collected across the entire traverse in as short a time as possible, usually within two hours instead of four to

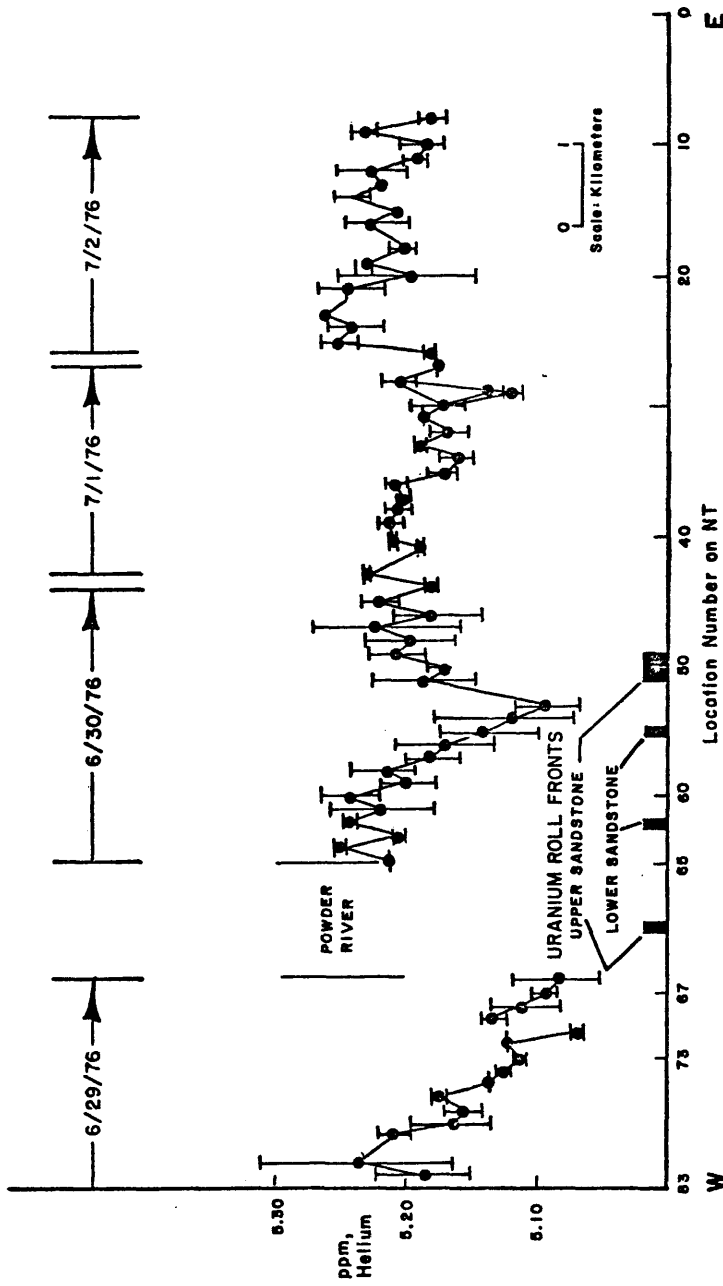


Figure 16. Helium concentration measured in syringe samples taken from 60-cm deep probes on the second run of the northern traverse of the Irigaray Ranch, June 29 - July 2, 1976. The points are averages of two analyses.



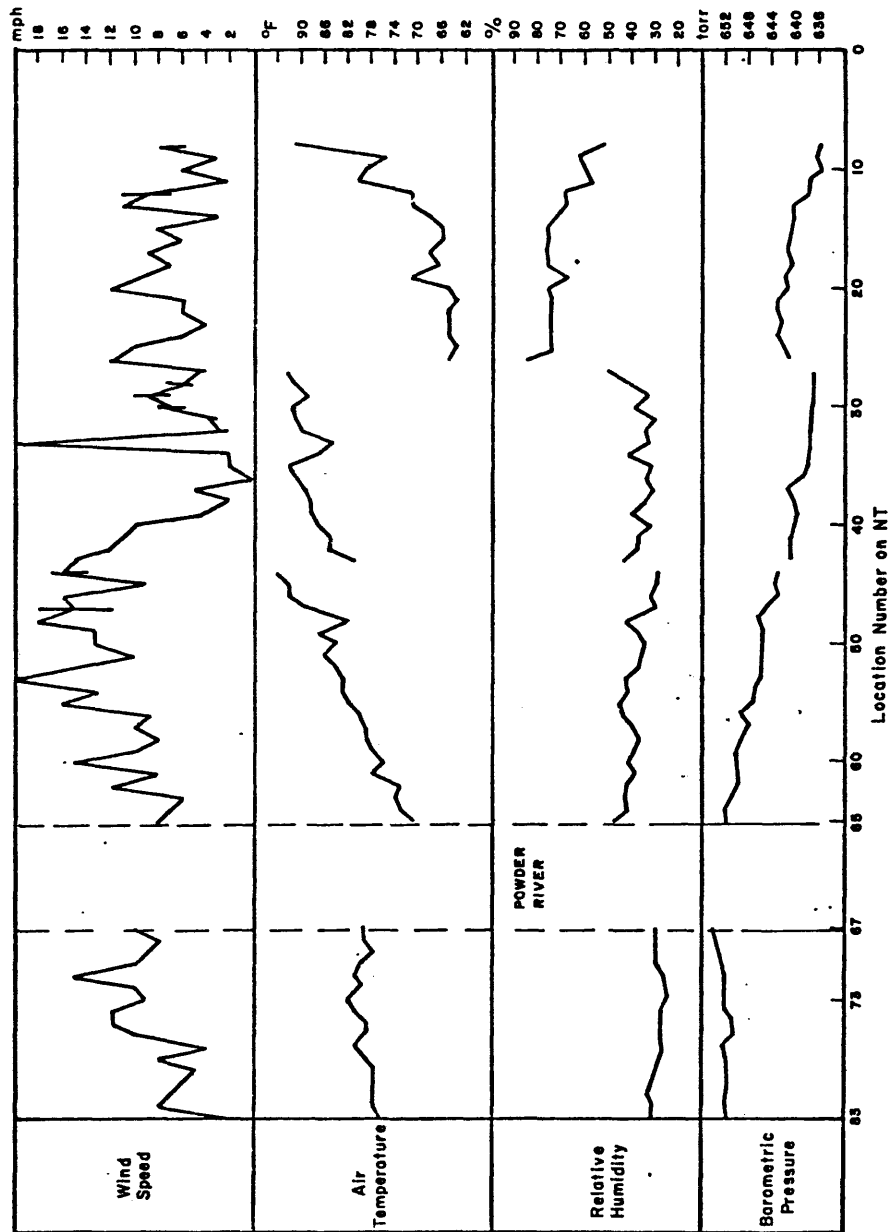


Figure 17. Meteorological data collected simultaneously with the second run on the northern traverse of the Irigaray Ranch.

seven days. The collected samples were then analyzed over a period of five to six hours. To justify holding the samples in the syringes for up to six hours, it was necessary to test the leak rate of the syringes (hospital-grade 20 cc hypodermic syringe and needle). Eighteen syringes were filled with the 7.65 ppm helium reference gas. One of the syringe samples was measured for helium concentration every 20 minutes for a total of six hours. By the end of six hours, the original 7.65 ppm had decreased to 6.95 ppm of helium by diffusion of the helium into the 5.24 ppm helium atmosphere. The leak rate is defined by the per cent decrease in the difference between the sample and the atmosphere. There was a 2.4 ppm differential existing between the syringe and the atmosphere. The leak rate was found to be five per cent per hour (figure 18). Presuming the decrease would be no more than five per cent per hour for lower differentials, holding the syringes for six hours after the collection of a gas sample will result in analyses that are not substantially different from their initial values. For example, an anomalous 5.35 ppm helium sample would have a differential above the atmosphere (5.24 ppm) of 0.11 ppm. If the syringe is held for six hours, the 30 per cent equilibration would lower the helium concentration 0.03 ppm resulting in a new concentration of 5.32 ppm. This concentration would still be anomalous. Changes due to temperature variations were very minor because the temperature of the truck was relatively constant. In later work, the syringe needles were capped with rubber stoppers resulting in a leak rate of 0.7 per cent of the differential per hour.

This syringe leak test justifies the use of rapidly collected, "instantaneous" profiles whereby soil-gas and atmospheric samples are

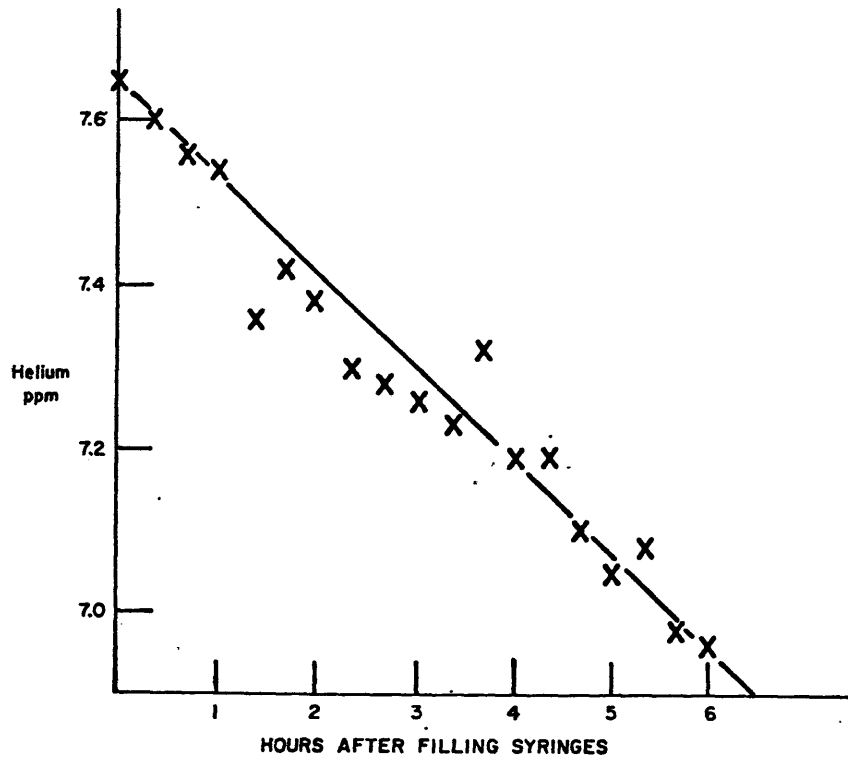


Figure 18. Leak rate measured from 18 syringes filled with R<sub>7</sub> calibration gas, indicating an average leak rate of 5%/hr of the differential helium concentration.

collected in syringes at a site within an hour or two of each other. Thus, the rapidly collected syringe samples minimize the effects of the rapidly changing environmental factors.

#### Helium Variations in a Local Area

Because of the erratic helium concentrations from station-to-station spaced 160 meters apart along the northern traverse, it was decided to examine the detailed helium variations at one station (PT-37, figure 15). Six 60 centimeter probes were inserted 60 cm apart along a line. The probes were left in the ground over a six-hour period and syringe samples were taken from each every hour. Simultaneously, atmospheric helium samples were taken at the location of probe 1 every hour at the ground surface, 15 cm, 30 cm, 60 cm, 90 cm, 120 cm, 150 cm, 180 cm, and 210 cm above the ground surface (figure 19).

As seen in figure 20, all six probes showed a general increase in helium concentration in the soil-gas throughout the 1230 to 1830 hours (7/7/76) duration of the test. The helium concentration, averaged over the six probes, increased from 5.14 ppm at 1230 to 5.24 ppm at 1830.

These data demonstrate that although there were fluctuations from probe to probe, the more significant changes occurred with time. Comparison with the meteorological data collected during the latter part of the test shows an inverse correlation with air temperature (figure 20).

#### Twenty-Four Hour Variations

The data shown in figure 20 strongly suggests that there is a diurnal variation in the concentration of helium in the soil-gas. Therefore, 12 probes were inserted 60 cm into the ground at stations NT-01,

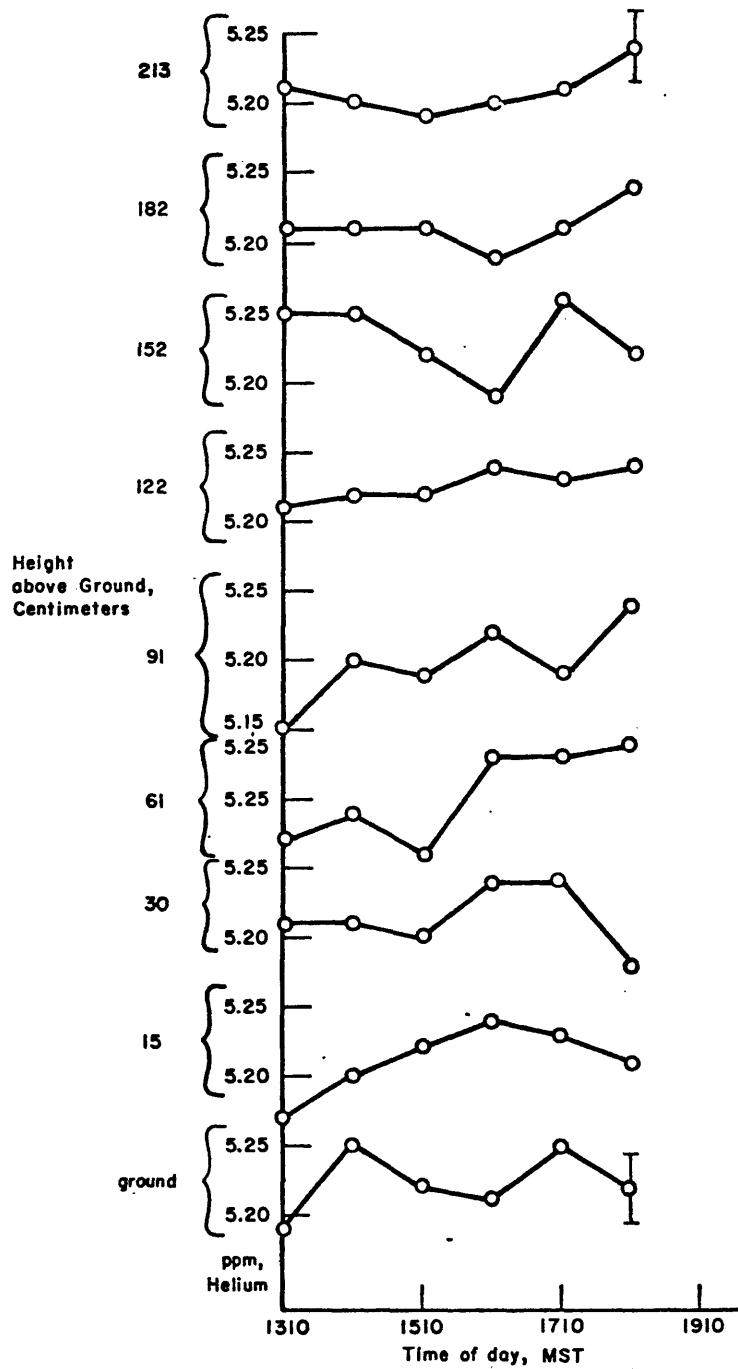


Figure 19. Measurements of helium concentration as a function of time and height above ground surface, July 7, 1976. Error bars denote instrumental accuracy.

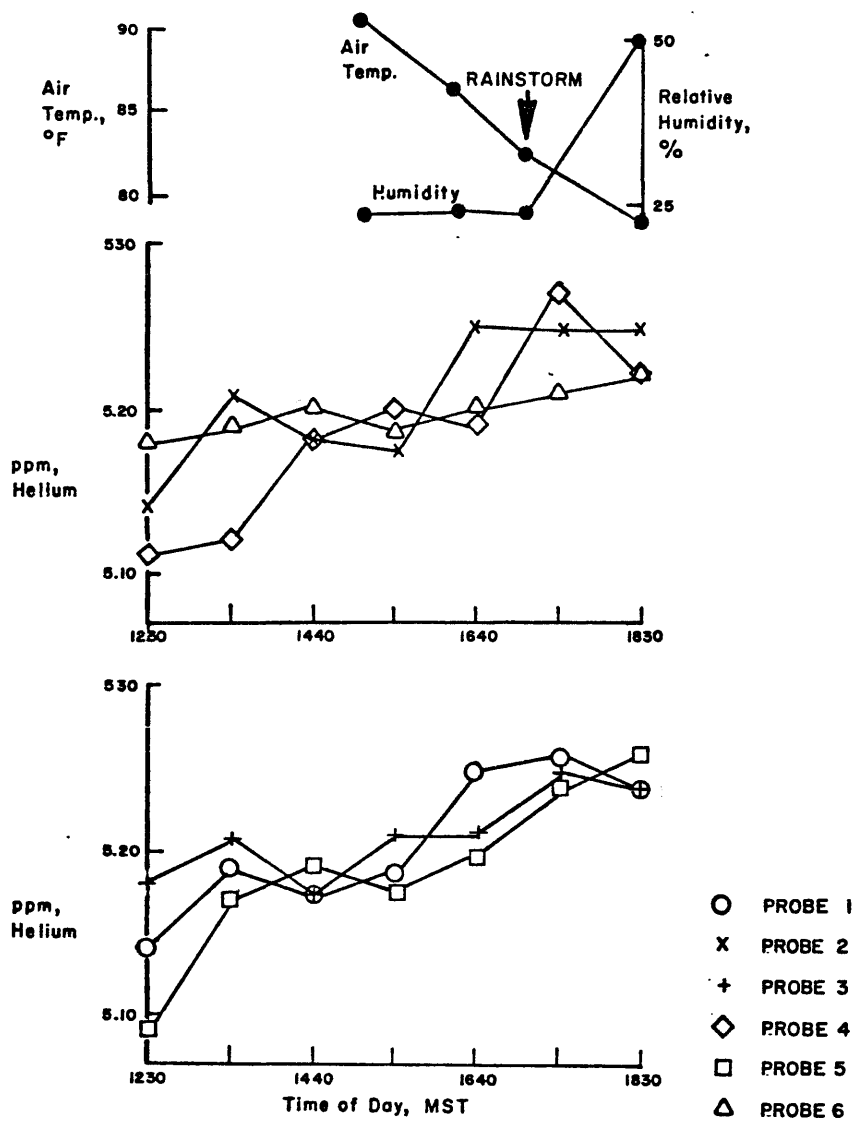


Figure 20. Hourly samples from six probes spaced 60 cm apart at PT-37, July 7, 1976.

-05, -11, -17, -23, -29, -35, -41, -47, -49, -51, and -55 (figure 12). Syringe samples were taken from these probes and from the atmosphere at ground level every two hours for a 24-hour period from 1700, 7/8/76 to 1700, 7/9/76.

The helium concentration in the atmosphere along the traverse varied from 5.15 to 5.32 ppm. All atmospheric stations experienced a 24-hour variation of at least 0.04 ppm and most varied from 0.08 to 0.15 ppm (figures 21 and 22). At any one time, the spread in atmospheric helium concentration measurements was 0.07 to 0.15 ppm. The average atmospheric helium concentration during the 24-hour test for all the sample stations was 5.224 ppm. No systematic atmospheric variations of helium concentration occurred during the 24-hour test, either diurnally or in relation to the buried uranium deposit along the traverse.

The variations of helium concentration in the soil-gas displayed several significant trends. During the daylight hours, the helium concentration of the soil-gas was lower (0.10 to 0.20 ppm) than the concentration in the atmosphere. During the cool hours of the day (generally 2100 to 0700), the helium concentration in the soil-gas increased to or above that of the atmosphere. The most abrupt changes in helium concentration in soil-gas occurred as a decrease from 0700 to 1500 hours (a decrease of as much as 0.16 to 0.18 ppm at several stations), and as an increase from 1500 to 2100 hours (as much as 0.15 to 0.21 ppm).

By 0900, the helium concentration in the soil-gas along the entire length of the traverse had become detectably lower (0.01 ppm or greater) than that of the atmosphere. The difference between the soil-gas and atmospheric concentration increased until 1500 when it began to diminish.

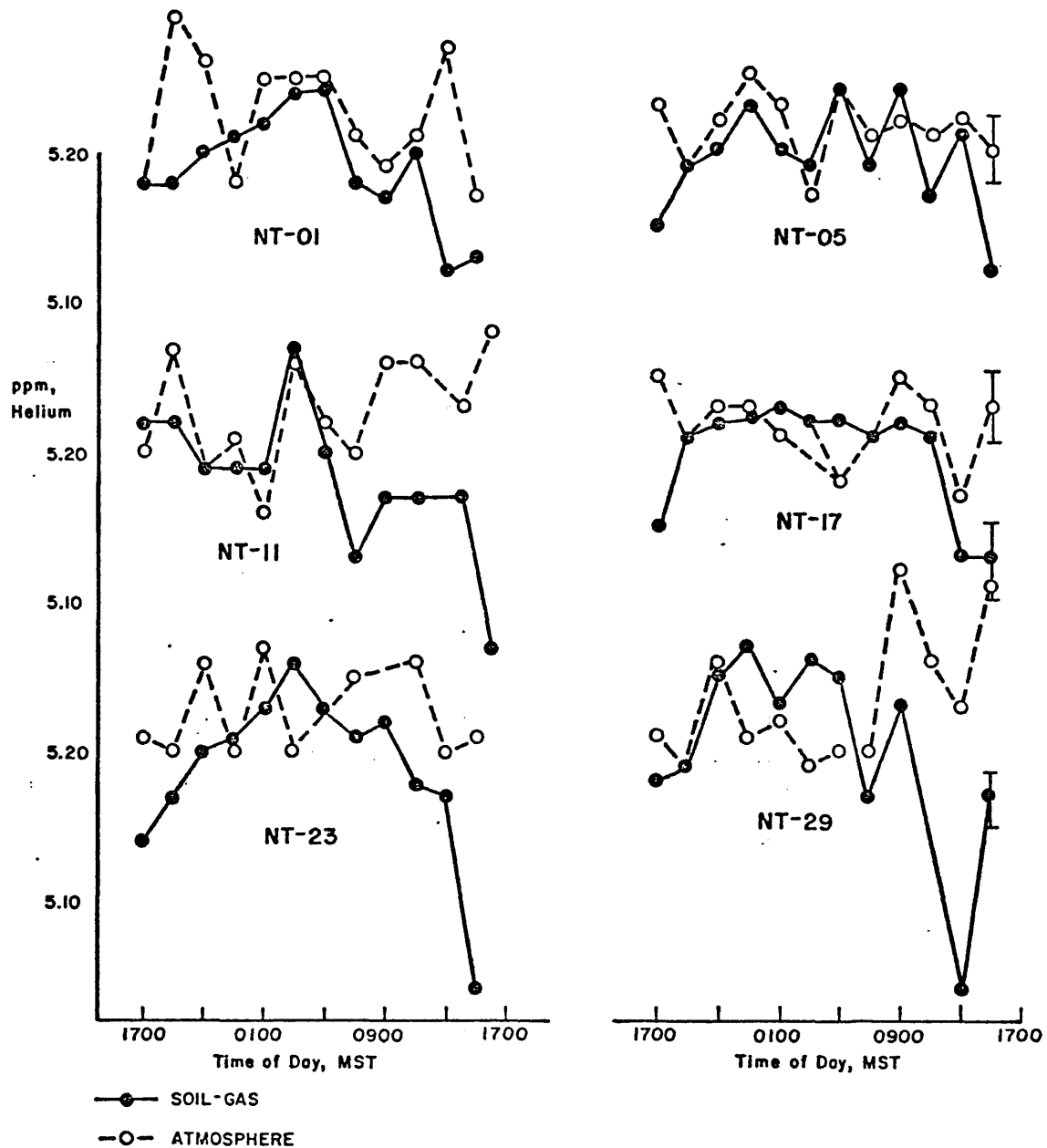


Figure 21. Helium concentration in soil-gas and atmosphere collected over a 24-hour period from northern traverse locations, NT-1, -5, -11, -17, -23 and -29 on 7/8/76 and 7/9/76. Error bars represent the instrument accuracy. MST indicates Mountain Standard Time.



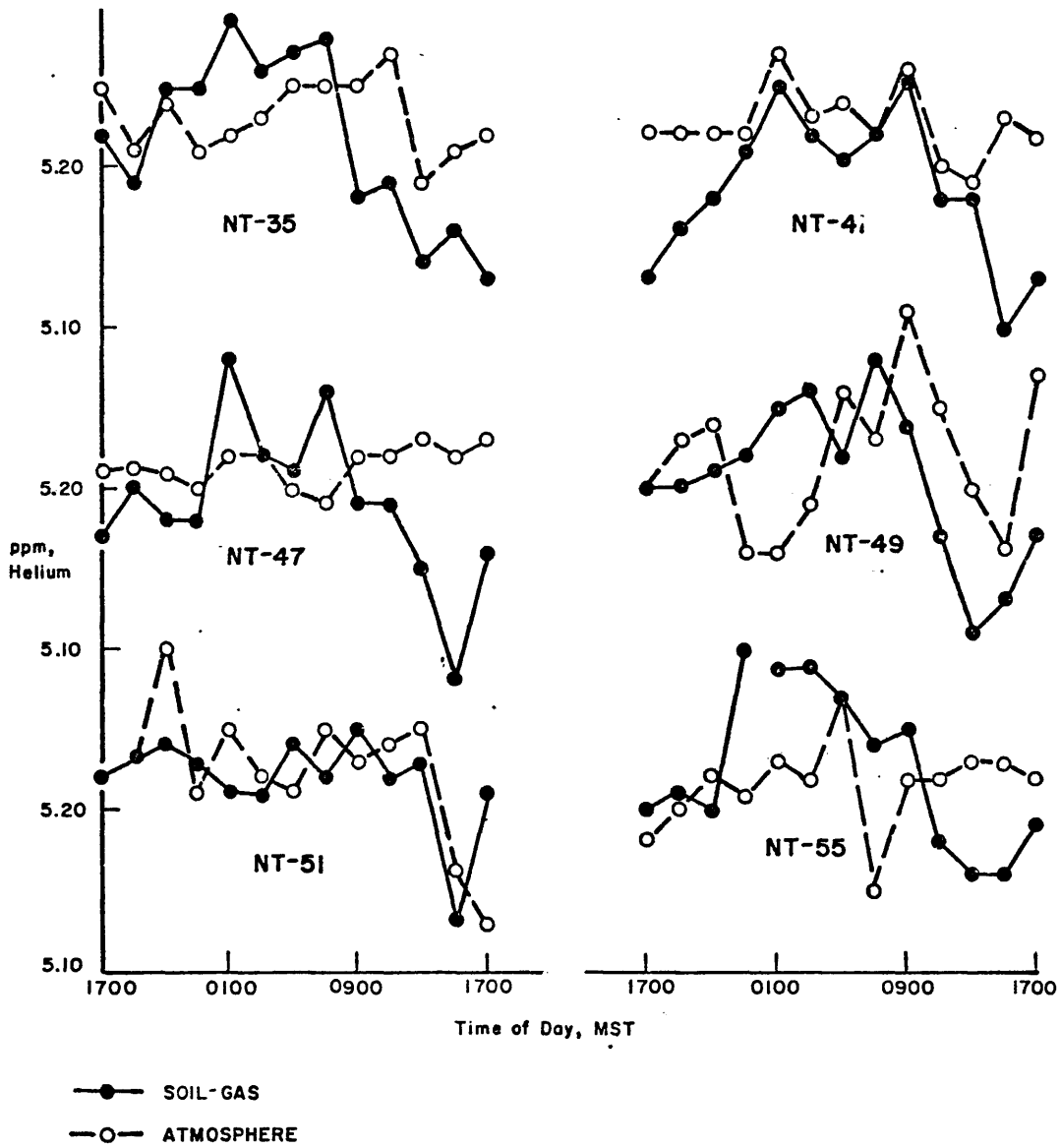


Figure 22. Helium concentration in soil-gas and atmosphere collected over a 24-hour period from northern traverse locations, NT-35, -41, -47, -49, -51 and -55 on 7/8/76 and 7/9/76.

Almost without exception, at each station the diurnal range of soil-gas helium values was greater than the atmospheric range of helium. However, the instantaneous range of helium in the atmosphere was often greater than the instantaneous range of soil-gas values.

No significant increase in helium concentration seemed to occur that was related to the subsurface uranium deposit.

In an attempt to analyze the data further, the data from five locations, NT-41, -47, -49, -51, and -55, were averaged together as "ore" locations. Data from the other seven locations, NT-1, -5, -11, -17, -23, -29, and -35, were averaged as "background" locations (figure 23).

The data clearly indicate a diurnal trend in the helium concentration in the soil-gas with a maximum in the early morning hours and a minimum around mid-afternoon. This was observed over the background as well as over the ore. The error bars shown on two of the points illustrate typical statistical fluctuations. This shows that the diurnal trend is significant in the soil-gas. The atmosphere does not show this trend. In addition, there is a marginal increase in helium in the soil above the ore compared with the background region.

The 24-hour test indicated that the environmental factors and time of day were extremely critical to the helium concentration measurements in the soil-gas at every locality. The strong decrease in soil-gas helium concentration during the daylight hours suggests the possible importance of: (a) soil-gas moisture variations related to temperature changes (figure 23); or (b) plant respiration or decay generating carbon dioxide, methane, ammonia or other gases which would have the effect of diluting the helium concentration diurnally. In

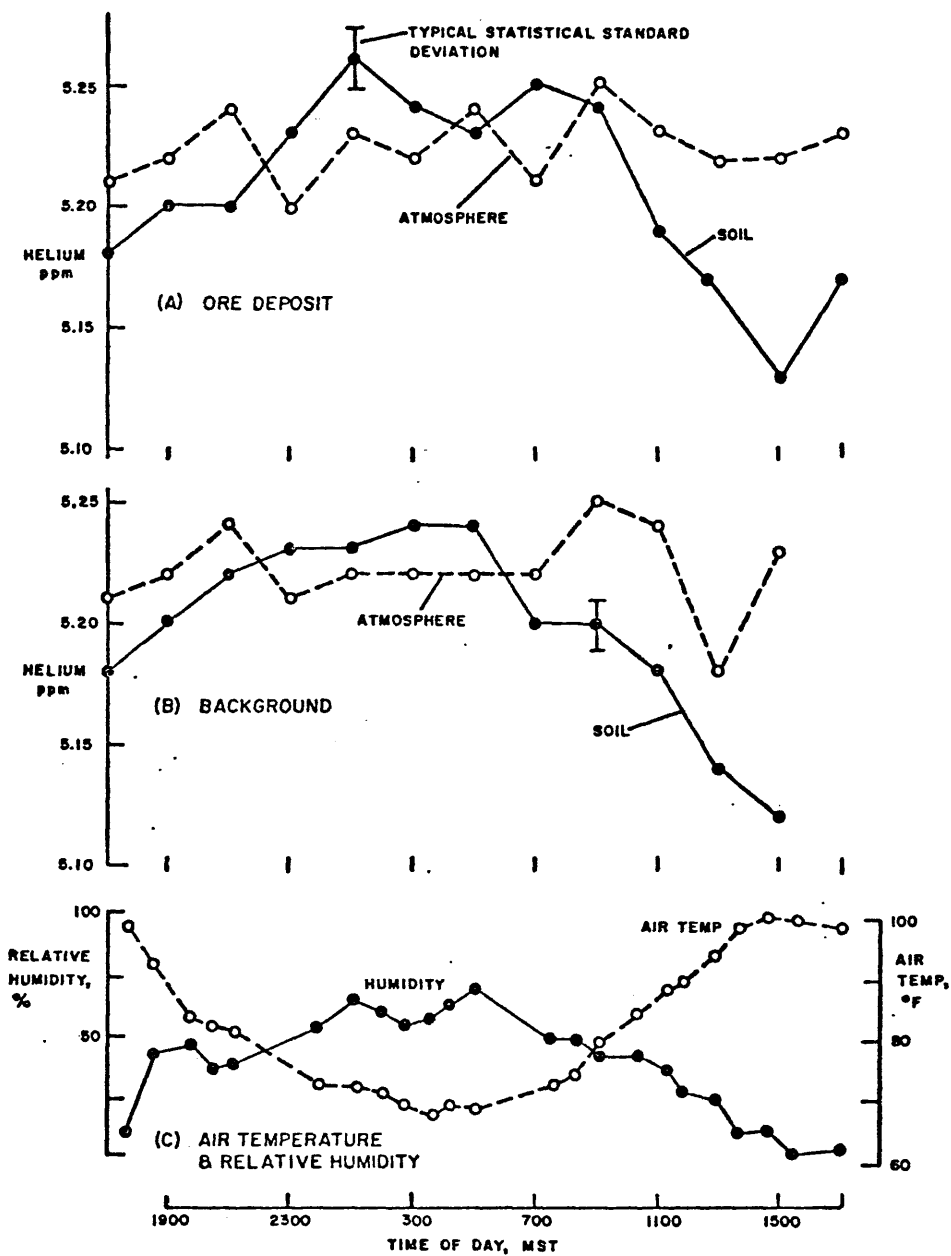


Figure 23. Twenty-four-hour run, July 8-9, 1976, across NT, average over locations NT-41, -47, -49, -51 and -55 over the "ore" deposit (a) and over locations NT-1, -5, -11, -17, -23, -29 and -35 over the background region (b). The corresponding air temperature and relative humidity taken at location NT-35 (c).

comparing the helium data with the air temperature, there seems to be a fairly strong inverse correlation. A possible mechanism causing this would be condensation of soil moisture in the upper portion of the probe which extends above the ground and is at air temperature. The cooler the air, the less moisture would remain in the soil-gas sample and the less dilution of helium concentration would occur. Thus, at the cooler temperature the helium concentration would appear higher, but the actual helium content in the soil-gas would not vary as much as it appears to vary.

#### Instantaneous Traverses

Six "instantaneous" traverses were conducted on the northern traverse with a station spacing of 160 meters. The surveys were conducted principally in the early morning (0330 to 0530) and mid-morning (0800 to 1100) hours of the day in attempts to gather data before the daytime heating caused the helium concentration measured in the soil gas to decrease. The two early-morning (0300 to 0530) traverses, on July 16 and July 21, 1976 (figure 24) show the greatest positive differential ( $\text{He}_{\text{sg}} - \text{He}_{\text{atm}}$ ) between the helium concentration in the soil-gas and atmosphere and the highest absolute helium soil-gas concentration along the entire length of the traverse of all the runs. The July 16 early-morning survey shows a greater positive differential ( $\text{He}_{\text{sg}} - \text{He}_{\text{atm}}$ ) and absolute helium concentration in soil-gas than the July 21 early-morning survey. This decrease in helium in soil-gas with the passage of days (at the same time of day) probably is related to the long-term drying out of the soil that occurred during this period.

The difference between soil-gas and atmospheric helium concentrations for the July 16 data (figure 24) are clearly indicated by

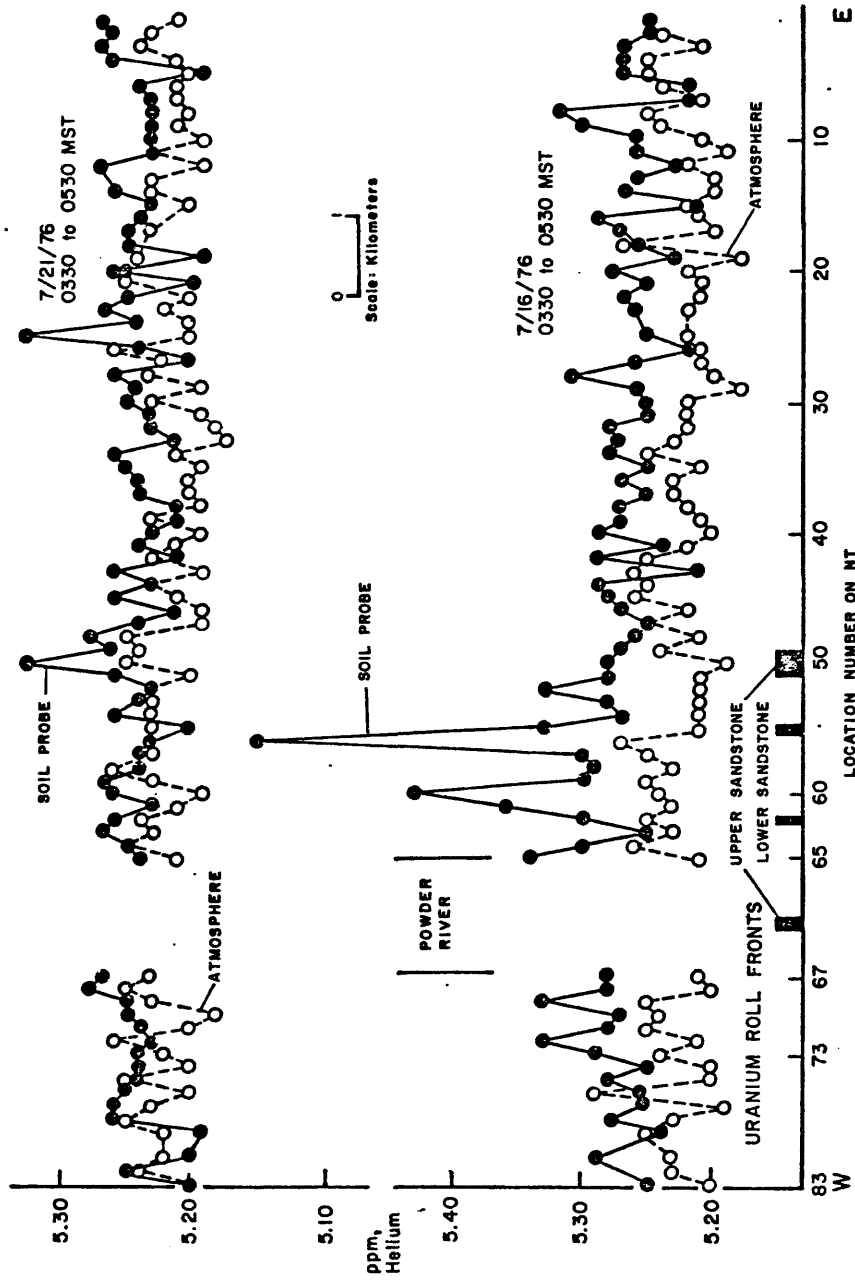


Figure 24. Helium concentration on northern traverse on early morning runs, Irigaray Ranch.

the comparison of the averaged data in table 2. This illustrates the statistical significance of the ( $\text{He}_{\text{sg}} - \text{He}_{\text{atm}}$ ) differential and the higher helium concentration in soil gas over the ore.

Table 2. ( $\text{He}_{\text{sg}} - \text{He}_{\text{atm}}$ ) Differential from 7/16/76 Survey  
Irigaray Ranch

Stations Averaged	Soil-gas	Atmosphere	Differential
NT-67 - 83 (Background)	$5.276 \pm 0.007$	$5.239 \pm 0.012$	$0.037 \pm 0.014$
NT-45 - 65 (Area of Ore)	$5.321 \pm 0.012$	$5.232 \pm 0.004$	$0.089 \pm 0.013$
NT-1 - 44 (Background)	$5.252 \pm 0.004$	$5.220 \pm 0.001$	$0.032 \pm 0.005$

The midmorning (0800 to 1100) runs were conducted on July 14, 15, and 20, 1976 (figure 25). The helium concentration in the soil-gas on all three surveys was generally equal to or slightly higher than the helium in atmosphere for the entire length of the traverse. The absolute helium in soil-gas values were approximately in the same range for these surveys.

The one afternoon traverse (1200 to 1600, July 8, 1976, figure 26) obtained lower helium in soil-gas values than any of the early morning or mid-morning surveys.

The average helium-in-soil-gas concentrations along the entire northern traverse are summarized in table 3. These averages again demonstrate the diurnal effect in that the highest values are from the two early morning surveys, lower values from the three mid-morning surveys and the lowest value from the midafternoon survey.

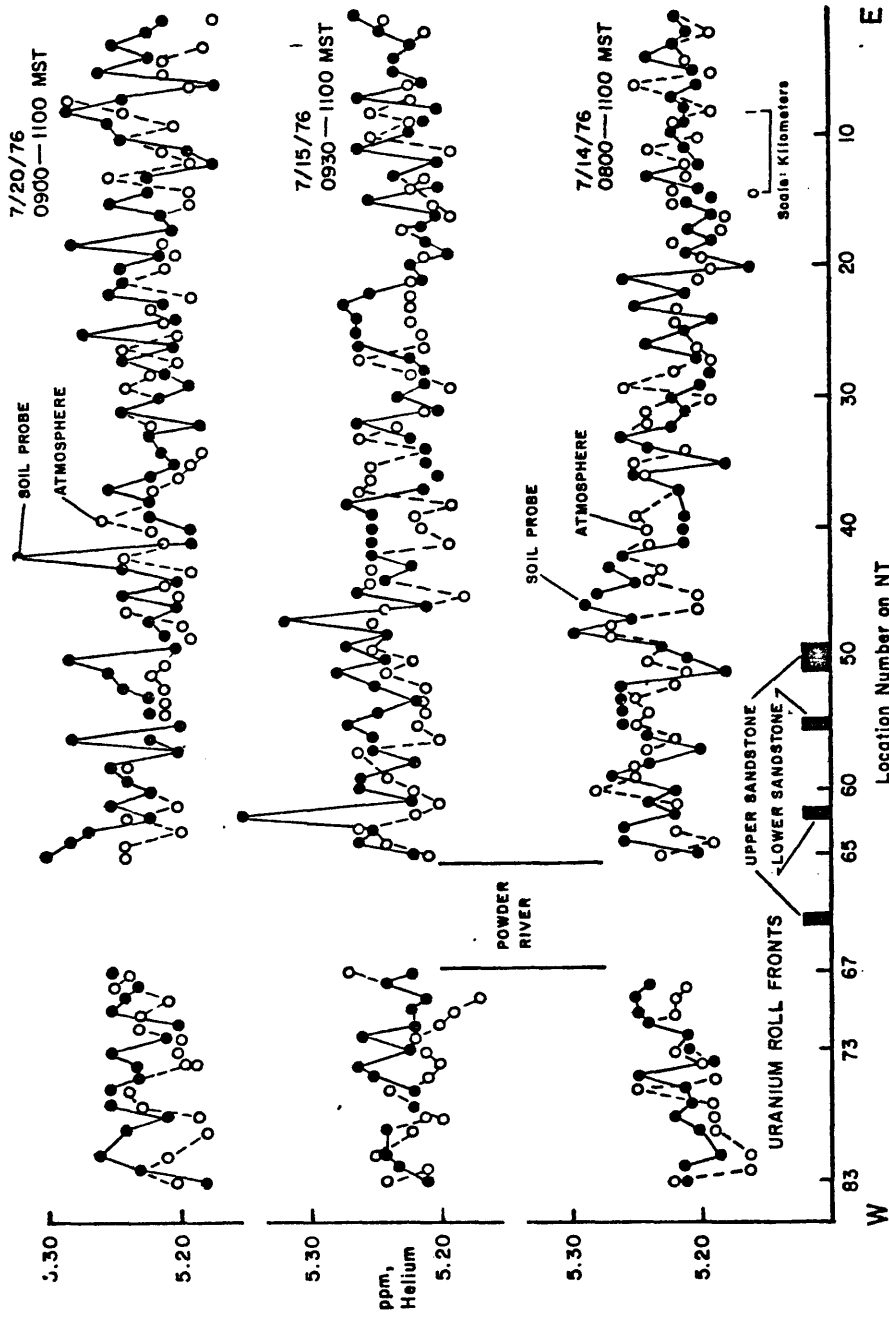


Figure 25. Helium concentration on northern traverse on mid-morning runs, Irigaray Ranch.

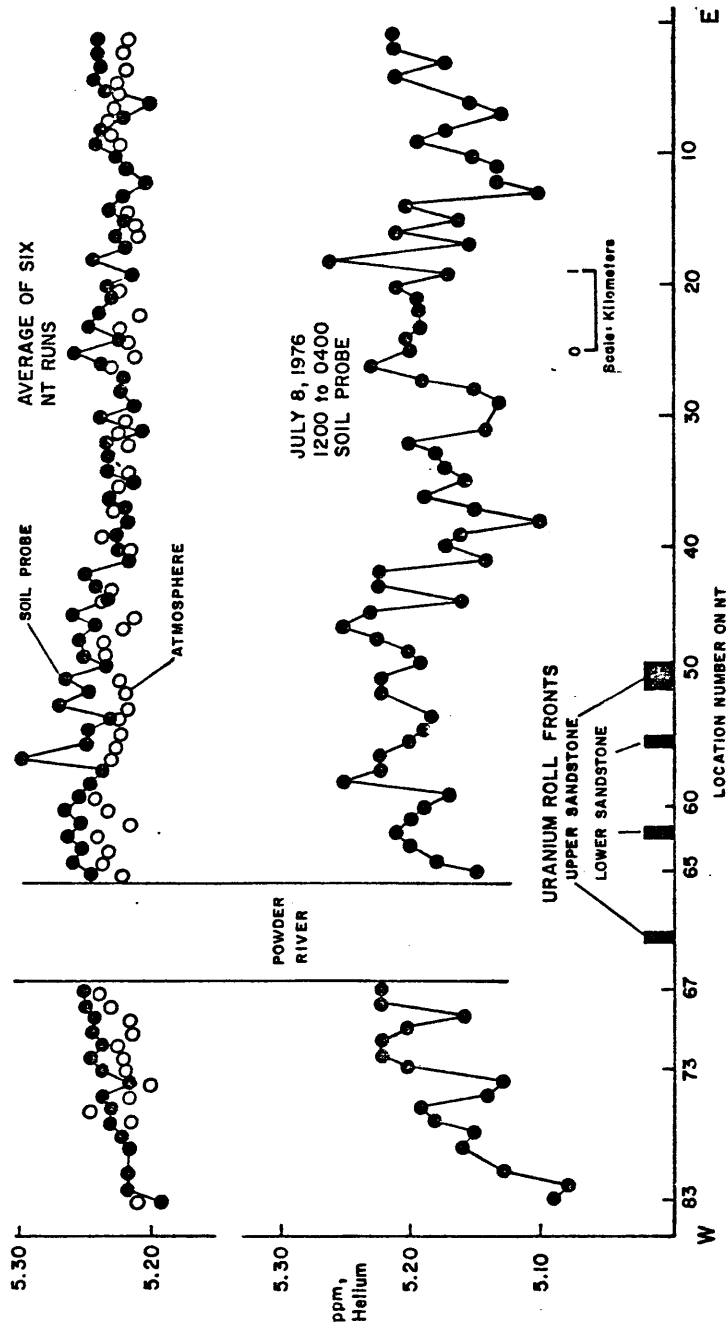


Figure 26. Helium concentration in soil-gas on northern traverse on afternoon run and averaged values of helium in soil-gas and atmosphere for all six NT "instantaneous traverses", Irigaray Ranch.



Table 3. Average Helium Concentrations, Irigaray Ranch

Date	Time	Average He in Soil-Gas (entire traverse) ppm
7/16/76	0330 to 0500	5.27
7/21/76	0330 to 0500	5.24
7/14/76	0800 to 1000	5.22
7/15/76	0930 to 1100	5.23
7/20/76	0900 to 1100	5.23
7/ 8/76	1200 to 1600	5.17

The data obtained on the July 8 afternoon (1200 to 1600), the July 14 mid-morning (0800 to 1000), the July 15 mid-morning (0930 to 1100), and the July 16 early morning (0330 to 0530) surveys show broad, umbrella-like, helium in soil-gas enhancement which varies in location from survey to survey. The anomaly was most pronounced for the July 8 afternoon and July 16 early morning surveys. The drying out of the soil through July suggests that the moist soil times of the year are the best times to sample soil-gas and detect a helium concentration enhancement.

The upper curves in figure 26 are values of helium in soil-gas and atmosphere averaged over the six northern traverse "instantaneous" sampling surveys shown in figures 24 and 25. As the averaging smooths out the data, the anomalous area over the uranium roll fronts appears more clearly, especially by comparing the soil-gas data to the atmospheric averages in this region. This indicates that an accumulative sampling system may help to define the areas of anomalous helium-in-soil gas.

The amplitude of the helium anomaly (averaged over the entire area of the enhancement) is 0.06 ppm on the early morning July 16 survey; the average background helium concentration was 5.26 ppm and the average anomalous helium concentration was 5.32 ppm, a one per cent anomaly for average values. Individual helium values of more than 5.40 to 5.50 ppm were obtained within the anomalous area. The amplitude of the anomaly decreased after the July 16, 1976 survey.

The "instantaneous" traverse on the southern traverse, conducted at 0900 to 1100 July 13, 1976, showed a helium in soil-gas concentration equal to or slightly greater than the atmosphere, but no clear anomaly related to the subsurface uranium deposits (figure 27).

#### Detailed 24-Hour Test

Because the grade, thickness, and continuity of uranium mineralization is not very great or well defined by drilling along the northern traverse, it was decided to test a traverse across the area of the eastern roll front that has a more significant uranium accumulation to see if the helium-in-soil-gas anomaly would be more detectable. The 24-hour test was conducted at background stations NT-17, -23, and -35, and stations 101, 102, 103, 104, 105, 106, 107, 108, and 109 at 30-meter centers above the ore body (figure 12). The test, conducted at 1000 MST, July 23, 1976, shows the diurnal "crossover" of helium in soil gas content with respect to the helium concentration in the atmosphere at most stations (figures 28 and 29).

The measurements from the nine ore zone locations were averaged together to get a 24-hour plot of the soil-gas and atmospheric helium concentration. This is shown in figure 30. Figure 31 shows

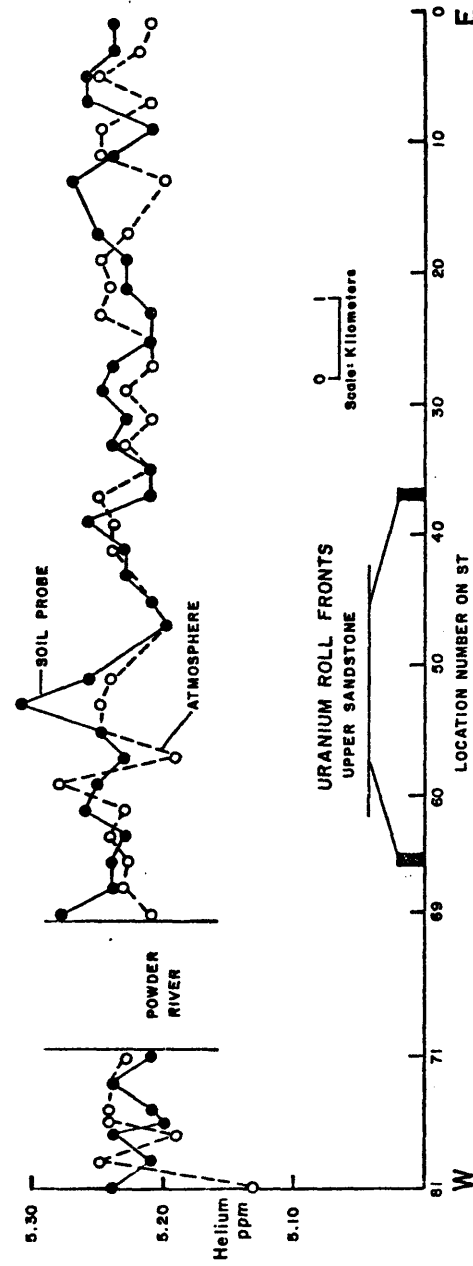


Figure 27. Helium concentrations in soil-gas and atmosphere, southern traverse, Irigaray Ranch, July 13, 1976.

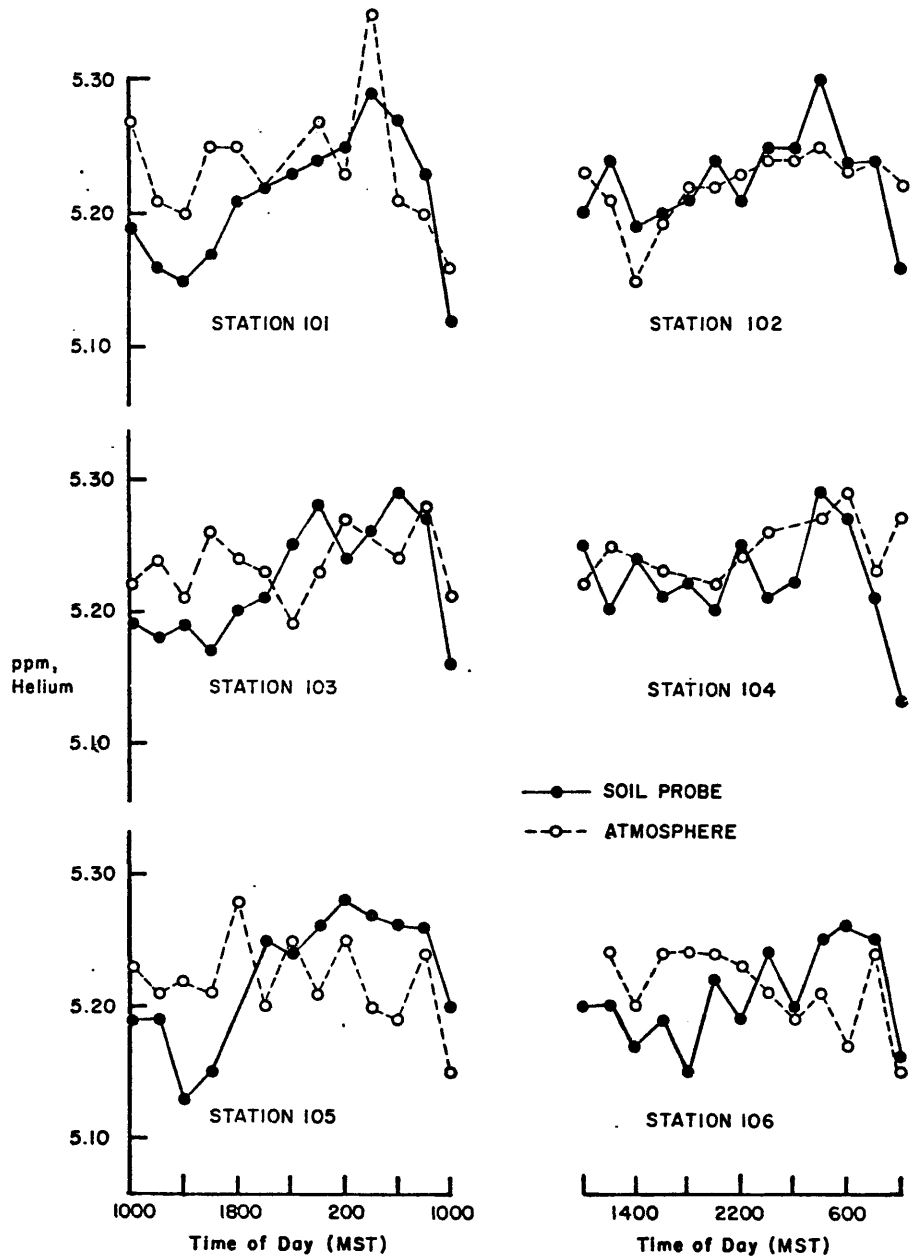


Figure 28. Helium concentrations in soil-gas and atmosphere collected over a 24-hour period from Wyoming Minerals' drill holes, 101, 102, 103, 104, 105 and 106 on July 22-23, 1976, Irigaray Ranch.

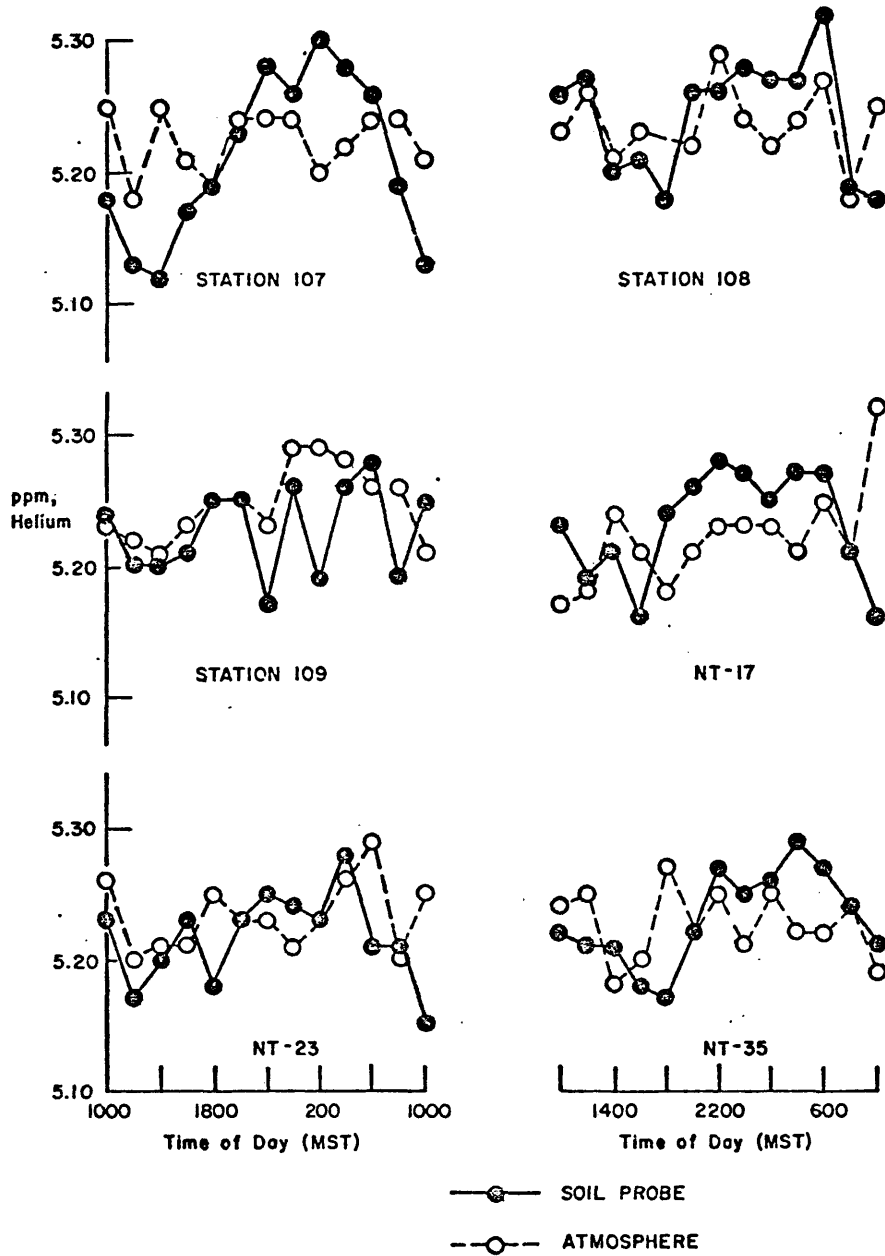


Figure 29. Helium concentrations in soil-gas and atmosphere collected over a 24-hour period from NT-17, -23, -35 and Wyoming Minerals' drill holes 107, 108 and 109, July 22-23, 1976, Irigaray Ranch.

the three background locations plotted for the 24 hours. Typical statistical standard deviations are shown on these graphs. The characteristic diurnal variation is observable. There is a good correlation between humidity and the soil-gas values and a strong inverse correlation between air temperature and soil-gas values. This is shown in figure 32.

The average helium concentration of the atmosphere for all stations ranged from 5.21 to 5.25 ppm. The individual values ranged from 5.15 to 5.35 ppm. The individual helium-in-soil-gas values ranged from 5.12 to 5.32 ppm. There appears to be no anomalous pattern of helium concentration related to the uranium mineralization.

Based on the data that has been accumulated to this point, the single helium traverse has limited applicability in the exploration for buried uranium deposits. The variability in helium concentration from day to day overshadows the helium anomalies that are related to the sub-surface uranium deposit.

### Helium Isotope Ratios

#### Basis of Helium Isotope Differences

The helium isotopes, helium-3 and helium-4, have different sources, so the ratio between the two isotopes can serve as an indicator of the source (Martin and Bergquist, 1977). Both isotopes were present in the primordial earth, and so are contained in the mantle. Since that time, helium-4 has been formed by the alpha-decay of the uranium and thorium series, and helium-3 is the daughter of tritium which is formed in a variety of nuclear interactions both in the atmosphere and in the soil. Helium that reaches the surface of the earth and can be measured

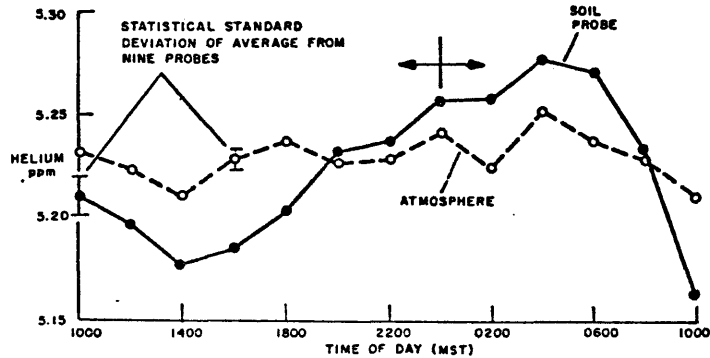


Figure 30.

a. Averages of Locations 101, 102, 103, 104, 105, 106, 107, 108, 109. Spaced 100 feet Apart Across Known Mineralization.

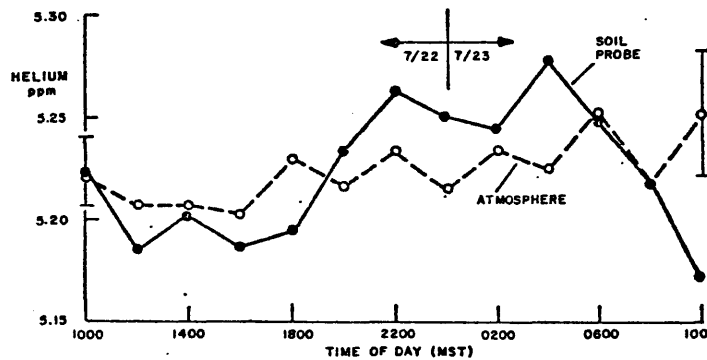


Figure 31.

b. Averages of Locations NI-17, 23, 35 Over Background Region of Northern Traverse.

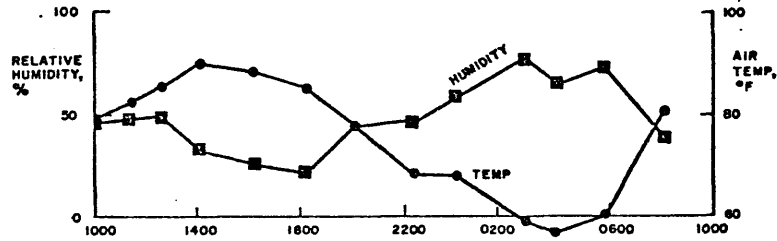


Figure 32.

c. Air Temperature and Relative Humidity during the Traverse.

Twenty-four-hour run on July 22-23, 1976, with closely spaced probes near known uranium mineralization located about one mile south of the northern traverse and crossing the parallel traverse.

in soil-gas is a combination of primordial helium released by the continuous outgassing of the earth's crust and mantle, the helium-4 from decay of the uranium and thorium series in rocks and soil, and any atmospheric component that might have diffused downward from the atmosphere or that might be carried in the groundwater system (Martin and Bergquist, 1977). The  $^3\text{He}/^4\text{He}$  ratio of the mantle is quite high relative to the atmospheric ratio, with values as high as  $1.4 \times 10^{-5}$  in volcanic gases (Naughton, et al., 1973) and hot springs water (Tolstikhin, et al., 1972) related to magma bodies at depth compared to  $1.3 \times 10^{-6}$  for the atmospheric ratio. As the alpha-decay component increases, the  $^3\text{He}/^4\text{He}$  ratio should decrease to well below the atmospheric value (Martin and Bergquist, 1977). Therefore, in a closed system as the uranium and thorium content of the rock increases, the  $^3\text{He}/^4\text{He}$  ratio should show a decrease. The total helium (or helium-4) concentration is subject to a number of uncertainties which should be clarified by measuring the  $^3\text{He}/^4\text{He}$  ratio.

### $^3\text{He}/^4\text{He}$ Measurements in the Vicinity of the Ore Body

The gas samples for the  $^3\text{He}/^4\text{He}$  ratio measurements were collected in pre-evacuated one-liter stainless steel containers from the soil-gas probe or the atmosphere. The gas samples for the  $^3\text{He}/^4\text{He}$  ratio were sent to Dr. David Emerson of the U.S. Bureau of Mines, Amarillo, Texas, Dr. John Lupton of the University of California at San Diego, California, and Dr. W.B. Clarke and Dr. Zafer Top of McMaster University, Hamilton, Ontario. The samples were analyzed by the three laboratories as indicated in table 4. In addition, ten samples collected by Teledyne Isotopes, Inc. were sent to Dr. Emerson's laboratory for helium-3 and helium-4 measurements. As a cross check,



three of these samples were split and sent to both Dr. Lupton's lab and Dr. Emerson's lab. The results are summarized in table 5. Accuracy of relative measurements are quoted at 0.6 per cent for Dr. Lupton, 0.3 per cent for Dr. Clarke, and  $\pm 20$  per cent for absolute helium-3 values and  $\pm 10$  per cent for the relative accuracy of Dr. Emerson's instrument.

The results for the measurements of  $^3\text{He}/^4\text{He}$  in the 46 samples identified in table 4 are given in table 6. The large variations in  $^3\text{He}/^4\text{He}$  ratio in Dr. Emerson's results seem to be related more to the accuracy of the helium-3 measurements rather than the helium-4 concentration. Except for two measurements, the range of helium-4 concentration was only 5.16 to 5.34 ppm (3.4 per cent), whereas the range of helium-3 concentration was 5.9 to 8.1 ppt (31 per cent). The range of  $^3\text{He}/^4\text{He}$  ratios determined by Dr. Lupton and by Dr. Clarke was only 1.232 to 1.415 (13.8 per cent).

Only two points in the soil-gas  $^3\text{He}/^4\text{He}$  data from the 24-hour run on 7/22 to 7/23/76 differed from the standard value of 1.40 by significantly more than the 0.3 per cent accuracy of the Clarke instrument. This demonstrates that the  $^3\text{He}/^4\text{He}$  ratio is essentially free of the diurnal variation seen in the helium-4 field measurements. Figure 33 shows the  $^3\text{He}/^4\text{He}$  ratio compared to the helium-4 field measurements for the 24-hour test. There is no consistency observable from the ratio measurements and the helium-4 measurements. The lowest  $^3\text{He}/^4\text{He}$  measurement, which should correspond to high helium-4 concentration, was at 1200 on 7/22 when the helium-4 field measurement was near its minimum. The two anomalously low values for  $^3\text{He}/^4\text{He}$  seen in figure 33 are not explained. If the helium-3 concentration is constant, this would represent helium-4 concentrations of 5.88 ppm and 5.49 ppm (Martin and Bergquist, 1977).

Table 4. Soil-Gas and Atmosphere Samples Collected for  $^3\text{He}/^4\text{He}$ ,  
Irigaray Ranch

Sampling Location	Sampling Date	Analysis by	Sampling Location	Sampling Date-Time	Analysis by
NT-07	6/21	DE (2)	104 Soil	7/22-1030	WBC
NT-09	6/21	DE (2)	104 S	7/22-1200	WBC
NT-11	6/21	DE (1)	104 S	7/22-1415	JL
NT-13	6/21	DE (1)	104 S	7/22-1615	WBC
NT-15	6/21	DE (1)	104 S	7/22-1810	WBC
NT-17	6/22		104 S	7/22-2000	WBC
NT-19	6/22	DE (1)	104 S	7/22-2210	WBC
NT-21	6/22	DE (1)	104 S	7/22-2400	WBC
NT-23	6/22	DE (1)	104 S	7/23-0200	WBC
NT-25	6/22	DE (1)	104 S	7/23-0400	WBC
NT-27	6/22	DE (1)	104 S	7/23-0620	WBC
NT-29	6/22	DE (1)	104 S	7/23-0822	WBC
NT-31	6/23	DE (1)	104 S	7/23-1015	WBC
NT-35	6/23	JL	104 Atmos	7/22-1035	
NT-37	6/23	DE (1)	104 A	7/22-1205	DE (2)
NT-39	6/23	DE (1)	104 A	7/22-1405	
NT-41	6/23	DE (1)	104 A	7/22-1600	DE (2)
NT-45	6/23		104 A	7/22-1805	
NT-46	6/23		104 A	7/22-2000	DE (2)
NT-47	6/24	JL	104 A	7/22-2216	
NT-49	6/25	JL	104 A	7/22-2400	DE (2)
NT-51	6/28	JL	104 A	7/23-0200	
NT-53	6/28	JL	104 A	7/23-0400	DE (2)
NT-55	6/28	DE (1)	104 A	7/23-0615	
NT-57	6/28	DE (1)	104 A	7/23-0815	
NT-49	7/19	DE (1)	104 A	7/23-1020	
NT-50	7/19	DE (1)			
NT-51	7/19	DE (1)			
NT-53	7/19	DE (1)			
NT-55	7/19	JL			
NT-57	7/19	DE (1)			

DE - Dr. David Emerson, U.S. Bureau of Mines, Amarillo, Texas

(1) - First Batch

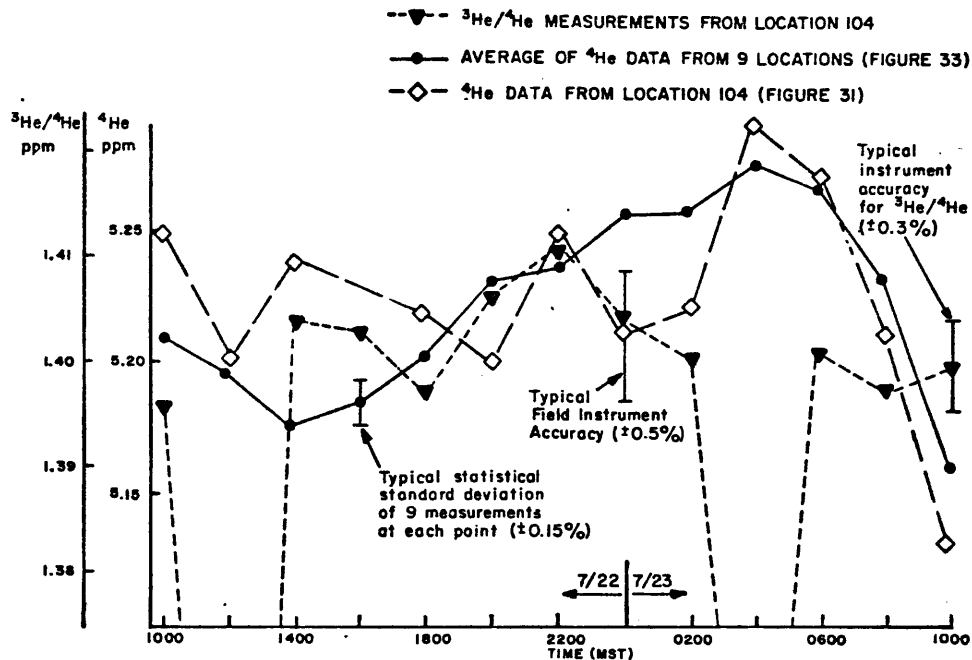
(2) - Second Batch

JL - Dr. John Lupton, University of California at San Diego

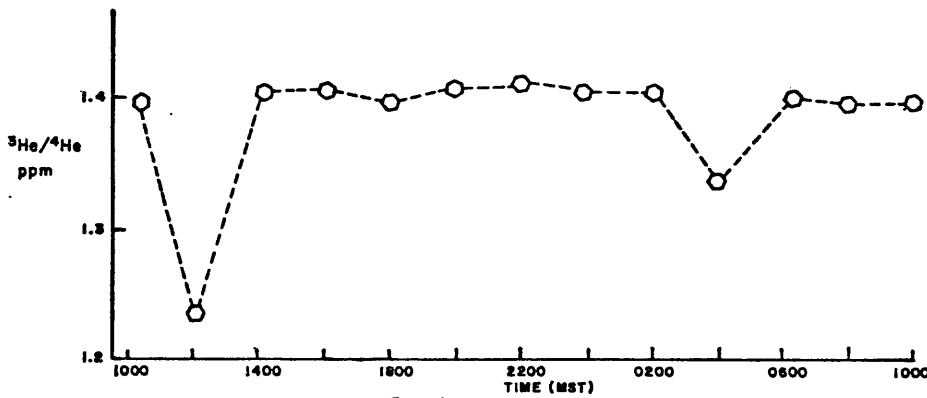
WBC - Dr. W. B. Clarke and Dr. Zafer Top, McMaster University,  
Hamilton, Ontario

Table 5.  $^3\text{He}/^4\text{He}$  Measurements in Soil-Gas Samples  
Collected by Teledyne Isotopes at the Irigaray Ranch Site

Sampling Location	$^3\text{He}$ , ppt	$^4\text{He}$ , ppm	$^3\text{He}/^4\text{He} \times 10^{-6}$	
			Emerson	Lupton
SW Cor. 107	8.0	5.37	1.49	1.37
108-1	7.2	5.34	1.35	
106-24	6.4	5.23	1.22	1.39
SW Cor. 105	5.4	5.34	1.01	1.40
NS6	7.0	5.24	1.34	
NT-29	7.0	5.19	1.35	
NT-31	6.9	5.21	1.32	
NT-55	7.1	5.22	1.36	
PT-36	6.7	5.25	1.28	
PT-34	7.6	5.36	1.42	
	$\pm 20\%$ (absolute)	$\pm 1\%$	$\pm 10\%$ (relative)	$\pm 0.6\%$



(A) COMPARISON AT  $^3\text{He}/^4\text{He}$  WITH  $^4\text{He}$  DATA



(B) COMPRESSED SCALE FOR  $^3\text{He}/^4\text{He}$

Figure 33.  $^3\text{He}/^4\text{He}$  ratio measurements by W. B. Clarke and Z. Top from samples collected during a 24-hour period at location 104, July 22, 23, 1976.  $^4\text{He}$  measurements at the same times are reproduced for comparison.

The data from tables 5 and 6 are plotted in figure 34. Although five of the measurements made by Dr. Emerson have low  $^3\text{He}/^4\text{He}$  values in the vicinity of the ore, the more accurate measurements of Dr. Lupton show no such effect at four of the five locations. At the fifth location, another measurement made by Dr. Emerson fails to reproduce the low  $^3\text{He}/^4\text{He}$  values.

The ratio of  $^3\text{He}/^4\text{He}$  could be an effective method of uranium exploration if more than a single traverse was considered and if the relative complexity of the analysis could be reduced. It is one possible means of eliminating the diurnal variations which would make it possible to sample regardless of time of day.

#### Analysis of Near Surface Soils

##### Gamma-Ray Scintillation and KUT Profiles

A Mount Sopris Model SC-131A gamma-ray scintillometer for measuring total gamma counts from the soil was used during the first run of the northern traverse. These data are shown in figure 35. Comparison of the counting rates with the various helium surveys across the northern traverse show no correlation.

The Bendix Field Engineering Corporation KUT (gamma-ray spectrometry) truck was driven across parts of the northern and parallel traverses (NT and PT, figure 36). Because of adverse topography, the survey was limited to five short traverses as shown in figure 36. The results are plotted in figures 37 a, b, c, d, e. The only significant uranium anomaly occurs on traverse number four at a distance of approximately 4.6 km from the start of the traverse, as shown on figure 36. This represents the Wyoming Mineral Corporation solution

Table 6.  $^3\text{He}/^4\text{He}$  Measurements in Soil-Gas Samples  
Collected by Martin Marietta at the Irigaray Ranch Site

Sampling Location	Sampling Date-Time	Laboratory	$^3\text{He}$ , ppt	$^4\text{He}$ , ppm	$^3\text{He}/^4\text{He}$ $\times 10^{-6}$
NT-07	6/21	DE (2)	7.3	5.29	1.38
NT-09	6/21	DE (2)	8.1	5.29	1.53
NT-11	6/21	DE (1)	7.2	5.16	1.40
NT-13	6/21	DE (1)	7.6	5.25	1.45
NT-15	6/21	DE (1)	7.6	5.23	1.45
NT-19	6/22	DE (1)	7.5	5.23	1.43
NT-21	6/22	DE (1)	6.8	5.27	1.29
NT-23	6/22	DE (1)	8.1	5.18	1.56
NT-25	6/22	DE (1)	6.6	5.22	1.26
NT-27	6/22	DE (1)	6.8	5.27	1.29
NT-29	6/22	DE (1)	6.9	5.24	1.32
NT-31	6/23	DE (1)	6.3	5.30	1.19
NT-35	6/23	JL			1.392
NT-37	6/23	DE (1)	7.6	5.25	1.45
NT-39	6/23	DE (1)	6.8	5.25	1.30
NT-41	6/23	DE (1)	7.8	5.23	1.49
NT-47	6/24	JL			1.406
NT-49	6/25	JL			1.394
NT-51	6/28	JL			1.401
NT-53	6/28	JL			1.411
NT-55	6/28	DE (1)	6.1	5.69	1.07
NT-57	6/28	DE (1)	5.9	5.20	1.13
NT-49	7/19	DE (1)	5.9	5.27	1.12
NT-50	7/19	DE (1)	7.5	5.29	1.42
NT-51	7/19	DE (1)	6.2	5.32	1.17
NT-53	7/19	DE (1)	6.3	5.26	1.20
NT-55	7/19	JL			1.415
NT-57	7/19	DE (1)	7.1	5.34	1.33
104 Soil	7/22-1030	WBC			1.396
104 S	7/22-1200	WBC			1.232
104 S	7/22-1415	JL			1.404
104 S	7/22-1615	WBC			1.403
104 S	7/22-1810	WBC			1.397
104 S	7/22-2000	WBC			1.406
104 S	7/22-2210	WBC			1.411
104 S	7/22-2400	WBC			1.404
104 S	7/23-0200	WBC			1.400
104 S	7/23-0400	WBC			1.336
104 S	7/23-0620	WBC			1.401
104 S	7/23-0822	WBC			1.397
104 S	7/23-1015	WBC			1.399
104 Atmos	7/22-1205	DE (2)	7.2	5.49	1.31
104 A	7/22-1600	DE (2)	8.1	5.23	1.55
104 A	7/22-2000	DE (2)	6.6	5.24	1.26
104 A	7/22-2400	DE (2)	5.9	5.26	1.12
104 A	7/23-0400	DE (2)	6.5	5.26	1.24

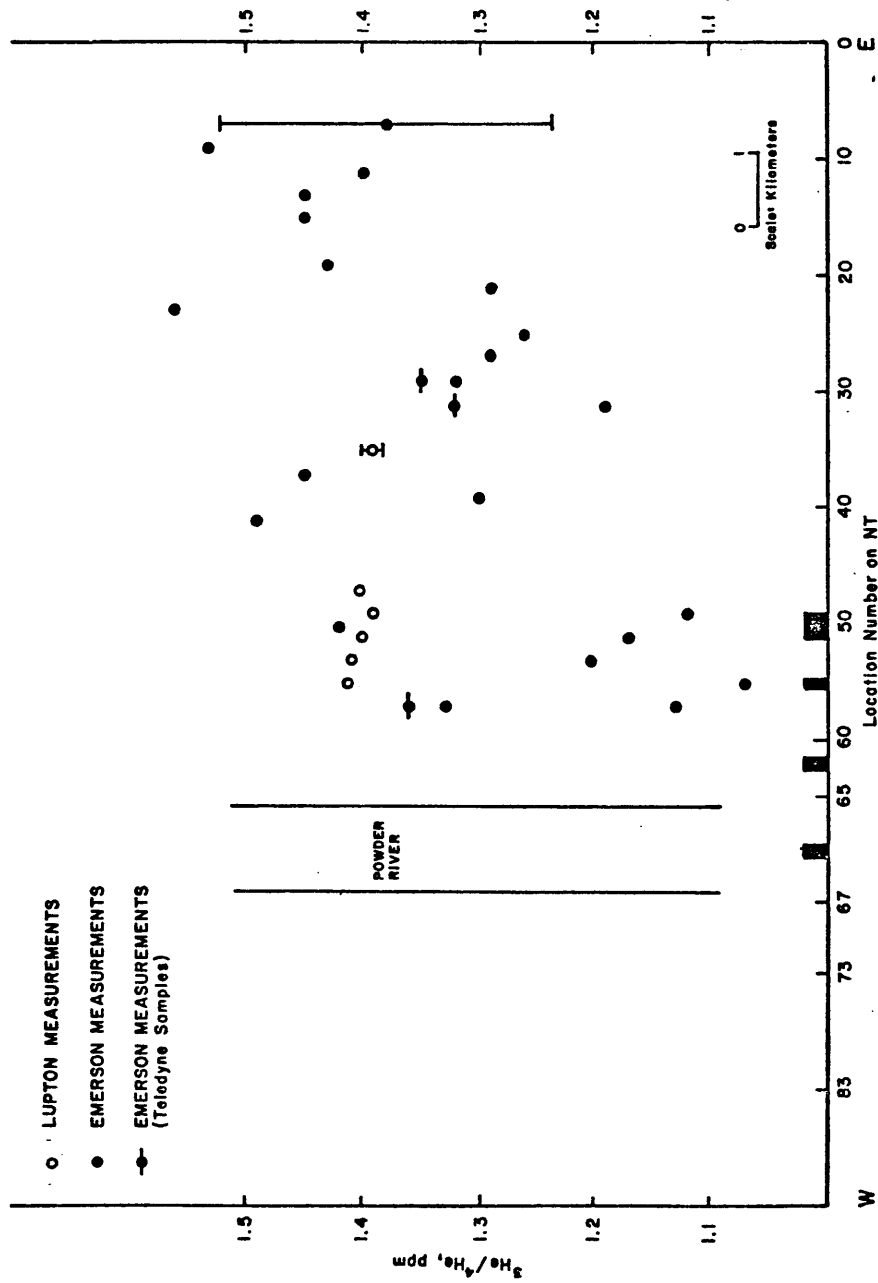


Figure 34.  $^3\text{He}/^4\text{He}$  ratio measurements from samples collected along the northern traverse.

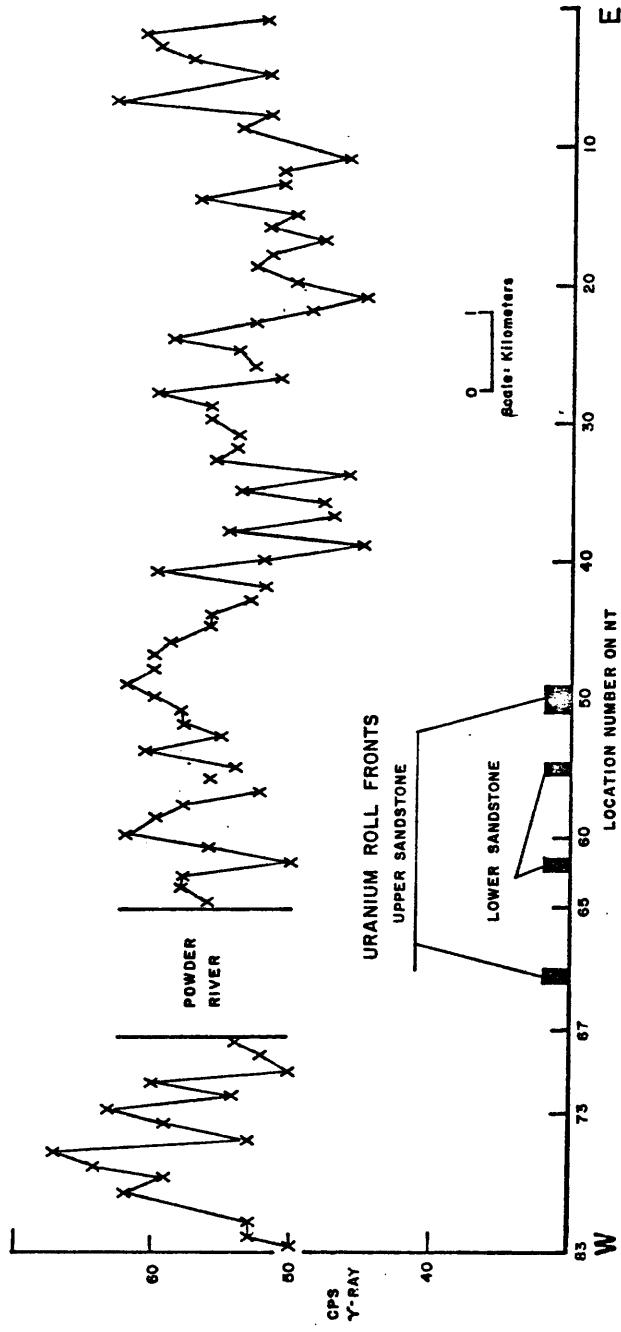


Figure 35. Gamma-ray scintillometer counting rates along the northern traverse of the Irigaray Ranch.



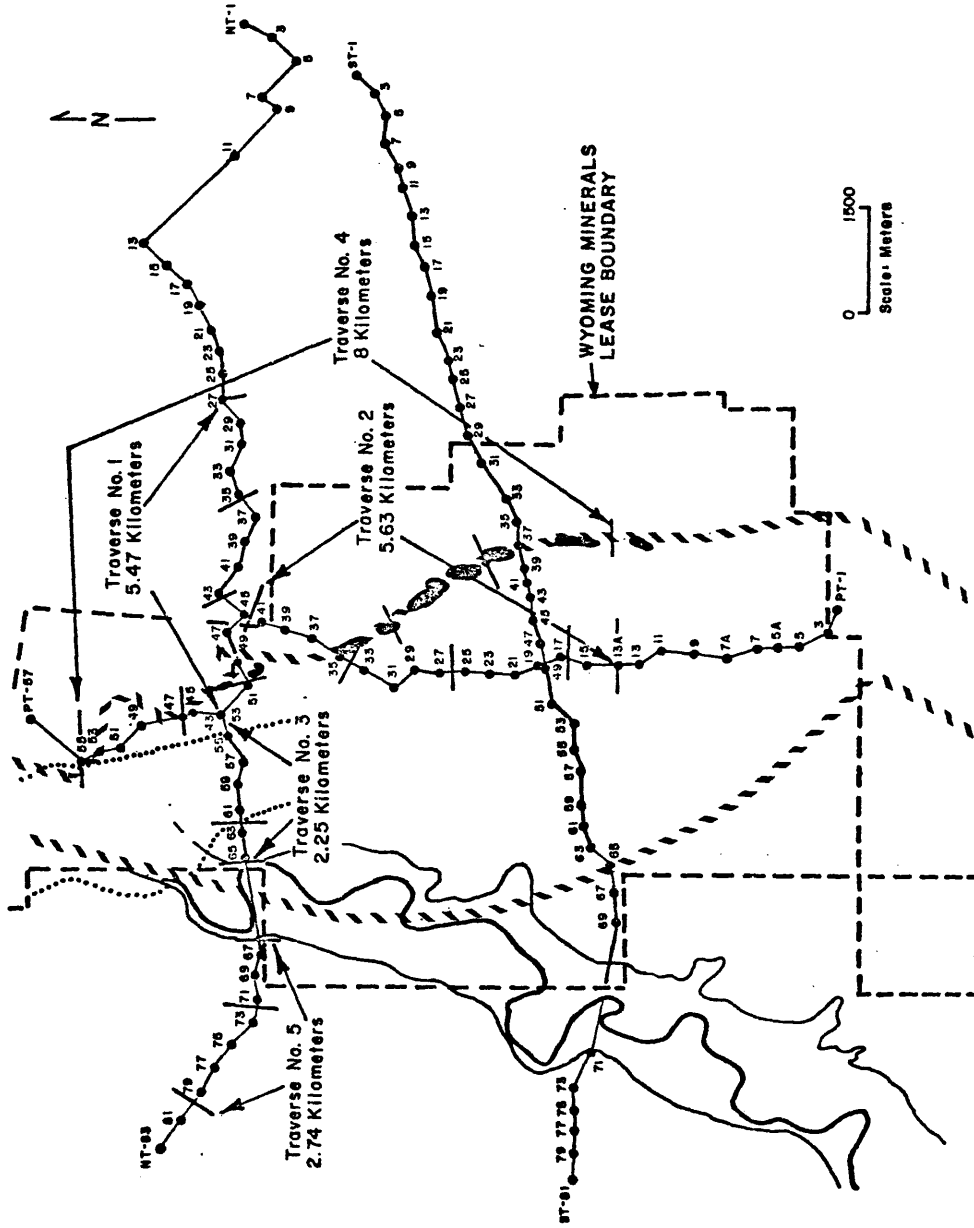


Figure 36. Map of the Irigaray Ranch exploration site showing the locations and mile markers for the five traverses in the KUT truck survey.

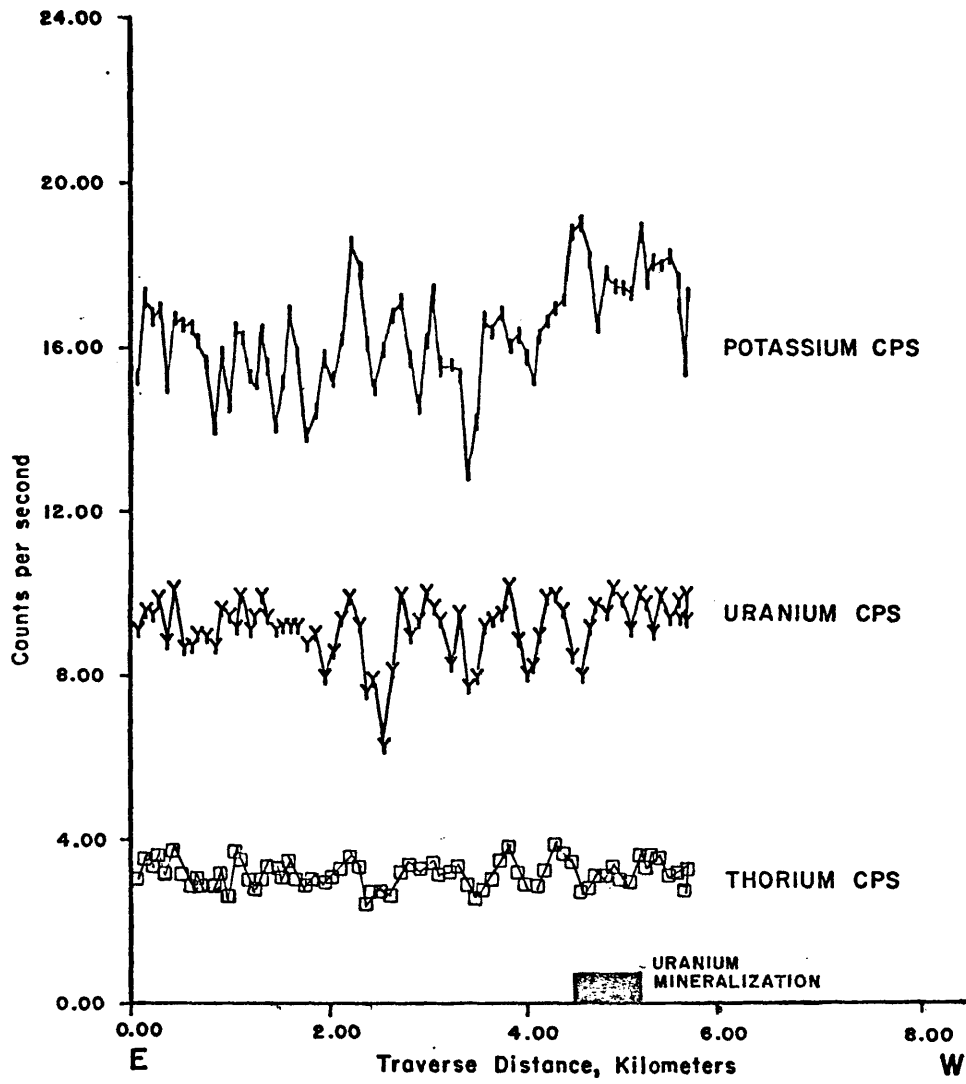


Figure 37a. KUT traverse No. 1.

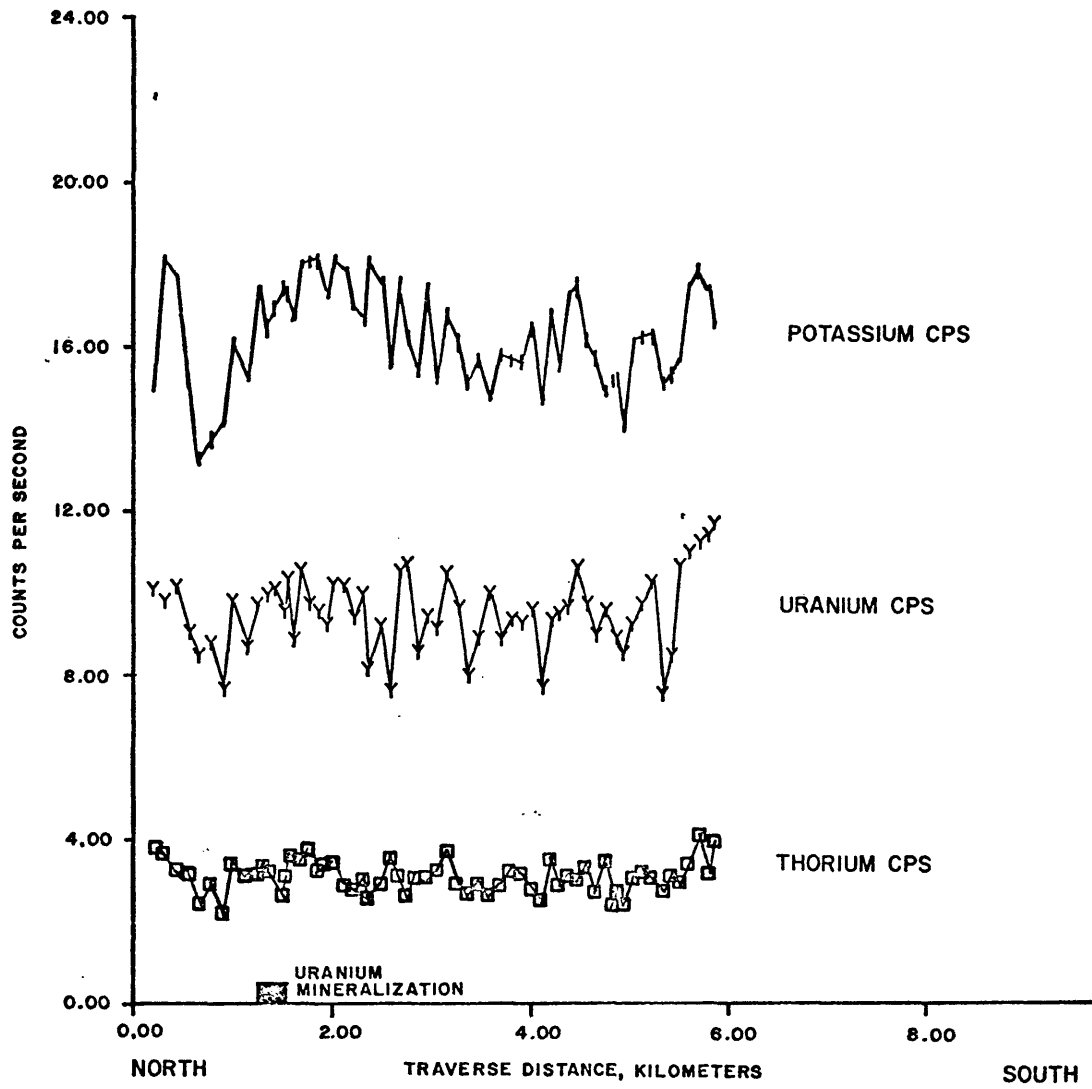


Figure 37b. KUT traverse No. 2.

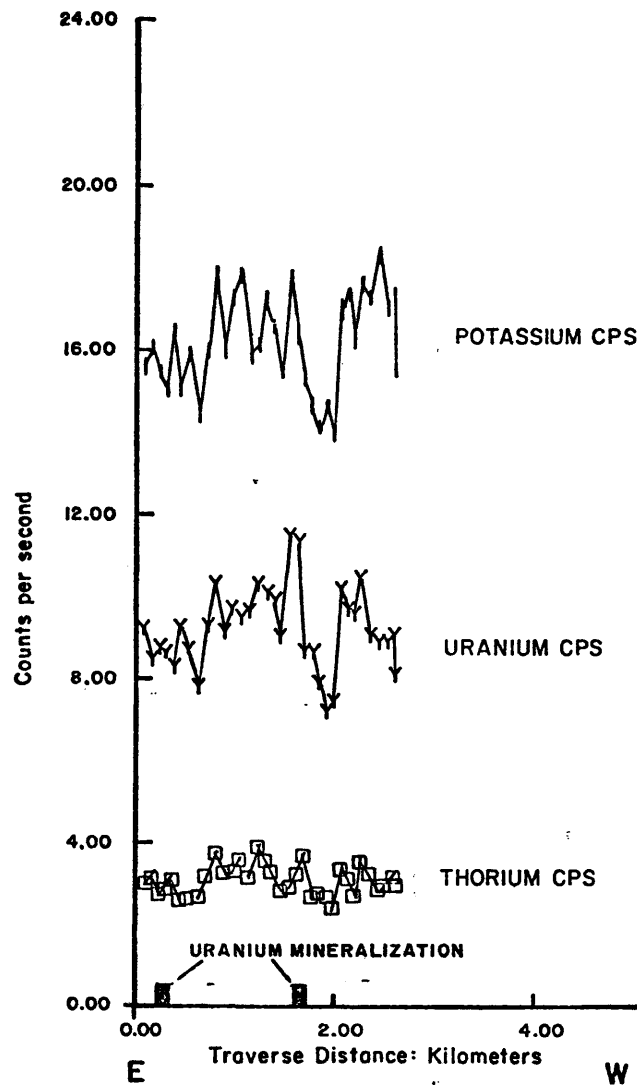


Figure 37c. KUT traverse No. 3.

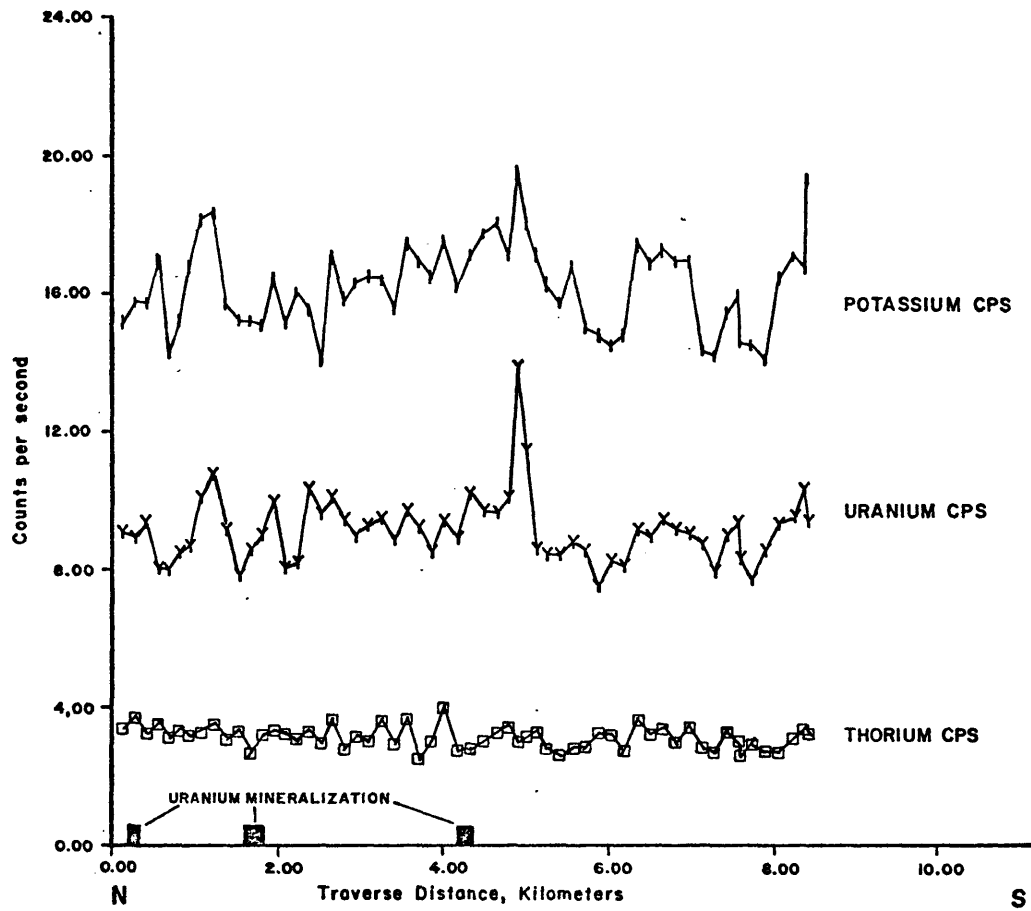


Figure 37d. KUT traverse No. 4.

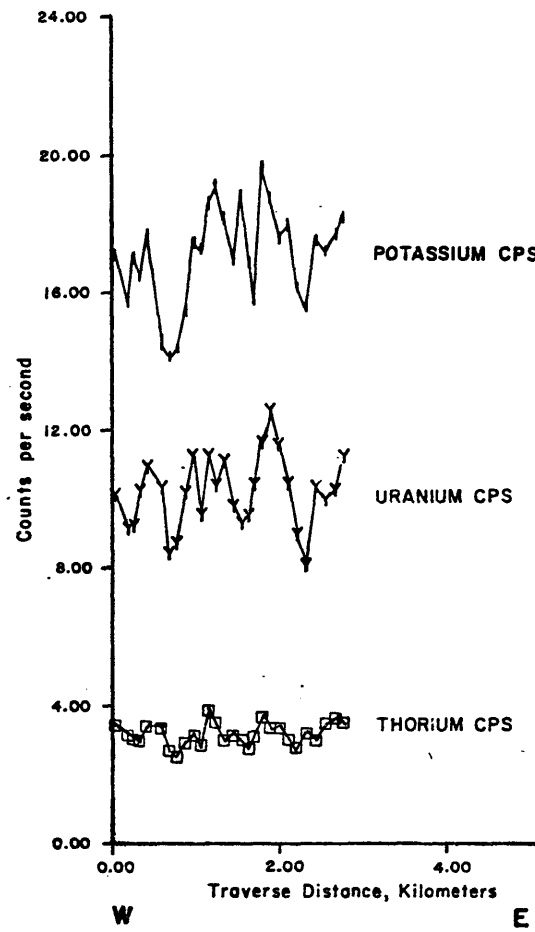


Figure 37e. KUT traverse No. 5.

mine where ore slurry is stored in metal barrels. The correlation between the KUT truck and the helium-in-soil-gas data is poor. The KUT survey is probably only detecting surface concentrations.

#### Gamma-Ray Spectrometric Analysis of Canned Soil Samples

A total of 132 soil samples were collected from the northern, southern and parallel traverses at a depth of 60 cm. Canning of the samples was done by Bendix Field Engineering Corporation (BFEC). Sixty-five of these samples were subsequently analyzed on a gamma-ray spectrometer for Bi-214, Th-208 by BFEC and 67 were analyzed (Bi-214 and Th-208) in Dr. Ken Edwards' laboratory at the Colorado School of Mines. The latter system uses a three inch by three inch NaI(Tl) scintillation counter in heavy lead shielding. Measurements were made in 10 minute runs which gave a precision of plus or minus two ppm thorium and uranium. Total background counting rate in the uranium channels is five counts per minute.

The BFEC system uses a four inch by five inch NaI(Tl) detector with lead and mercury shielding. Counting is done for 40 minutes giving an accuracy of one ppm for uranium, 2 ppm for thorium, and 0.1 per cent for potassium.

The gamma-ray spectrometer results are given in figures 38, 39, and 40. There are several large uranium peaks in these analyses at locations NT-21, NT-41, NT-71, ST-11, ST-51, and PT-5, PT-15, PT-53. These peaks do not correlate significantly with the uranium deposits or the helium-in-soil-gas data except at PT-53 which coincides with the uranium roll front in the upper sandstone.

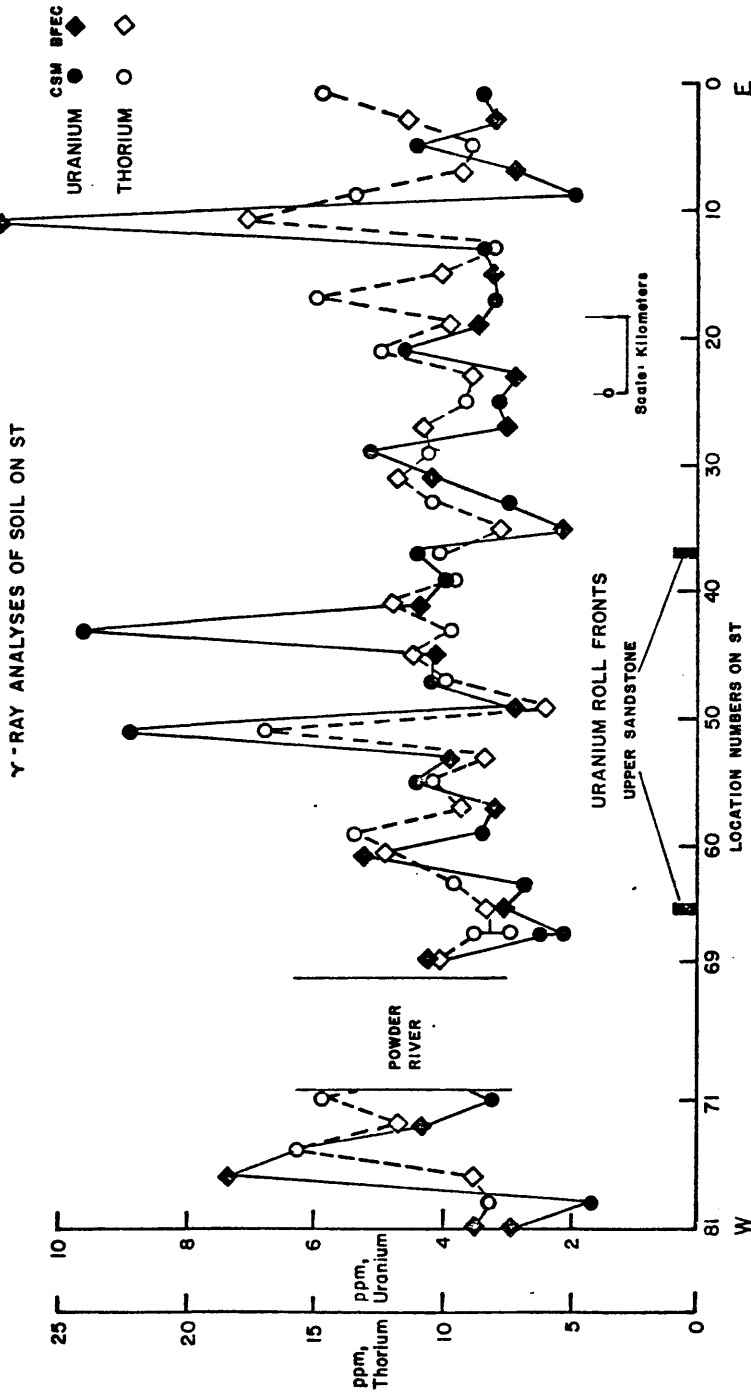


Figure 38. Uranium and thorium content by gamma-ray spectrometer analysis of soil samples collected from 60 cm deep drill holes on the southern traverse of the Irigaray Ranch.



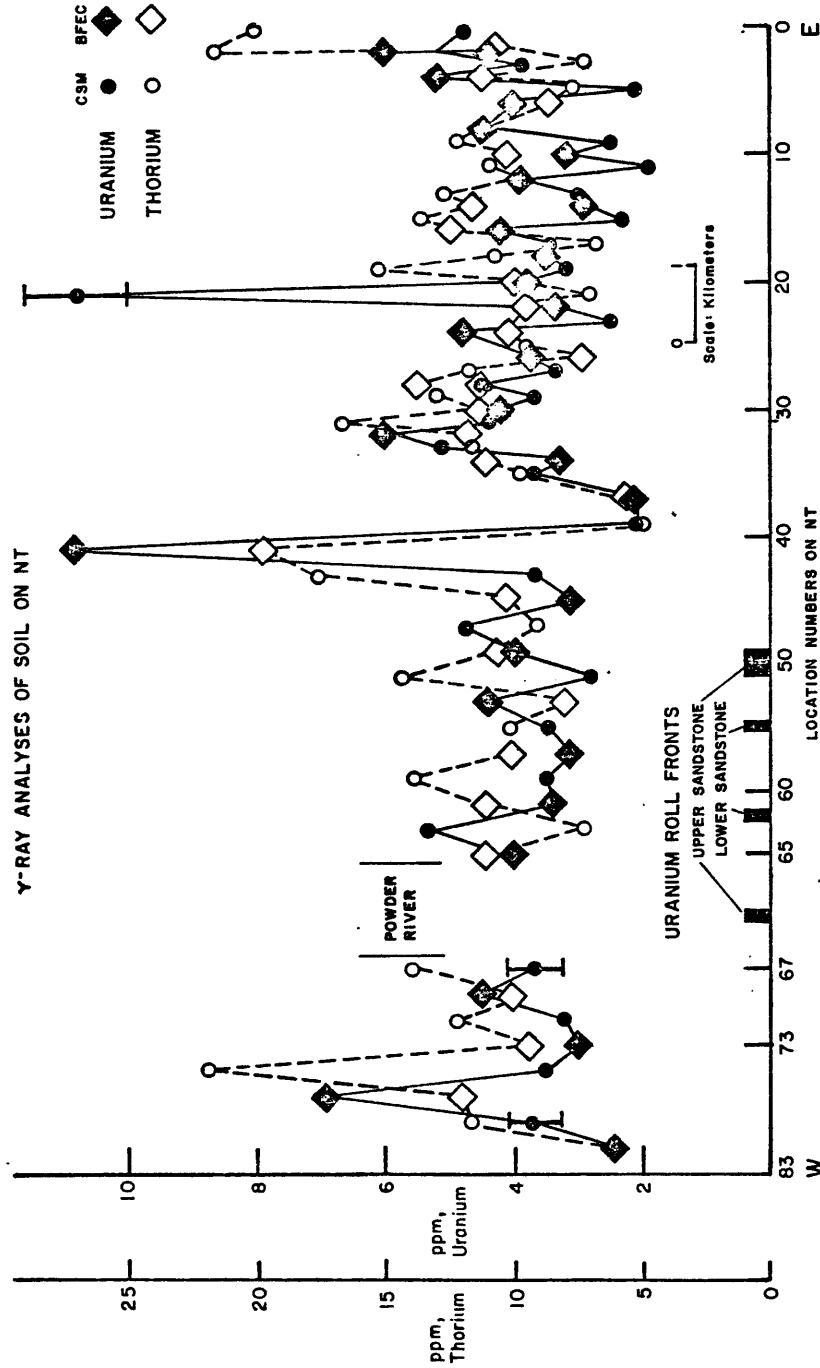


Figure 39. Uranium and thorium content by gamma-ray spectrometer analysis of soil samples collected from 60 cm deep drill holes on the northern traverse of the Irigaray Ranch.

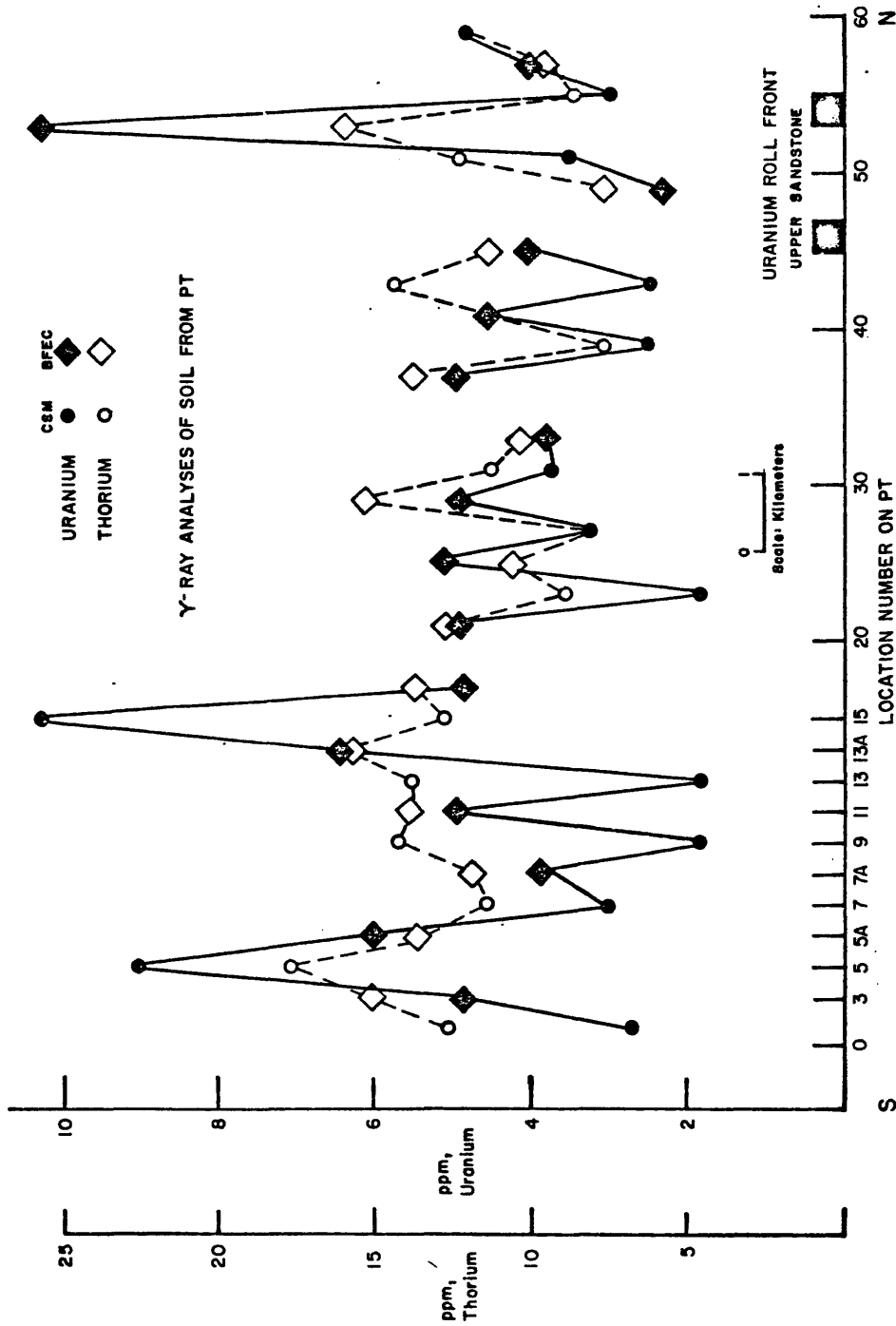


Figure 40. Uranium and thorium contents by gamma-ray spectrometer analysis of soil samples collected from 60 cm deep drill holes on the parallel traverse of the Irigaray Ranch.

The general trend of the gamma-ray spectrometer analyses on the northern traverse (figure 38) shows a fair correlation with the scintillometer survey of figure 35. The correlation of the KUT truck survey and the uranium and thorium analysis is poor. This is probably a result of the difference in sample depth.

#### Chemical Analysis of Soil Samples

Sixteen of the soil samples were split and analyzed chemically for uranium, thorium, radium, and selenium. The results are shown in figure 41. Table 7 gives the ratio between the chemical and gamma-ray spectrometer analyses for uranium and thorium, showing a poor correlation between these results. Since the gamma-ray uranium analysis is really a measure of the bismuth-214 concentration, this would give a reliable indication of the amount of uranium present only if the sample had not been weathered for approximately one million years. The thorium series is less affected by weathering because of the much shorter half-lives of the daughter products. Therefore, the chemical and gamma-ray spectrometric analyses for thorium should be much closer than they are. It can only be assumed that the scatter in the thorium ratios is due to uncertainties in the measurements. There does not appear to be any correlation between the subsurface uranium and the radium and selenium concentrations.

#### In-Situ Radon Detection with Alpha Detectors

##### Miniature Electronic Radon Alpha Counters

A set of miniature electronic radon alpha counters (MERAC) was used at the Irigaray site to obtain a measure of the in-situ radon

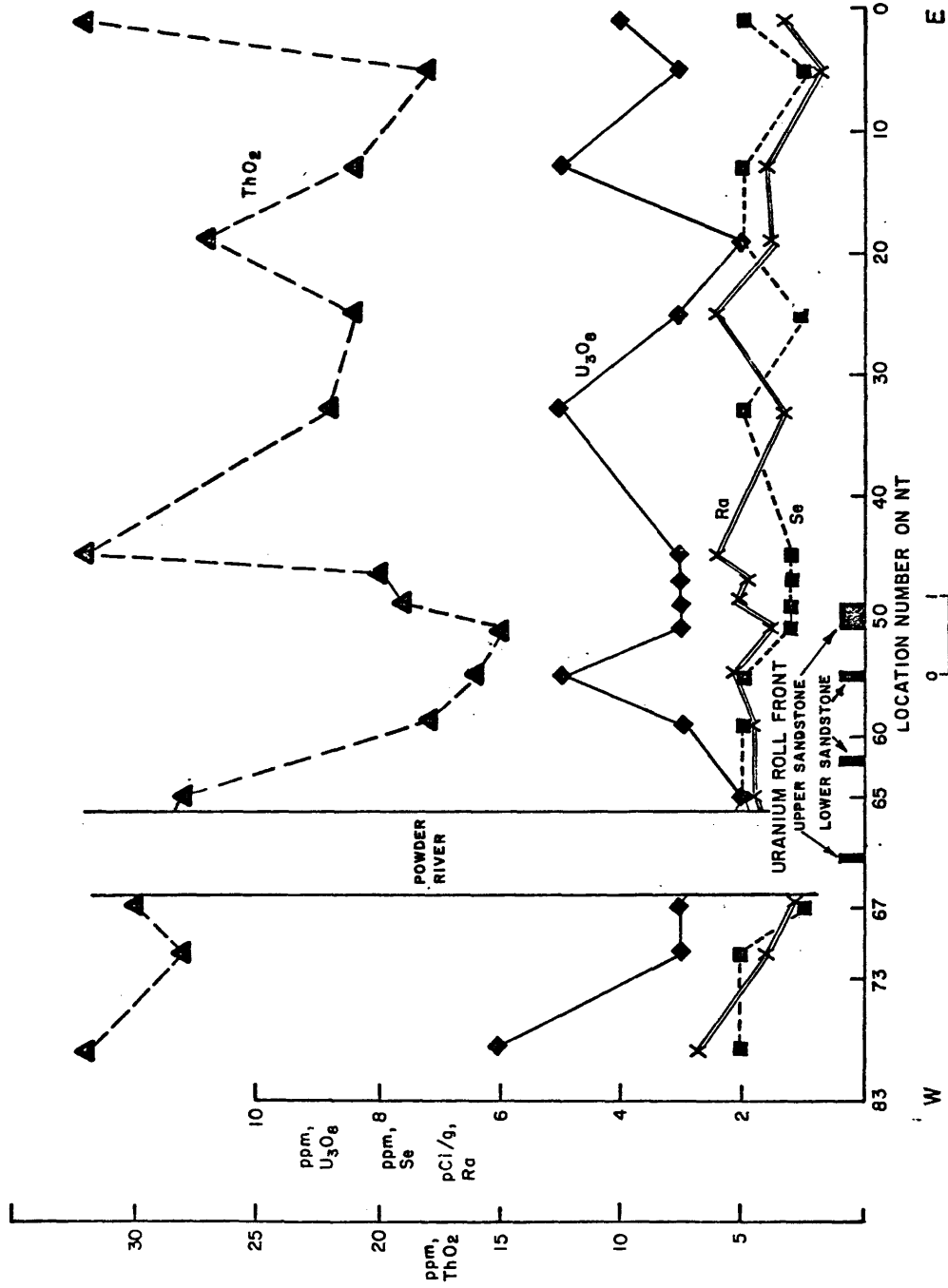


Figure 41. Chemical analyses by BFEC of soil samples collected from 60 cm deep drill holes on the northern traverse of the Irigaray Ranch.

Table 7. Ratios of Chemical to Gamma-Ray Spectrometer  
Determinations of Uranium and Thorium in Soil Samples,  
Irigaray Ranch

Location	Chemical ppm, U	$\gamma$ -ray ppm, U	U ratio $\frac{\text{Chemical}}{\gamma\text{-ray}}$	Chemical ppm, Th	$\gamma$ -ray ppm, Th	Th ratio $\frac{\text{Chemical}}{\gamma\text{-ray}}$
NT- 1	4	4.8	0.83	32	20	1.6
NT- 5	3	3.9	0.77	18	7.3	2.5
NT-13	5	3.0	1.67	21	12.6	1.7
NT-19	2	3.2	0.62	27	15.2	1.8
NT-25	3	3.7	0.81	21	11.2	1.9
NT-33	5	5.1	0.98	22	11.7	1.9
NT-45	3	3.1	0.97	32	10.4	3.1
NT-47	3	4.8	0.63	20	9.2	2.2
NT-49	3	4.0	0.75	19	10.7	1.8
NT-51	3	2.8	1.07	15	14.5	1.0
NT-55	5	3.5	1.43	16	10.1	1.6
NT-59	3	3.5	0.86	18	14.0	1.3
NT-65	2	4.0	0.5	28	11.2	2.5
NT-67	3	3.7	0.81	30	14.0	2.1
NT-71	3	3.2	0.94	28	12.2	2.3
NT-77	6	6.9	0.87	32	12	2.7

gas concentration in the soil. Thirty-six MERAC's were planted on June 17, 1976, alongside Track-etch cups along the northern traverse at 320 meter intervals. They were read for a total of eight days. On July 13 and 14, they were planted alongside cups on the southern traverse, again on 320 meter spacing. The MERAC's were read approximately every day for 10 days. Typically the counters would average between 0.4 counts per minute and 5.90 counts per minute. At any location the counting rates were rather steady ( $\pm 17$  percent).

The results of the MERAC measurements are shown in figures 42 and 43. The average counting rates are plotted at each location. To see the comparative trends between the MERAC counting rates and the gamma-ray analysis of uranium from the soil, both measurements are plotted in figures 42 and 43. Only those gamma-ray analyses points which had corresponding MERAC data points were plotted in the figures.

The correlation on the southern traverse (figure 43) is very good, indicating that the radon is probably due to uranium in the near surface soil. On the northern traverse, the correlation is poorer. Particularly interesting are inverse correlations at stations NT-11, NT-13, and NT-21. These points represent an increase in sand content in an otherwise siltstone and claystone facies. This would increase the porosity at the stations giving a lower soil radon concentration.

#### Track-etch Cups

The Track-etch cups which were planted along the northern, southern, and parallel traverses were recovered and sent to Terradex for analysis. The cups were also planted at a depth of 60 cm. The cups were in the ground from 76 to 79 days. Figure 44 shows each cup

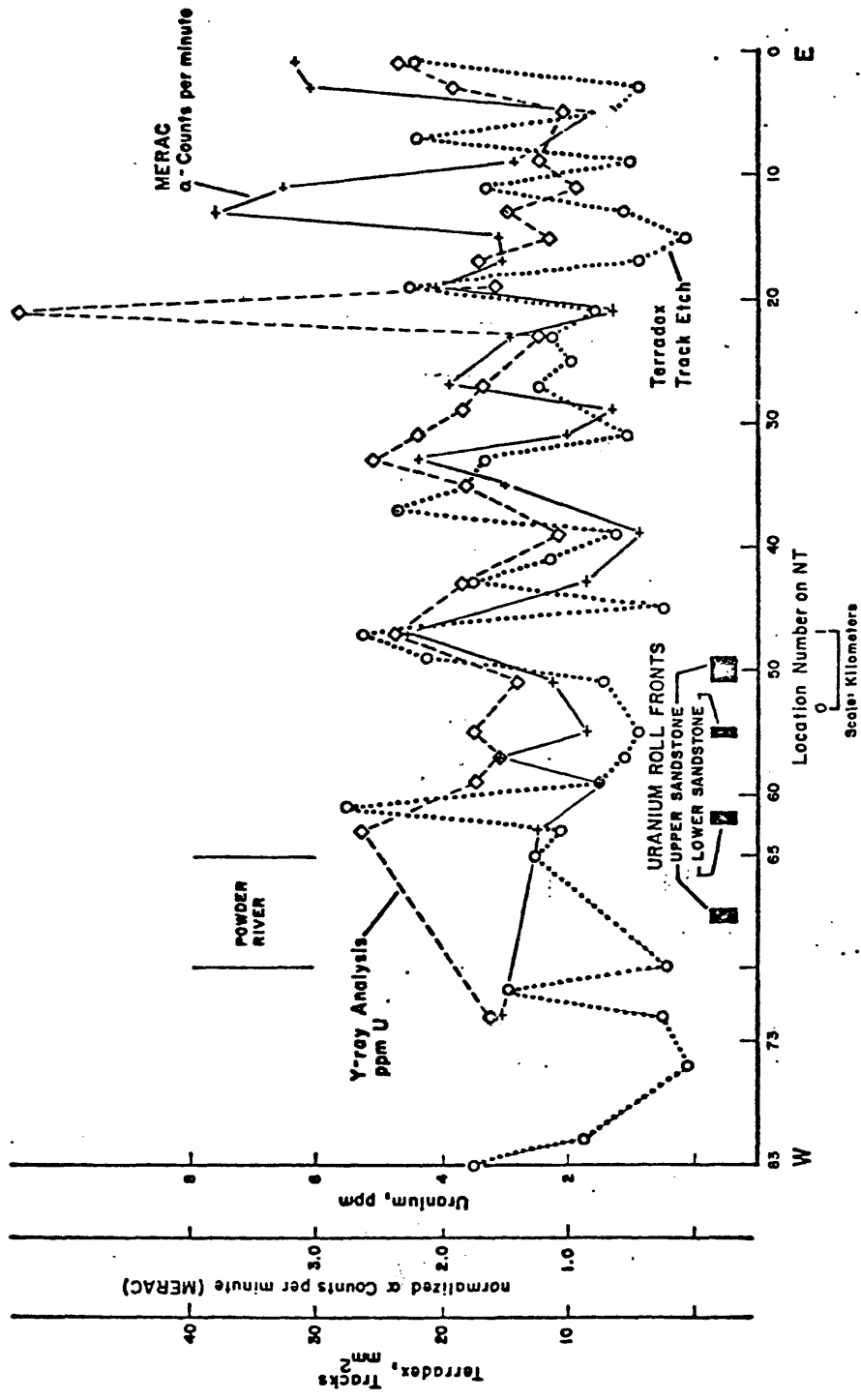


**Figure 42.** MERAC counting rates averaged over eight days along the northern traverse. The gamma-ray spectrometer analysis uranium contents from the corresponding soil samples and the Terradex cup readings are shown for comparison. The MERAC counting rates are normalized according to the relative calibration discussed in the text.

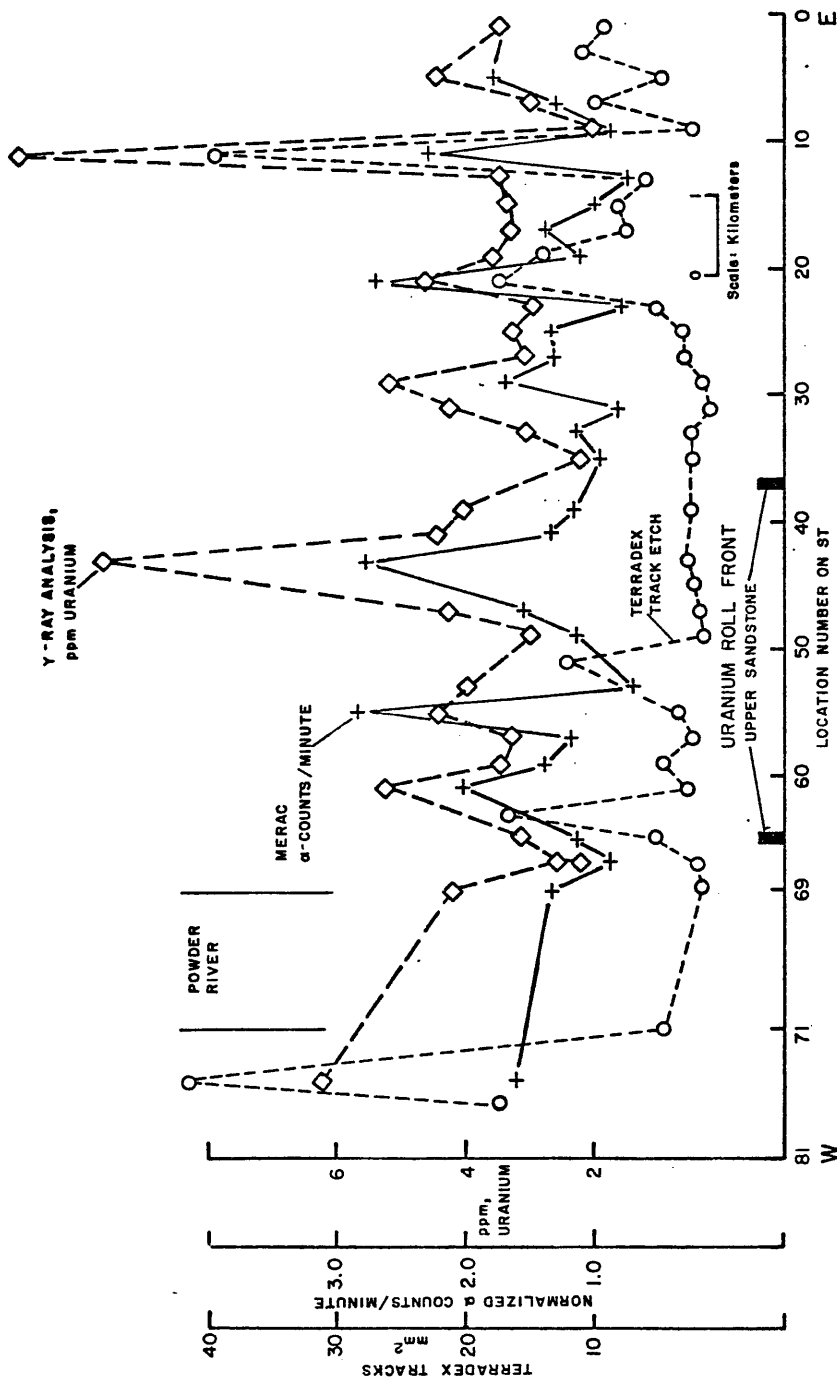


Figure 43. MERAC counting rates averaged over 10 days along the southern traverse. The uranium gamma-ray analyses from the corresponding soil samples and the Terradex cup readings are shown for comparison. The MERAC counting rates are normalized according to the relative calibration discussed in the text.



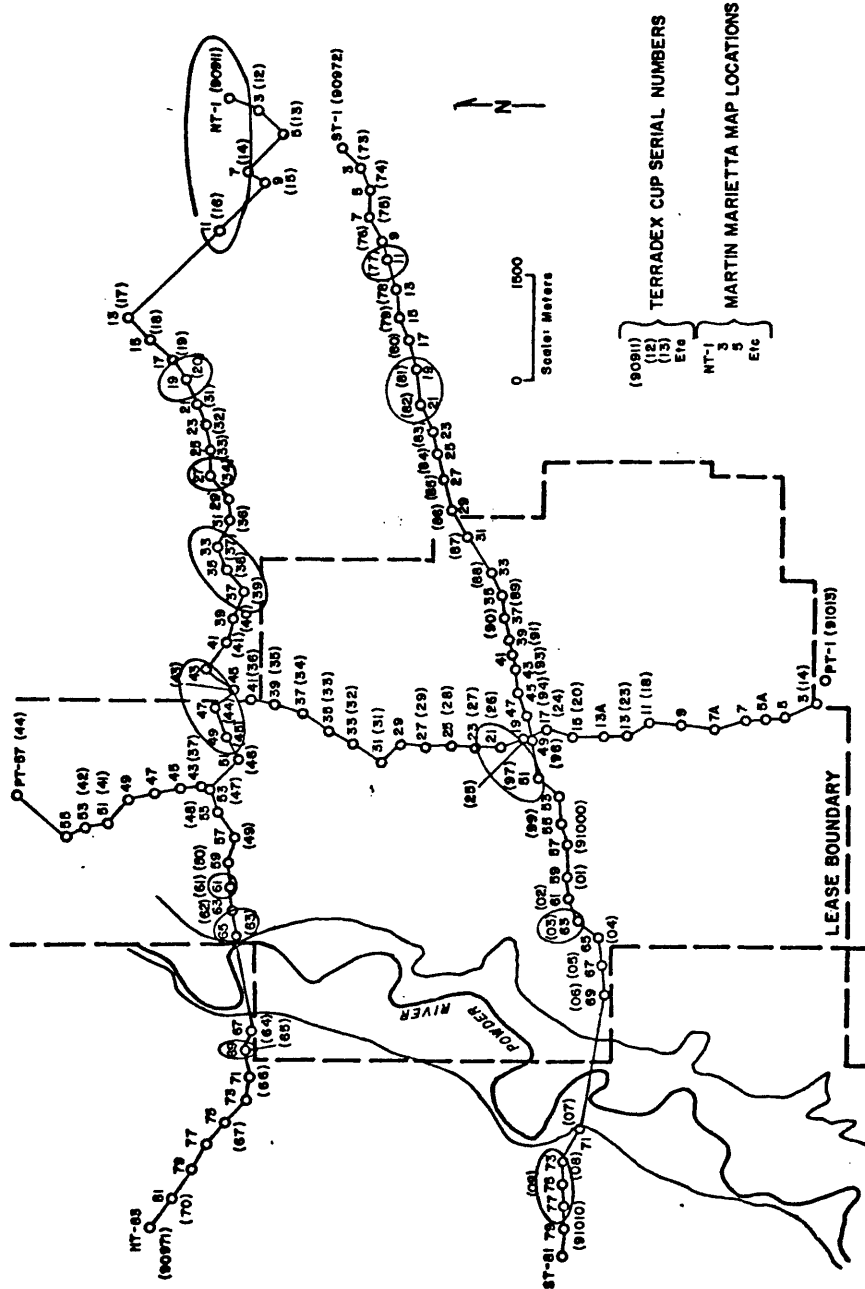


Figure 44. Location map for Terradex cup locations, circles show location of Track-etch readings greater than 12.0 tracks/mm<sup>2</sup>. Background corresponds to 4.8 tracks/mm<sup>2</sup>.

location and the corresponding location numbers. It also shows the 25 locations with track densities greater than 12.0 tracks per square millimeter.

The data from the northern and southern traverses are plotted on figures 42 and 43 along with the MERAC data and the bismuth-214 data. There is good correlation between the MERAC data and the Track-etch data on the northern traverse. On the southern traverse, the correlation is good only up to station ST-23. Beyond this location, there is a very low track density on all cups. Because this anomalously low area does not correlate with either the MERAC data or the bismuth-214 analyses, the decrease in track density is assumed to be due to a problem with the cups.

Generally, there was no correlation between the Track-etch data and the helium-in-soil-gas data. It is thought that the alpha particles detected by the Track-etch cups were derived from the near-surface soil whereas the helium was derived from depth.

### Test Site B

#### Geology and Hydrology

Test site B is located north of Douglas, Wyoming at the site of an extensively drilled zone of uranium mineralization within the Fort Union Formation. In the southern part of the study area, the mineralization is in a sandstone at a depth of 6 to 24 meters; to the northwest, the mineralized sandstone increases to a depth of 30 to 60 meters. The redox fronts are coincident with the eastern edge of the mineralization.

Figures 45 and 46 are generalized geologic cross sections across the test site showing typical stratigraphic relationships. The groundwater flow direction is to the northeast in the study area.

#### Helium Soil-Gas and Atmosphere Measurements

Helium soil-gas samples were collected along three roughly north-south lines (figure 47) spaced approximately 240 and 365 meters apart, respectively, from east to west. The station spacing along the lines ranged from 60 to 300 meters. Data were also collected along two generally east-west traverses as shown in figure 47, with one traverse extending well beyond the mineralization in both directions and the other extending well beyond it in a westerly direction.

The survey of soil and atmospheric gases was conducted at nine different times on five different days as shown in table 8. Generally, the samples were collected twice on each day, at sunrise and in the mid-afternoon.

Table 8. Times and Dates of Surveys at Test Site B

Day	Time of Day*	Day	Time of Day*
July 29, 1976	1020 - 1050 1345 - 1415	August 7, 1976	0500 - 0730 1350 - 1500
July 30, 1976	0430 - 0530 1300 - 1400	August 12, 1976	0530 - 0820
August 5, 1976	0500 - 0600 1350 - 1430		

\*All times presented as Mountain Standard Time

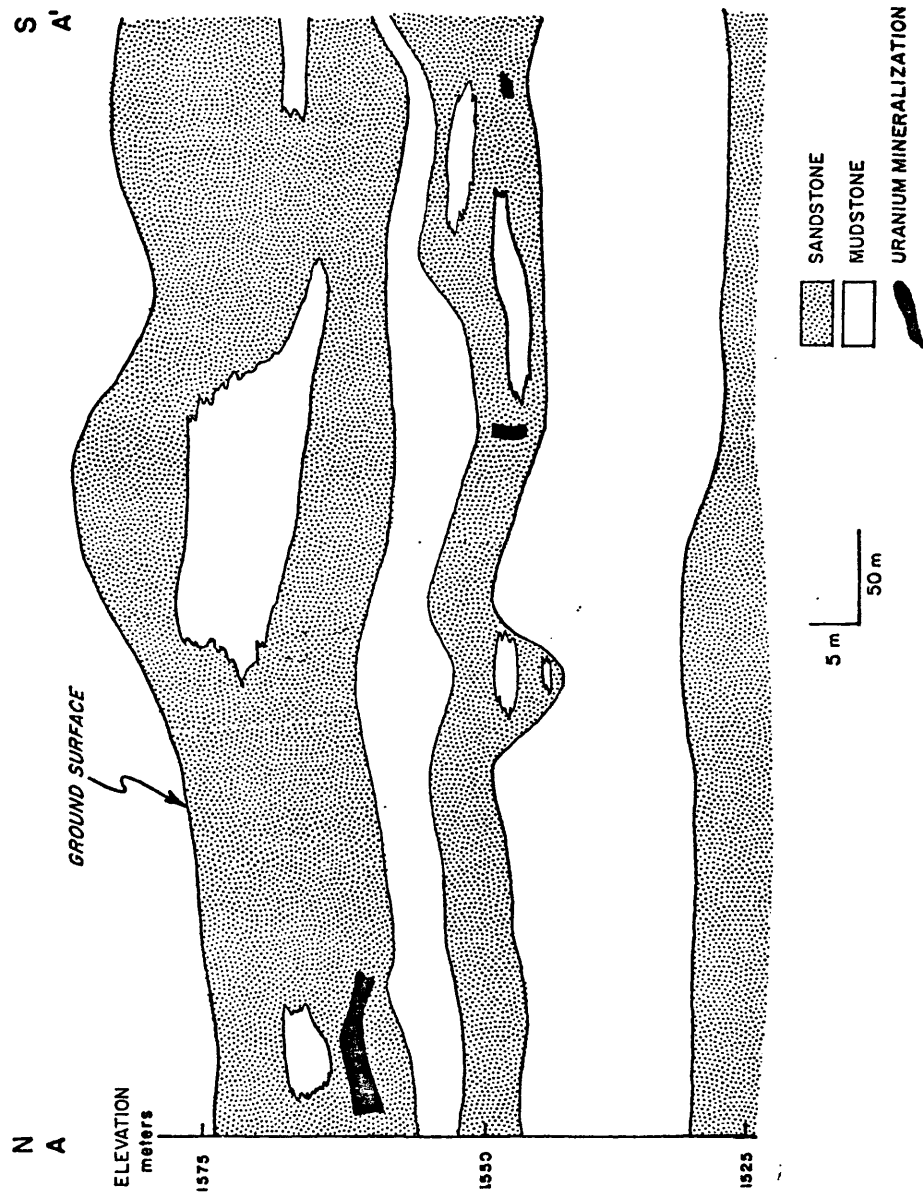


Figure 45. Generalized north-south geologic cross section of test site B.

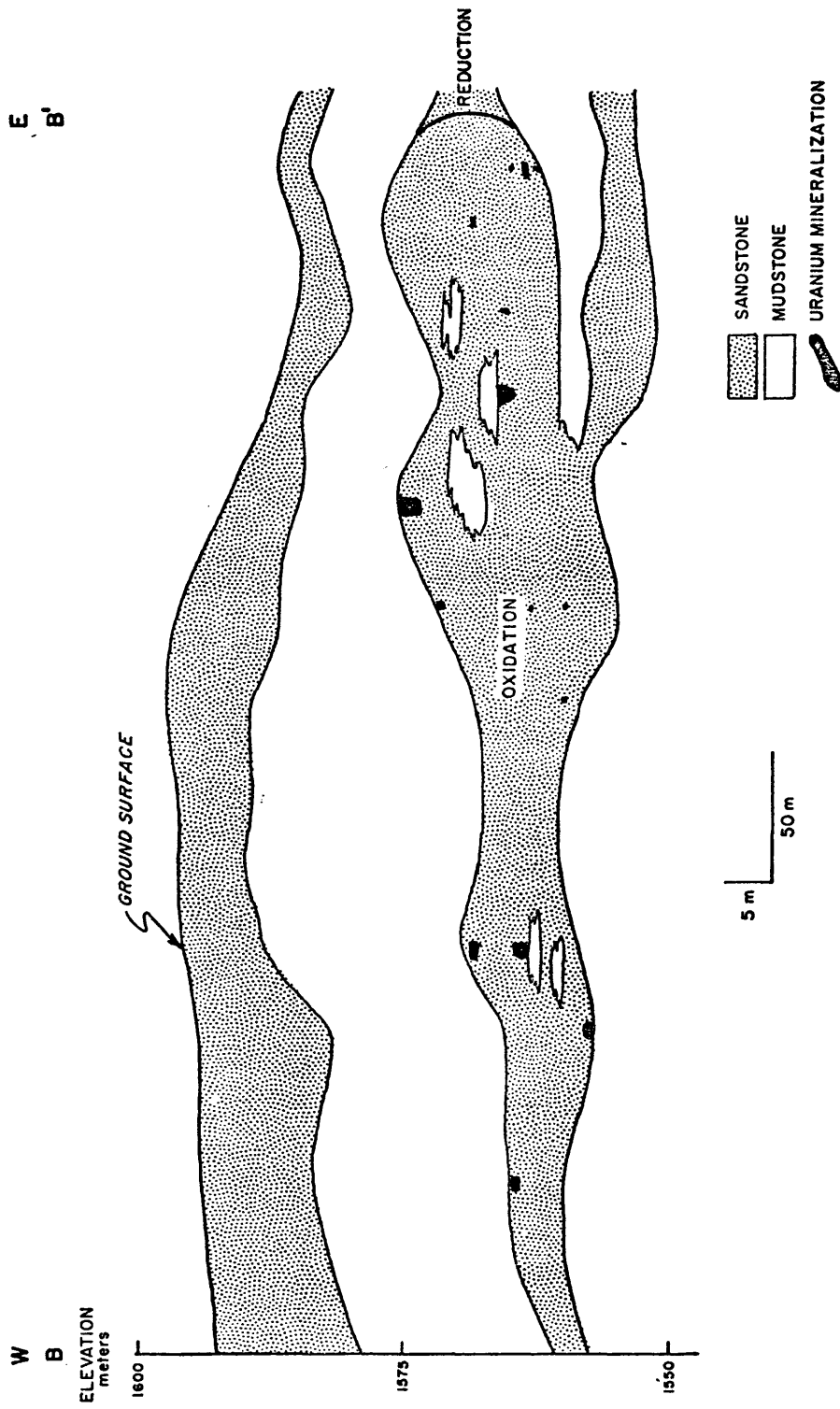


Figure 46. Generalized east-west geologic cross section of test site B.

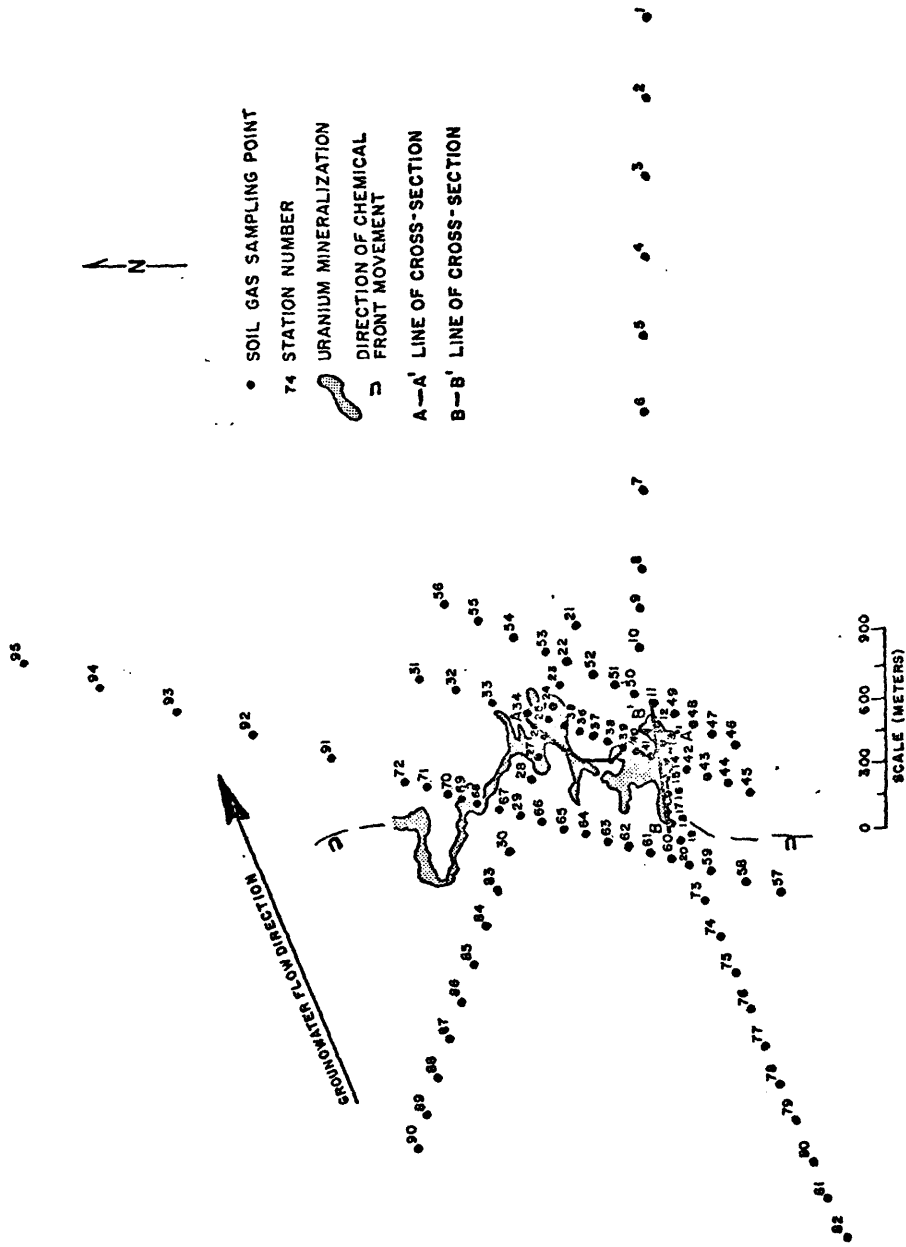


Figure 47. Location map showing soil gas sampling station numbers for all helium soil gas data collected at test site B.

Table 9 summarizes the helium soil-gas data from all of the surveys at test site B. The first two surveys in the study area were single line traverses as shown in figure 48. These traverses again show the difficulty in interpreting single line surveys. There appears to be an anomaly related to the mineralization in the afternoon survey on July 29 but not on the early morning survey of the same day. The same line of the survey from the July 30th runs is also shown in figure 48. Again the early morning run does not show any anomalous helium in soil gas related to the uranium mineralization, whereas the July 30th afternoon traverse does repeat the helium-in-soil-gas anomaly that was observed on July 29. From July 30 to August 12, the data was taken on a semi-rectangular grid (table 9). All of the surveys conducted from the afternoon run on July 30 to the end of the work on test site B recorded a clearly detectable anomaly that can be associated with the region of uranium mineralization. These data, plotted on figures 49 through 54, show that the anomaly shifts in both position and amplitude from one survey to the next but maintains a close spatial relationship to the mineralization.

In addition to the soil gas measurements, a syringe of atmospheric gas was collected at the ground surface at each sample location. Typical atmospheric helium contents are shown on figures 55 and 56. No significant helium anomalies are observable in the atmosphere that can be related to the subsurface uranium mineralization.

Several general conclusions can be drawn from the helium concentration data (table 9):

- 1) The helium concentrations in the soil-gas (at a depth of 60 cm) generally show a systematic variation

Table 9. Helium-in-soil-gas Anomalies, Test Site B.

Day	Time of Day*	Nature of Grid	Range of He Concentration (in ppm)	Background Threshold He Concentration (BGT) (in ppm)	Position of He-in-soil-gas Anomaly(ies)	Size of Anomaly	Amplitude of Anomaly over Known Uranium
7/29/76	1020-1050	1 line (20 stations)	5.17 -5.27	5.20	To east of known uranium and weak over ore	180 m wide (E-W)	Up to 70 ppb > BGT 10 ppb over ore
	1345-1415	1 line (20 stations)	5.17 -5.29	5.21	Over leading edge of "roll-front" mineralization	120 m wide (E-W)	Up to 80 ppb > BGT
7/30/76	0430-0530	3 lines (44 stations)	5.26 -5.33	5.30	No pattern		None
	1300-1400	3 lines (45 stations)	5.16 -5.29	5.22	Continuous N-S anomaly over leading edge of mineralization (roll)	240 m wide (E-W) 1100 m (?) long (N-S)	Up to 70 ppb > BGT
8/ 5/76	0500-0600	3 lines (45 stations)	5.23 -5.31	5.28	Large cluster over ore, generally at leading edge	370 m E-W by 550 m N-S	Upto 30 ppb > BGT
	1350-1430	5 lines (44 stations)	5.16 5.33	5.21	Over portions of northern and southern ore deposits, not over middle ore	90 m E-W by 800 m N-S	Up to 120 ppb > BGT
8/ 7/76	0500-0730	5 lines (72 stations)	5.21 -5.30	5.25	Over and in front of leading edge of southern ore and over northern ore.	430 m N-S by 490 m E-W	Up to 50 ppb > BGT
	1350-1500	5 lines (72 stations)	5.18 -5.31	5.23	Generally over entire area of mineralization.	2 broad areas	Up to 80 ppb > BGT
8/12/76	0530-0820	5 lines extended (88 stations)	5.23 -5.31	5.26	Over leading edges of 3 areas of strongest mineralization.	90 m by 400 m (southern) and other smaller areas	Up to 50 ppb > BGT
Average all Data		5 lines (95 stations)	5.215-5.270	5.240	Over entire area of mineralization.	300 m by 300 m	Up to 30 ppb > BGT

\* All times presented as Mountain Standard Time



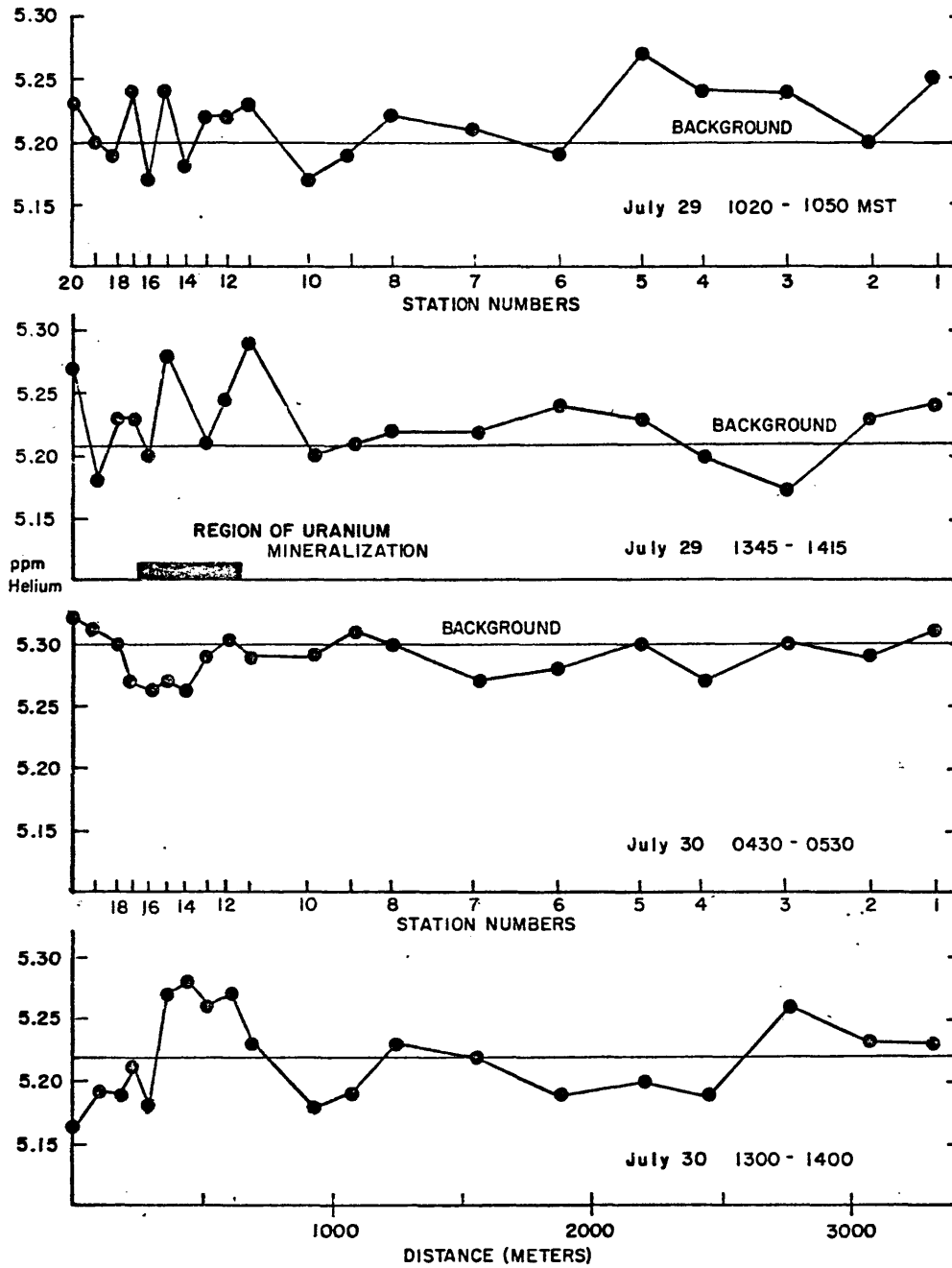


Figure 48. Comparison of morning and afternoon runs at Test site B showing helium concentration anomaly-in-soil -gas over ore in the afternoon runs.

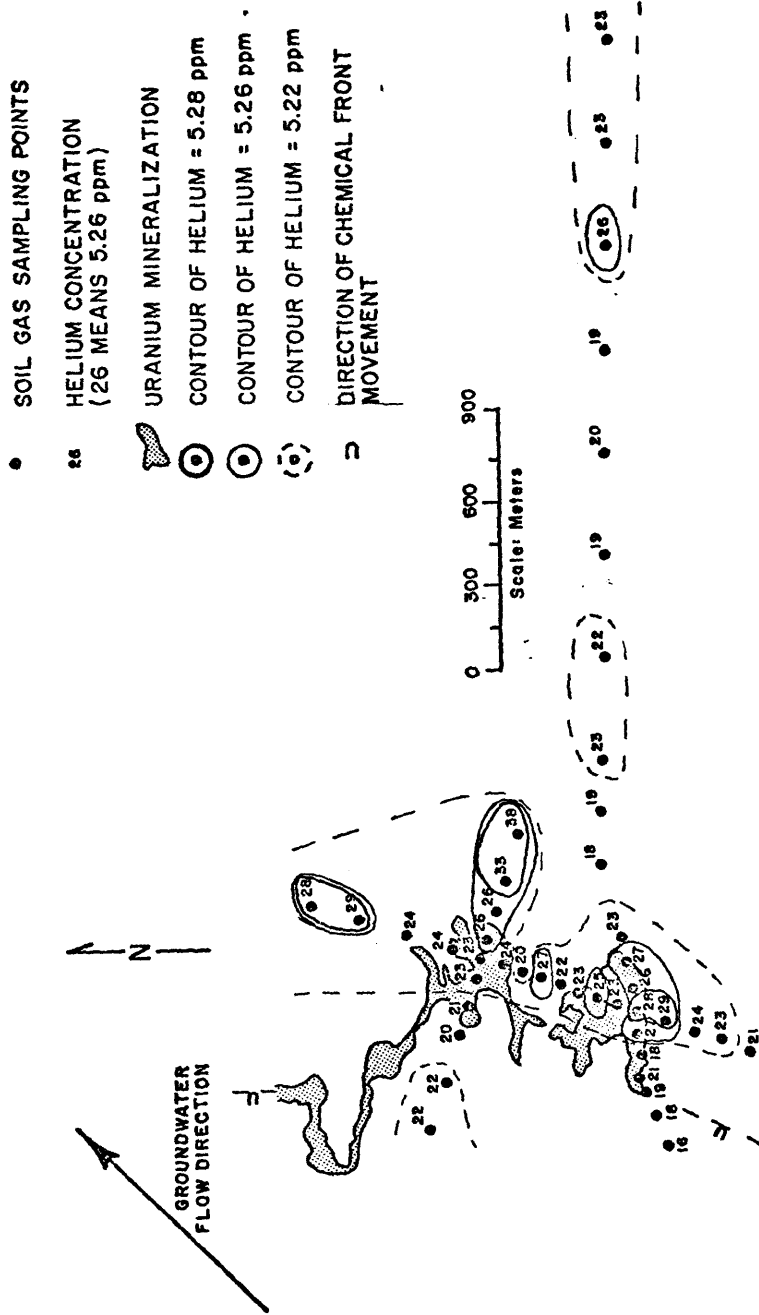


Figure 49. Helium concentration in soil gas at test site B on July 30, 1976. Samples collected 1300 - 1400 MST.

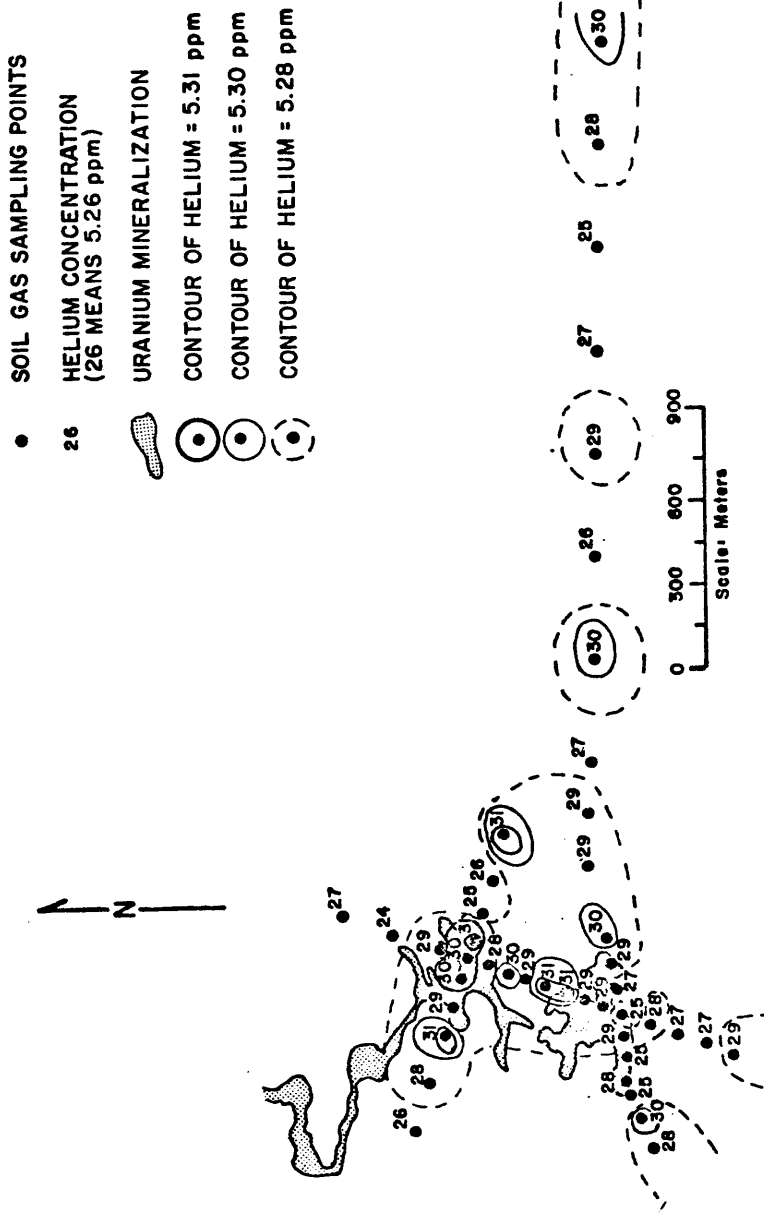


Figure 50. Helium concentration in soil gas at test site B on August 5, 1976. Samples collected 0500 - 0600 MST.

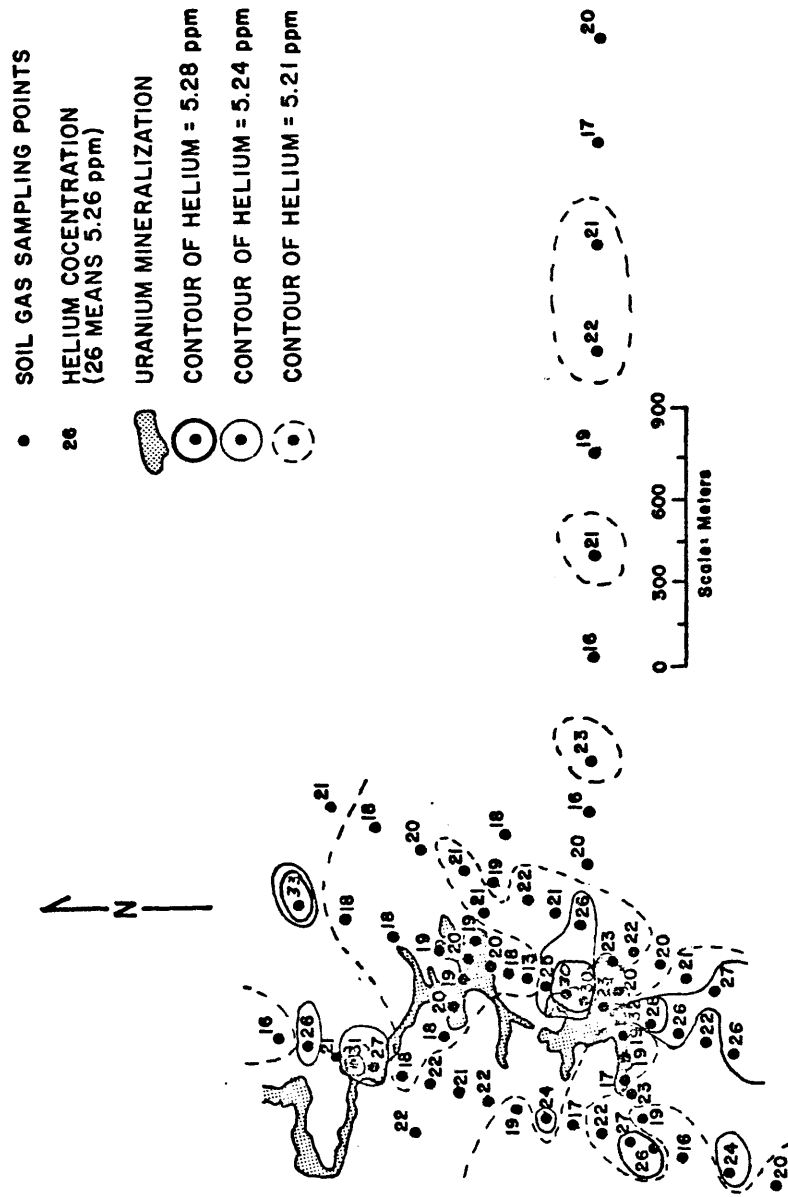


Figure 51. Helium concentration in soil gas at test site B on August 5, 1976. Samples collected 1350- 1430 MST.

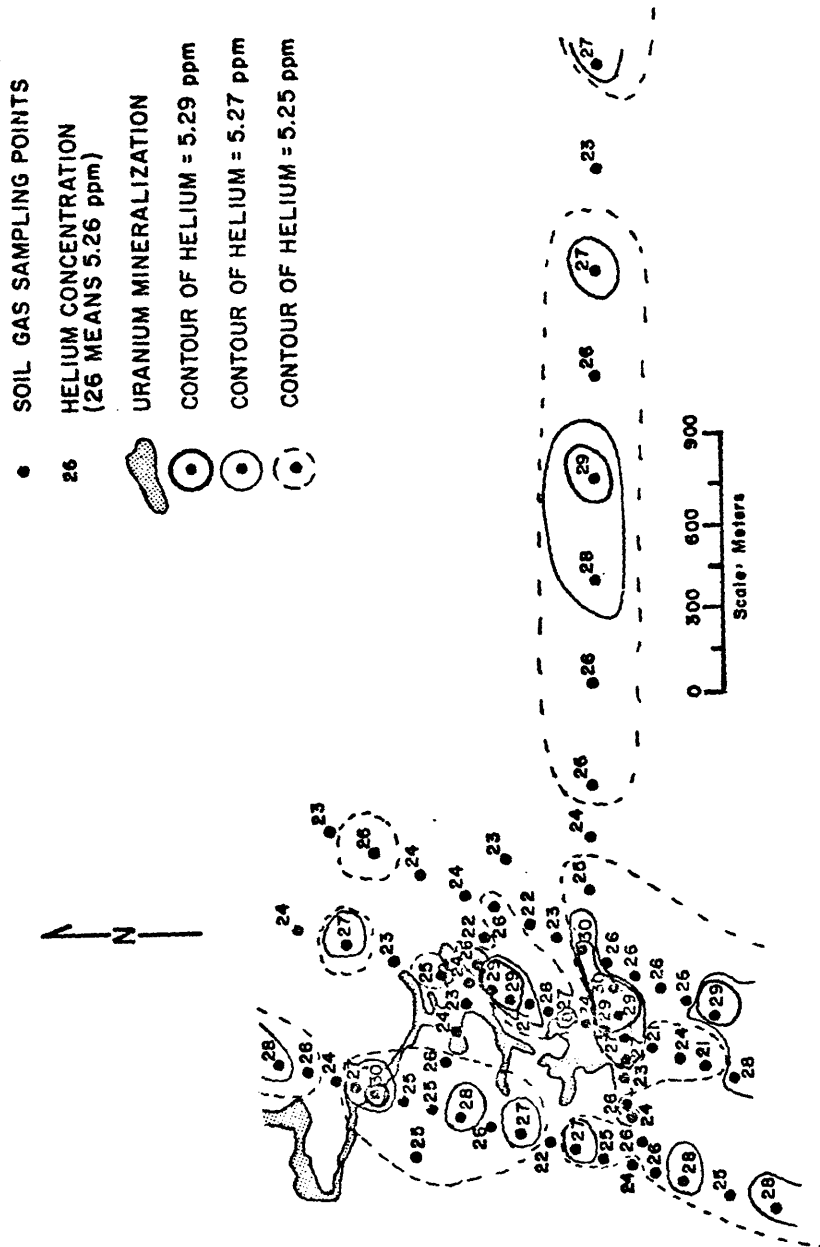


Figure 52. Helium concentration in soil gas at test site B on August 7, 1976. Samples collected 0500 - 0730 MST.

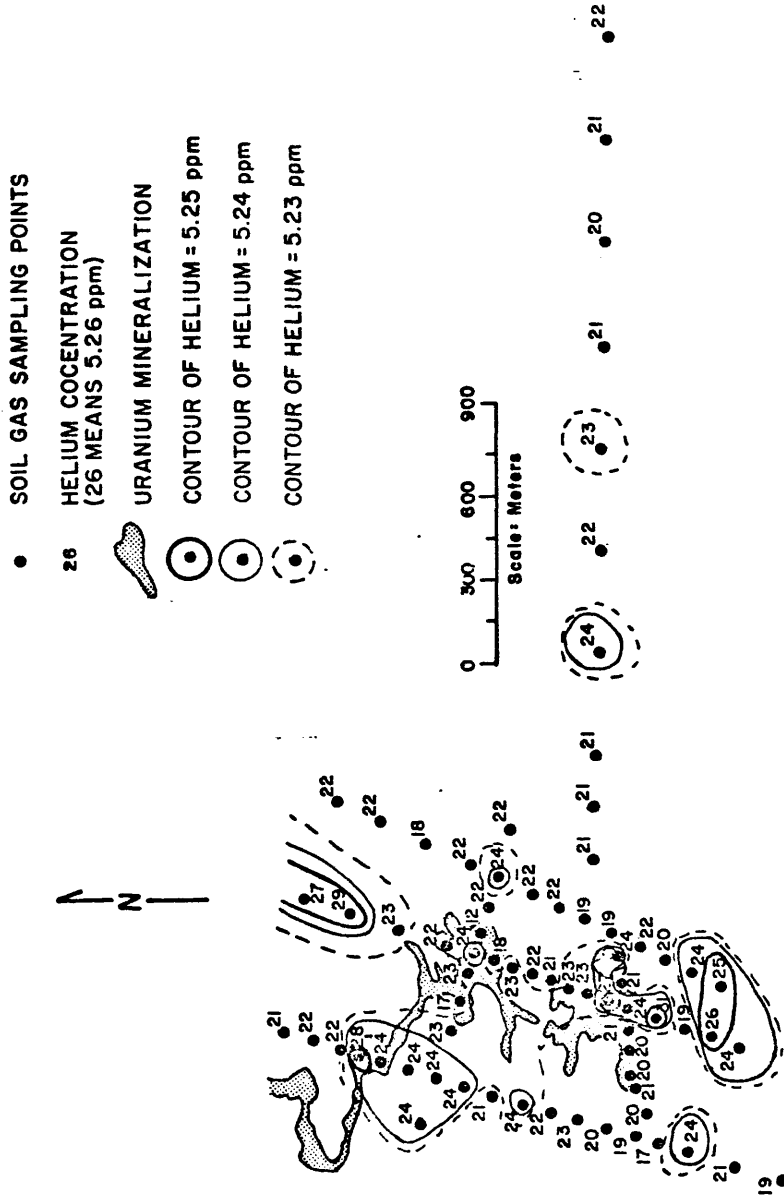


Figure 53. Helium concentration in soil gas at test site B on August 7, 1976. Samples collected 1350 - 1500 MST.

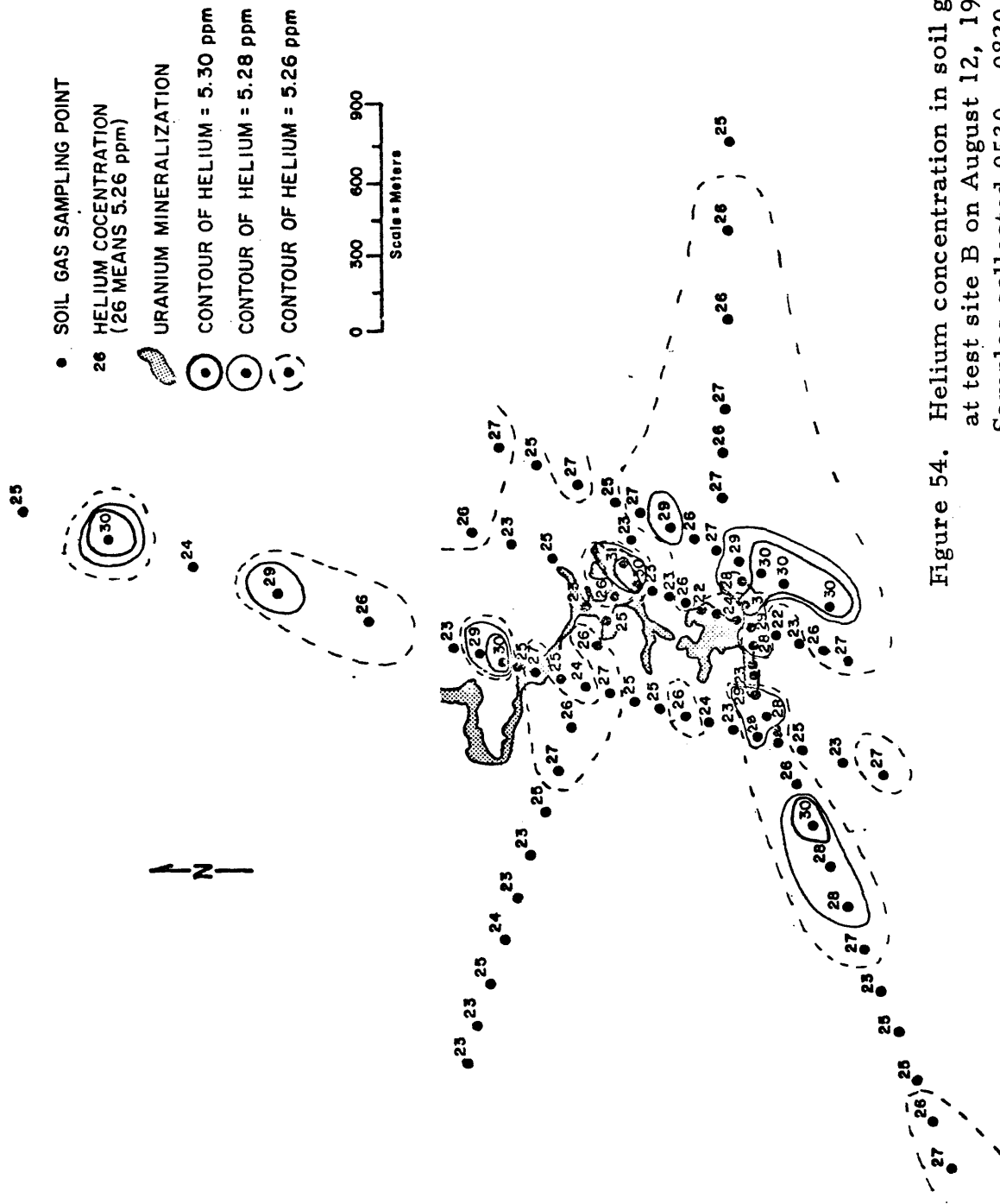


Figure 54. Helium concentration in soil gas at test site B on August 12, 1976. Samples collected 0530 - 0820 MST.

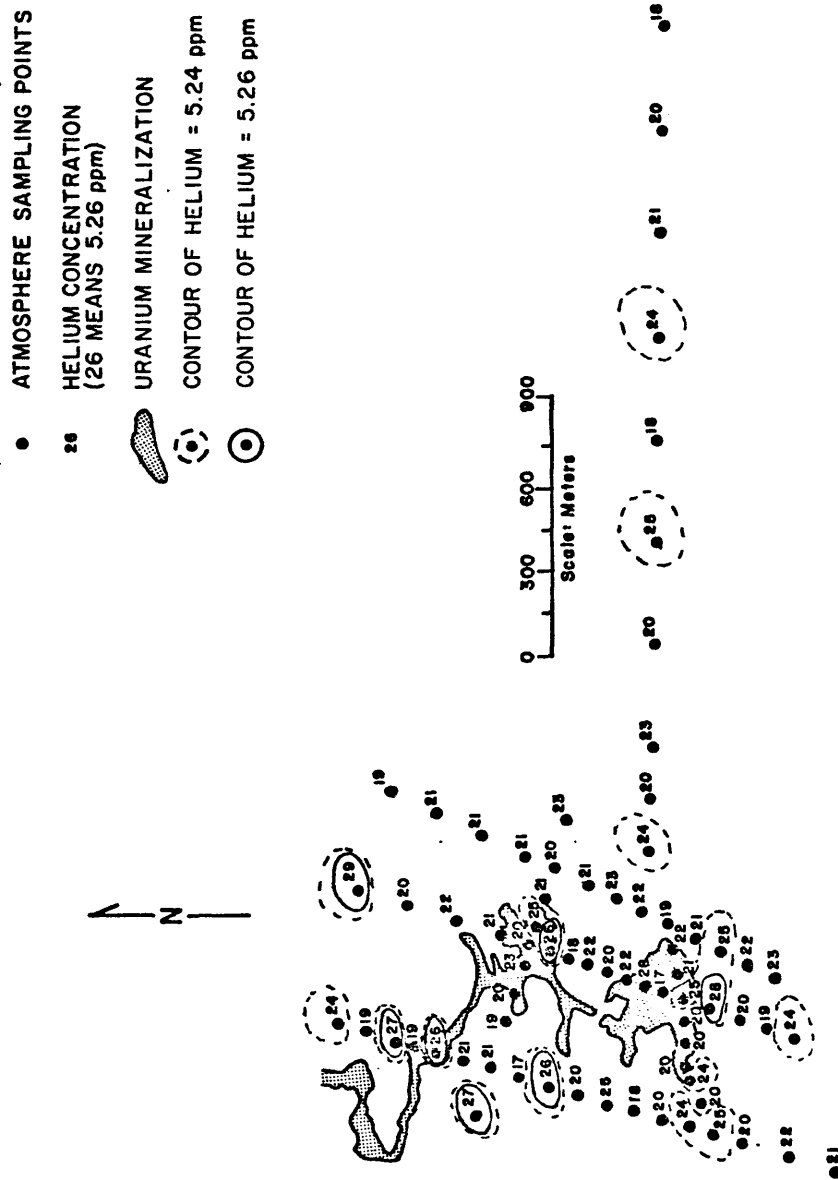


Figure 55. Helium concentration in atmosphere at test site B on August 5, 1976. Samples collected 1350 - 1430 MST.



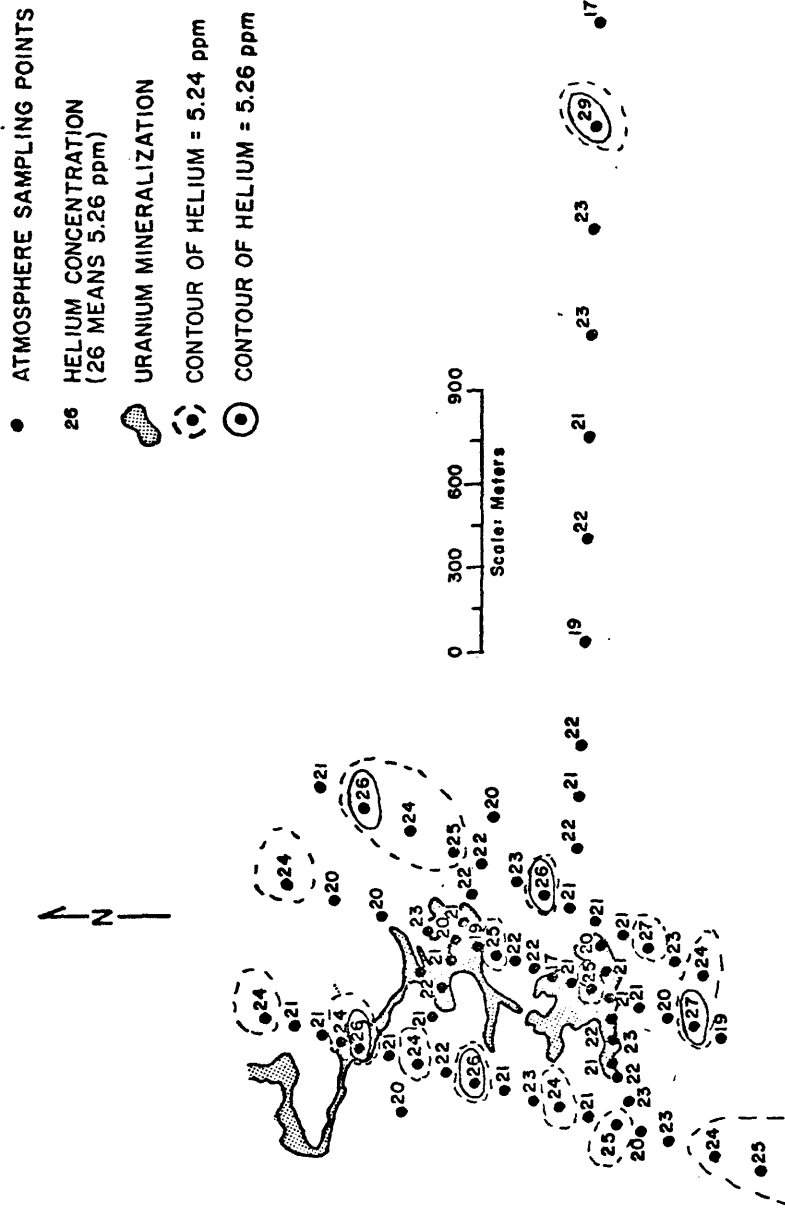


Figure 56. Helium concentration in atmosphere at test site B on August 7, 1976. Samples collected 0500 - 0730 MST.

diurnally, irrespective of position with respect to the subsurface uranium mineralization. On each day when data were collected both in the morning and in the afternoon, the helium concentration in soil-gas generally decreased from 10 to 130 ppb at any one station. Virtually all stations showed this decrease in helium concentration in soil-gas from the morning to afternoon on every day.

- 2) The patterns of highest helium concentrations in soil-gas vary from time to time throughout a single day and from day to day; however, significant areas of anomalous helium in soil-gas (up to 120 ppb above the background threshold concentration) occurred over the subsurface uranium deposits at this test site on seven of the nine times that the survey was conducted. The background threshold is chosen so that most of the measurements (>70%) that fall below this level are within the range of instrument fluctuations. This level tends to be lower for afternoon runs than for morning runs because of the diurnal effect.
- 3) The last column of table 9 shows that on each day that soil-gas data were collected both in the morning and afternoon, the amplitude of the helium-in-soil-gas anomaly above the background threshold was greater in the afternoon than in the morning. Thus, although morning runs yield higher helium concentrations, the afternoon runs showed a greater difference in helium concentration above buried ore and background areas.

- 4) Atmospheric gas samples collected approximately simultaneously over the test site show helium concentrations that range from 5.16 to 5.29 ppm. The instantaneous spread in atmospheric helium concentrations measured in any one run was from 60 to 100 ppb. The average helium concentration of the atmosphere from survey to survey ranged in value from 5.208 to 5.229 ppm. The overall average was 5.223 ppm.
- 5) Atmospheric helium concentrations do not fluctuate systematically in response to diurnal environmental changes.
- 6) No anomalous helium concentrations related to the subsurface uranium deposit have been observed in the atmosphere.

These results indicate that a helium-in-soil-gas grid survey is a viable exploration method for uranium mineralization down to 60 meters. The optimum time for sampling was shown to be in the afternoon. The atmospheric helium concentration, although showing minor fluctuations, shows no correlation to subsurface uranium mineralization.

#### Average Values of Helium in Soil Gas at Test Site B

Figure 57 shows the results of averaging all of the helium-in-soil-gas data from the nine separate runs at this test site. Of a total of 95 sample locations, 14 averaged helium concentration in excess of 5.26 ppm. Five of these are clustered together over the shallower

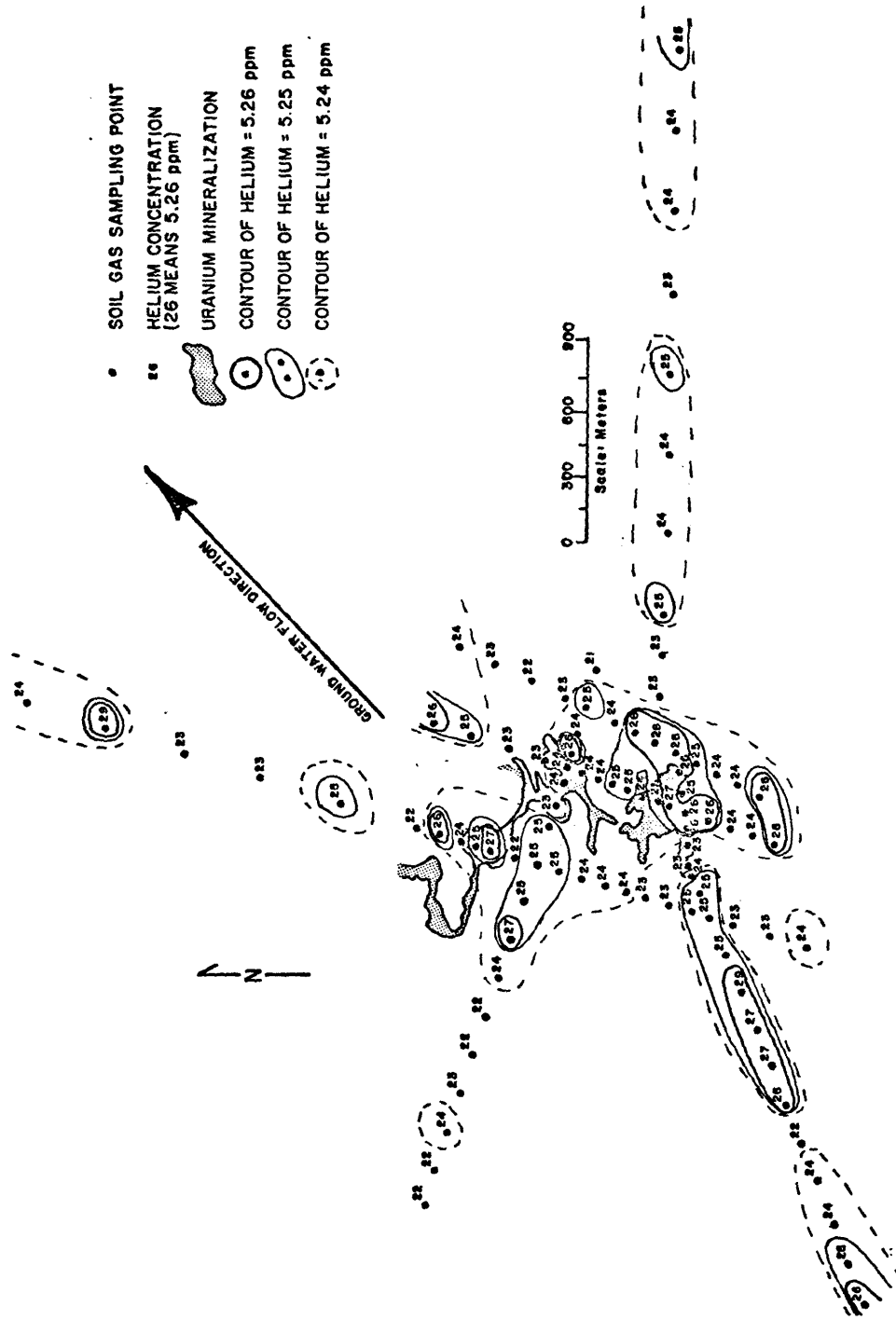


Figure 57. Helium concentration in soil gas. Average of all soil gas measurements at test site B.

mineralization. Also six of these are located on lines where data were collected on only one run (locations 73 through 95) and are, therefore, of less statistical significance. These six high values were from an early morning survey which normally has higher background concentrations. Therefore, these six high values are of much less significance than the other eight.

For the average of all the soil-gas measurements (as seen in figure 57), the entire area of the known uranium mineralization is essentially delineated and overlain by the broad helium-in-soil-gas anomaly. The highest portion of the anomaly occurs on the eastern edge, the leading edge of the uranium roll front. This is probably related to the groundwater movement in the study area. The clearer coincidence of the areas of anomalous helium-in-soil-gas and the known uranium mineralization on the average map (figure 57) versus any individual map (figures 49 through 54) indicates that the detection of helium anomalies would probably be greatly enhanced by the use of a cumulative collection device.

### Test Site C

#### Geology and Hydrology

Test site C is also located north of Douglas, Wyoming, several kilometers north of test site B. Uranium mineralization occurs along sinuous roll fronts in four fluvial sandstones from 110 to 150 meters deep. The regional relationships of the host sandstones are shown in the cross section of figure 58. The sediments consist of medium- to coarse-grained arkosic sandstones deposited as point-bar sequences

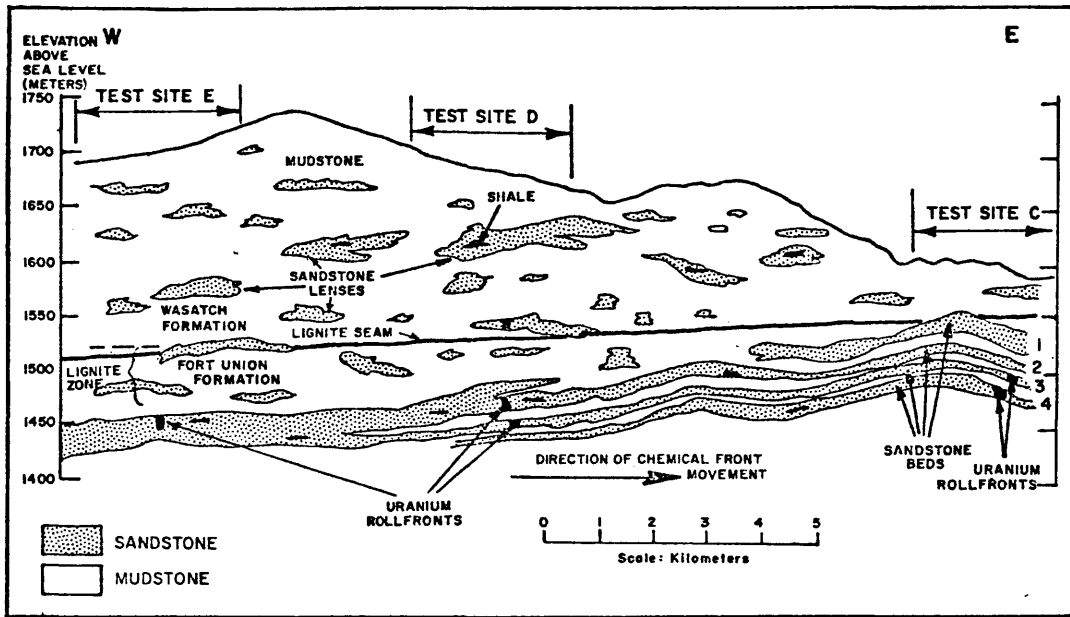


Figure 58. Generalized cross section of the Wasatch and Fort Union formations in the southern Powder River Basin.

in meander-belt fluvial systems. Carbonaceous and tuffaceous material are common. The groundwater flow is from southwest to northeast.

A reference map for this test site is shown in figure 59. The depths to the indicated roll fronts are shown in figure 58.

#### Helium Soil Gas and Atmosphere Measurements

Initially, atmospheric and soil gas samples were collected on 90 to 150 meter spacing along a 2.4 km traverse. The stations are shown in relation to the mineralization in figure 59 (station 1 to 23). The soil gas results for five passes along the traverse are shown in figure 60. The samples for the first run were collected on August 6, 1976. The other four were performed on August 9, 1976. There was no detectable helium anomaly over any of the uranium mineralization on any of the runs. The helium measurements of the atmosphere are not shown since they do not add anything of significance.

The difficulty in observing any significant helium anomaly in single line traverses is again illustrated here. Consequently, work performed at subsequent test sites was done only in grid arrays. The sample coverage at this test site was expanded on August 13, 1976, to include a western extension of the original line, another east-west traverse further north as well as a north-south traverse cutting through the other two. The helium concentration in soil gas collected on August 13 between 0810 and 1040 Mountain Standard Time on these three traverses is shown in figure 61. This map shows a pattern of anomalous helium concentration associated with the mineralization but displaced in the direction of groundwater flow. The largest area of

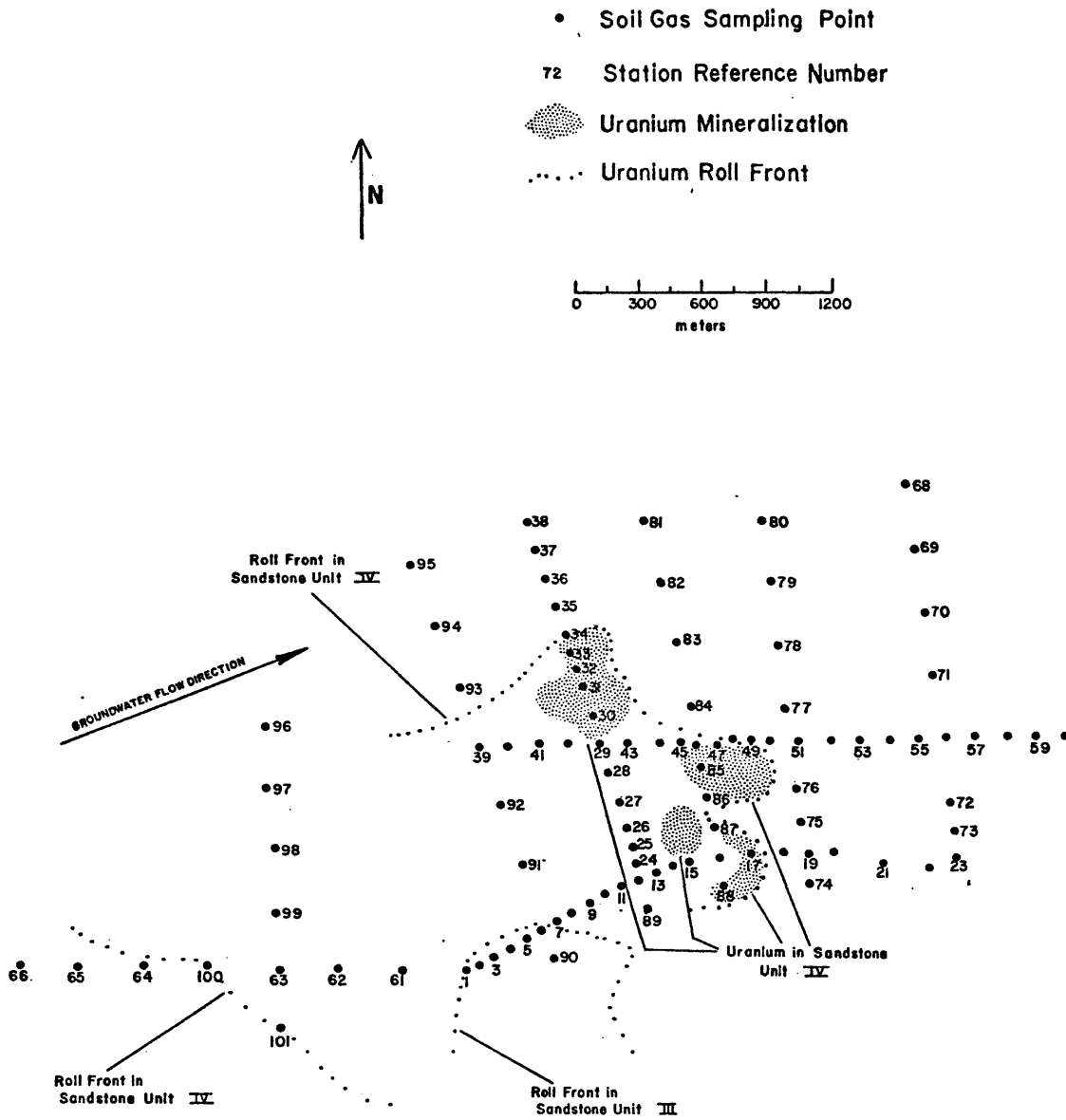


Figure 59. Uranium deposits and helium sampling stations, test site C. Beds III and IV shown on figure 58.



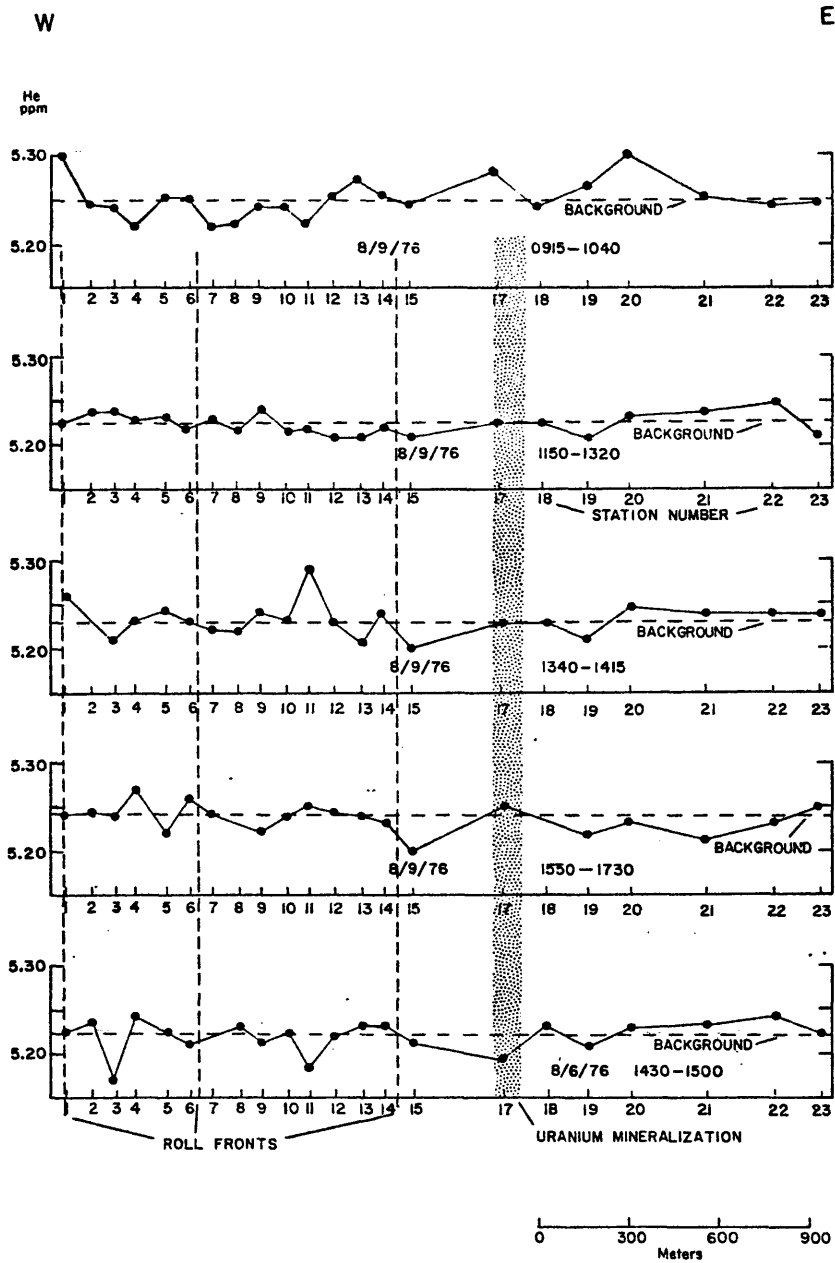


Figure 60. Helium concentration in soil gas measured five times on east-west traverse of test site C. Uranium mineralization in sandstones III and IV, as shown in figures 58 and 59.

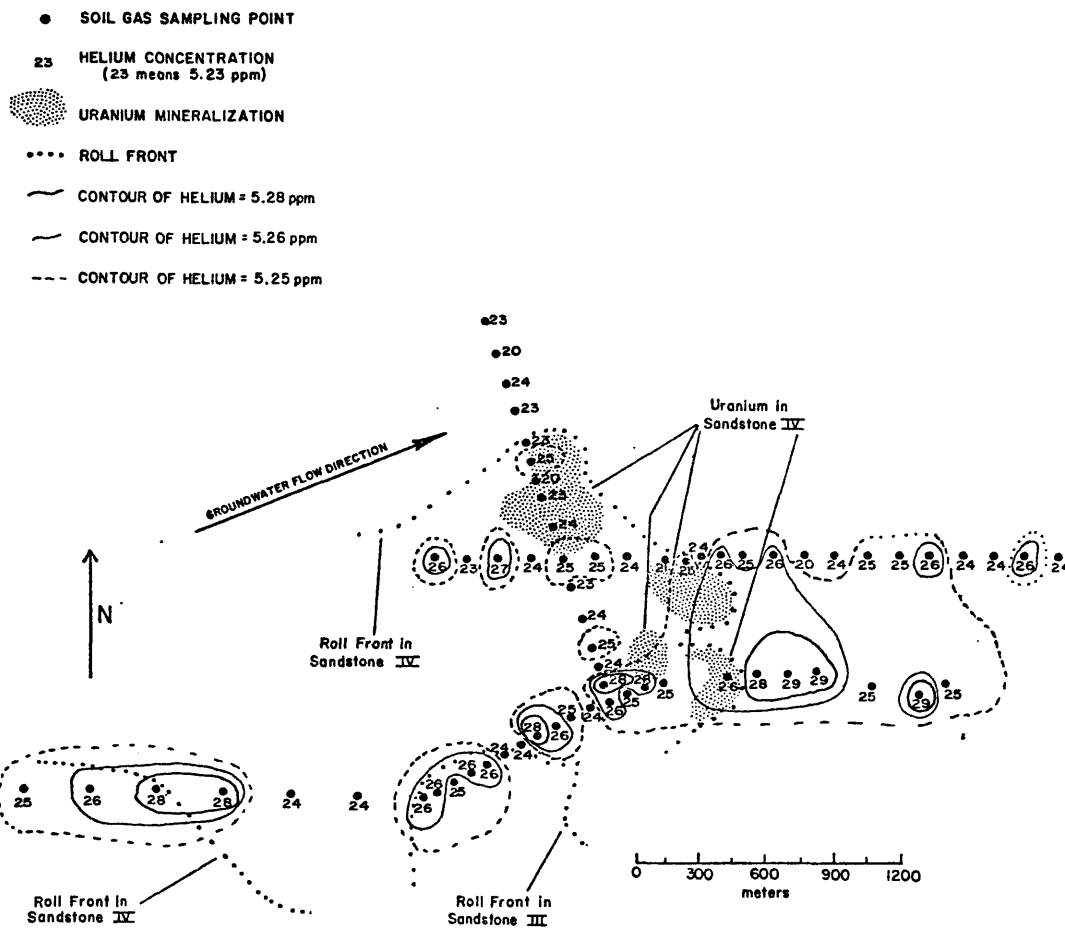


Figure 61. Helium concentration in soil gas for samples collected on August 13, 1976 between 0710 and 0940 MST at test site C. Sandstone beds III and IV shown on figure 58.

helium enhancement is east of the largest zones of mineralization. Slight enhancements occur southeast of the roll fronts in the reduced portion of the sand.

The next sample collection took place on August 21, 1976 between 0700 and 1200 Mountain Standard Time. For this survey, the collection area was expanded to include five more north-south lines as shown in figure 62. Again a helium anomaly is observable to the east-southeast of the major deposits and a repetition of the enhancement occurs at the western roll front. In addition, however, a strong helium anomaly was detected to the west of the ore bodies. This is somewhat surprising but may be due to uranium mineralization along the northern roll front west of the mineralization that is shown on the map.

Measurements of helium in the atmosphere were also made at the same times that soil gas measurements were made. The data are not included here since they do not add anything of significance. As an indication of the difference between atmosphere and soil gas measurements, all 97 points measured at test site C on August 21, 1976 averaged  $5.226 \pm 0.0166$  ppm helium for atmospheric samples and  $5.273 \pm 0.264$  ppm helium for soil gas samples. The higher average values and the greater standard deviation reflects the existence of positive anomalies in the soil gas data. The spread of data also illustrates this. In the atmosphere, data range from 5.18 to 5.27 ppm helium, while for the soil gas the data range from 5.22 to 5.34 ppm helium.

The shifting pattern and location of the helium-in-soil-gas anomalies with time suggest that helium prospecting would be more

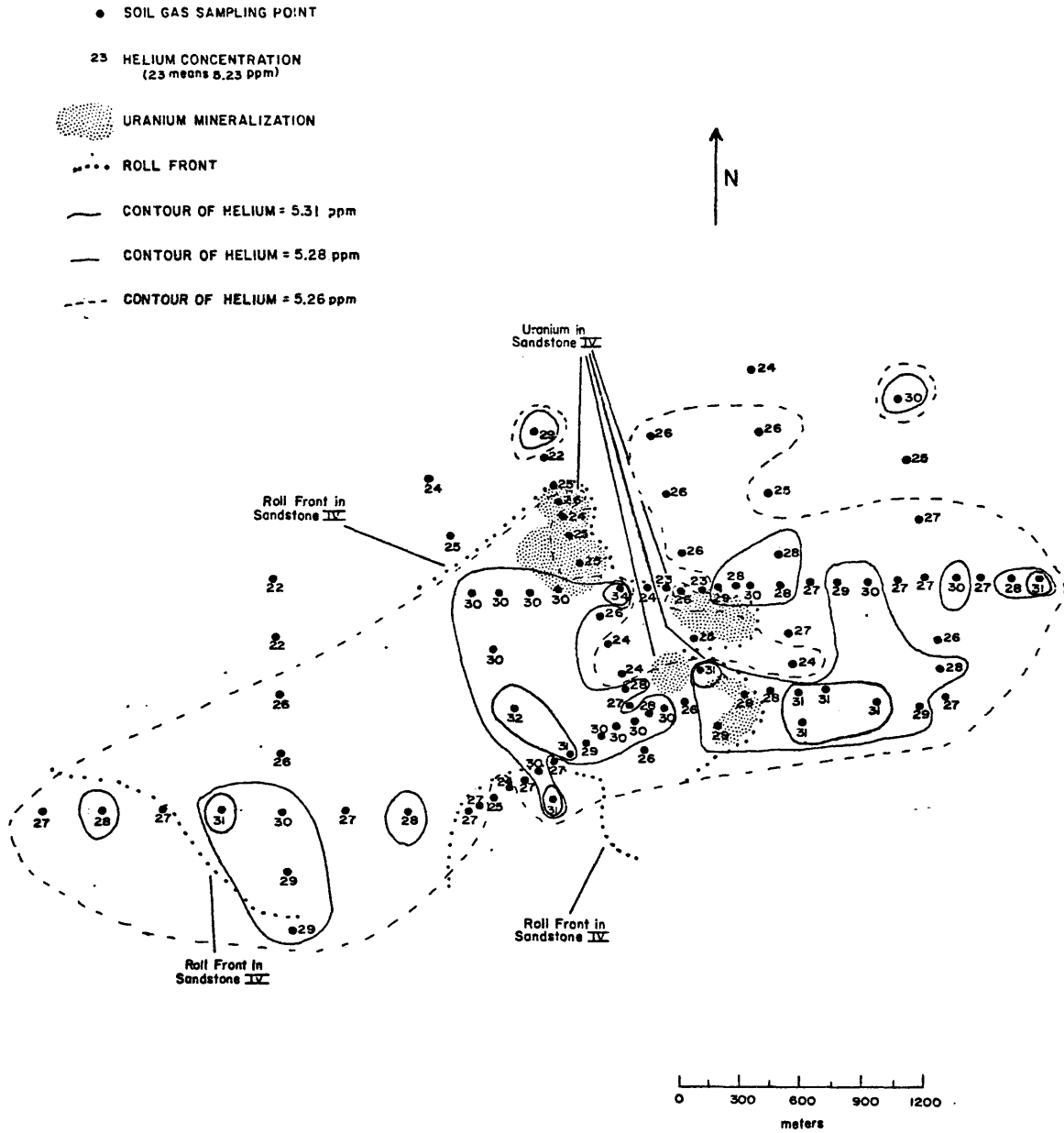


Figure 62. Helium concentration in soil gas for samples collected on August 21, 1976 between 0600 and 1100 MST at test site C. Sandstone beds III and IV shown on figure 58.

useful in the detection and discovery, with reconnaissance-fence drilling, of an area of uranium mineralization rather than the exact location of an individual uranium deposit. A summary of all the soil gas runs conducted on test site C is given in table 10.

#### Helium Dissolved in Well Water

Samples of water from 14 wells within test site C were collected in one-liter plastic bottles and analyzed for their helium content. All of the wells extend to the lowest mineralized horizon, are cased over the entire length, are perforated at the four sands shown in figure 58, and are capped with a tap. The wells which were not operating at the time of sampling were allowed to flow for five minutes before collecting a sample, thus insuring that the water sample was fresh from the aquifer and not contaminated by the atmosphere. The helium concentration in the air in the space above the water in the bottle was measured after equilibrating with the helium concentration in the water. The helium-in-well-water data are shown in figure 63. A clustering of wells having helium concentrations in excess of 6.0 ppm is observable to the west of the ore bodies. This western displacement is probably attributed to mineralization to the west of that shown in figure 63.

#### Test Site D

##### Geology and Hydrology

Test site D is several kilometers west of test site C. It is a continuation of the fluvial system described at test site C; consequently, mineralization occurs within the same sandstones (figure 58).

Table 10. Helium-in-soil-gas Anomalies at Test Site C.

Day	Time of Day*	Nature of Grid	Range of He Concentration (in ppm)	Background Threshold He Concentration (BGT) (in ppm)	Position of He-in-soil-gas Anomaly(ies)	Size of Anomaly	Amplitude of Anomaly over Known Uranium
8/ 6/76	1430-1500	1 line (22 stations)	5.16 -5.24	5.22	No pattern		None
8/ 9/76	0915-1040		5.22 -5.30	5.25	Over and in front of leading edge of principal uranium ore.	600 m wide	Up to 50 ppb > BGT
	1150-1320	1 line	5.21 -5.25	5.23	No pattern		None
	1340-1415	(22 stations)	5.20 -5.29	5.23	300 m to east of mineral-ization.	600 m wide (E-W)	
	1555-1730		5.20 -5.27	5.24	Generally over uranium mineralization.	300 m wide and spotty	Up to 30 ppb > BGT
8/13/76	0710-0940	3 lines (65 stations)	5.20 -5.29	5.25	Over and at leading edge of roll-front mineralization	600 m by 300 m	Up to 40 ppb > BGT
8/21/76	0600-1100	8 lines (100 stations)	5.22 -5.3	5.26	Over and spread out from roll-front mineralization.	900 m N-S by 2100 m E-W	Up to 60 ppb > BGT
Average of Data of 8/13, 8/21		8 lines (97 stations)	5.250-5.330	5.290	Over & in front of leading edge of roll-front mineralization.	Up to 450 m by 450 m	Up to 40 ppb > BGT

\*All times presented as Mountain Standard Time

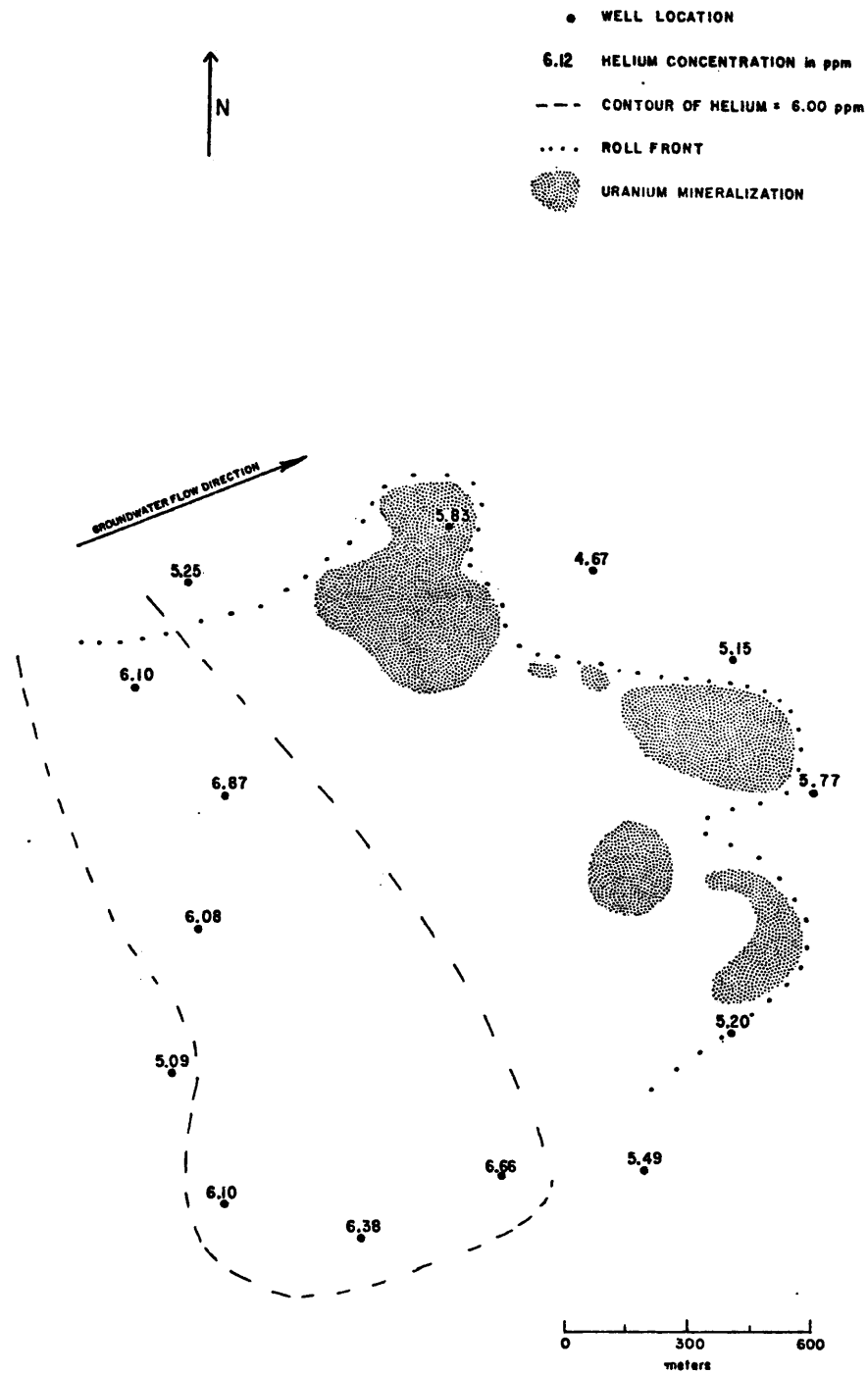


Figure 63. Helium concentration in ground water collected on October 26, 1976 from wells in test site C.

Due to the slight westerly dip on this flank of the basin, the mineralization at test site D is down dip of mineralization of test site C. Mineralization occurs at depths of 140 to 240 meters. Groundwater flow is to the northeast.

#### Helium Soil-Gas and Atmosphere Measurements

A helium-in-soil-gas survey was conducted at this test site without prior knowledge of the location of the uranium mineralization. As seen in figure 64, a semi-rectangular grid pattern was used with samples taken on 150 and 300 meter spacing. A subsequent survey was made on an expanded grid utilizing 34 of the original sample locations with stations on 300 meter spacing.

Soil-gas and atmosphere samples were collected at test site D from 0600 - 1000 MST on August 27, 1976. After the samples were analyzed, the location of the subsurface mineralization was provided by the mining personnel. A large helium-in-soil-gas anomaly of greater than 5.31 ppm was found to overlie three subsurface zones of mineralization, as seen in figure 65. The general area of mineralization was overlain by a helium envelope of greater than 5.29 ppm. The area away from the mineralization, the background, averaged less than 5.27 ppm.

Samples from the atmosphere, collected at the same time as the soil-gas, failed to show any significant enhancement (figure 66). Because of their lack of significance, this represented the last time during this research that atmospheric samples were collected on a routine basis.



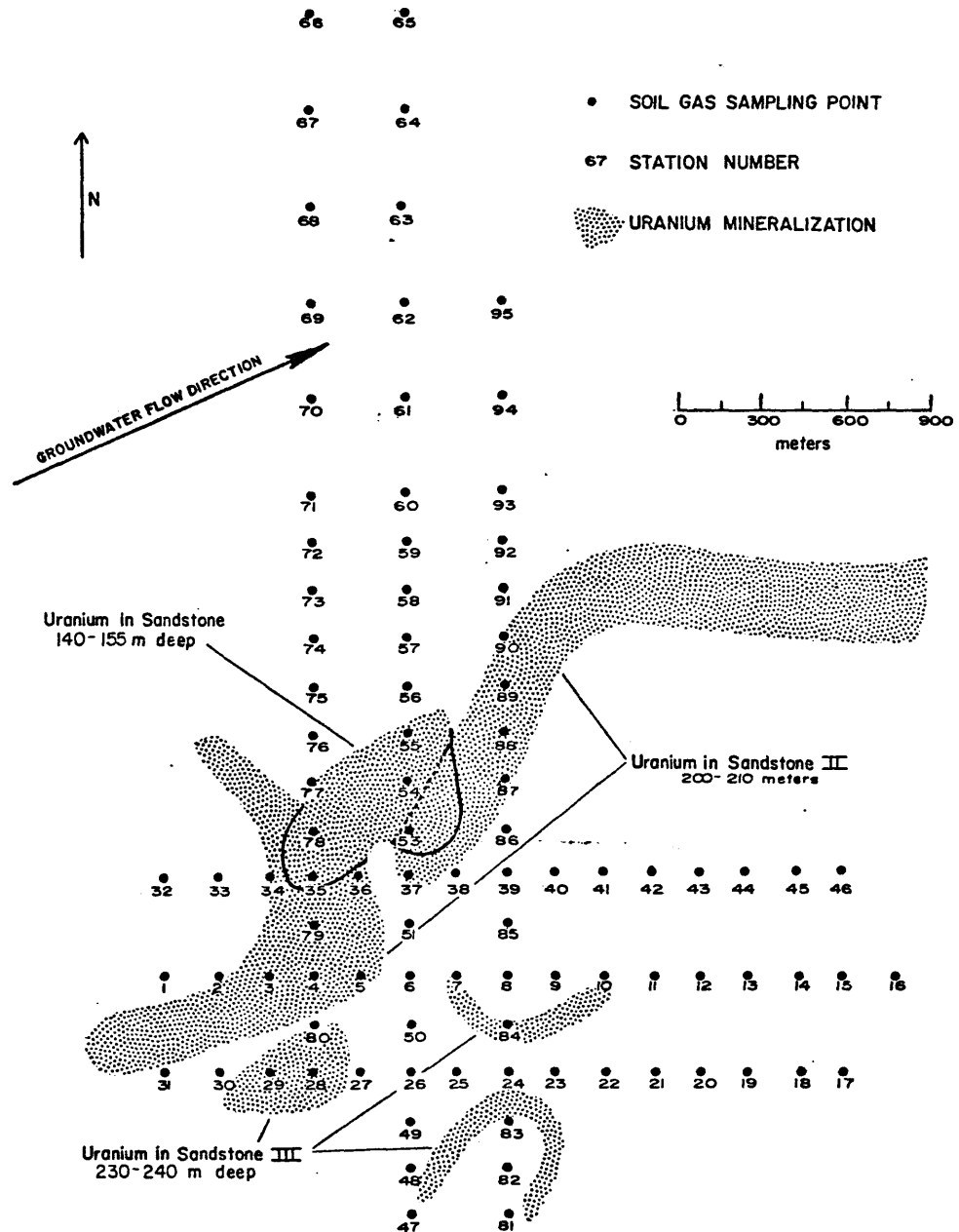


Figure 64. Uranium ore deposits and helium sampling stations for the August 27, 1976 survey, test site D.

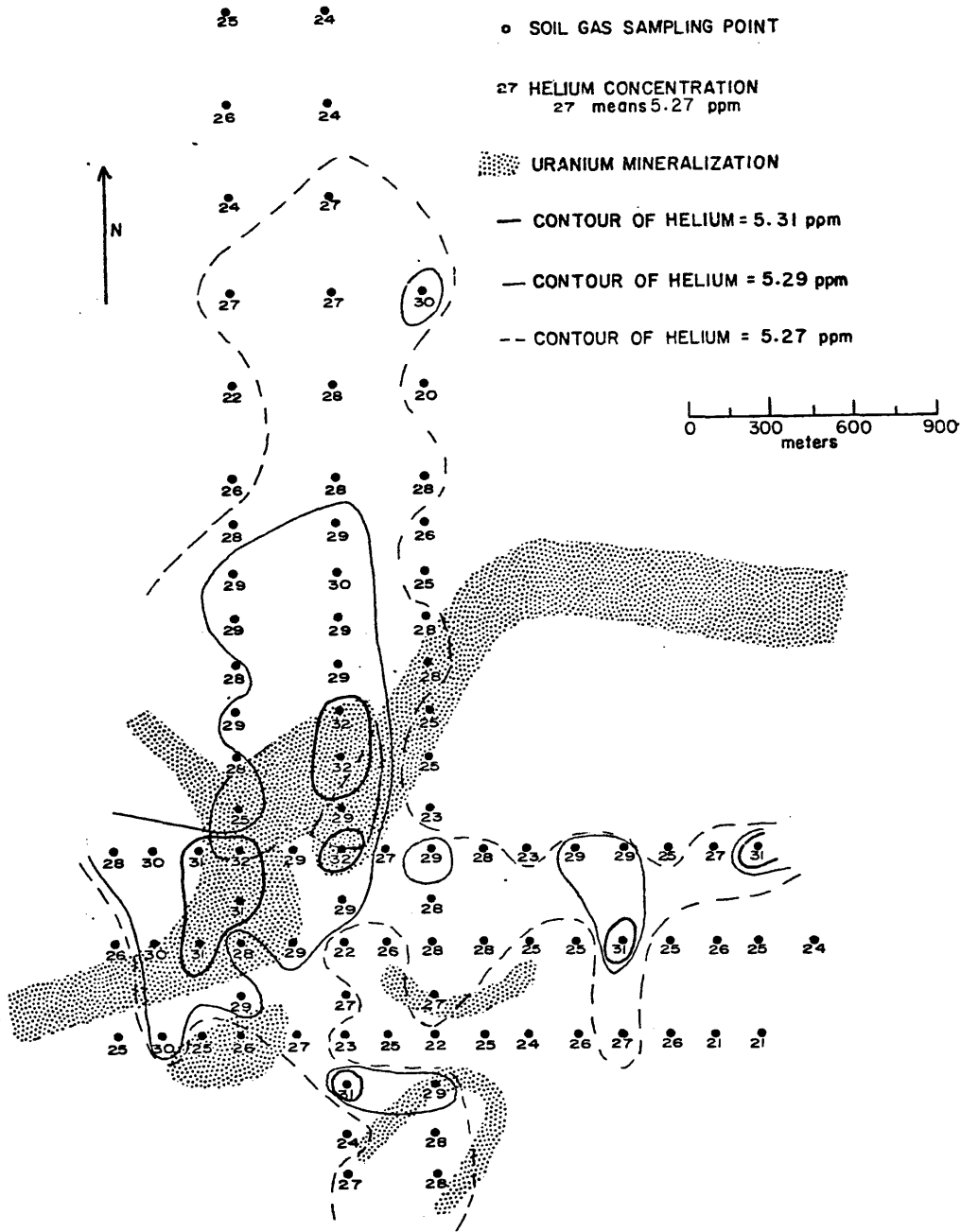


Figure 65. Helium concentration in soil gas collected on August 27, 1976 from 0600 to 1000 MST, test site D.

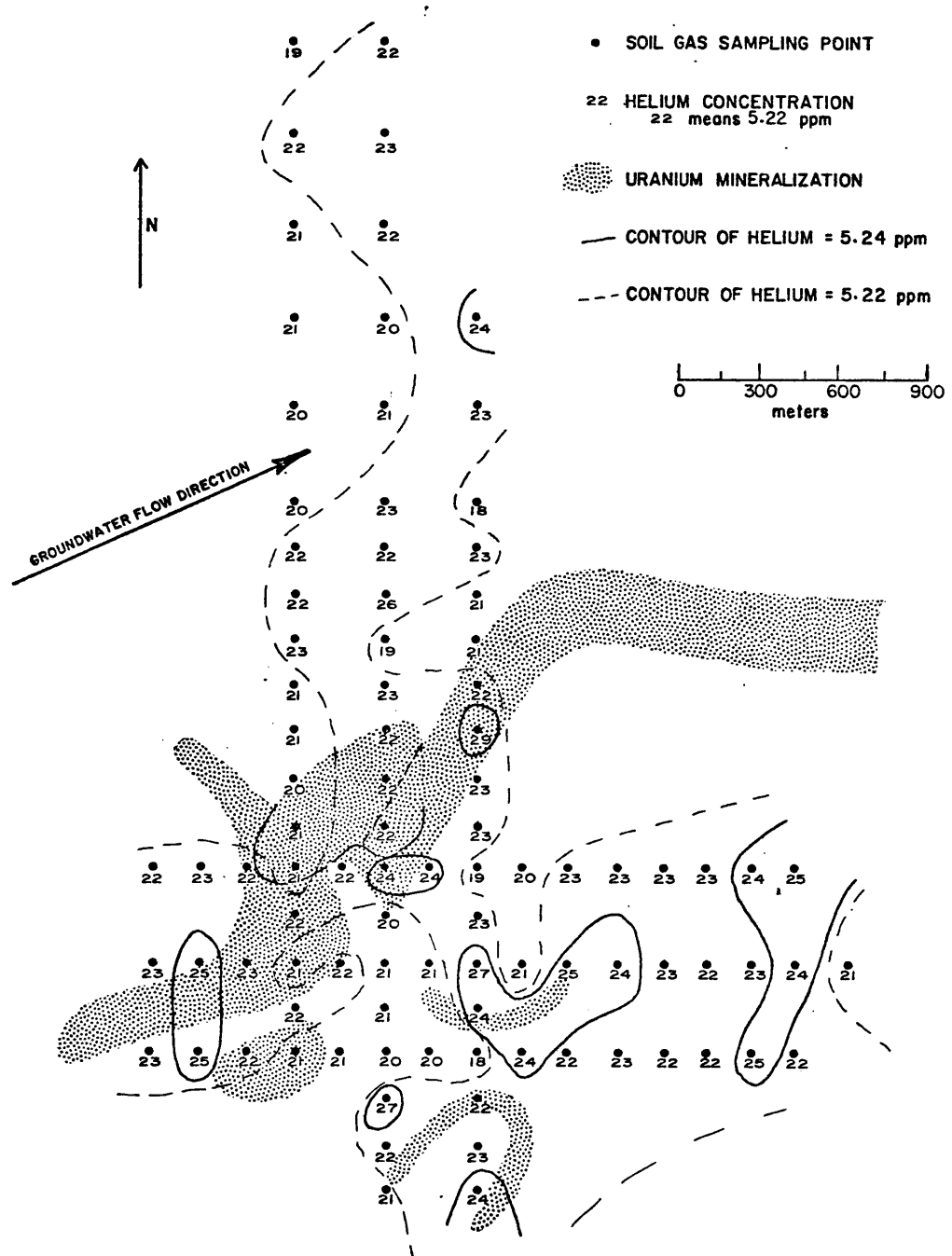


Figure 66. Helium concentration for atmosphere samples collected at test site D on August 27, 1976 from 0600 to 1000 MST.

On September 17, 1976 the survey was performed on the expanded grid. One hundred and fifteen samples were taken. The results are shown in figure 67. Again a large halo of helium enhancement is observed over the uranium mineralization. There is also an extension of anomalous helium concentration to the southwest. This is possibly related to minor amounts of mineralization to the west of that shown. Two large areas of background concentration were seen to the northwest and southeast.

These surveys show the greater utility of the grid pattern sampling over the single line traverses. The advantage of making the survey large enough to include a suitable amount of background area is also shown.

#### Diurnal Test of Helium Concentration as Related to Moisture Content

In previous work, diurnal variations in helium concentration in soil-gas were observed. Consistently during the summer months helium values in soil gas were high during the night time and early morning hours and showed a decrease in the midday compared to a relatively constant atmospheric helium concentration. This variation showed an inverse correlation with air temperature. A possible explanation of this is that the relative amount of water vapor in the sample is changing as a result of temperature (Joe Martin, 1977, personal communication). At night time, as the comparatively warm soil-gas is drawn through the cooler probe, condensation of the water vapor may occur which would increase the relative amount of helium in the sample.

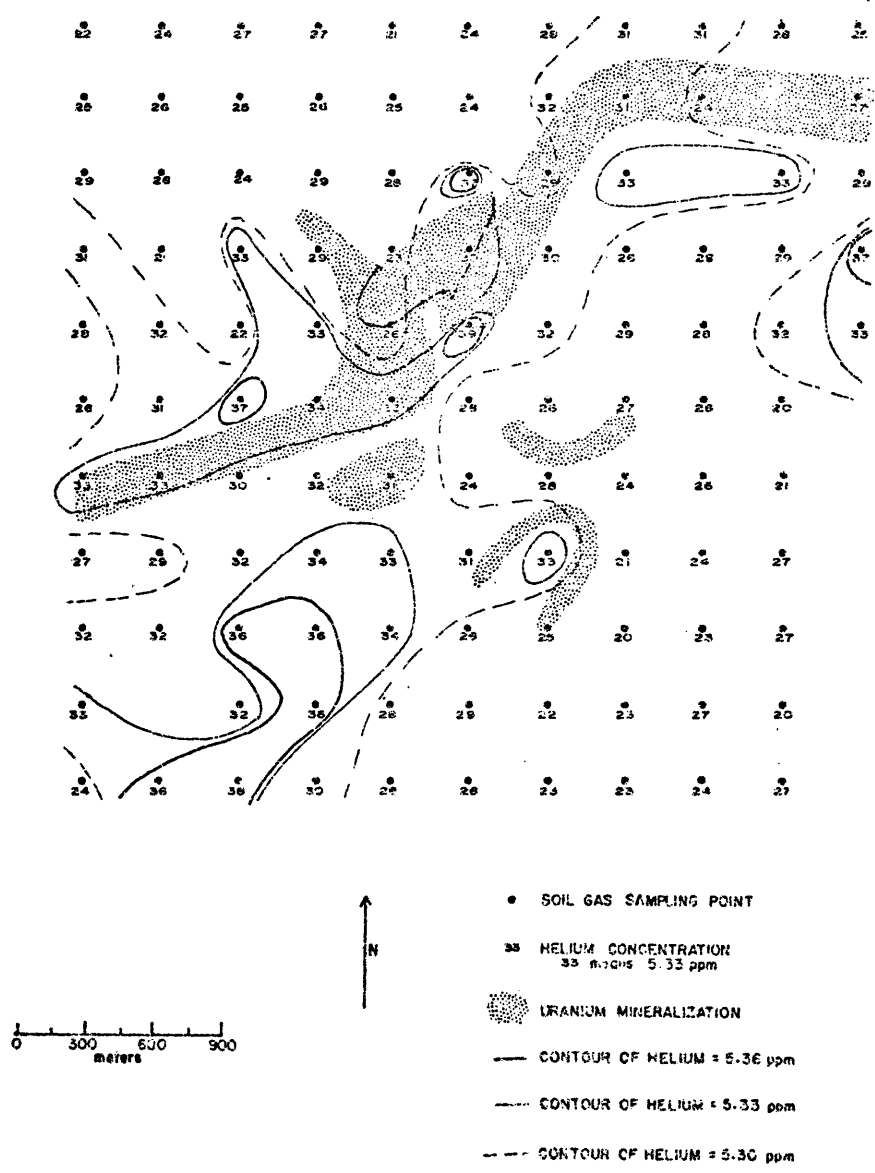


Figure 67. Helium concentration in soil gas collected on October 17, 1976 from 0900 to 1400 MST, test site D.

It was decided to test this hypothesis by performing another twenty-four hour test. This was done from 1200 MST to 1200 MST on October 23-24, 1976. Six probes were left in the ground at test site D. The method was to collect two samples from each probe every two hours. One sample was collected in the normal way while the second sample was drawn through a phosphorus pentoxide dessicant. The results are shown in figure 68. No systematic diurnal helium-in-soil-gas variations were detected, either with or without the dessicant. On the day that the test was made, the range in air temperature was from 40°F (4.4°C) to 28°F (-2.2°C). When the greatest diurnal variations were noted during the summer, the temperature ranged from a high of 100°F (37.8°C) to a low of 45°F (7.2°C). The decrease in range of air temperature virtually eliminated the diurnal variation at this test at test site D. This is seen in the undried samples in figure 68. Because the helium concentration in the soil gas was now maintaining a level of constancy, it was no longer necessary to collect samples only within a two to three hour period.

#### Syringe Diffusion Leak Test

Leak tests performed earlier in the program resulted in a five per cent per hour decrease in the helium-content differential between the sample and the atmosphere. In the short time between when the samples were collected and their analysis, any anomalies would still be detectable. In order to expand the program, to lessen the dependence on storage time in the syringe, and to increase accuracy, the sample syringes were treated to make them more leak resistant. The syringes were capped with rubber stoppers and the needle fittings and rubber plungers were coated with high vacuum grease. Also, the syringes

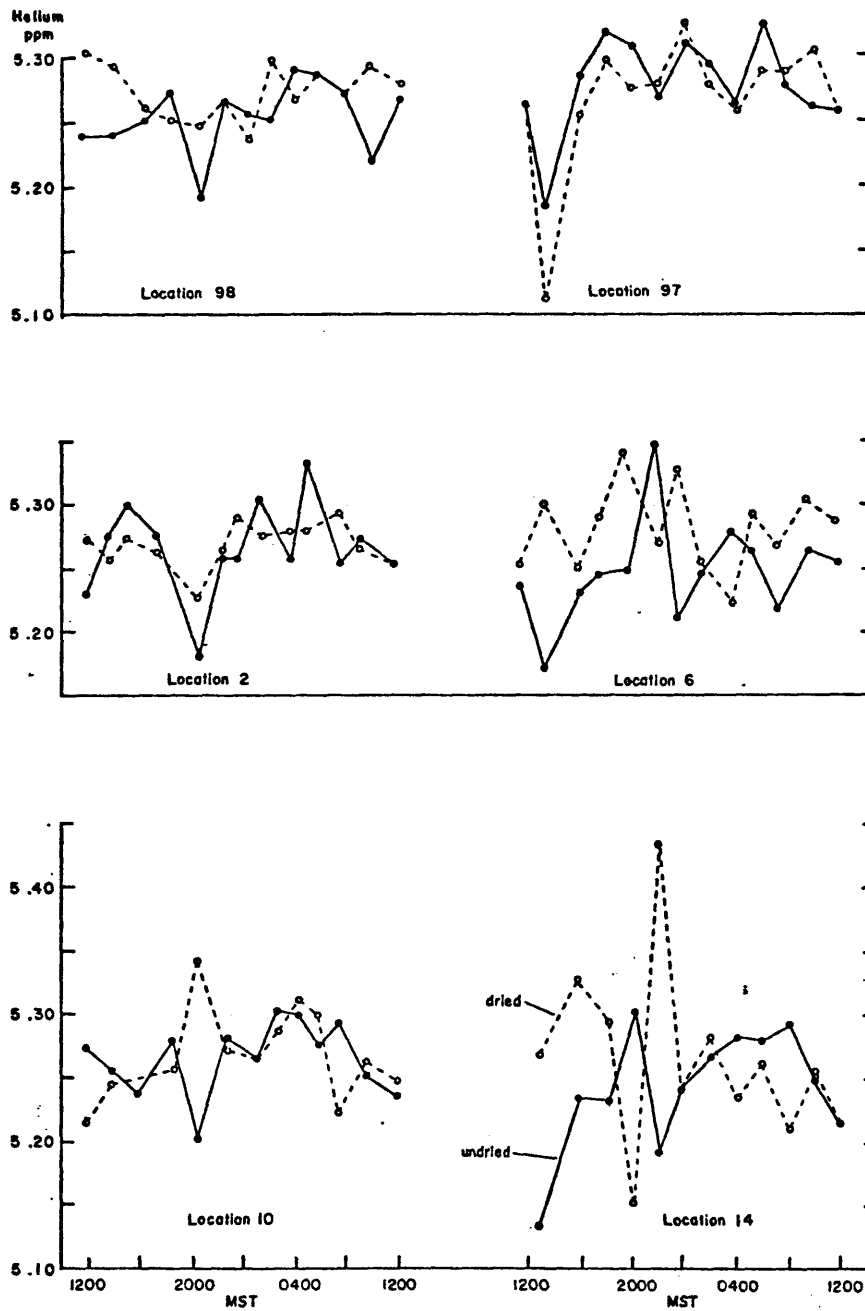


Figure 68. Helium concentration in soil gas collected from probes at six locations across test site D at two-hour intervals over a 24-hour period on October 23-24, 1976, with undried and dried samples ( $P_2O_5$  dryer).

were discarded when dirt began to accumulate and they showed signs of wear. This procedure started when work began at test site B, but the leak rate was not tested until the twenty-four hour test described above.

Twenty-eight syringes were filled with the 7.65 ppm reference gas. Two syringes were measured approximately every two hours throughout the twenty-four hour test. The results are shown in figure 69. With this procedure the leak rate amounted to an average 0.69 per cent decrease in the differential per hour. This was an order of magnitude decrease from the earlier leak rate and made it possible to hold the samples up to twenty-four hours if it was needed. This test also gave an estimate on the consistency of the syringes. Two of the twenty-eight syringes appeared to leak more than the others.

#### Radon Counting Rates Measured with MERAC's

MERAC alpha counters were planted at thirty of the sample locations at test site D on October 21, 1976. They were read five times through November 8, 1976. The results of this are shown in figure 70. There is a high degree of similarity between the helium results of figure 70 and the MERAC data. This was the closest correlation between the helium and radon data for any of the test areas.

#### Gamma-Ray Analyses of Soil Samples

Thirty-four soil samples were collected from the MERAC holes to compare several non-gaseous isotopes with the radon and helium data. The soil samples were analyzed for bismuth-214 and thalium-208 by Geolabs division of Natural Resources Laboratory.



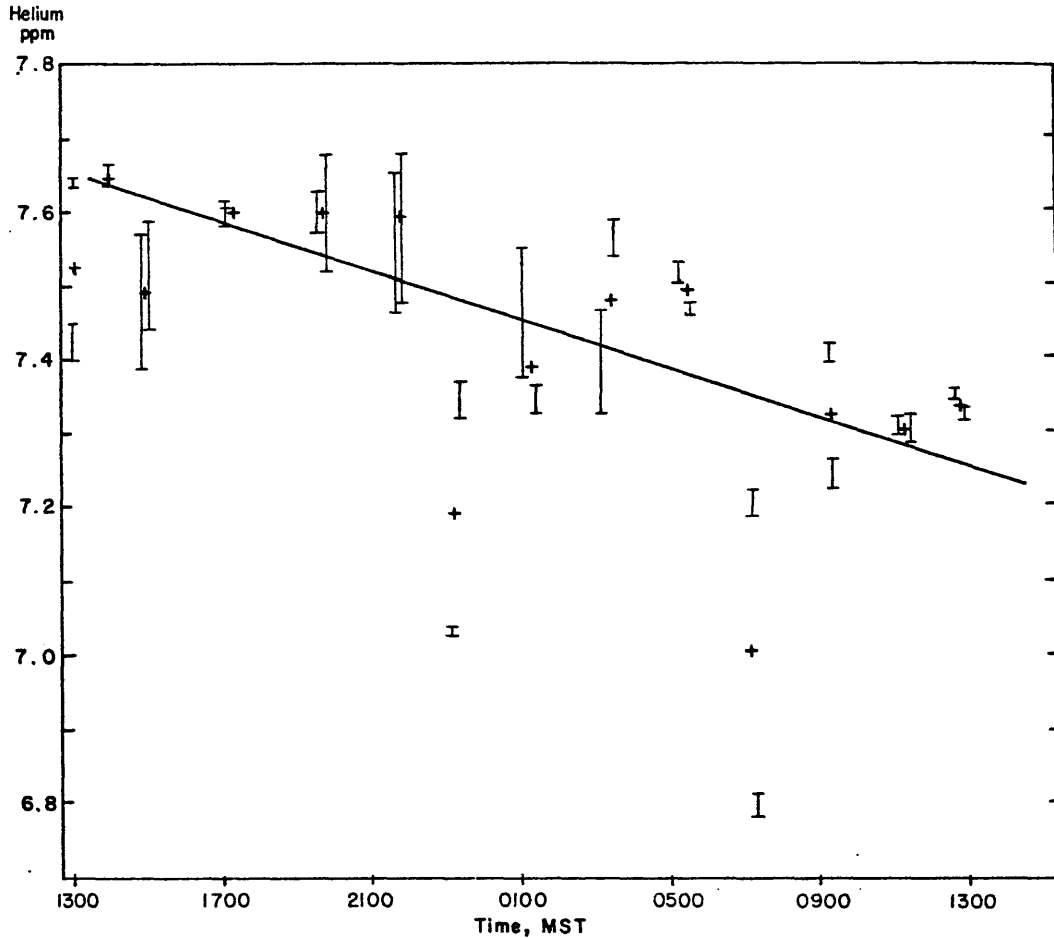


Figure 69. Syringe leak test over a 24-hour period with 24 capped B-D syringes all loaded with R<sub>7</sub> reference gas at the start of the period. The average leak rate measured is 0.69%/hr. (represented by the solid line) of the concentration differential between inside and outside the syringe. Two syringes were measured at each two-hour interval with three measurements from each syringe. The error bars represent the extremes of the three measurements from one syringe. The x's represent the average from the two syringes. Evidently, two syringes (measured at 2400 and 0800 MST) were particularly leaky.

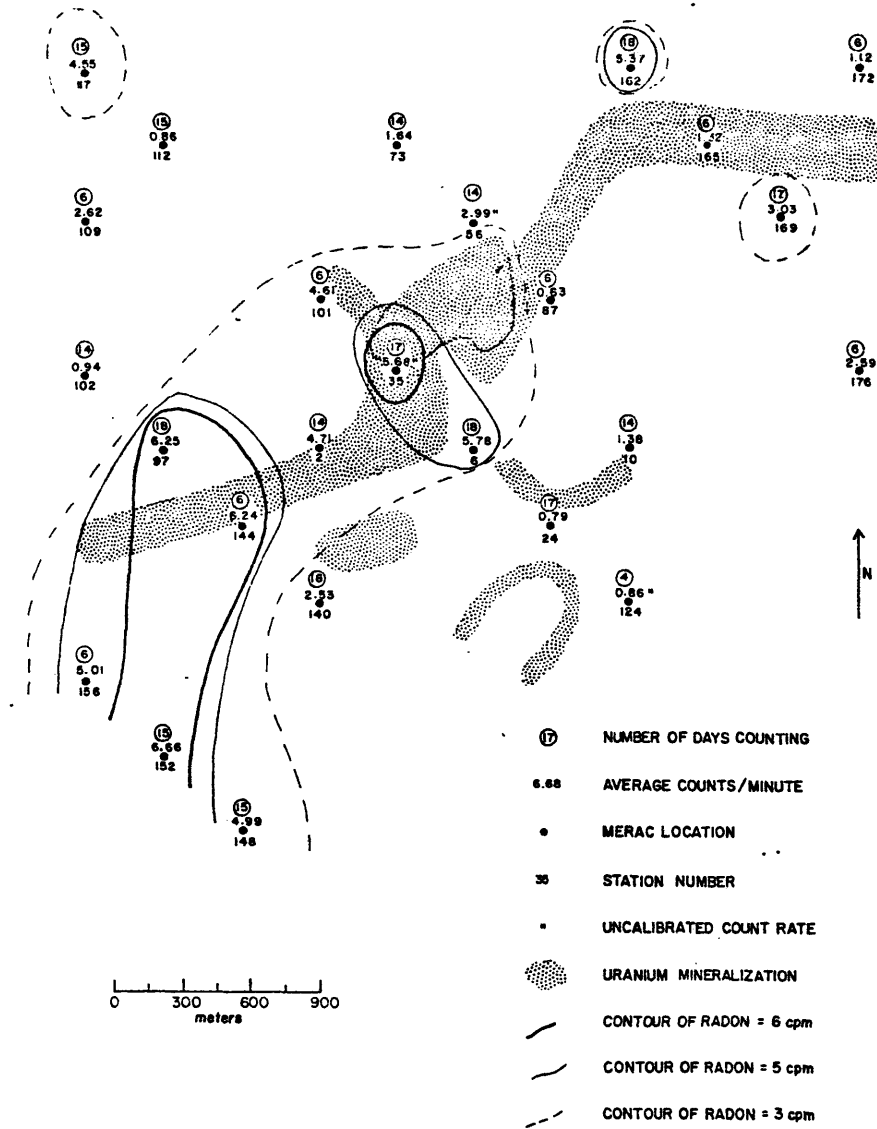


Figure 70. Radon counting rates measured with MERAC's buried 60 cm deep at the locations where average counts/min are indicated, test site D.

Before analysis, twelve of the samples were split and sent to Teledyne Isotopes for further gamma-ray analyses. The Geolab results are shown in table 11 and figure 71. Teledyne Isotopes analyzed the soil samples for potassium-40, cesium-137, actinium-228, radium-226, bismuth-214 and lead-210. These results are shown in table 12. Figure 71 is similar to both the helium and radon contour maps (figures 67 and 70). There is a cluster of points that exceed four ppm  $eU_3O_8$  that extend to the northwest, however. The dissimilarity between figures 70 and 71 suggests that the radon (and helium) are not a result of near-surface production but are from mineralization at depth. Stations 117 and 109 are anomalous in both figures, however. This similarity, along with a lack of subsurface mineralization at these stations, indicates that in those localities the radon is probably being produced in the soil.

For comparison, the data from tables 11 and 12 are plotted along with MERAC data in figure 72 at the different stations. In the thorium related isotopes, there is a good correlation between the actinium-228 and thalium-208. There is also a moderate correlation with the lead-212. The correlation between the thalium-208 measurements from the two laboratories is not as good as expected. This is possibly due to sample inhomogeneity.

In the uranium series, there is a good correlation between the radium-226 and bismuth-214 data. Again the correlation between the two bismuth-214 analyses is not as good as expected.

Unfortunately, the isotopic data were not abundant enough to show which isotope or ratios would be beneficial in uranium detection. The similarity between the radon-222 and lead-210 is encouraging.

Table 11. Uranium and Thorium Concentrations in Soil  
 Samples from Test Site D Determined by  
 Gamma-Ray Analysis by Geolabs.

Sample Location Number	eU, ppm ( $^{214}\text{Bi}-\gamma$ )	eTh, ppm ( $^{208}\text{Tl}-\gamma$ )	Sample Location Number	eU, ppm ( $^{214}\text{Bi}-\gamma$ )	eTh, ppm ( $^{208}\text{Tl}-\gamma$ )
D-2	3	8	D-117	7	13
D-6	4	7	D-119	3	12
D-12	3	10	D-123	2	6
D-18	2	11	D-124	3	14
D-24	4	11	D-129	2	7
D-35	6	12	D-134	2	14
D-39	4	7	D-137	2	11
D-56	2	10	D-140	4	10
D-73	3	9	D-144	8	6
D-87	3	20	D-148	3	13
D-97	3	11	D-152	2	10
D-101	5	12	D-156	3	14
D-102	2	10	D-162	2	12
D-107	4	11	D-165	2	10
D-109	4	11	D-169	1	11
D-112	1	11	D-172	2	9
D-114	3	12	D-176	3	11

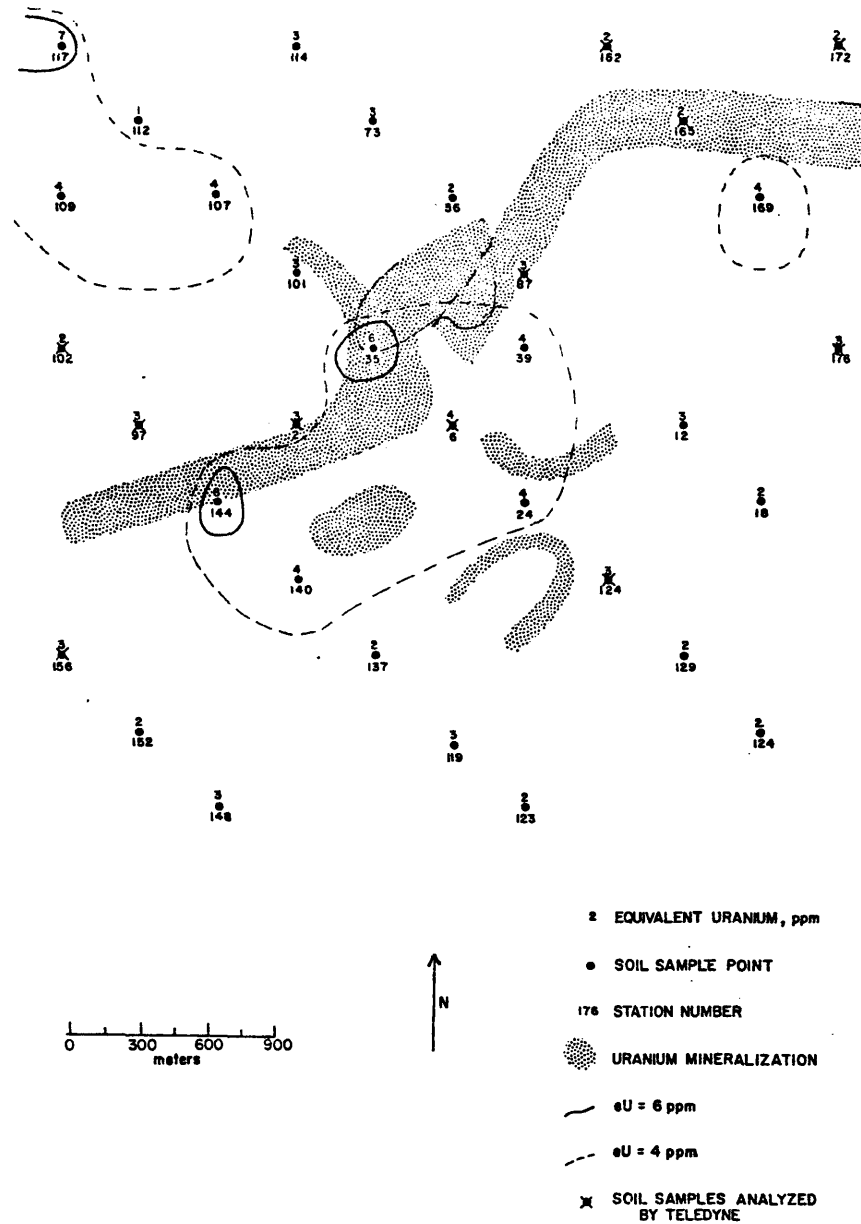


Figure 71. Equivalent uranium (eU) concentration in soil samples collected from test site D. The concentrations are determined by gamma spectroscopy using the  $^{214}\text{Bi}$  gamma ray as indicator of uranium.

Table 12. Gamma-Ray Activities Recorded in Soil Samples from Test Site D by Gamma Spectrometry by Teledyne Isotopes

Sample Station Number	40K	137Cs	228Ac	226Ra	210Pb	214Bi	208Tl
D- 2	22.9	0.242±0.030	1.44±0.17	2.23	1.1	1.5 ±0.2	1.32
D- 6	18.0	0.169±0.022	1.49±0.22	2.73	1.1	1.1 ±0.2	1.13
D- 35	18.2	0.080±0.015	1.46±0.20	2.46	1.5	1.4 ±0.2	1.38
D- 87	19.3	0.220±0.044	1.85±0.26	3.76	1.0	1.9 ±0.3	1.66
D- 97	21.6	0.125±0.026	1.65	2.47	1.3	1.4 ±0.2	1.44
D-102	29.6	0.233±0.033	1.08	0.96±0.15	0.61	0.66±0.21	1.02
D-124	16.9	0.339±0.050	1.63	2.15	1.2	1.3 ±0.3	1.40
D-156	19.3	0.070±0.022	1.55	2.36	.98	1.2 ±0.2	1.36
D-162	17.3	0.045±0.013	1.10±0.21	2.30	1.7	1.4 ±0.3	1.06
D-165	15.2	0.221±0.024	1.44±0.21	2.19	1.2	1.0 ±0.2	1.25
D-172	18.3	0.153±0.040	1.87±0.22	2.64±0.48	1.1	1.4 ±0.1	1.82
D-176	14.8	0.235±0.030	1.53±0.17	2.60	1.6	0.99±0.16	1.40

The error of each measurement is within ± 10% unless otherwise indicated.

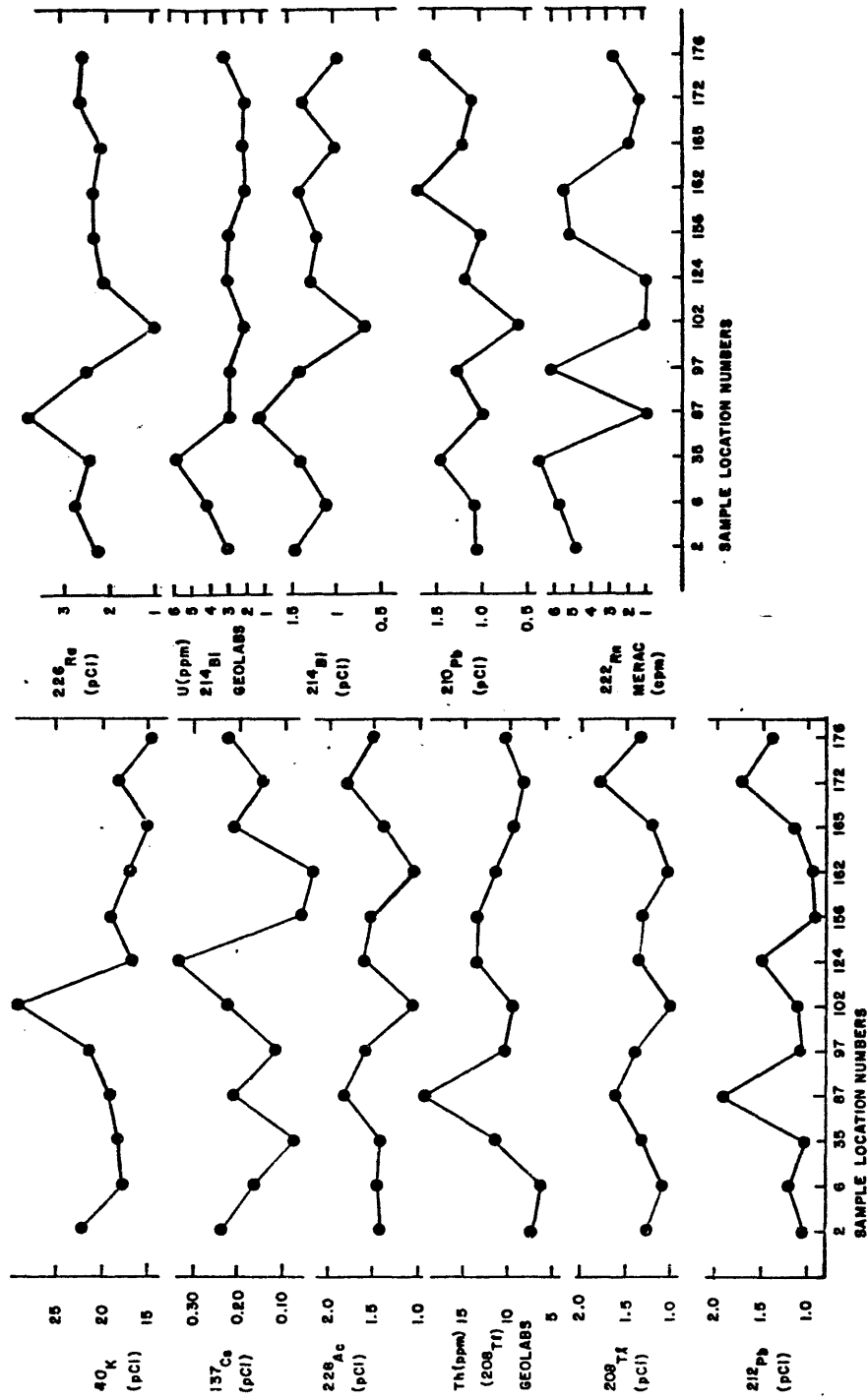


Figure 72. Comparisons of Teledyne gamma-ray spectrometry data for 21 soil samples collected from test site D. Radon counting rates measured by MERAC and the gamma measurements for Th and U by Geolabs at the soil sample locations shown.

Since the lead-210 is a daughter of the radon-222 and has a half-life of 21 years, it can give a cumulative estimate of the radon-222. This would be helpful in exploration in the case of test site D.

#### Laboratory Analyses of Soil Gas Samples

Five one-liter stainless steel containers were filled with soil-gas at stations 2, 6, 97, 156, and 162. These were sent to the Martin Marietta lab to be analyzed for noble gases. Five other four-liter containers were filled with soil-gas from stations 2, 6, 35, 162, and 172 and were sent to Teledyne Isotopes to be analyzed for radon-222, argon-36, and helium-4. The results of these measurements are shown in table 13. The radon data were corrected to 1200 MST, November 9, 1976, the time of collection. In the Teledyne Isotopes data there is an anomalous amount of helium at station 6. This was not confirmed, however, in the Martin Marietta analyses. Two stations (97 and 156) were found to be anomalous in helium when the helium was compared to the argon-36. This was not duplicated in the helium-neon measurements. The use of ratios may lead to valuable results in the future when the accuracy of the measurements can be increased and size of the sample can be reduced. At this time there does not appear to be any advantage over the helium-4 field measurement.

### TEST SITE E

#### Geology and Hydrology

Test site E lies several kilometers west of test site D. As seen in figure 58, the mineralized sandstones of test site D coalesce to form



Table 13. Laboratory Soil Gas Analyses from Test Site D Samples.

Sample Location Number	Teledyne		Martin Marietta		
	$^{222}\text{Rn}$ $\pm 10\%$ pCi/l	$^4\text{He}/^{36}\text{Ar}$ $\pm 10\%$	$^4\text{He}/^{36}\text{Ar}$	$^4\text{He}/^{22}\text{Ne}$	$\delta^4\text{He}\%$
D- 2	2665	0.168	0.180	3.320	+1.4
D- 6	1644	0.199	0.165	3.082	-6.3
D- 35	5163	0.162			
D- 97			0.221	3.421	+4.5
D-156			0.220	3.381	+3.2
D-162	1122	0.171	0.179	3.311	+1.1
D-172	819	0.158			

an arkosic sandstone approximately 35 meters thick. The area has been extensively drilled, resulting in the discovery of uranium mineralization from 250 to 300 meters deep. This thick sandstone sequence is thought to be near the axis of the meandering fluvial system (Dahl and Hagmaier, 1974). The regional groundwater flow is to the northeast at test site E.

#### Helium Soil-Gas Measurements

Soil gas samples were collected over a ten-square-kilometer area with stations at 320-meter intervals. Samples were collected on November 11 and 13, 1976. The results are shown in figures 73 and 74, respectively. The results of the two surveys are very similar. The general shape of the anomaly is the same in both cases. Most impressive are the large anomalies in the north. These are spatially related to the mineralization directly to the south and represent a groundwater displacement to the north-northeast. The anomalies at stations 87 and 92 on figure 74 are probably related to mineralization that is south of the survey area. The zone of mineralization on the east side of the grid does not show a helium anomaly probably because groundwater displacement would move any anomaly east of the survey. Figure 75 is a composite map of figures 73 and 74. By combining the two surveys, the spurious values are eliminated thus giving a more meaningful set of data.

#### Radon Counting Rates Measured with MERAC's

Twenty-five MERAC's were planted on November 16, 1976 and were read once on November 23, 1976. The results of this survey are shown in figure 76. In general, there is a lack of correlation

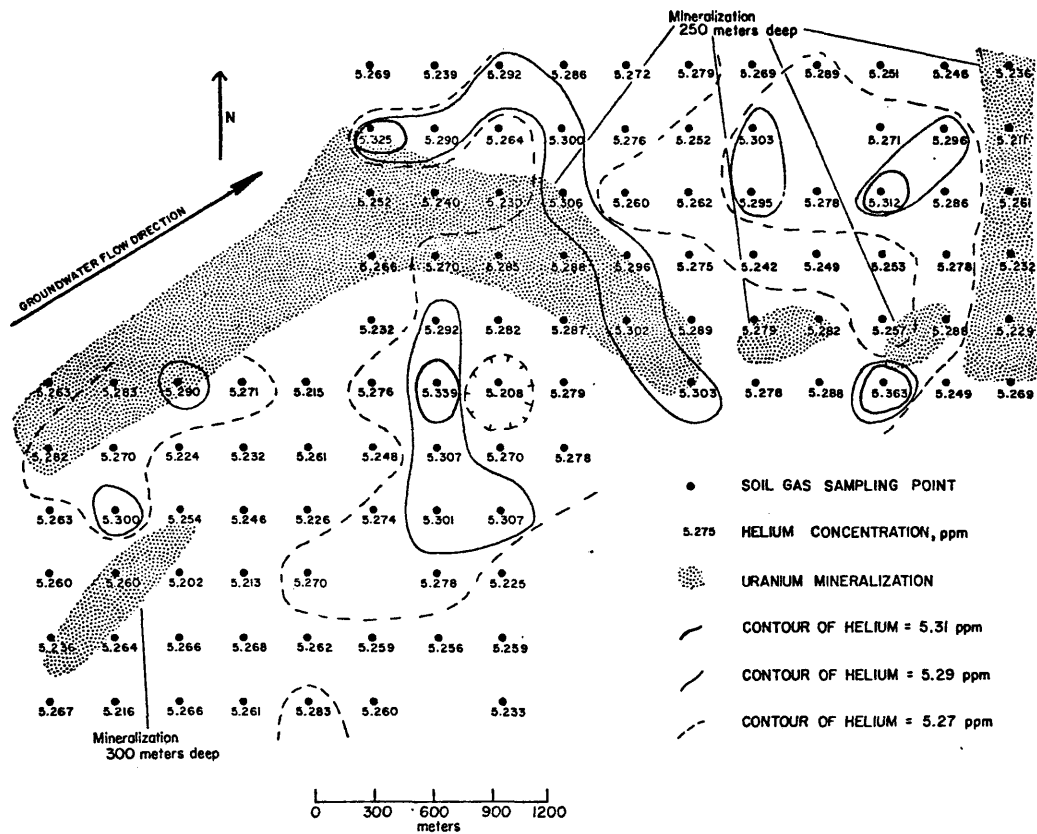


Figure 73. Helium concentration in soil gas collected on November 11, 1976, showing mineralization buried at a depth of 244 m, test site E. Sample interval spacings are 320 m (0.2 mi.).

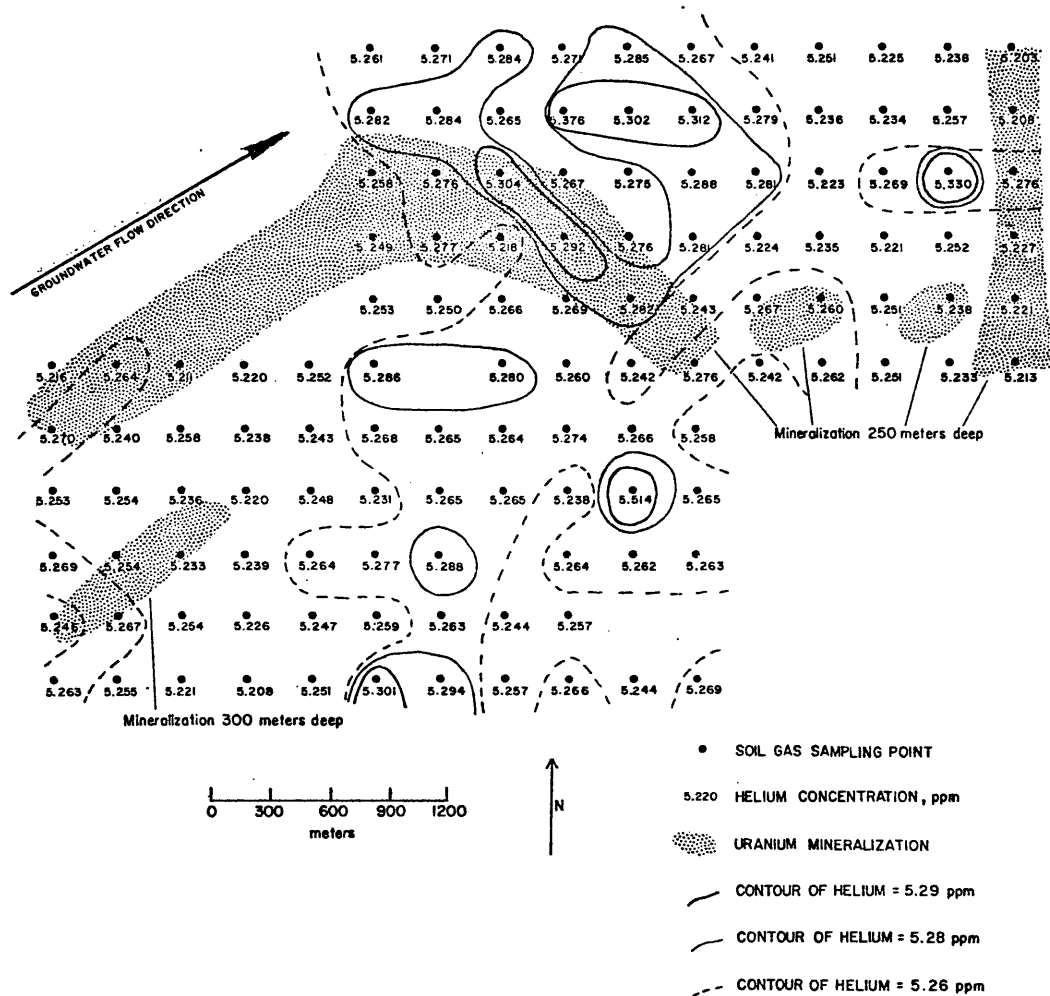


Figure 74. Helium concentration in soil gas collected on November 13, 1976, test site E. The sampling pattern is identical to that shown in figure 73.

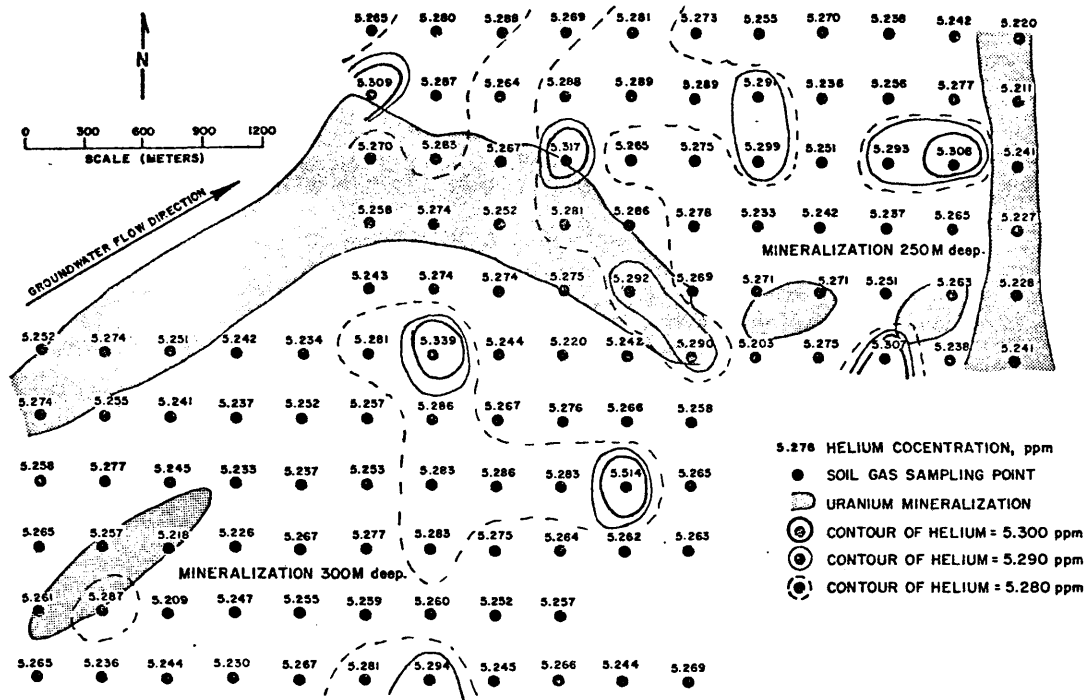


Figure 75. Contours of helium concentration in soil gas derived from averages of data accumulated on November 11, 1976 and November 13, 1976 at test site E.

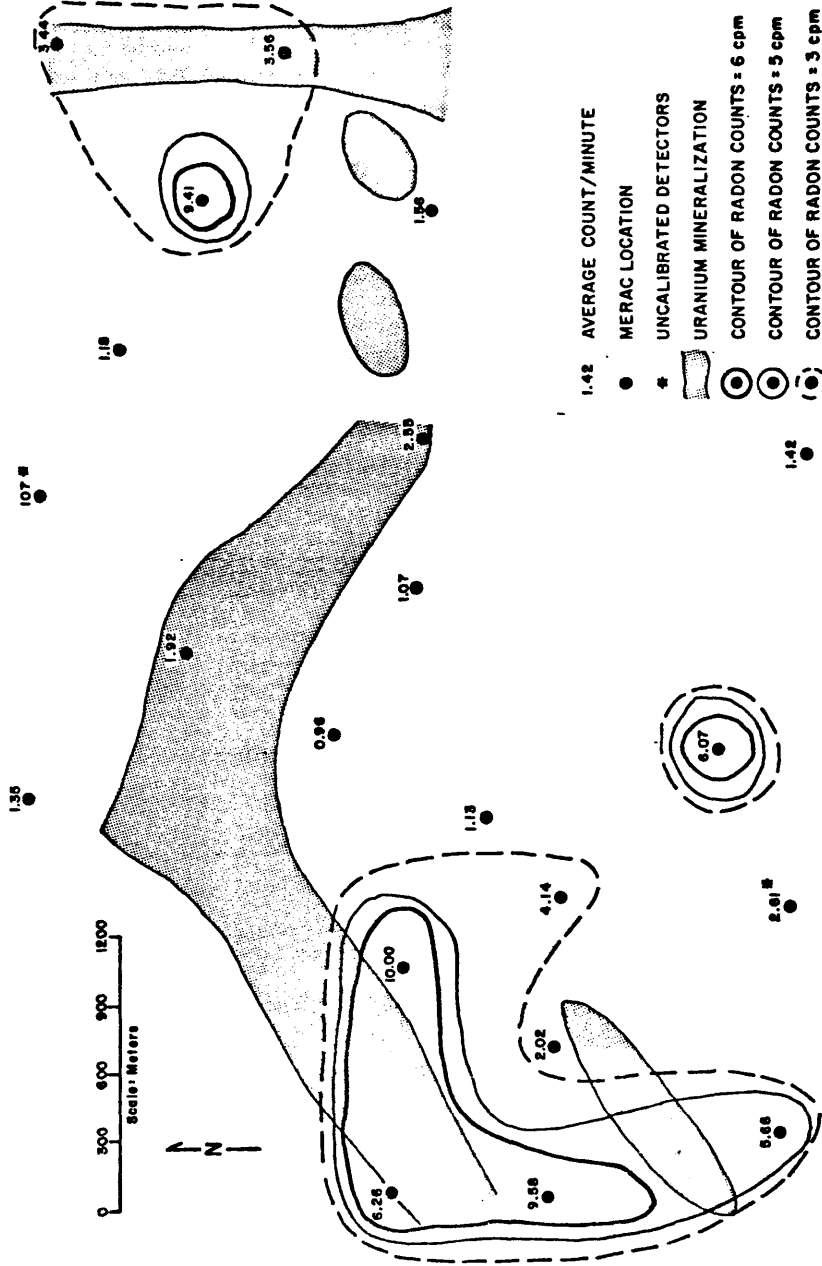


Figure 76. Radon counting rates measured with MERAC's averaged over seven days, buried 60 cm deep at the locations indicated, test site E. The grid array points are the helium sampling locations of figures 73 and 74.

between the radon and helium data. This can be attributed to one of two possibilities: (1) the accumulation time was not long enough to generate significant data, or (2) the radon is being generated in the near surface soil and does not represent the subsurface mineralization. This will be seen to be the case in the next section.

#### Gamma-Ray Spectrometric Analysis of Soil Samples

Soil samples were collected from 23 locations, 18 of which coincide with MERAC locations. The Geolab spectrometer results are given in table 14. Equivalent uranium and thorium data are plotted in figures 77 and 78 respectively. Comparison of figures 77 and 78 with the MERAC data (figure 76) shows an excellent correlation. This indicates that the radon is being derived from the near-surface soil. The helium results (figure 75) do not correlate with either the radon or the spectrometer results, suggesting that the helium is being derived from a subsurface source.

#### Regional Surveys

In addition to the detailed surveys at specific deposits, several tests were made to assess the applicability of helium sampling for regional exploration. This was done by traversing the Powder River Basin in a north-south direction and by analyzing for helium and uranium in groundwater.

#### Helium in Ground Water

During October, 1976, ground water was sampled from all of

Table 14. Uranium and Thorium Concentrations in Soil  
 Samples from Test Site E, Determined by  
 Gamma-Ray Analysis by Geolabs.

Sample Location Number	eU, ppm ( $^{214}\text{Bi}-\gamma$ )	eTh, ppm ( $^{208}\text{Tl}-\gamma$ )	Sample Location Number	eU, ppm ( $^{214}\text{Bi}-\gamma$ )	eTh, ppm ( $^{208}\text{Tl}-\gamma$ )
E- 3	1	15	E- 66	2	7
13	3	11	67	2	6
16	3	10	77	2	8
24	1	7	85		6
29	2	10	88	5	13
31	2	11	96	2	7
39	3	8	100	6	8
42	3	6	104	3	16
43	1	11	112	2	9
44	2	13	115	3	14
52	2	11	126	3	12
56	1	14			



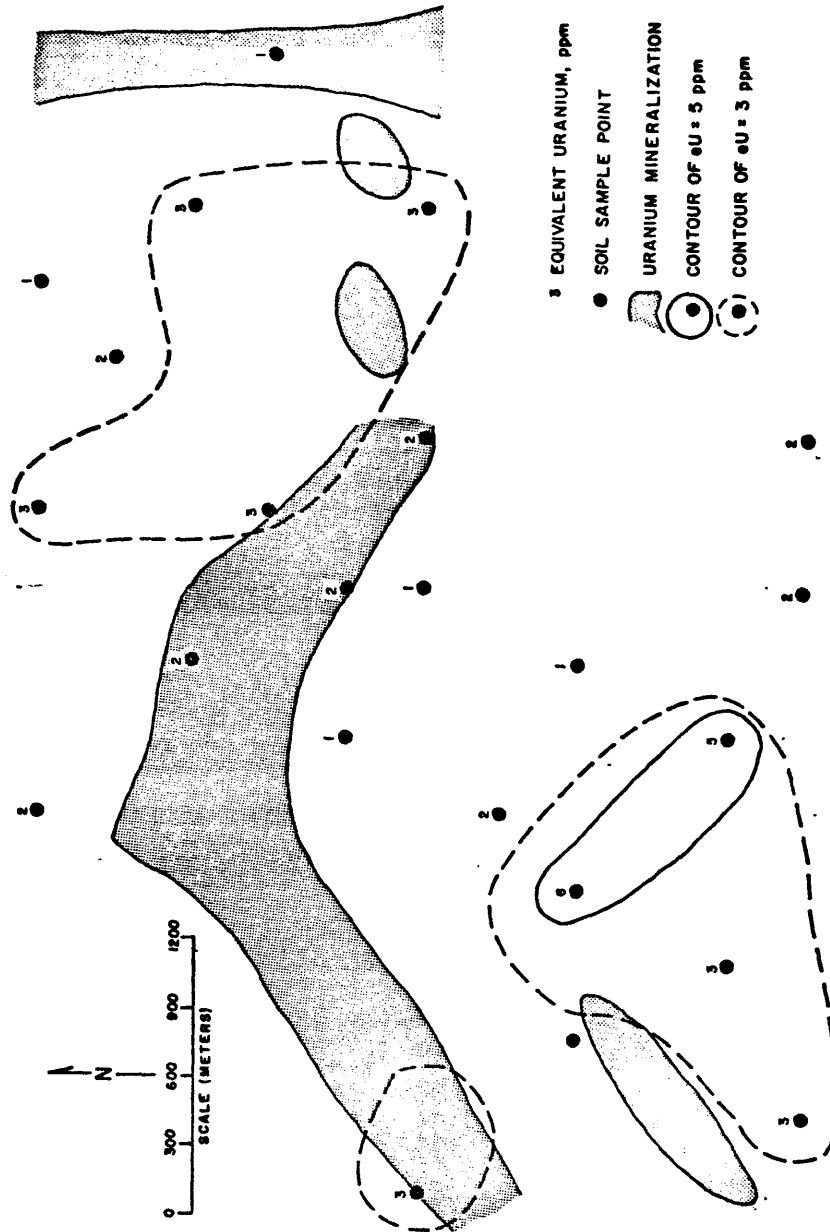


Figure 77. Equivalent uranium (eU) measurements from soil samples collected from MERAC holes at test site E, determined by  $^{214}\text{Bi}$  gamma spectroscopy.

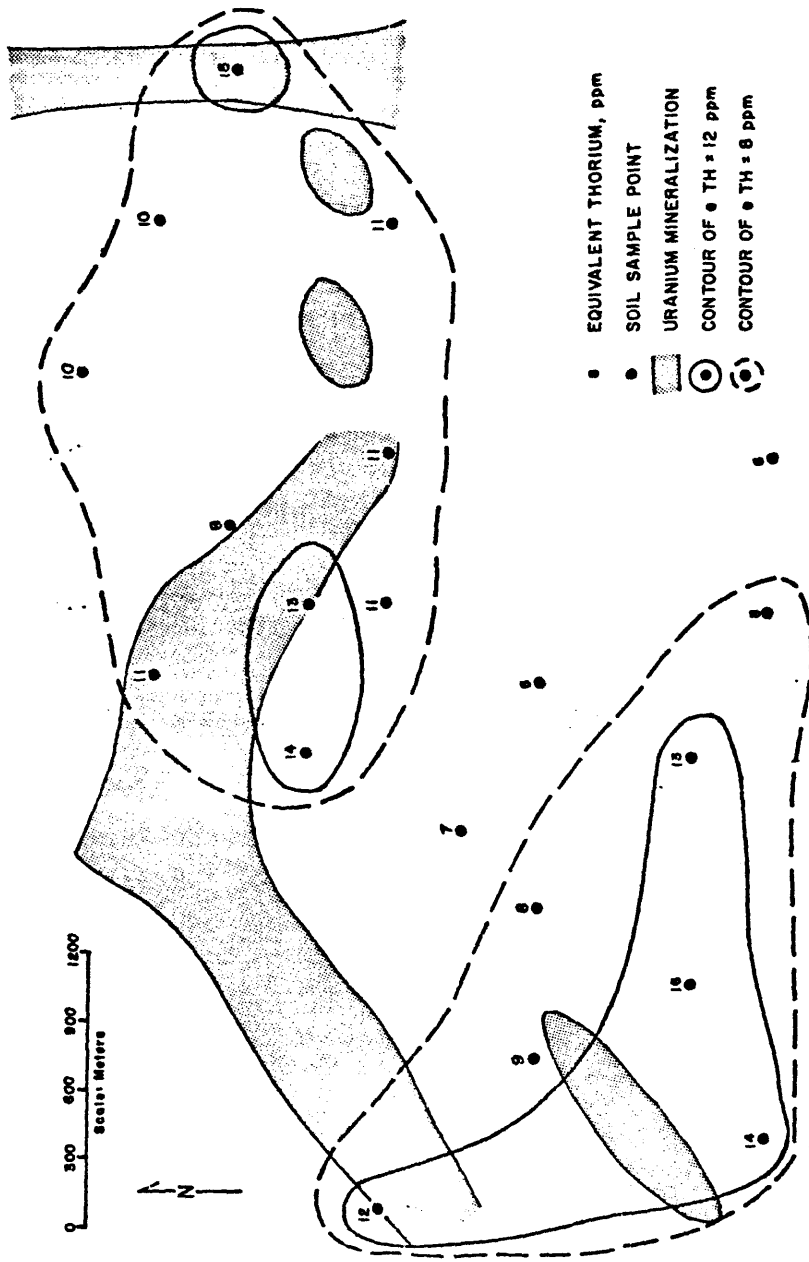


Figure 78. Equivalent thorium (eTh) measurements from soil samples collected from MERAC holes at test site E, determined by  $^{208}\text{Tl}$  gamma spectroscopy.

the pumping wells in a 2300-square-kilometer area in the southern part of the Powder River Basin. This area included test sites B through E (see figure 79).

A total of 48 water samples were collected and analyzed for helium. The results are shown in figure 79. Values ranged from 4.71 to 16.09 ppm.

An extensive study of the hydrology of the Powder River Basin was reported by J. L. Hagmaier (1971) as his Ph.D. thesis. An analysis of his static level measurements yields the static level contours for the wells in this region and the resultant ground water flow shown in figure 79. These ground water flow directions are significant in interpreting the helium concentration in ground water samples. It appears from the distribution of helium in ground water, shown in figure 79, that the large region of high helium concentration lies downstream from the uranium ore deposits.

It is curious, however, that between the region of high helium concentration and the uranium deposits there is generally a region depleted in helium. In a closer examination of the work by Dahl and Hagmaier (1974), as seen in figure 80, the ground water flow pattern has a vertical component that permits communication of aquifers through siltstones and claystones. There is a downward migration of ground water in recharge areas and an upward flow in areas of discharge. It is thought that the majority of the helium produced in the uranium deposits is trapped in the downward-migrating waters of the recharge area. It is then carried eastward in the deep aquifers. In the discharge area when the ground water approaches the surface, the helium can be detected in the ground water of shallow wells.

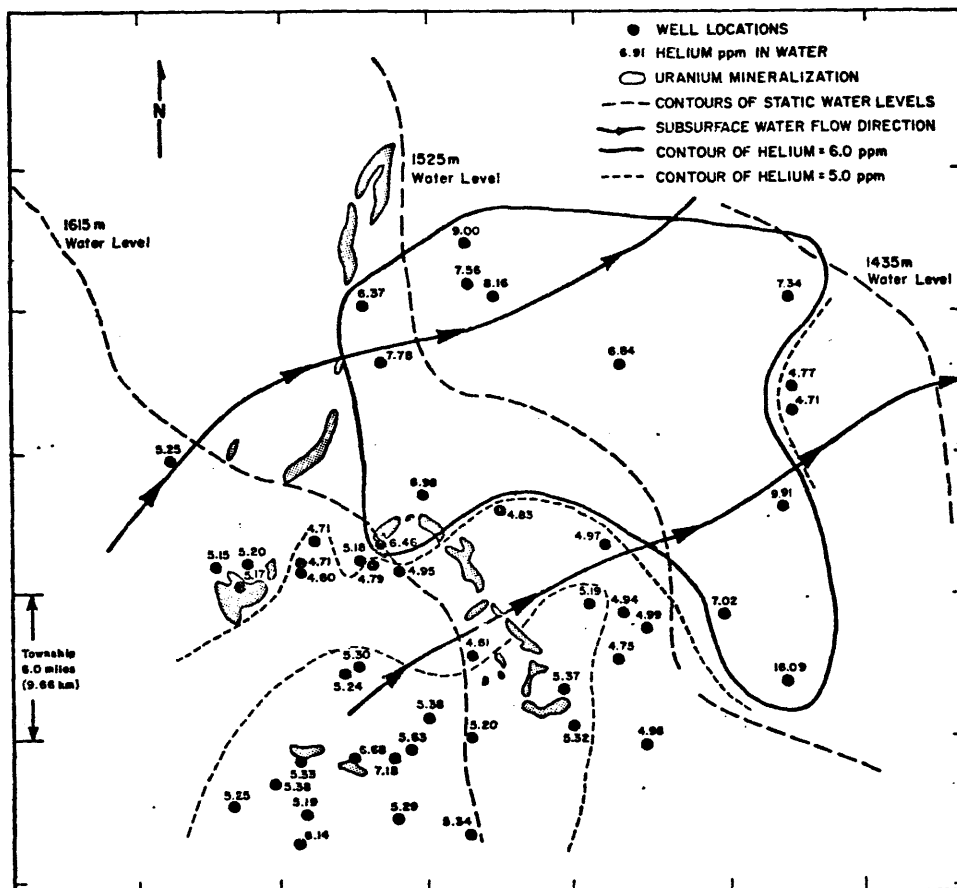


Figure 79. Helium concentration in ground water collected from water wells in the southern Powder River Basin. Water level and water flow information from Hagmaier (1971). Areas of uranium mineralization are shown also.

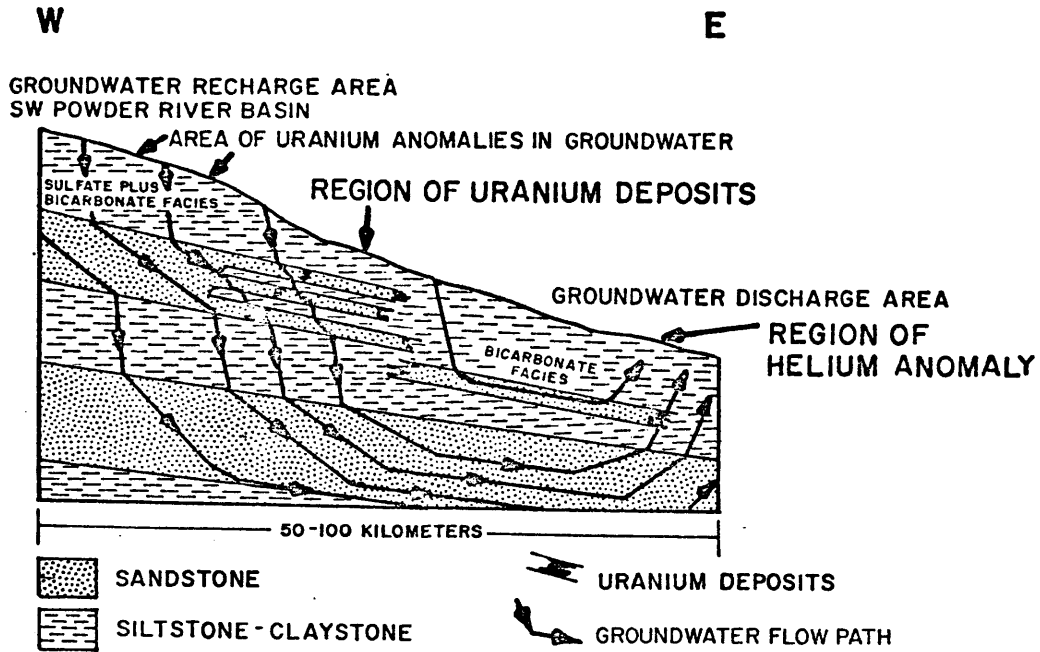


Figure 80. Generalized diagram showing the chemical facies of the ground water flow system in the southern Powder River Basin and its relationship to the Highland uranium deposits (Dahl and Hagmaier, 1974).

The general absence of anomalous ( $\geq 6.0$  ppm) helium in shallow ground water in the immediate area of the subsurface uranium deposits and the large area of strikingly anomalous helium in shallow ground water displaced down the ground water flow path from the uranium deposits indicate that helium analysis of ground water can be a useful and important reconnaissance technique in exploration for uranium deposits. However, the hydrology of the area must be understood in order to interpret the results of such a survey.

#### Uranium in Ground Water

Water samples from 11 of the 48 wells sampled for helium were sent to Geolabs for analysis of dissolved uranium. These uranium in ground water data, as well as those reported by Hagmaier (1971) from the 37 samples which he collected in this region, are plotted in figure 81. The uranium in ground water data show a region of higher concentration (5-230 ppb) just west of the ore bodies, i. e., upstream in the ground water flow and very low concentrations (1 ppb) downstream. This pattern of uranium in ground water relative to the uranium deposits is consistent with the oxidized nature of the sandstones and high solubility of uranium (in the form of uranyl dicarbonate) upstream to the southwest of the uranium deposits and the reduced nature of the sandstones and corresponding very low solubility of uranium in these rocks to the north and east, downstream of the deposits. Thus, the uranium-in-ground-water data indicate that uranium is currently being solubilized and precipitated in this region. These data illustrate the potentially great utility of uranium-in-ground-water data in reconnaissance and detailed exploration for uranium. In fact, the helium-in-ground-water data, as well as the uranium-in-ground-water data,



assume greater significance and yield the most meaningful interpretation for uranium exploration when used in conjunction with one another.

#### Helium in Soil Gas Along Basin-wide Traverse

A regional survey of the Powder River Basin from Douglas, Wyoming north to the Wyoming-Montana border was conducted on September 3-4, 1976 along a 300-kilometer traverse following county roads. Helium-in-soil-gas samples were collected from probes at a depth of 60 cm on 1.6 km spacing along the traverse. A second traverse over the same roads was undertaken on November 15-16, 1976. The data from both traverses are plotted in figure 82.

In interpreting the September, 1976 traverse, one observes that there are three clusters of high helium concentration defined by having a significant number of points above an arbitrary background threshold of 5.25 ppm. These clusters are found in the southern Powder River Basin and Pumpkin Buttes uranium districts and an area just south of Gillette where there is no known uranium occurrence. These results led to the tentative conclusion that helium detection might have been useful in a reconnaissance evaluation of the uranium potential of the basin prior to discovery of uranium in the Powder River Basin.

Examination of the November, 1976 data with the same criteria of clustering above a 5.25 ppm threshold, however, shows poor reproducibility of the September, 1976 results. Again, three clusters are recognized but only one (south of Gillette) was reproduced in both traverses. All three clusters on the second traverse were over regions where there is no known uranium mineralization. The tentative



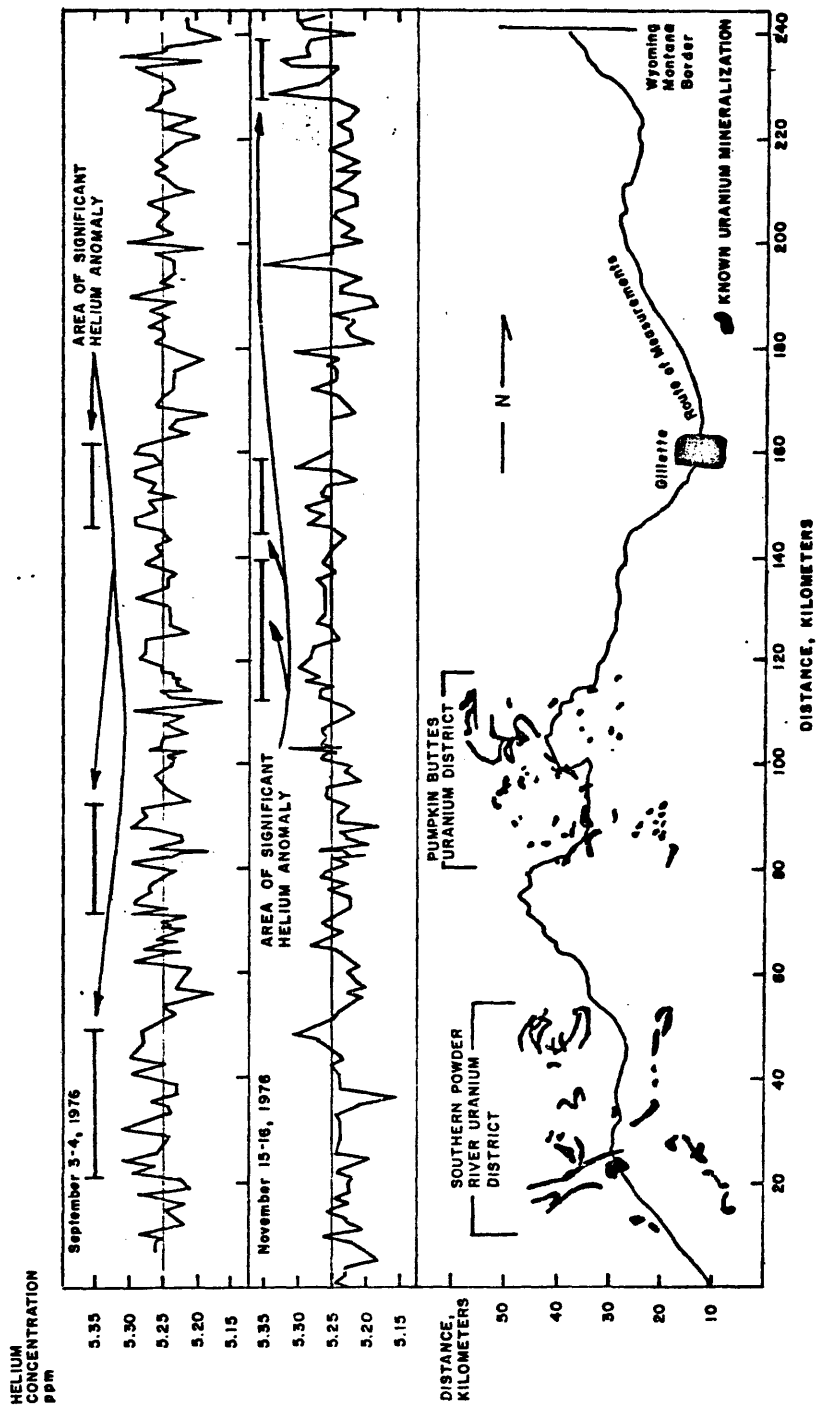


Figure 82. Helium in soil gas, basin-wide traverse, Powder River Basin, Wyoming.

conclusion of the usefulness of this type of survey in locating districts for further uranium exploration was not supported by the second survey.

## GRANTS-AMBROSIA LAKE REGION, NEW MEXICO

### Introduction

Extensive field work began on the Chaco Slope of the San Juan Basin in December of 1976. This area was chosen because of its highly faulted nature, widely varying depths of deposits, and outcrops of the ore-bearing units. Of particular interest was a test to determine if there was an up-dip migration of helium from the mineralization at depth and whether there was a detectable helium concentration emanating from the deposits of great depth.

Helium research work consisted of detailed soil-gas grid sampling on two test sites (F and G), regional soil gas sampling along county roads in the district and regional ground water sampling in the vicinity of the uranium district.

### General Geology

In the Ambrosia Lake district, uranium mineralization occurs in the Westwater Canyon Member of the Morrison Formation of Late Jurassic age, the Todilto Limestone of Late Jurassic age and the Dakota Sandstone of Early and Late Cretaceous age. Figure 83 is a diagram of the Cretaceous and Jurassic stratigraphic relationships of the Ambrosia Lake area.

The Morrison Formation in northwestern New Mexico consists of three members, the Recapture, the Westwater Canyon, and the

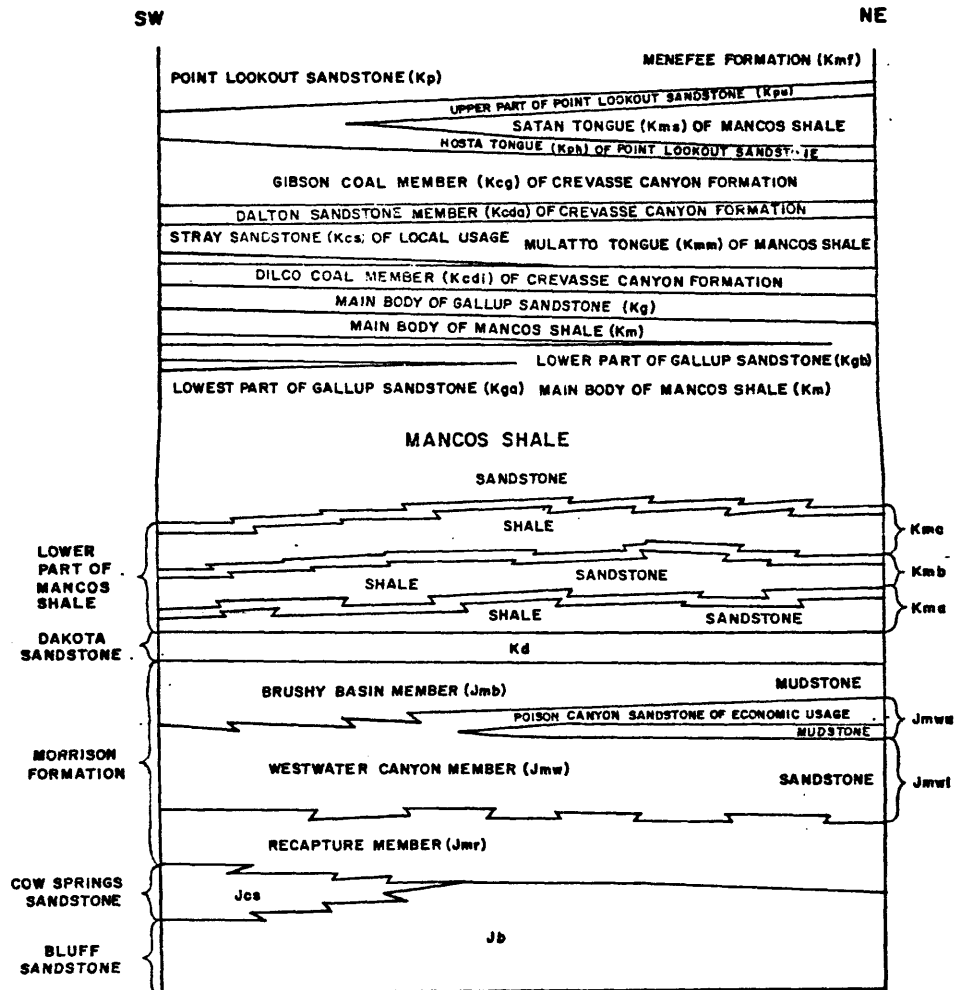


Figure 83. Schematic diagram of stratigraphic relations of Cretaceous and Jurassic rocks, Ambrosia Lake area (Santos and Thaden, 1966).

Brushy Basin (Santos, 1963). It is overlain unconformably by the Dakota Sandstone and underlain by the Bluff Sandstone of Early Jurassic age.

The Recapture Member (Santos, 1963) consists of alternating mudstones that range in color from greenish gray, purplish, and grayish red. It also includes minor amounts of buff and light gray to white sandstone. The Recapture Member varies in thickness from 42 to 70 meters and forms steep slopes and badlands (Santos, 1963).

The Westwater Canyon Member is primarily a tuffaceous, arkosic sandstone but includes minor amounts of mudstone. Intertonguing relationships with the overlying Brushy Basin and the underlying Recapture produce a variation in thickness of from 10 to 80 meters (Santos, 1963). The facies distribution indicates that the provenance area of the Westwater Canyon was in west-central New Mexico, an area of pre-existing igneous, metamorphic, and sedimentary rocks (Santos, 1963). The environment of deposition appears to be a broad, fan-shaped, alluvial plain traversed by braided streams (Santos, 1963). The colors range from pale yellowish gray, reddish brown, and yellowish orange at the outcrop to light gray, pale yellowish orange, dark yellowish orange, dusky red, and moderate reddish brown in the subsurface (Santos, 1963). Gray-green mudstones from 2 cm to 10 m thick are interbedded with the sandstones. They are lithologically similar to the mudstones of the Brushy Basin Member. The sandstone is commonly cemented with calcite, iron oxide or clays. Mudstone pebbles, cobbles and boulders are scattered throughout the Westwater Canyon section (Santos, 1963). Sedimentary structures present are simple and trough crossbedding. The grain sizes range from very fine to very coarse (Santos, 1963).

The sandstones were deposited in northwest-trending channels in the lower two thirds of the Westwater Canyon and northeast in the upper one third (Santos, 1963).

The Brushy Basin Member consists mainly of a grayish green, tuffaceous mudstone with minor amounts of sandstone and sandy claystone (Santos, 1963). Erosion at the top and an interfingering relationship with the Westwater Canyon below produce a variation in thickness of from 20 to 40 meters of the Brushy Basin Member. It is a steep slope former.

Ninety percent of the known uranium mineralization in the Ambrosia Lake district occurs in the Westwater Canyon Member. Two types of ore are recognized in the Ambrosia Lake trend--prefault trend ore and postfault redistributed ore. Deposition of the trend ore appears to be controlled entirely by sedimentary structures including mudstone lenses and disconformities (Santos, 1963). Deposition of the redistributed ore was controlled by a combination of sedimentary and tectonic features (Santos, 1963). The west-northwest trend of the prefault ore was modified or is absent in the postfault redistributed ore.

#### Test Site F

##### Geology and Hydrology

Test site F lies on the eastern end of the Ambrosia Lake trend. The uranium mineralization occurs in the Westwater Canyon Member of the Morrison Formation. This is shown in a generalized geologic cross section in figure 84. As can be seen in the cross section, a

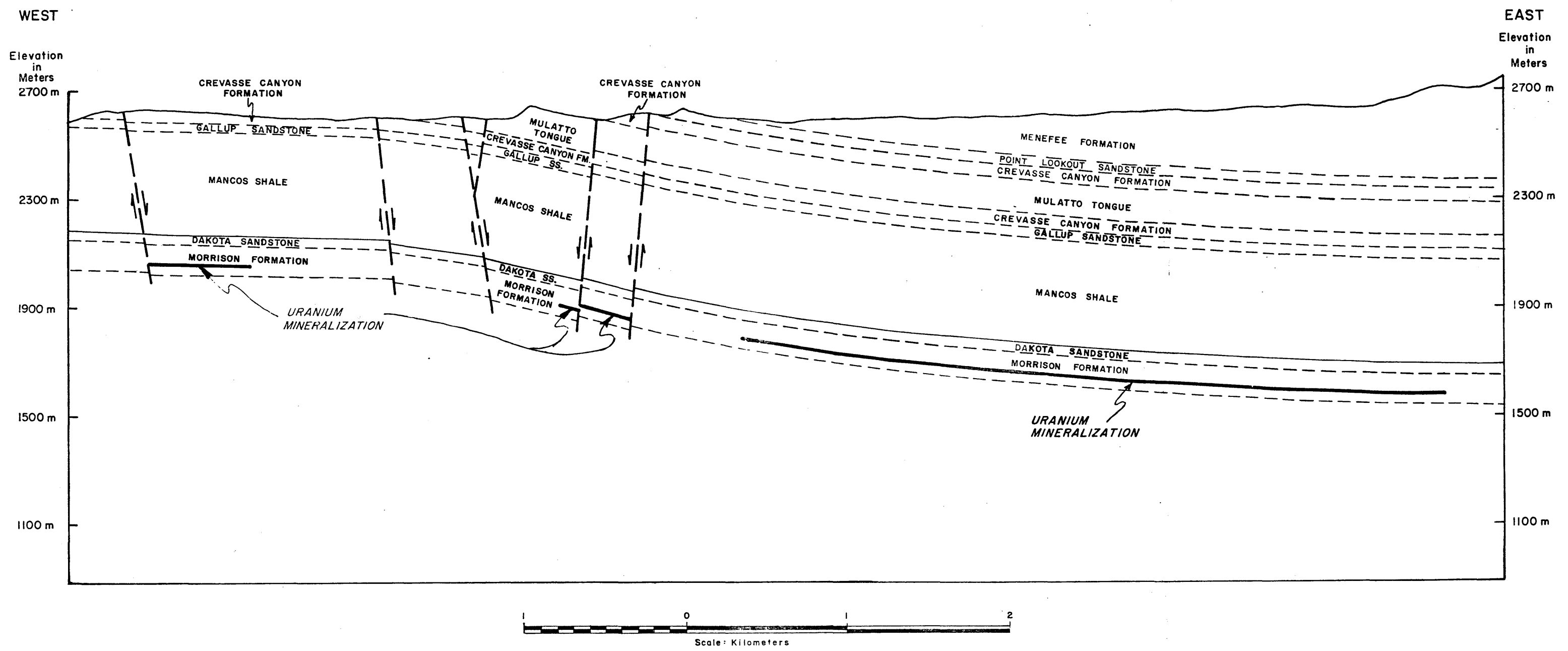


Figure 84. Generalized geologic cross section of test site F in the Grants-Ambrosia Lake region.

thin alluvial soil covers the bedrock geology in the lowland areas. The Menefee Formation, of Cretaceous age, occurs at the surface over most of the test site to the east of the eastern-most fault shown in figures 84 and 85. The Point Lookout, Crevasse Canyon, Mulatto tongue, Gallup and Mancos crop out to the west of the fault within the test site. As seen in the cross section (figure 84), the uranium mineralization increases in depth to the east. Average depths to the mineralization near the west boundary of the test site are approximately 240 meters increasing to 610 to 915 meters on the eastern side.

Principal aquifers of concern in the Ambrosia Lake area include the Westwater Canyon Member, Dakota Sandstone, Menefee Formation, Gallup Sandstone, Crevasse Canyon Formation, Todilto Limestone, and the Quaternary alluvium. Regional ground water directions are to the north-northeast.

#### Helium Soil-Gas Measurements

Helium-in-soil-gas samples were collected with the probe and syringe method over an area with maximum dimensions of 10 by 10 kilometers as shown in figure 85. Sampling was conducted twice during February, 1977, utilizing a grid sample spacing of 300 m. The survey included 485 samples.

Because of the large area and number of sample stations, the surveys were conducted without any attempt to collect samples in a short time period or at a particular time of day, in contrast to surveys in the Powder River Basin, Wyoming. However, it appeared from the cool weather data obtained in Wyoming that at this time of year the long collection time should not have been a concern with respect to significant





diurnal background variations.

The first helium-in-soil-gas survey at test site F was conducted from February 5-13, 1977. During the course of the survey, soil gas samples from nearby reference stations were collected every two or three hours to provide a measure of the diurnal and climatically induced helium variations during the time of the survey. The helium concentration of the soil gas at the reference stations is shown in figure 86 for each day of collection. The reference station sample probes remained in the ground throughout the survey. The reference station measurements show a fairly erratic pattern of helium concentration in soil gas, however, there is a general diurnal decrease in helium concentration in soil gas during the sunlight hours. This is shown in figure 87 where all the reference station data are plotted together and averaged over one hour intervals. The helium concentration of the reference station soil gas shows a range from 5.114 to 5.391 ppm, although most of the values are in the 5.21 to 5.27 ppm range.

In examining the data of figures 86 and 87 it is seen that although there is some evidence of a diurnal trend, the large variations of the soil gas concentrations at each base station make it rather meaningless to use these base station results to apply any kind of data correction to the soil gas measurements.

The atmospheric samples again show a much narrower range of helium concentration (5.203 to 5.263 ppm), as shown in figures 86 and 87.

The helium concentration of the soil gas samples collected during the first survey from February 5-13, 1977, are shown in figure 88. The helium-in-soil-gas concentration measured in this

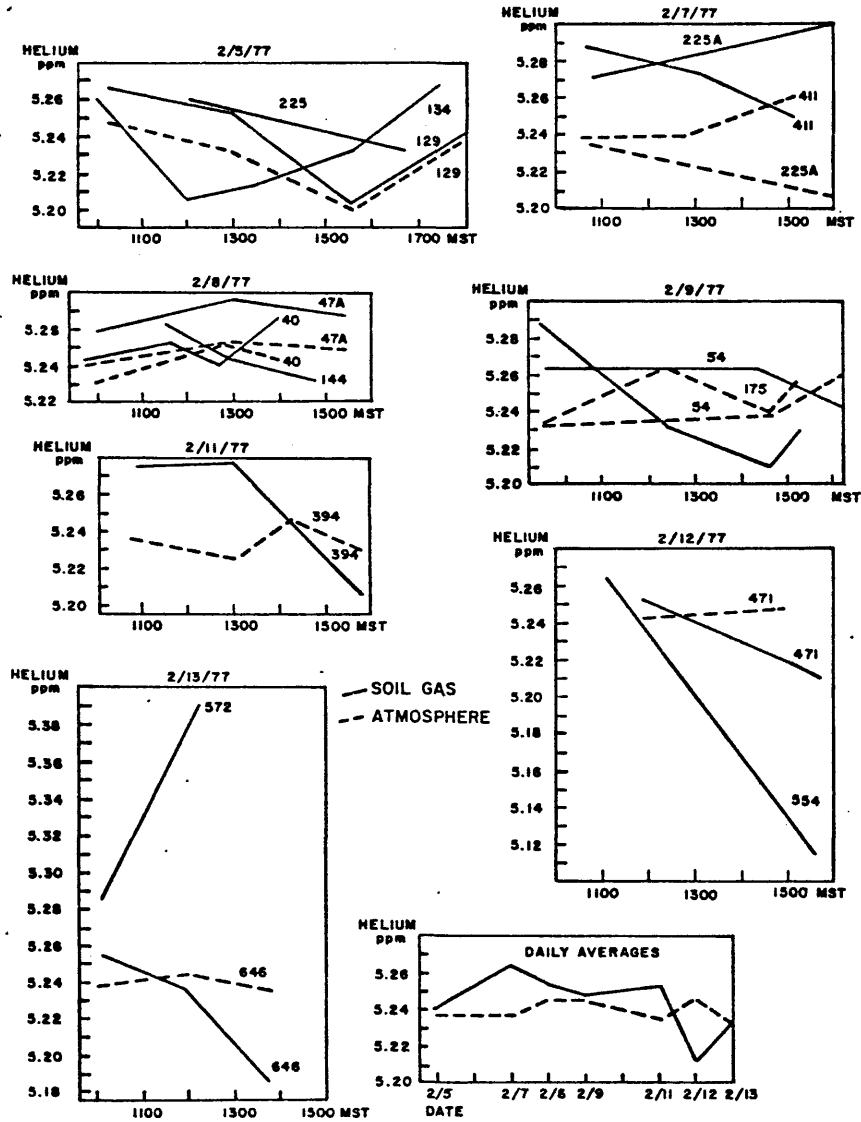


Figure 86. Helium concentrations in atmosphere and soil gas at reference stations from February 5 to February 13, 1977 at test site F. The reference station numbers are shown on each curve.

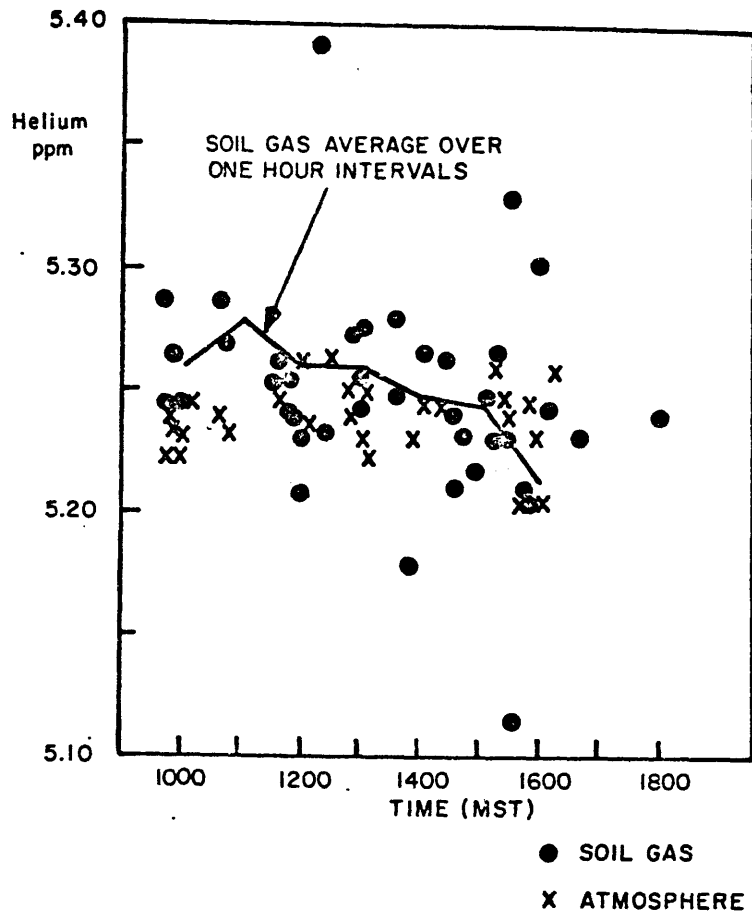


Figure 87. Composite data, helium concentrations in atmosphere and soil gas at reference stations, from February 5 to February 13, 1977, averaged over one-hour intervals.

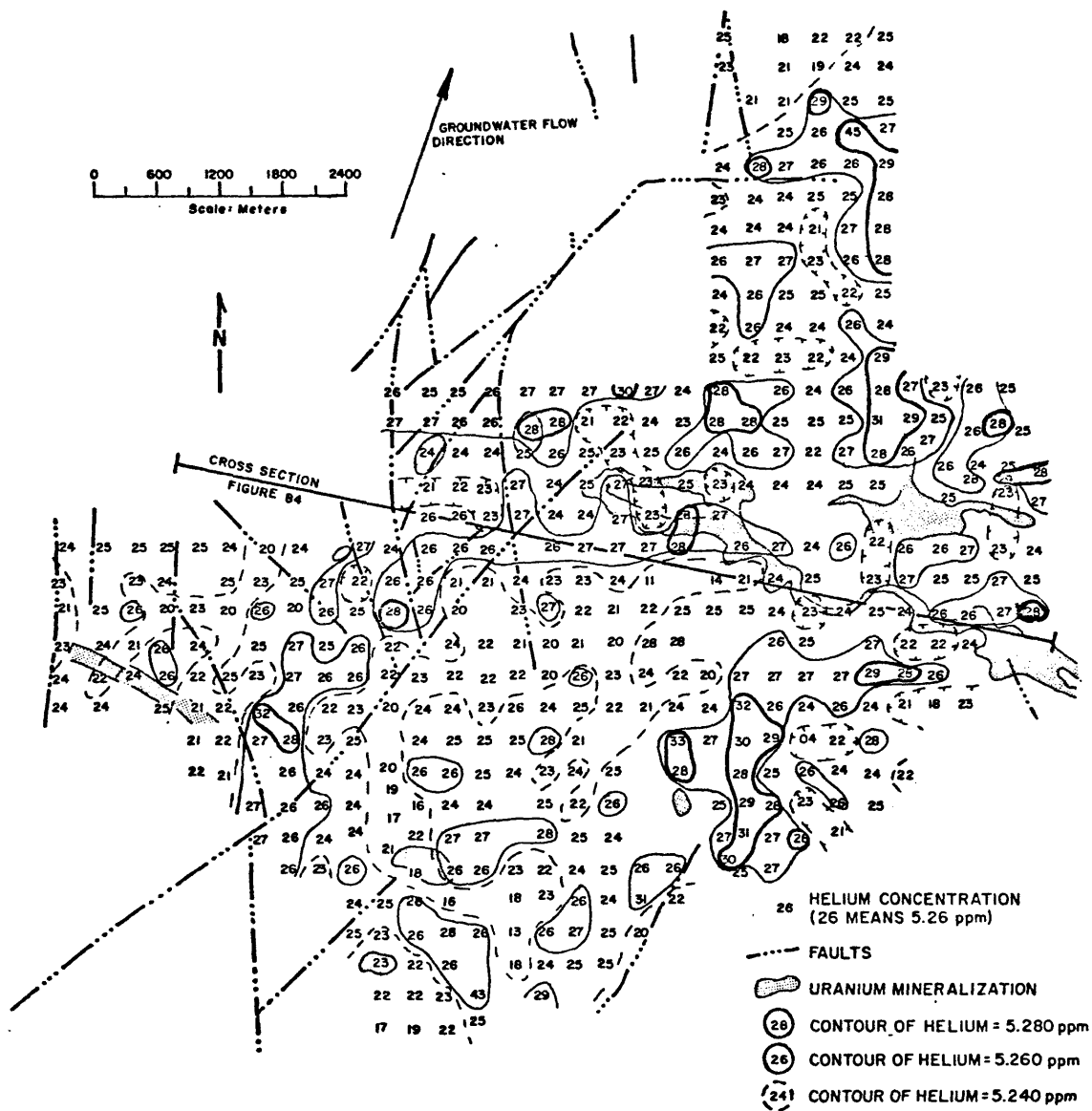


Figure 88. Contours of helium concentrations in soil gas measured at test site F from samples collected during the period from February 5, 1977 to February 13, 1977.

survey ranged from 5.133 to 5.432 ppm. The helium contours plotted in figure 88 show a random pattern of anomalous helium concentration with regard to the subsurface uranium mineralization. There appears to be very little correlation between the known distribution of subsurface mineralization and anomalous helium-in-soil-gas concentrations. Also there are no fault-controlled linear helium anomalies suggesting that the faults are not open conduits detectable with the 300-meter sample spacing. An attempt was made to correct the data for diurnal variations introduced by the long sample collection time, however, this plot showed as random a pattern with respect to the mineralization as the uncorrected data. Therefore, the diurnally adjusted data are not presented here.

The second helium-in-soil-gas survey at test site F was conducted from February 15 to 20, 1977. Again, as with the previous survey, soil gas samples from nearby reference stations were collected every two or three hours with the intention of providing some measure of the average diurnal and climatically induced helium variations during the survey. The reference stations were sampled throughout the day from February 15 to 20, 1977 as shown in figure 89. As in the first survey, the sampling probes at the reference stations remained in the ground throughout the survey.

There is no clear trend in the individual reference station data as shown in figure 89. All of the reference station data are plotted at the bottom of figure 89 as a function of time of day. This plot shows a minor diurnal trend (decrease in helium concentration with time of day) and the difficulty of applying any diurnal correction to the data. The helium concentrations of the reference stations from this survey range

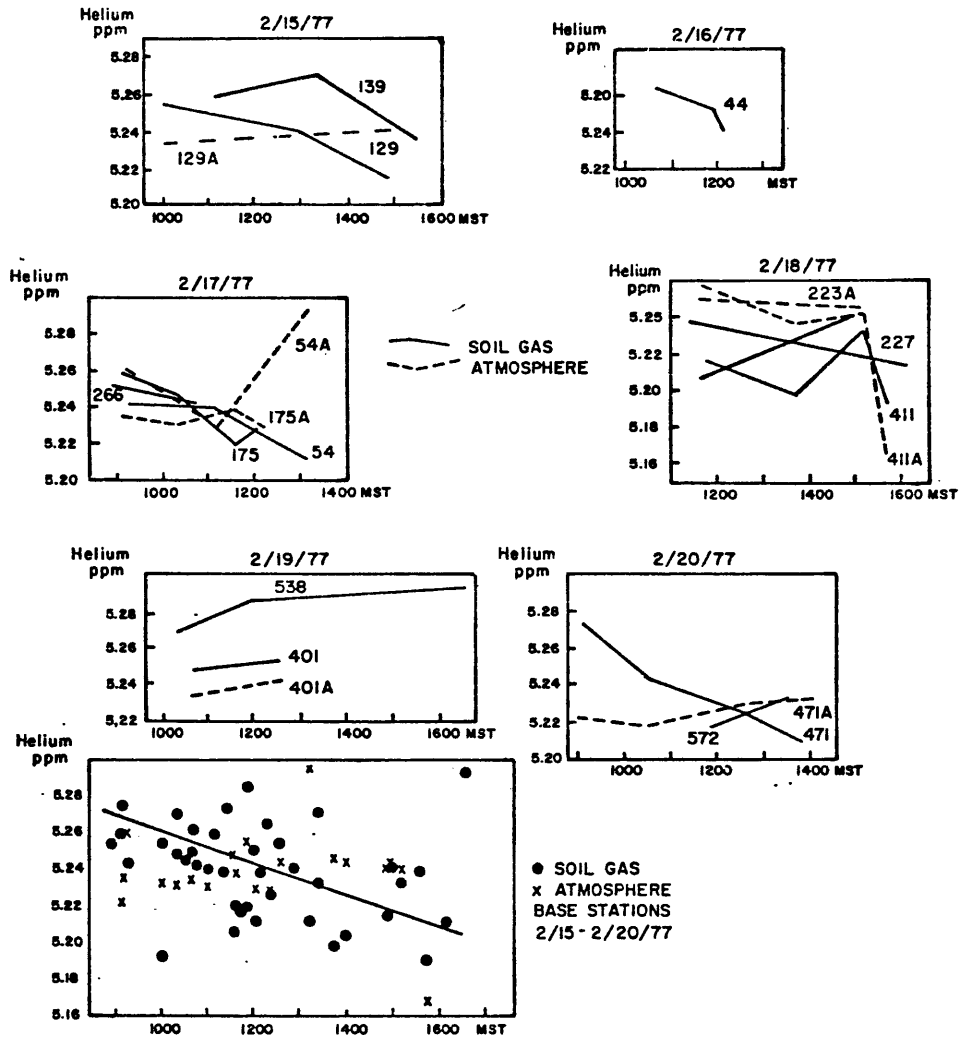


Figure 89. Helium concentrations in atmosphere and soil gas at reference stations from February 15 to February 20, 1977 at test site F (survey 2). The reference station numbers are shown on each curve. The bottom frame shows these data all plotted on a single time of day presentation.

from 5.191 to 5.293 ppm with most of the values in the 5.21 to 5.27 range, which is very similar to the range of the first survey.

Except for two extreme values of 5.168 and 5.294 ppm, the helium concentration in the atmosphere samples ranged over a much narrower range than the soil gas samples (5.224 to 5.260 ppm).

The helium concentrations of the soil gas samples from the second survey of test site F are shown in figure 90. The helium concentration ranged from 5.072 to 5.345 ppm in the soil gas. Again, the contours in figure 90 show predominantly a random pattern with respect to the subsurface uranium mineralization. Two helium anomalies are displaced in the direction of ground water flow and may be related to uranium mineralization. There were no linear helium anomalies that can be attributed to faulting. An attempt to correct this data for the diurnal effect yielded random helium anomalies, as it did in the first survey.

Figure 91 shows the average helium-in-soil-gas concentration plotted at each station from the two surveys. It was hoped that the average of the two sets of data would tend to reduce atmospheric and other short-term variations, making the helium content due to subsurface uranium more discernable. Unfortunately, the average data also show a random pattern of anomalous helium.

It is the opinion of the author that this test site was too large in which to utilize an instantaneous collection system. Even in winter months when environmental conditions were not changing rapidly, variations that affected the helium concentration in the soil gas did occur from day to day. An integrated collection system where helium concentration is averaged over a month's time would be more



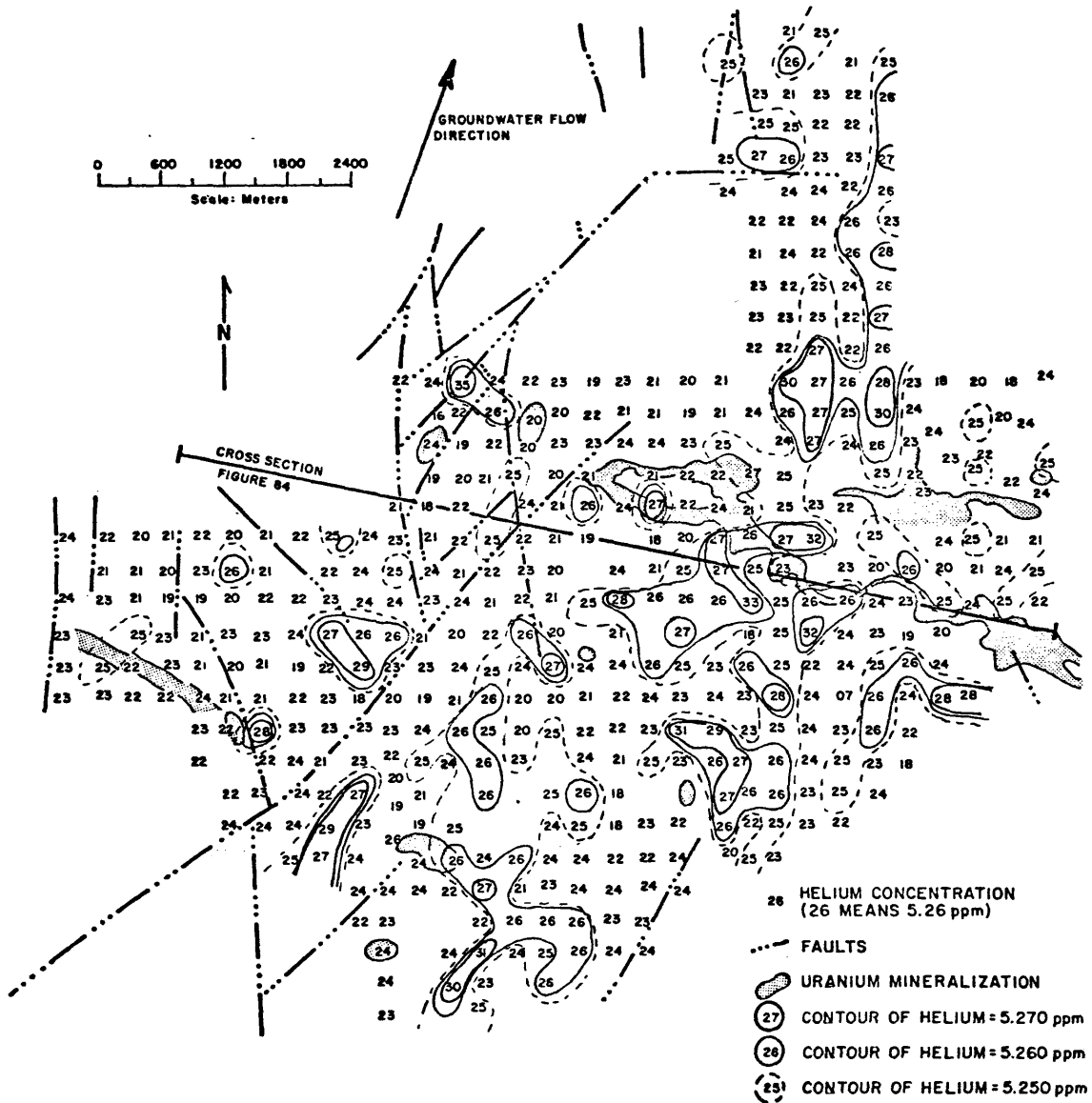


Figure 90. Helium concentration in soil gas, February 15 to February 20, 1977, test site F.

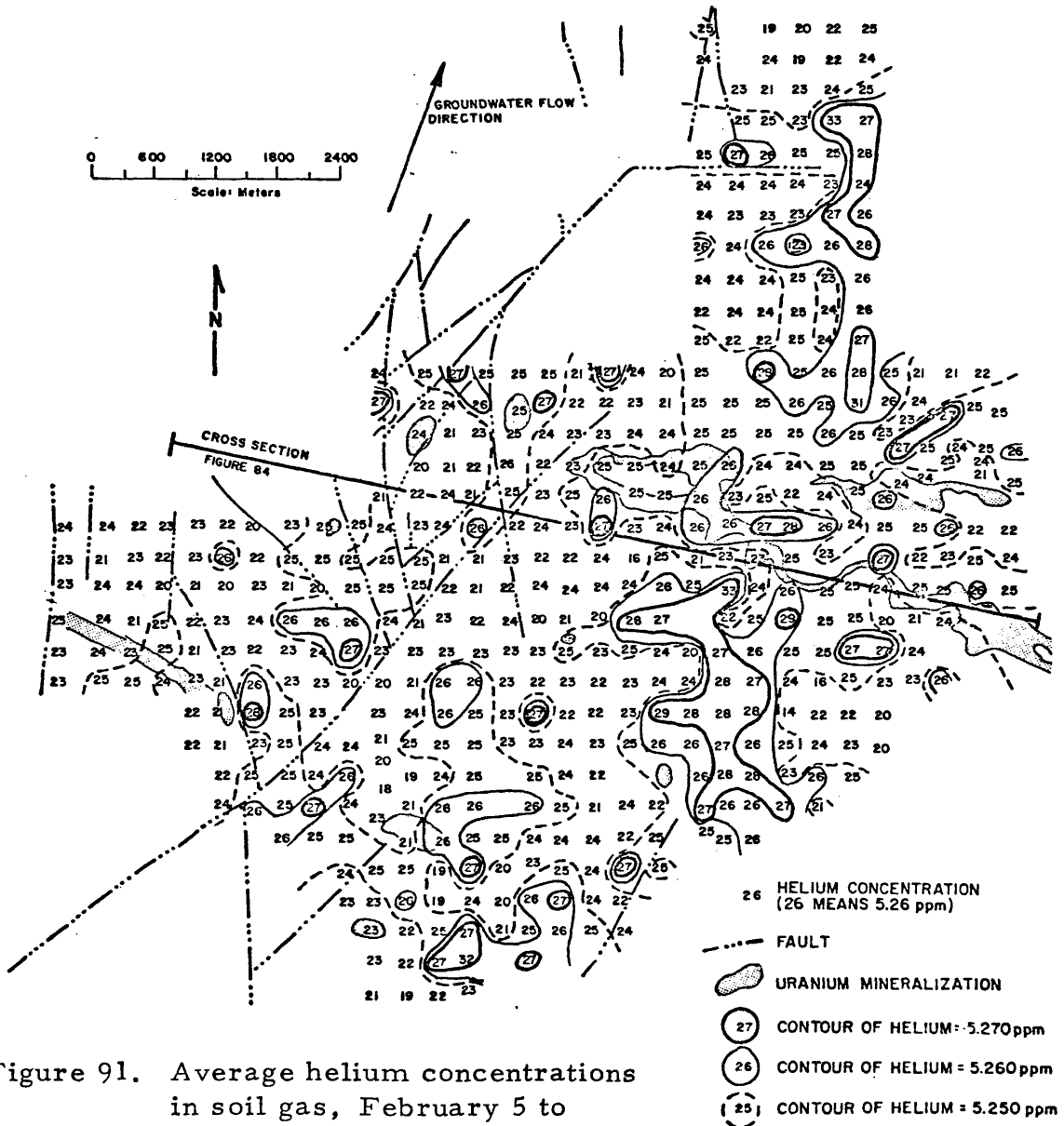


Figure 91. Average helium concentrations in soil gas, February 5 to February 20, 1977, test site F (from figures 88 and 90).

applicable to a survey of this size.

#### Radon Counting Rates Measured with MERAC's

The MERAC counters were planted twice throughout test site F, first for the nine-day period of February 4-13, 1977, and then for the five-day period from February 16-21, 1977. Data from the 28 MERAC sites from the first survey are shown in figure 92. The data from the 23 MERAC sites from the February 16-21 survey (including 21 of the same sites as the first survey) are shown in figure 93. Contour lines shown are for visual guides only, since data is too sparse to contour rigorously.

The range of radon counting rates observed during the first survey was 0.440 to 6.713 cpm; the average was 1.366 cpm. The range observed during the second survey was 0.030 to 9.648 cpm averaging 1.463 cpm. All of the MERAC data, including the averages for each station, are shown in table 15. Table 15 also shows that at most stations the counting rates are reproducible to  $\pm 50$  percent, indicating the reliability of the data. The counting rates of stations 264 and 646 should be disregarded due to the tenfold fluctuation observed from the first to second survey. The data at stations 161, 291, 330 and 396 differ by more than 100 percent from one survey to the next and should be used cautiously. As seen in figures 92 and 93, the data from both periods show an area of anomalous radon in soil gas associated with the subsurface mineralization. While this suggests that radon counting would have been a useful exploration tool in the discovery of this deposit, this conclusion is subject to speculation as will be seen in the next section.

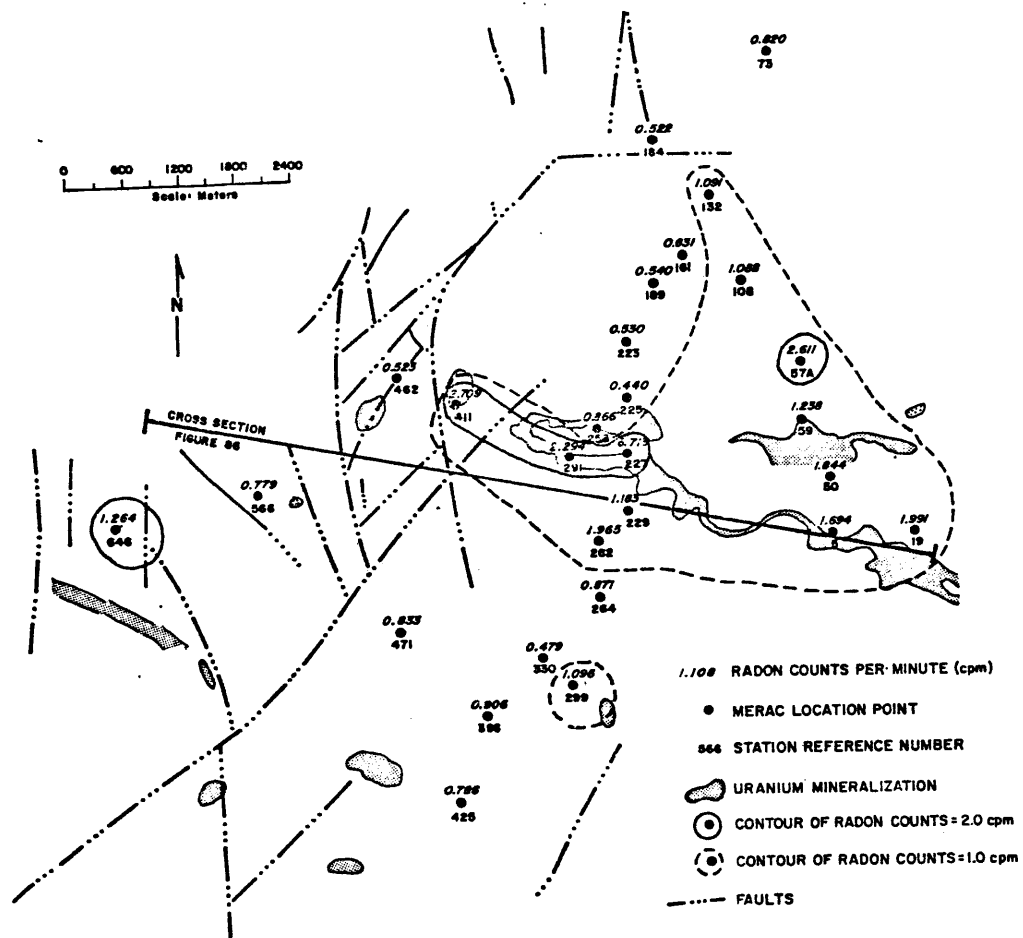


Figure 92. MERAC data, February 4 to February 13, 1977 at test site F.

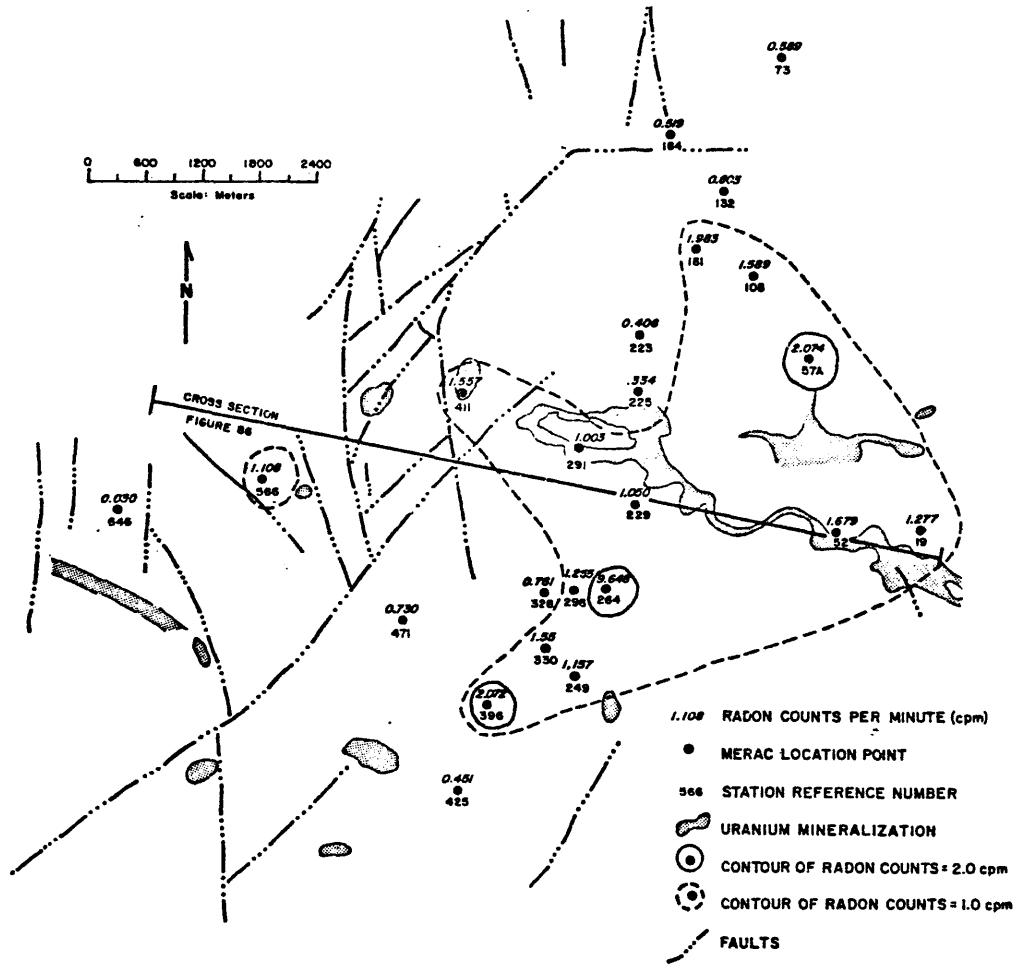


Figure 93. MERAC data, February 16 to February 21, 1977 at test site F.

Table 15. MERAC Data at Test Site F

Station No.	Radon Counts per Minute (cpm) ***		Average
	2/4/77-2/13/77	2/16/77-2/21/77	
F- 19	1.991	1.277	1.634
F- 50	1.846	-	1.846
F- 52	1.694	1.674	1.684
F- 57A	2.611	2.074	2.342
F- 59	1.234	-	1.234
F- 73	0.820	0.589	0.704
F-108	1.088	1.589	1.338
F-132	1.091	0.803	0.947
F-161*	0.631	1.983	0.807
F-184	0.522	0.519	0.520
F-189	0.540	-	0.540
F-223	0.530	0.406	0.468
F-225	0.440	0.334	0.387
F-227	6.713	-	6.713
F-229	1.105	1.050	1.100
F-258	0.866	-	0.866
F-262	1.965	-	1.965
F-264**	0.871	9.648	5.259
F-291*	2.294	1.003	1.648
F-296	-	1.255	1.255
F-299	1.096	1.157	1.126
F-328	-	0.761	0.761
F-330*	0.479	1.595	1.037
F-396*	0.906	2.172	1.489
F-411	2.709	1.557	2.133
F-425	0.786	0.451	0.618
F-462	0.523	-	0.523
F-471	0.833	0.730	0.781
F-566	0.779	1.103	0.941
F-646**	1.264	0.030	0.647
Average (all stations)	1.366	1.463	1.444

\* Data at these stations differ by greater than 100% from one recording period to the other.

\*\* Data at these stations differ vastly (greater than tenfold) from one recording period to the other and, consequently, should be disregarded.

\*\*\* A qualitative calibration of the counters (17) yields a sensitivity of 70 (picocuries per liter)/(count per minute).

### Gamma-Ray Spectrometric Analysis of Soil Samples

Soil samples were collected from all 30 of the MERAC locations of test site F described above. Their equivalent uranium and equivalent thorium contents were determined by gamma-ray spectrometry by Geolabs. These data are shown in figure 94. The equivalent uranium content of the soil ranges from 1-4 ppm; the equivalent thorium content ranges from 3-12 ppm.

There is a good correlation between the anomalous (greater than 8 ppm) equivalent thorium and anomalous radon rates. This is shown by comparing figures 93 and 94. This suggests that the anomalous radon-220 is derived from the thorium decay series in the near-surface soil.

There does not appear to be any correlation between the uranium content in the soil and anomalous radon or subsurface mineralization.

### Micro-Environment Test

Helium-in-soil-gas measurements were made in a small area around station 40 at test site F on February 16, 1977, to test sampling and regional variability. Soil gas samples were collected at nine locations in a square area, 207 meters on a side with station 40 in the center. Figure 95 shows the position of the micro-environment test in relation to stations of the larger survey at test site F. The helium-in-soil-gas data collected during 1030-1225 and 1330-1425 hours on February 16, 1977 are presented in table 16. Generally, soil gas was obtained from two probes approximately five to ten meters apart at each station.

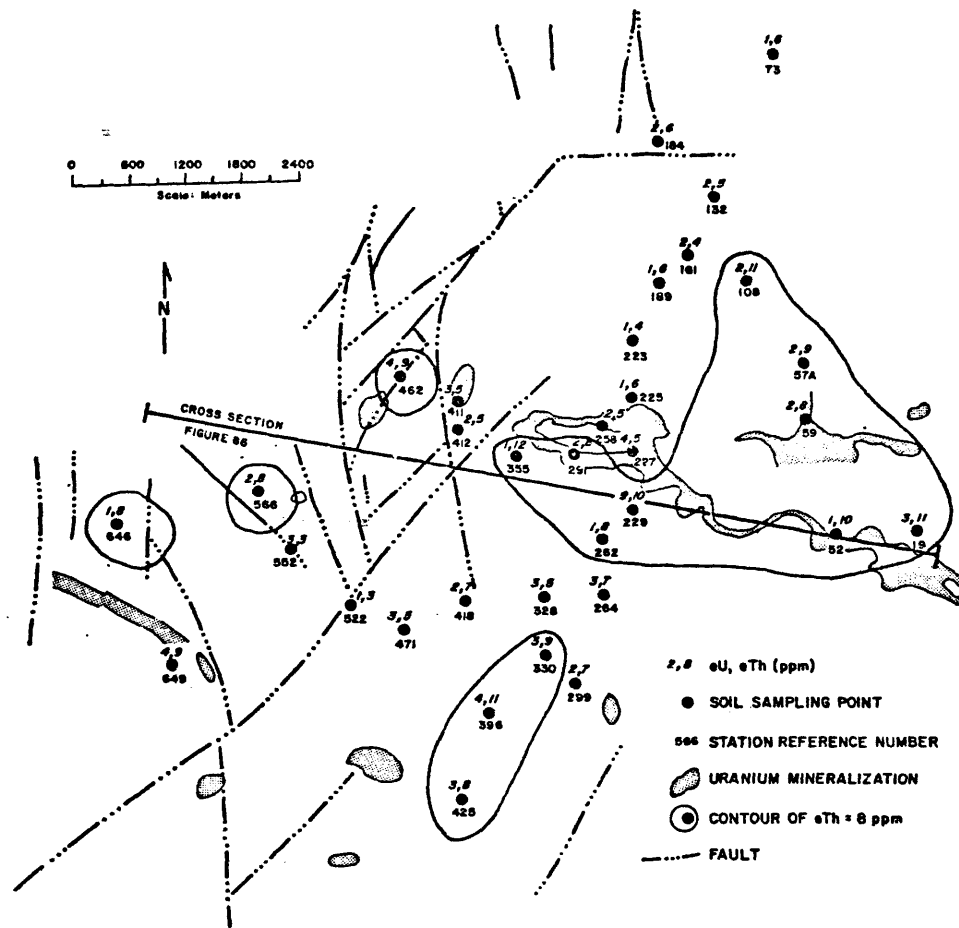


Figure 94. Equivalent uranium and thorium data from soil samples from MERAC holes at test site F, determined by  $^{214}\text{Bi}$  and  $^{208}\text{Tl}$  spectroscopy.



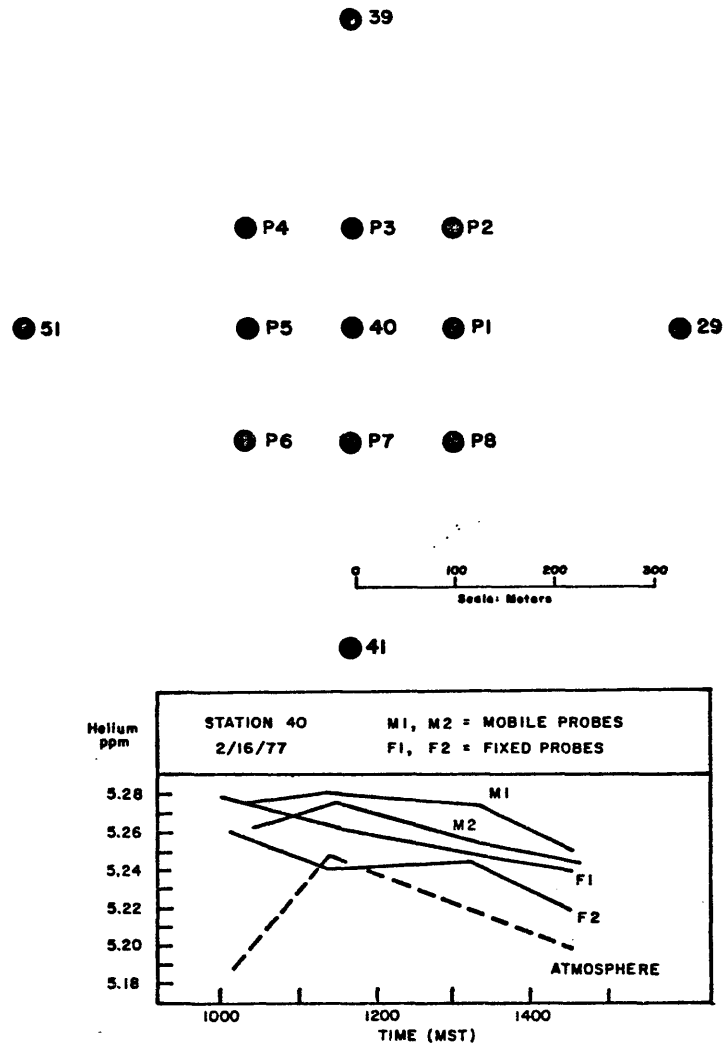


Figure 95. Micro-environment tests and time of day variations of helium in soil gas at reference station 40 at test site F.

Table 16. Helium in Soil Gas Concentrations  
for the Micro-Environment Test, Test Site F (in ppm).

Station	1030-1225 hrs.		1330-1425 hrs.		Average of Both Times
	2 probes	average	3 probes	average	
40	5.254 5.267	5.260	5.252 5.239	5.245	5.252
P-1	5.249 5.269	5.259	5.239 5.232	5.236	5.247
P-2	5.267 5.257	5.262	5.258 5.250	5.254	5.258
P-3	5.246 5.235	5.241	5.230 5.233	5.232	5.236
P-4	5.261 5.255	5.253	5.251 5.243	5.247	5.250
P-5	5.268 5.260	5.264	5.246 5.239	5.243	5.253
P-6	5.242 5.261 5.258	5.254	5.210 5.236	5.223	5.238
P-7	5.236 5.239	5.237	5.238 5.222	5.230	5.233
P-8	5.238 5.224	5.231	5.242 5.196	5.219	5.225
Average of all stations		5.251		5.237	5.244

The helium concentrations measured in soil gas at each sample location within five to ten meters of each other were usually within 10 ppb of each other. Samples from one station to another 100 meters away produced helium concentrations in soil gas that varied by as much as 30 ppb. This implies that most of the variability in sampling can be attributed to differences between stations. This makes it possible to detect regional helium enhancements due to subsurface mineralization. Individual readings between stations ranged from 5.208 to 5.270 ppm, averaging 5.244 ppm.

The plot of helium concentration versus time variation from station 40 (shown in figure 95) shows that a general decrease in helium concentration in the soil gas occurred from 1000 to 1430 hours on February 16, 1977. Similarly, as seen in table 16, the helium concentration measured in the micro-environment test decreased at every station from the 1030-1225 hour readings to the 1330-1425 hour readings. These data suggest that, even during the cold weather of February, diurnal variations are important and significantly influence the results and reliability of helium data collected over long periods of time (several hours or days in length).

The more rapid decrease (figure 95) in helium concentrations from the fixed probes (left in the ground and used for several subsequent readings) than from the mobile probes (probes removed from the ground after each reading) suggest that the withdrawal of gas from the soil in the vicinity of the probe causes a relative depletion in helium. This is probably caused by differential gas migration through the soil.

This micro-environment test suggests that the long duration of time for collection of soil-gas samples over test site F may have

permitted significant environmental changes that would have affected the helium readings making it meaningless to correlate the data from day to day. Therefore, the lack of correlation between helium anomalies and subsurface mineralization is probably due to changes in temperature or barometric pressure that overshadowed any possible anomalous helium derived from the deposit.

#### $^4\text{He}/^{36}\text{Ar}$ and $^4\text{He}/^{22}\text{Ne}$ Ratios in Soil Gas

One-liter stainless steel soil-gas containers were loaded with soil gas collected from 60 cm deep sampling probes at 25 sample locations at test site F (figure 96). The samples were collected from 1410-1625 hours on February 21, 1977, and from 1523-1755 hours on February 24, 1977, as shown in table 17. Samples were returned to Martin Marietta for noble gas analyses by the Finnigan quadrupole mass spectrometer system.

The results of the helium-4, argon-36, and neon-22 in soil gas measurements are shown in table 17 and figure 96. The  $^4\text{He}/^{36}\text{Ar}$  percentage and  $^4\text{He}/^{22}\text{Ne}$  percentage, which indicate the percentage deviation from an assumed constant ratio in the atmosphere, are also shown in table 17. Only the variations greater than five to ten percent of the atmospheric ratio of 0.168 for  $^4\text{He}/^{36}\text{Ar}$  and 3.275 for  $^4\text{He}/^{22}\text{Ne}$  are considered to be significant due to the instrument precision of  $\pm 10$  percent.

None of the data for either the  $^4\text{He}/^{36}\text{Ar}$  ratio or  $^4\text{He}/^{22}\text{Ne}$  ratio vary below the atmospheric ratios by more than 8.3 percent, which is well within the instrumental precision. Several stations, however, did show ratios significantly greater than 10 percent above



Table 17.  ${}^4\text{He}/{}^{36}\text{Ar}$  and  ${}^4\text{He}/{}^{22}\text{Ne}$  Data, Test Site F.

Sample Location Number	${}^4\text{He}/{}^{36}\text{Ar}$	$\delta {}^4\text{He}/{}^{36}\text{Ar}\%$ *	${}^4\text{He}/{}^{22}\text{Ne}$	$\delta {}^4\text{He}/{}^{22}\text{Ne}\%$ **
F- 50	0.147	-12.5	3.027	- 7.6
F- 52	0.236	+40.5	5.491	+67.7
F- 57	0.230	+36.9	5.170	+57.9
F- 59	0.154	- 8.3	3.051	- 6.8
F- 73A	0.166	- 1.2	3.313	+ 1.2
F-108	0.154	- 8.3	3.075	- 6.1
F-132	0.156	- 7.1	3.075	- 6.1
F-161	0.155	- 7.7	3.203	- 2.2
F-184	0.161	- 4.2	3.167	- 3.4
F-189	0.164	- 2.4	3.248	- 0.8
F-223A	0.162	- 3.6	3.194	- 2.5
F-225	0.160	- 4.8	3.050	- 6.9
F-227	0.165	- 1.8	3.203	- 2.2
F-229	0.160	- 4.8	3.203	- 2.2
F-258	0.186	+10.7	3.381	+ 3.2
F-262	0.176	+ 4.8	3.230	- 1.4
F-264	0.165	- 1.8	3.352	+ 2.4
F-291	0.171	+ 1.8	3.411	+ 4.2
F-299	0.208	+23.8	3.515	+ 7.3
F-330	0.168	0.0	3.411	+ 4.2
F-396	0.157	- 6.5	3.221	- 1.6
F-425	0.238	+41.7	3.526	+ 7.7
F-471	0.161	- 4.2	3.221	- 1.6
F-566	0.165	- 1.8	3.660	+11.8
F-646	0.164	- 2.4	3.313	+ 1.2

\* From an assumed constant ratio in the atmosphere of 0.168.

\*\* From an assumed constant ratio in the atmosphere of 3.275.

the atmospheric ratios. These are stations 52, 57, 299, 425 and 566. Assuming a constant value of argon-36 and neon-22 in the earth's atmosphere and soil, these stations exhibit an anomalous concentration of helium-4 in the soil gas. These gas samples, because of their short collection time, were affected very little by environmental fluctuations. Therefore, the anomalous helium concentration may be due to subsurface mineralization.

Figure 96 shows the distribution of anomalous  ${}^4\text{He}/{}^{36}\text{Ar}$  and  ${}^4\text{He}/{}^{22}\text{Ne}$  ratios. In most cases, the stations with anomalous ratios can be attributed to subsurface mineralization. The ratios also point to several other target areas that are as yet unexplored, such as south of station 566 and southwest of station 425.

Despite the limited sample points, the data suggest that instantaneous  ${}^4\text{He}/{}^{36}\text{Ar}$  and  ${}^4\text{He}/{}^{22}\text{Ne}$  ratios may be useful in the detection of subsurface uranium mineralization to a depth of from 600 to 900 meters. However, to have more credibility, the survey should include a greater number of sample stations.

Table 18 shows these laboratory analyzed data and the previously obtained helium-in-soil-gas data for the same sample locations. Of the five gas samples analyzed in the lab which were anomalous in helium-4 concentration as demarked by the positive  ${}^4\text{He}/{}^{36}\text{Ar}$  (stations 52, 57, 258, 299 and 425), only stations 57 and 299 were found by the field method to have anomalous helium-in-soil-gas concentrations.

The ratio work in comparison with the field helium-in-soil-gas data suggests several conclusions:

- 1) diurnal changes caused substantial variations in the

Table 18. Helium Data Comparison, Test Site F

Sample Location Number	Laboratory Gas Analysis		Field Probe Analysis		Time of day collected		
	$\delta \frac{4}{36}\text{He}\%$	Time of day collected x 2/21/77 v 2/24/77	$\frac{4}{22}\text{He}\%$	Time of day collected			
50	-12.5	1610 x	- 7.6	+ 7	1032	-11	1223
52	+40.5	1625 x	+67.7	+ 12	1227	- 5	1344
57	+36.9	1550 x	+57.9	+ 38	1430		
59	- 8.3	1600 x	- 6.8			-32	1353
73A	- 1.2	1520 x	+ 1.2	- 9	1114	- 4	1327
108	- 8.3	1535 x	- 6.1	+ 10	1237	-26	1110
132	- 7.1	1505 x	- 6.1	- 40	1341	- 8	1203
161	- 7.7	1435 x	- 2.2	+ 1	1413	-29	1223
184	- 4.2	1450 x	- 3.4	+ 25	1553	+15	1035
189	- 2.4	1420 x	- 0.8	+ 12	1507	-25	1254
223A	- 3.6	1410 x	- 2.5	+ 33	1125	-44	1134
225	- 4.8	1450 x	- 6.9	+ 10	1200	- 5	1226
227	- 1.8	1615 x	- 2.2	+ 24	1615	-12	1120
229	- 4.8	1755 v	- 2.2	-107	1610	+17	1050
258	+10.7	1520 x	+ 3.2	+ 1	1150	-29	1240
262	+ 4.8		- 1.4	+ 1	1300	+ 9	1110
264	- 1.8	1609 v	+ 2.4	- 30	1515	- 1	1105
291	+ 1.8	1545 x	+ 4.2	- 20	1145	+17	1140
299	+23.8	1618 v	+ 7.3			+12	1115
330	0.0	1614 v	+ 4.2			-26	1420
396	- 6.5	1625 v	- 1.6	- 1	1245	- 4	1117
425	+41.7	1630 v	+ 7.7	- 68	1556	-39	1212
471	- 4.2	1550 v	- 1.6	- 11	1510	+24	0906
566	- 1.8	1540 v	+11.8	- 11	1235	-33	1256
646	- 2.4	1523 v	+ 1.2	0	1007	-36	1339

\* Deviation from background (assumed to be 5.250 ppm He).



- helium concentration of the soil gas during the collection of the soil gas samples;
- 2) a general decrease in the helium concentration of the soil gas occurs as the time of day progresses;
  - 3) it is difficult to correlate helium-in-soil-gas data that is collected over several days with anomalous helium concentrations related to subsurface mineralization;
  - 4) to detect realistically anomalous helium concentrations in soil gas derived from subsurface mineralization, it is necessary to:
    - a) collect instantaneous samples over a short period of time, or
    - b) utilize a cumulative collection device where the sample represents soil gas accumulated over a longer time period.

### Test Site G

#### Geology and Hydrology

Test site G encompasses approximately 15 square kilometers in a north-south band 1.6 kilometers wide across the "main trend" of uranium ore deposits in the Ambrosia Lake and Dos Lomas Quadrangles, McKinley County, New Mexico, as seen in figure 97. This test site was selected to test the utility of measuring the helium concentration in soil gas over known subsurface uranium deposits approximately 180-215 meters deep on widely spaced (600 meters) grid sample spacing.

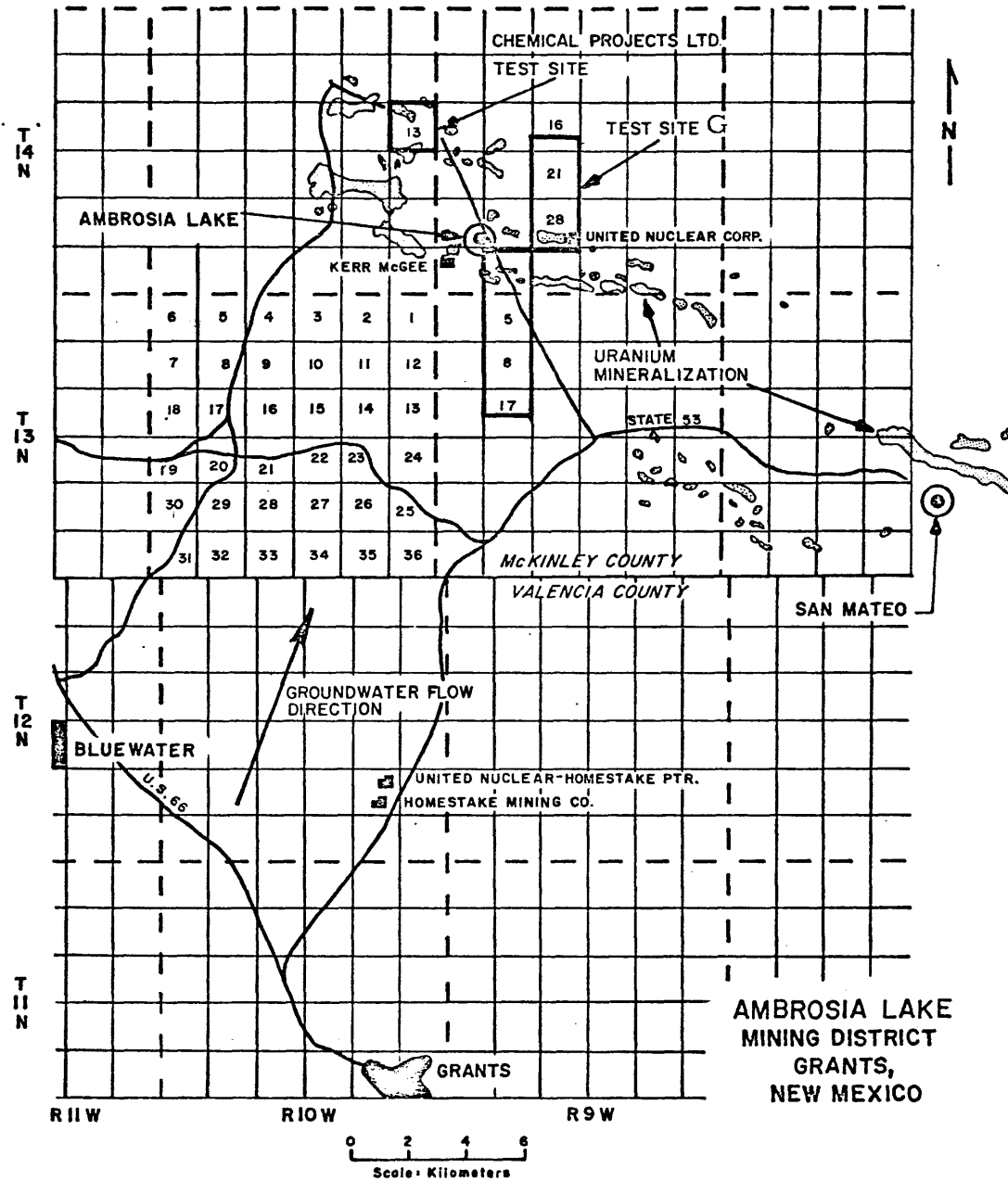


Figure 97. Regional map of the Grants - Ambrosia Lake Uranium District showing the location of test site G.

The survey was conducted principally in Sections 21, 18, and 32, T. 14 N., R. 9 W. and Sections 5 and 8, T. 13 N., R. 9 W. on land controlled by United Nuclear Corp., United Nuclear-Homestake Partners, and Hydronuclear, Inc.

The bedrock geology of test site G (figure 98) is essentially one of Mancos Shale at the surface of the site except for the southernmost ten stations (stations 36, 37, 46, 47, 55-57, and 65-67; see figure 99), where the Dakota Sandstone crops out. The bedrock units dip gently (1-2 degrees) to the northeast into the San Juan Basin, as shown in the cross section of figure 98. A number of north-northeast trending, high-angle, normal faults occur throughout the test site. The locations of the known uranium deposits in the Westwater Canyon Member in Sections 28, 29, 32, and 33, T. 14 N., R. 9 W., and the small deposits in the Poison Canyon Member of the Morrison Formation in Sections 6 and 7, T. 13 N., R. 9 W., are shown in figure 99. A thin veneer of surficial alluvial and colluvial deposits cover the bedrock units over most of the test site. The ground water gradient is to the northeast as shown in figure 99.

#### Helium Measurements in Soil Gas

Soil gas was sampled by means of the probe and syringe method for field analysis on a 600-meter grid spacing including 65 sample locations. Soil gas sampling was conducted once on February 23 and once on February 24, 1977. In order to test the utility of helium-soil-gas surveys in a practical exploration mode, the grid sample spacing was large and the survey was conducted without any attempt to collect samples in a short time period.

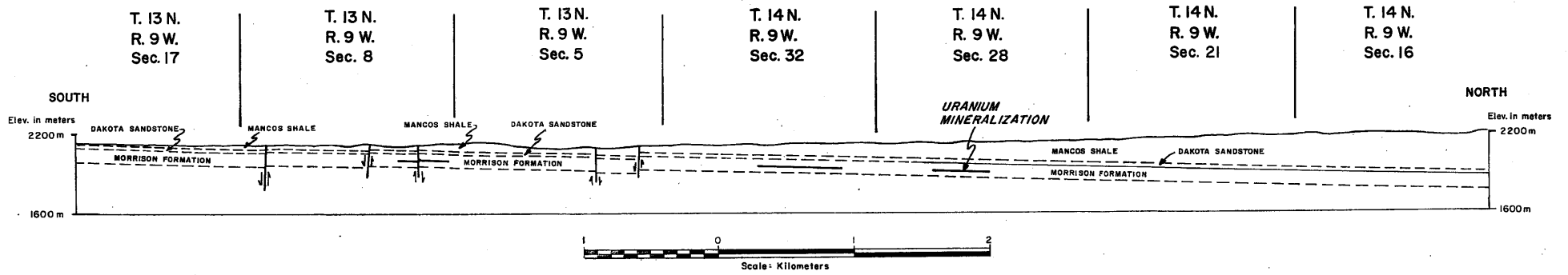


Figure 98. Geologic cross section of test site G.

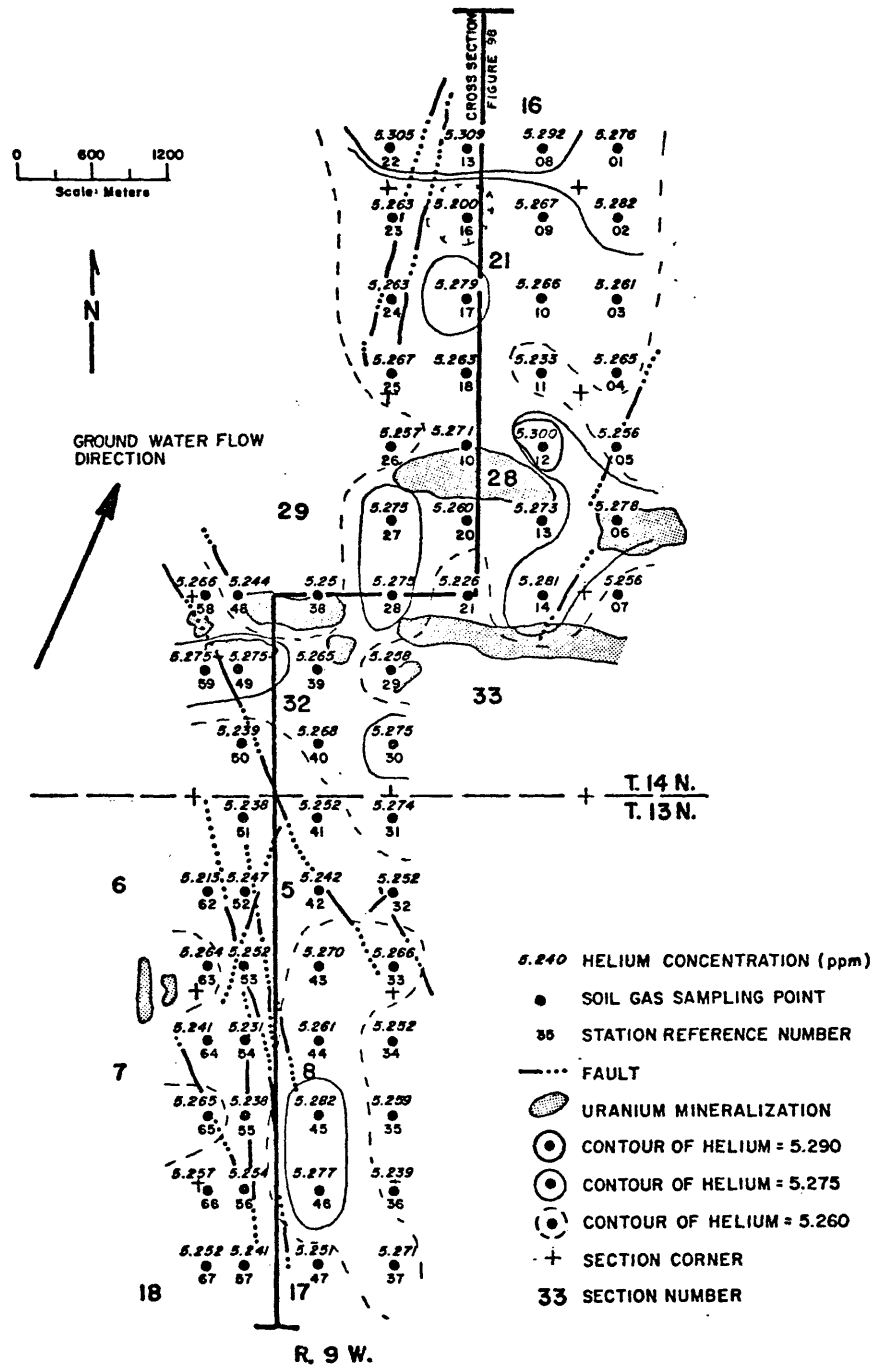


Figure 99. Helium concentration in soil gas on February 23, 1977, at test site G.

The results of the February 23 survey are shown in figure 99. The areas of highest helium concentration show no direct correlation with the areas of subsurface mineralization but are displaced northward in the direction of ground water movement. The faults which are mapped at the surface do not appear to affect the helium-in-soil-gas distribution.

The results obtained on the February 24 survey are shown in figure 100. During analysis, the chemical pump malfunctioned yielding erroneous analytical results for some samples. These data are omitted on figure 99. Again, the samples were obtained throughout the course of the day, thus being subject to diurnal and other environmental changes. The February 24 data generally show lower helium values than the February 23 data. However, the pattern of highest helium values are similar in both surveys. Again, a northward displacement is noted in the direction of ground water flow. The surface faults in the test site do not appear to affect the helium-in-soil-gas distribution.

The results of the two surveys indicate that helium-in-soil-gas anomalies can be detected that are related to subsurface mineralization in small surveys with a single day collection time. More consistent results probably would have been obtained if the samples were collected in a very short time on both days.

At this scale of sampling, faulting does not appear to affect the distribution of helium-in-soil-gas.

#### Regional Surveys

R.H. De Voto (1976, personal communication) had reported

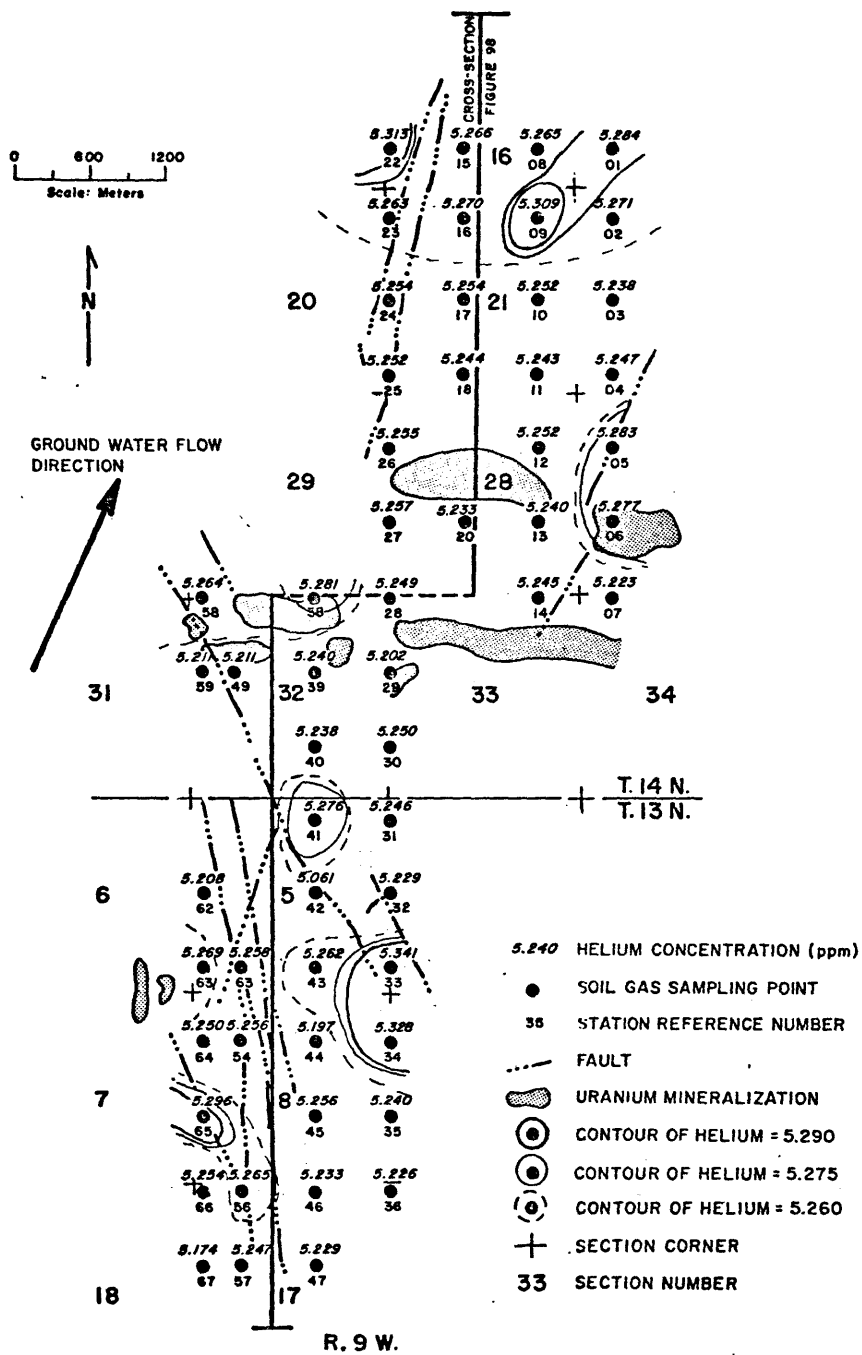


Figure 100. Helium concentration in soil gas on February 24, 1977, at test site G.

that a broad area of anomalous uranium concentration in ground water within the Morrison and Dakota aquifers exists in the immediate vicinity of the Ambrosia Lake district. An attempt was made in mid-December, 1976, to sample ground water and analyze for the helium and uranium contents from every available water well in the area from the Morrison Formation outcrop northward, as shown in figure 101. Many water wells, windmills and stock-storage tanks were shut down for the winter and were unavailable for sampling, so the data is sparse.

Water samples were collected in polyethelene bottles to be analyzed for their helium content later and duplicate ground water samples were sent to Geolabs for fluorometric uranium analysis. The helium and uranium concentrations of the 17 ground water samples obtained are shown in table 19 and on figure 101. The depth of the well and stratigraphically lowest aquifer (Cooper and John, 1967) are also shown in table 19. The bedrock geologic units (Chapman, et al., 1973) and the major uranium deposits are also shown in figure 101. It is assumed from the regional river pattern that the area of figure 101 is a regional ground water recharge area.

#### Uranium in Ground Water

The range of uranium concentration in ground waters in the survey was from less than 2 ppb to 980 ppb. The background concentration of uranium in ground water within the sandstone aquifers in the region (Menefee Formation, Point Lookout Sandstone, Crevasse Canyon Formation) is in the range of 0 to 17 ppb.

Ground water samples taken from wells which yield water from the Westwater Canyon Member in proximity to uranium mineralization



Table 19. Helium and Uranium Concentrations in Ground Water  
in the Grants-Gallup-Ambrosia Lake Region.

Well Location		Section	Uranium Concentration (ppb)	Helium Concentration (ppm)	Well Depth (meters)	Lowest Producing Aquifer
Township	Range					
T. 20N.	R. 12W.	6	3	12.57	295	Kmf
T. 20N.	R. 13W.	23	10	7.56	125	Kmf
T. 19N.	R. 13W.	9	7	5.90	143	Kgc
T. 18N.	R. 9W.	22	7	5.72		
T. 17N.	R. 13W.	24	10	8.81	67	Kgc
T. 17N.	R. 9W.	15	8	4.92		
T. 16N.	R. 10W.	22	12	5.09	195	Kplh
T. 15N.	R. 12W.	17	16	4.95	372	Jmw
T. 15N.	R. 10W.	6	17	5.32	305	Kcdi
T. 14N.	R. 10W.	10	63	7.44	224	Jmw
T. 14N.	R. 10W.	14	74	44.73	214	Jmw
T. 13N.	R. 9W.	22	320	4.65	91	Jmw
T. 13N.	R. 9W.	32	980	4.52		Jt
T. 13N.	R. 8W.	11	< 2	5.20	61	Kmf
T. 13N.	R. 8W.	19	520	4.88		
T. 13N.	R. 8W.	22	2	6.95		Kmf
T. 13N.	R. 8W.	25	< 2	10.77	45.72	Kmf
T. 13N.	R. 8W.	26	2	13.46	213	Kpl
T. 12N.	R. 8W.	4	< 2	12.82		Kmf

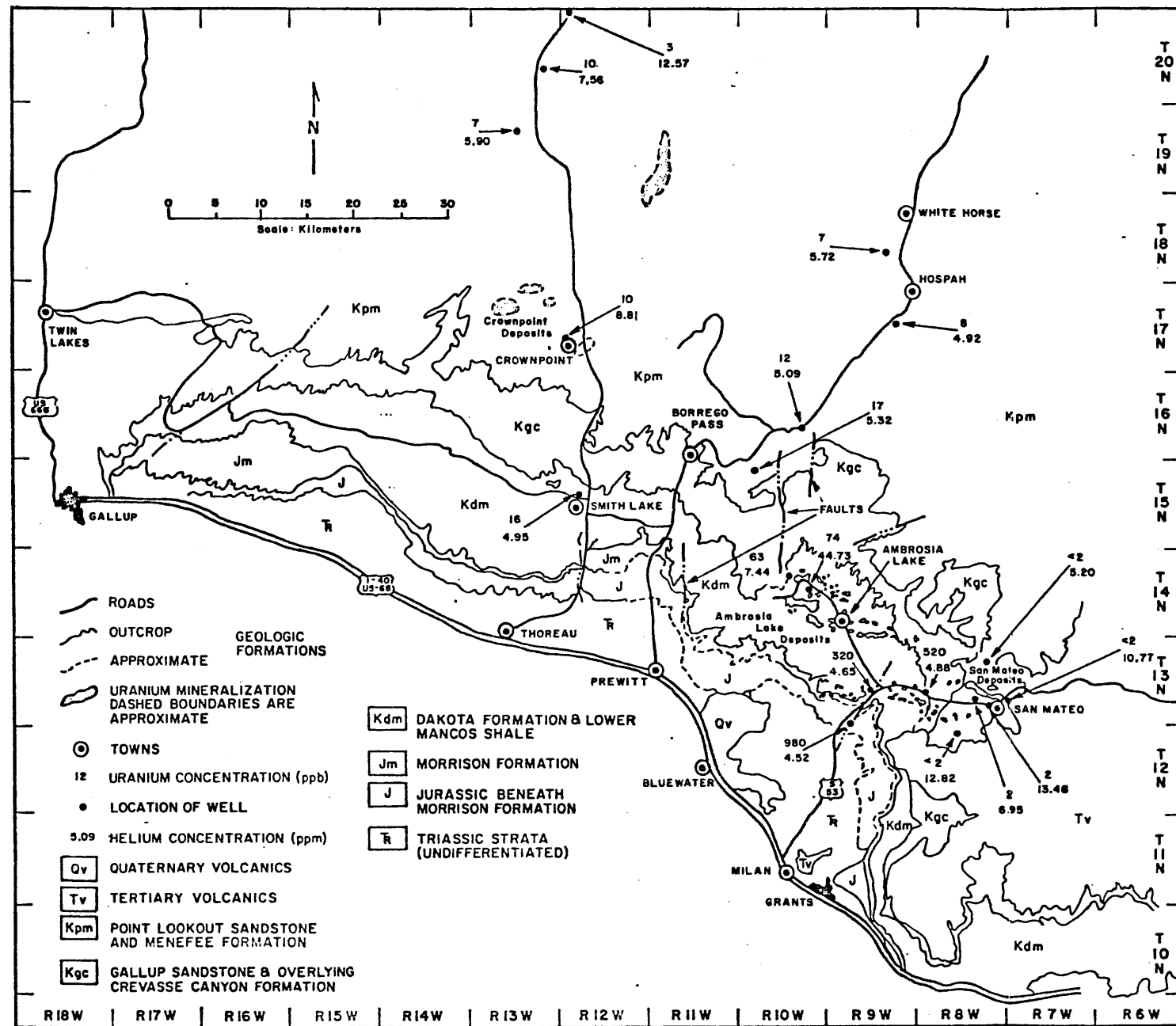


Figure 101. Helium and uranium concentrations in ground water in the Grants-Gallup-Ambrosia Lake region. The geologic formations in the region are shown also. Geologic data from Chapman, Wood and Griswald (1973).

contain highly anomalous uranium (63 and 74, respectively, in T. 14 N., R. 19 W., near uranium deposits in the Westwater Canyon Member and 320 and 520 ppb uranium, respectively, in Section 22, T. 13 N., R. 9 W., and Section 19, T. 13 N., R. 8 W., near uranium mineralization in the Poison Canyon sandstone of the Morrison Formation). Morrison ground water at some distance from uranium deposits or in the direction of ground water recharge contain background levels (16 ppb at T. 15 N., R. 12 W.).

Ground water samples taken from wells which draw water from sandstones stratigraphically above the Westwater Canyon Member show background concentrations of uranium. This is true even in the immediate vicinity of uranium deposits, such as the background uranium concentration in water from wells in the San Mateo area that were derived from the Menefee and Point Lookout sandstones. The other highly anomalous uranium-in-ground-water value, 980 ppb in Section 32, T. 13 N., R. 9 W., was obtained from a well in the Todilto Limestone near a uranium deposit within that unit.

Thus, a uranium-in-ground-water survey can be extremely useful in exploration for uranium deposits if water can be sampled from the aquifers that are potential hosts for the uranium mineralization. The utility of uranium-in-ground-water surveys diminishes, however, as the stratigraphic distance from and hydraulic discontinuity with the uraniumiferous aquifer increases. Thus, as exploration for uranium deposits becomes deeper and deeper, sampling of ground water from shallow water wells for their uranium concentration becomes less and less useful. Sampling the water from exploration drill holes from several, and possibly all, aquifer horizons that are potential hosts for

uranium mineralization, however, can be an important exploration tool. This is effectively a search for a geochemical halo related to an undiscovered uranium deposit. A procedure of water recovery from water-bearing zones in deep exploration drill holes followed by geochemical analysis of the water for uranium, helium, radon, and other constituents, could be an extremely cost-effective technique in exploration for deeply buried uranium deposits. In order to be effective in determining accurately which formation hosts the water tested in this procedure, packer isolation of aquifers in the drill hole is necessary.

#### Helium in Ground Water

The helium concentrations in the ground water samples ranged from 4.52 to 44.73 ppm. Background helium levels in the water samples range from 4.5 to 5.5 ppm. The data on figure 101 show a distinct lack of correlation between anomalous helium concentrations in ground water and anomalous uranium concentrations in the same water samples.

Four of the water samples in the area of the San Mateo uranium deposits, all from sandstones stratigraphically above the ore-bearing Morrison sandstones, contain highly anomalous helium concentrations (from 6.95 to 13.46 ppm) and background levels (<2 ppb) of uranium. The two water samples in T. 14 N., R. 10 W., in close proximity geographically and stratigraphically to the Westwater Canyon ore deposits of the Ambrosia Lake area, both have anomalous helium and uranium concentrations, including one with the highest observed helium concentration, 44.73 ppm, in the area. The three ground water samples with the highest uranium concentrations, those in T. 13 N., R. 9 W., and Section 19, T. 13 N., R. 8 W., however, have background helium levels.

The ground water sample from the Menefee sandstones in the area of the Crown Point uranium deposits (which are in the Westwater Canyon Member of the Morrison Formation) has an anomalous helium concentration of 8.81 ppm, but a background uranium level (10 ppb). Most of the other water wells from the Menefee Formation contain background levels of both helium and uranium, with the exception of one in Section 23, T. 20 N., R. 13 W., where the helium concentration is anomalous (7.56 ppm) and the uranium concentration is not (10 ppb) and another in Section 6, T. 20 N., R. 12 W., where the helium concentration is anomalous (12.57 ppm) and the uranium concentration is not (3 ppb). No uranium deposit is known which may be the source of the anomalous helium in these two water wells.

The helium data show that helium moves with the ground water as well as through the ground water vertically from subsurface uranium deposits. Thus, anomalous helium concentrations can often be found in ground waters located in stratigraphically higher horizons than the uranium-bearing horizons. This movement of helium toward the atmosphere, with little dependence on the ground water movement and through rocks relatively impervious to water, permits surveys for helium in ground water to be extremely useful in exploring for uranium deposits at depth. Hence, sampling of water from shallow water wells may be efficacious in detecting anomalous helium concentrations derived from the radioactive decay of a uranium deposit which is substantially deeper. At San Mateo, in T. 13 N., R. 8 W., it appears that a uranium deposit 900 meters deep yielded anomalous helium concentrations of 10-13 ppm in ground water 760-850 meters stratigraphically above the uranium deposit, within shallow water-well depths. Thus, helium analysis should be conducted routinely on all

ground water samples obtained in a hydrogeochemical exploration survey or encountered in an exploration drilling program.

#### Helium in Soil Gas Along Four Regional Traverses

A regional helium-in-soil-gas survey was conducted along county roads in the Grants-Gallup-Ambrosia Lake area of northwestern New Mexico. Samples of soil-gas were obtained by the probe-syringe collection system and analyzed for their helium concentration with the truck-mounted portable mass spectrometer. The samples were generally collected at 1.6 kilometer (one mile) intervals along four roads north of U.S. Highway 66, north from Gallup, Thoreau, Prewitt, and Milan, and along an east-west road which connects the north-south roads. The location of the roads and sample spacing along the traverses are shown with respect to the bedrock geologic units and the location of the uranium deposits in figure 102. The intent of this regional survey was to determine if regional helium-in-soil-gas surveying could have delineated favorable areas within a sedimentary basin to prospect for buried uranium deposits. The lines were laid out, therefore, to traverse some areas of known subsurface uranium deposits, the San Mateo, Ambrosia Lake, and Crown Point areas, as well as some relatively barren areas. The sample spacing was reduced to 300-meter spacing across the outcrop band of the Morrison Formation, in an attempt to discern if any helium was escaping up the dip of the Morrison Formation from the uranium deposits to the surface.

Soil gas samples were collected twice, from December 14-16, 1976, as shown on figure 102, and on December 21, 1976, as shown on figure 103. The helium concentration in soil gas along the December 14-16, 1976 traverses ranged from 5.142 to 5.424 ppm.

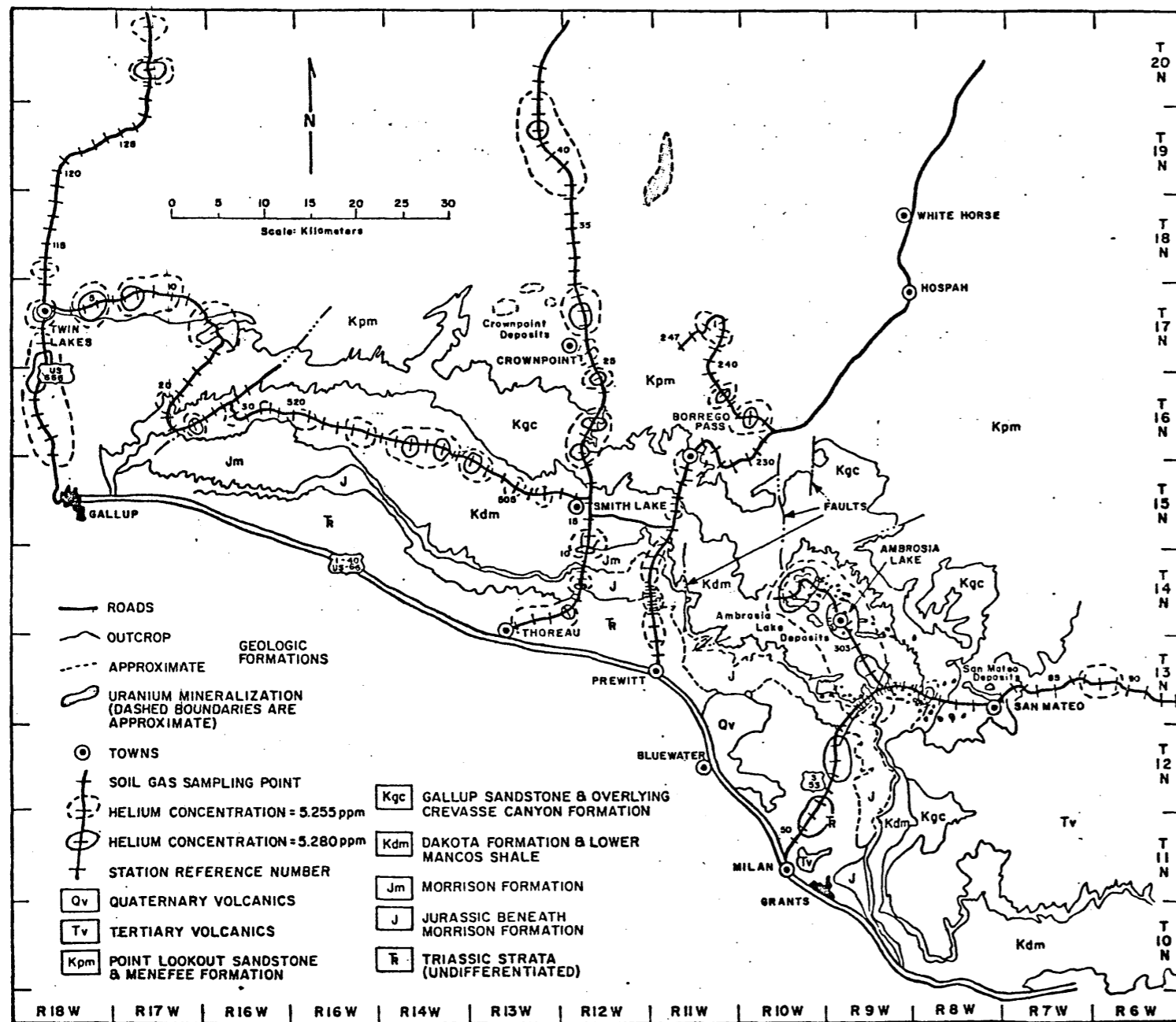


Figure 102. Helium concentration in soil gas collected at 1.6 kilometer (1 mile) intervals along roads in the Grants-Gallup-Ambrosia Lake region from December 14, 1976 to December 16, 1976. Geologic data from Chapman, Wood and Griswald (1973).

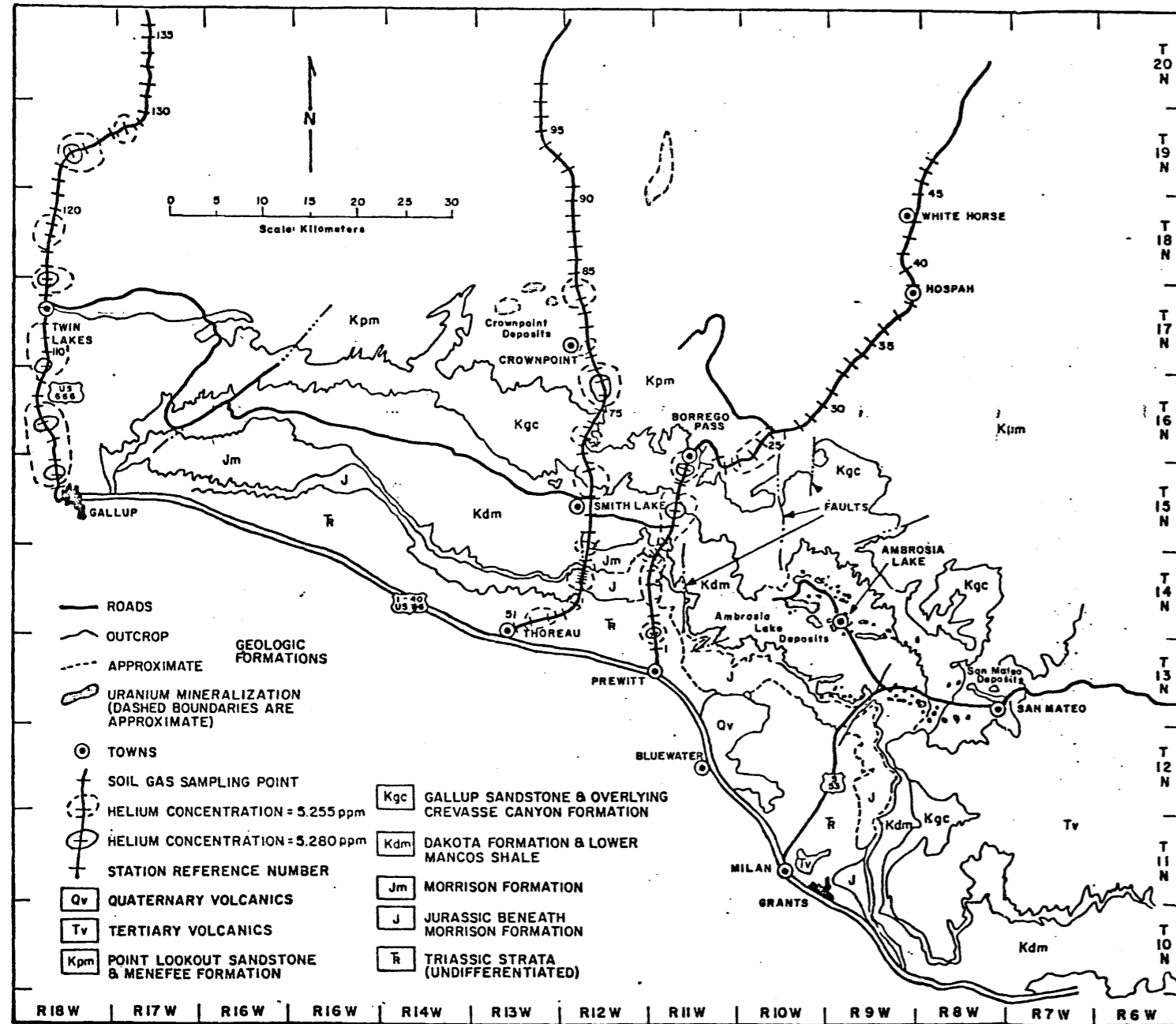


Figure 103. Helium concentration in soil gas collected at 1.6 kilometer (1 mile) intervals along roads in the Grants-Gallup-Ambrosia Lake region on December 21, 1976. Geologic data from Chapman, Wood and Griswald (1973).



It is difficult to draw any conclusions from the December 14-16 traverse data except that the region of most of the uranium deposits, the Ambrosia Lake area, shows the greatest concentration of helium in soil gas values greater than 5.28 ppm. Anomalous helium in soil gas in the Crown Point area may also reflect the known subsurface uranium deposits. Otherwise, the December 14-16 soil gas values show little correlation with the bedrock geology or the subsurface uranium deposits.

The December 21, 1976 survey was conducted only along three roads north of U.S. Highway 66, two of which were in common with the December 14-16, 1976 survey. The helium-in-soil-gas concentrations of the December 21, 1976 survey ranged from 5.204 to 5.344 ppm. Again, there is no clear coincidence of anomalous helium in soil gas with subsurface uranium deposits, except in the area of Crown Point.

A general increase in helium concentration also seems to occur at the outcrop band of the Morrison Formation, on all lines on both times of traverse. This suggests that up-dip migration of helium may be occurring and may afford a regional exploration technique by running helium-in-soil-gas surveys along the outcrop band of favorable host rocks. Unfortunately, the Morrison outcrops were only traversed in three locations during this survey and, in each case, with some uranium mineralization down dip.

The areas of high helium concentration in the December 21, 1976 survey (figure 103) correspond fairly well to similar high helium areas in the December 14-16 survey (figure 102). These regional soil gas surveys, however, are difficult to interpret but might be improved by use of a grid sampling system with reference station data for diurnal

and environmental corrections.

It appears from these regional results, as well as those in the southern Powder River Basin, that regional ground water helium measurements have a better potential for identifying the presence of uranium ore than the regional soil gas surveys. However, the ground water approach may be limited by the availability of wells.

## FRONT RANGE, COLORADO

Schwartzwalder Mine Area, Colorado

The final location for research was at the Schwartzwalder uranium mine near Golden, Colorado. The deposit is quite different from the other test sites investigated in that it is a vein uranium deposit that occurs in metamorphic terrane.

The field tests in this area were performed in May and June, 1977, with permission from the Cotter Corp. which operates the Schwartzwalder mine. The field expenses for the third survey conducted on June 16, 1977 were funded by them.

Geology and Uranium Deposits

The geology of the Schwartzwalder mine area is characterized by foliated Precambrian schists and gneisses of the Idaho Springs Formation. The Precambrian units strike approximately east-west and dip from 70°N to 70°S but are nearly vertical in the vicinity of the mine (Young, 1977).

Major zones of fracturing and brecciation occur within the area. The Rogers Fault is the most important in the area of the mine, showing as much as 670 meters of vertical displacement (Fisher, 1976) (figure 105). Most of the displacement probably occurred during the Precambrian with renewed movement during the Laramide. The Laramide movement probably prepared the rocks for deposition of remobilized uranium. The major ore-bearing veins strike approximately N15W

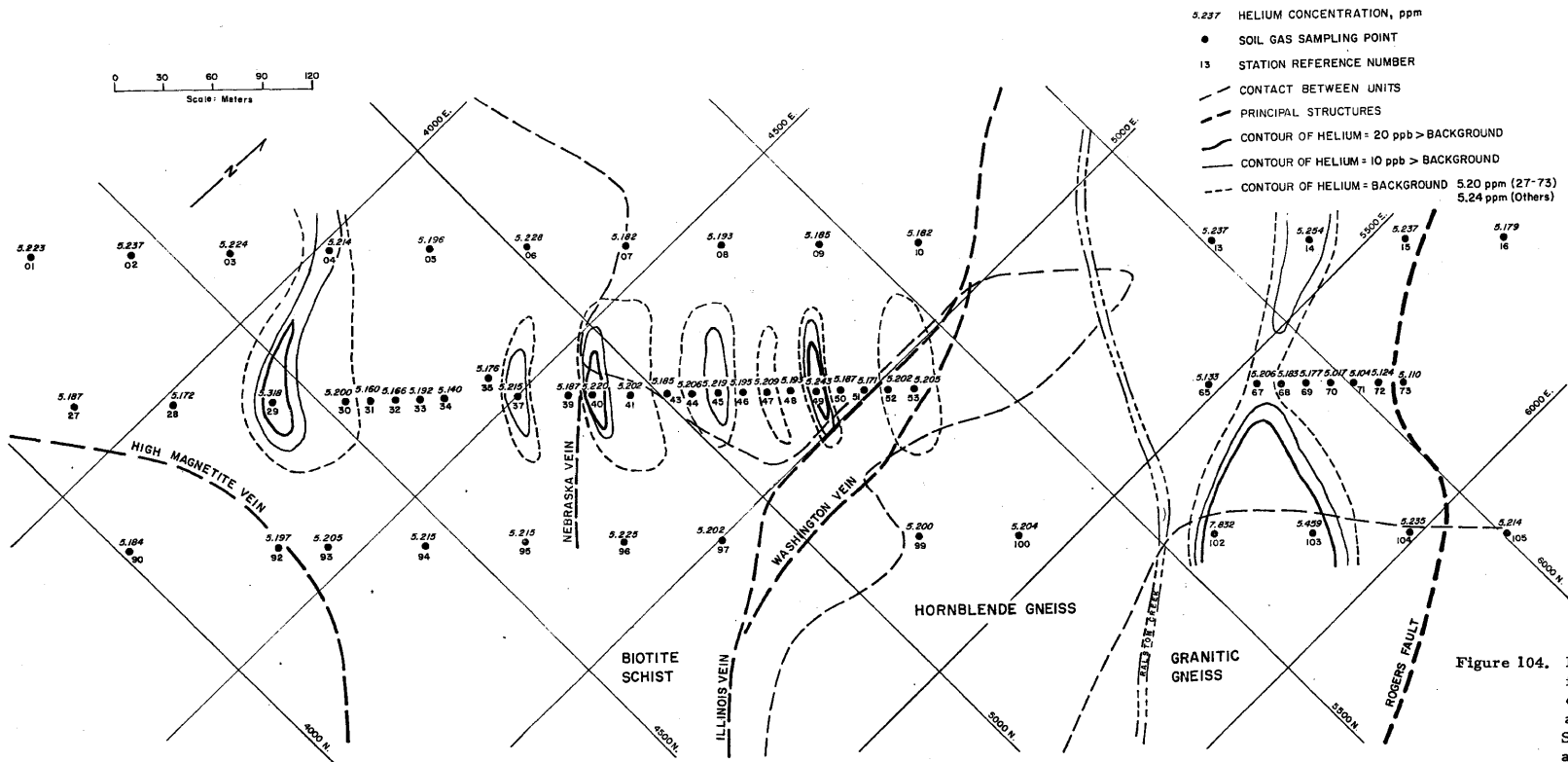


Figure 104. Helium in soil gas for samples collected on May 6, and May 9, 1977, Schwartzwalder mine area. Geologic data from Young, 1977.

and dip steeply to the west. The Illinois vein is the longest and most persistent and dips approximately  $75^\circ$  to the west. On the hanging wall of these major structures numerous low angle veins, "horse-tails," extend to the west, as can be seen in figure 105. The ore is intimately associated with fault breccias and fractures. The veins and fracture system within the mine are generally open and, as a result, fairly permeable and should be preferred pathways for helium migration from the uranium mineralization.

The mineral of economic importance within the mine is uraninite. Associated minerals include pyrite, chalcopyrite, bornite, ankerite, molybdenite, jordisite, siderite and calcite (Fisher, 1976). Alteration of the wall rock is usually quite minimal.

#### Helium-in-Soil-Gas Surveys

Helium surveys were conducted on May 6, May 9, May 24, and June 16, 1977, during which a total of 150 soil-gas samples were collected. The surveys were conducted using the syringe-probe collection system and helium field analysis mass spectrometer. In the first orientation survey, conducted on May 6 and May 9, sample station spacing was approximately 60 meters in background areas and 15 meters in the area of the mine. This is illustrated in figure 105. Three N45W lines were traversed approximately 90 meters apart. The center line was traversed on May 6 and the two outer lines on May 9. Helium concentrations in the soil-gas of this survey ranged from 5.08 ppm to 7.83 ppm with an average of 5.25 ppm. The helium concentration contours shown in figure 105 have been drawn with two different background threshold values, 5.20 ppm for the May 6 data and 5.24 ppm for the May 9 data. This was due to a 24-hour delay which occurred in

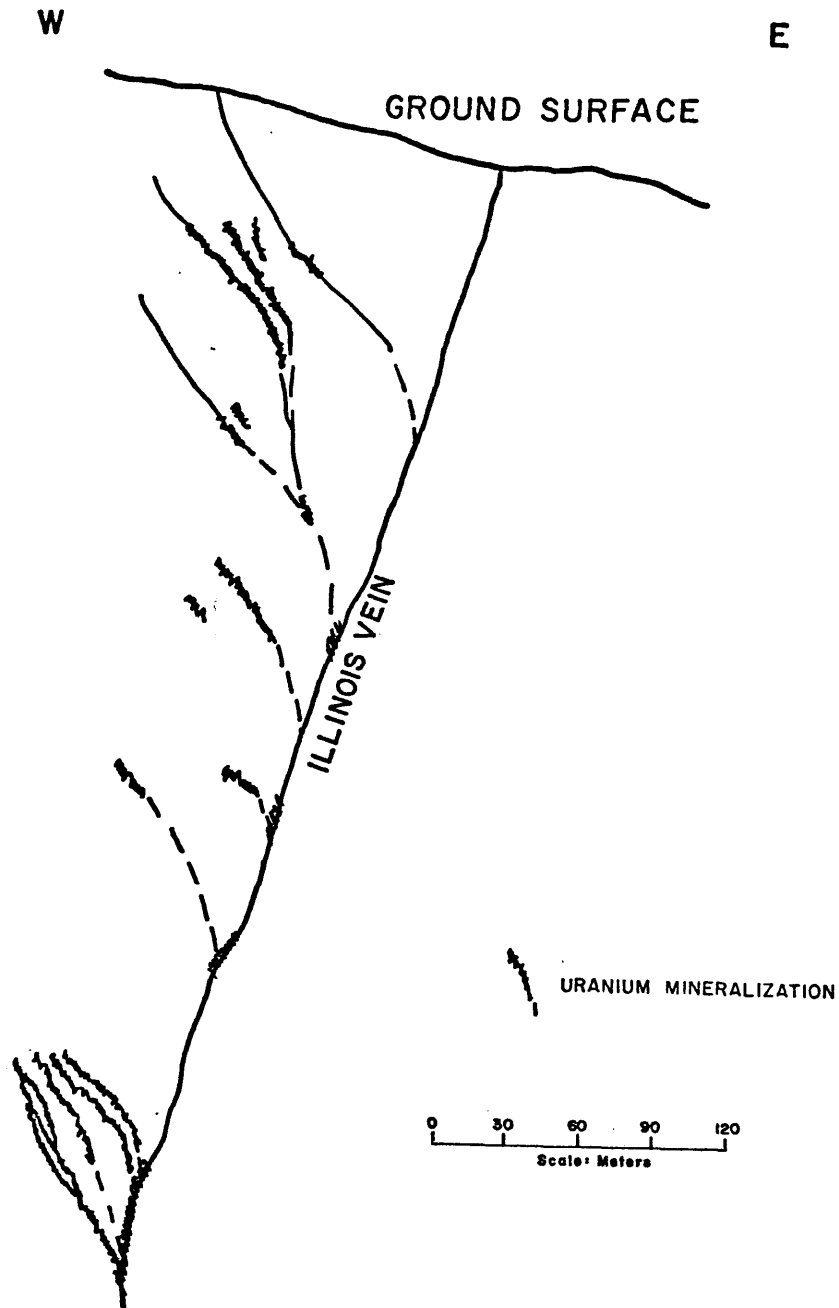


Figure 105. Schematic geologic cross section of the Schwartzwaldler mine, showing the Illinois vein and "horse-tails" which contain most of the known ore deposits (Paschis, personal communication).

the mass spectrometric analysis of the May 9 soil gas samples. Choosing the atmospheric level of 5.24 ppm helium as the background level for these samples insured that samples which might have equilibrated with the atmosphere would not be erroneously considered as anomalous. This is a conservative treatment of the data but still shows unequivocally the high amplitude anomaly to the northeast of Ralston Creek. Several single and double-point anomalies were detected west of the mine that are attributed to helium migration in the "horse-tails". The anomaly detected east of the mine, between Ralston Creek and the Rogers Fault had considerably greater helium concentration (from 5.4 to 7.8 ppm) than had previously been detected at any location in this entire research program. This area was the site for further detailed testwork on May 24, with a grid type survey having 30-meter east-west spacing between stations and 15-meter north-south spacing, as shown in figure 106. This detailed test work showed helium concentrations in soil gas ranging from 5.17 ppm to 6.58 ppm, and averaging 5.30 ppm. A 30 x 100 meter, east-west anomaly greater than 5.25 ppm, including one value of 6.58 ppm, was detected by this detailed test work.

A second detailed test on a 15-meter grid spacing was conducted in the same vicinity on June 16, 1977. These data are shown in figure 107. Helium concentrations in this test ranged from 5.12 ppm to 6.22 ppm, averaging 5.29 ppm. A 30 x 70 meter, helium-in-soil-gas anomaly was detected with helium concentration up to 970 ppb above the background threshold of 5.25 ppm.

The results of all of the helium-in-soil-gas data obtained to the northeast of Ralston Creek in the three surveys are summarized





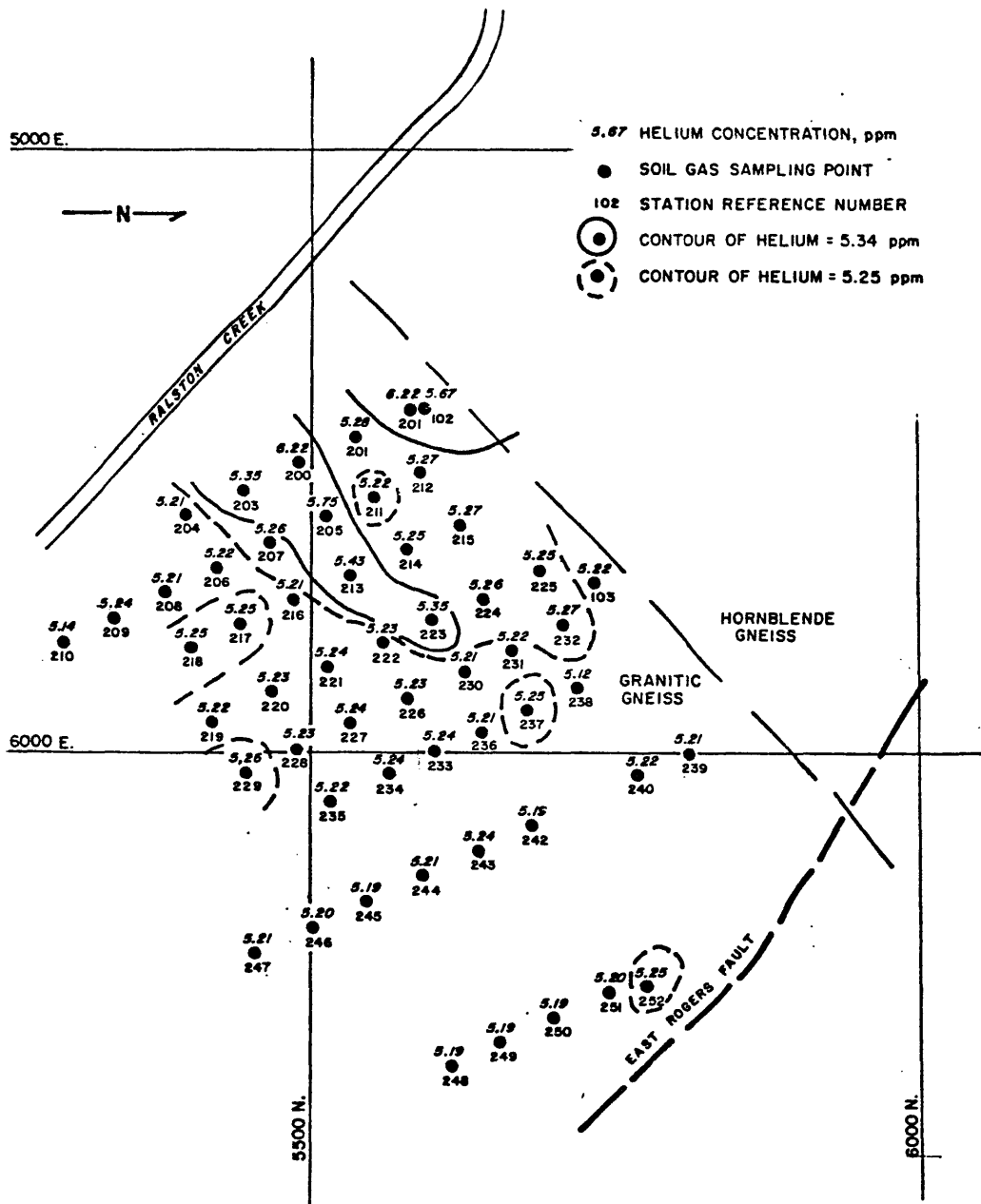


Figure 107. Helium-in-soil-gas collected during the second detailed survey (June 16, 1977), Schwartzwaldler mine. Geologic data from Young, 1977.

in figure 108. This composite helium soil-gas map shows two regions of anomalous helium greater than 100 ppb above the background threshold, surrounded by a broader region 10-100 ppb above the background threshold. The anomalies are separated by a pegmatite intrusion of probable Silver Plume age. Figure 108 also shows the anomalies in relation to the Rogers Fault, the contact between hornblende gneiss and granite gneiss, and Ralston Creek. The Rogers Fault does not appear to be the source of the helium because the helium concentration in soil gas near the fault is at background levels. The area of the hornblende gneiss-granitic gneiss contact displays anomalous helium in soil gas in the vicinity of Ralston Creek, but not to the northeast. This contact is gradational, and the granitic gneiss appears to be a result of feldspathization of the hornblende gneiss (Jim Paschis, 1977, personal communication). Thus, it seems that the contact itself is not the source of the helium. The anomalous area is open ended toward Ralston Creek, which, if structurally controlled, may represent the source of the helium. Figure 109 is a cross section in the area of the mine showing the two major structures in the mine, the Illinois and Washington veins and the associated mineralized "horse-tails". A westward inclined Cotter Corp. core hole (Drill Hole 4) intercepted a 45-centimeter fracture zone with uranium content of twenty times background. This fracture zone dips 29° to the east. There is a high degree of similarity between this mineralized zone and the mineralized "horse-tails" off the Illinois vein. This mineralized zone plus the high helium anomalies in the vicinity of Ralston Creek lead to the postulation (as shown in figure 109) of a major structure parallel to the Illinois vein beneath Ralston Creek that may be the source of the helium-in-soil-gas anomaly discovered by this

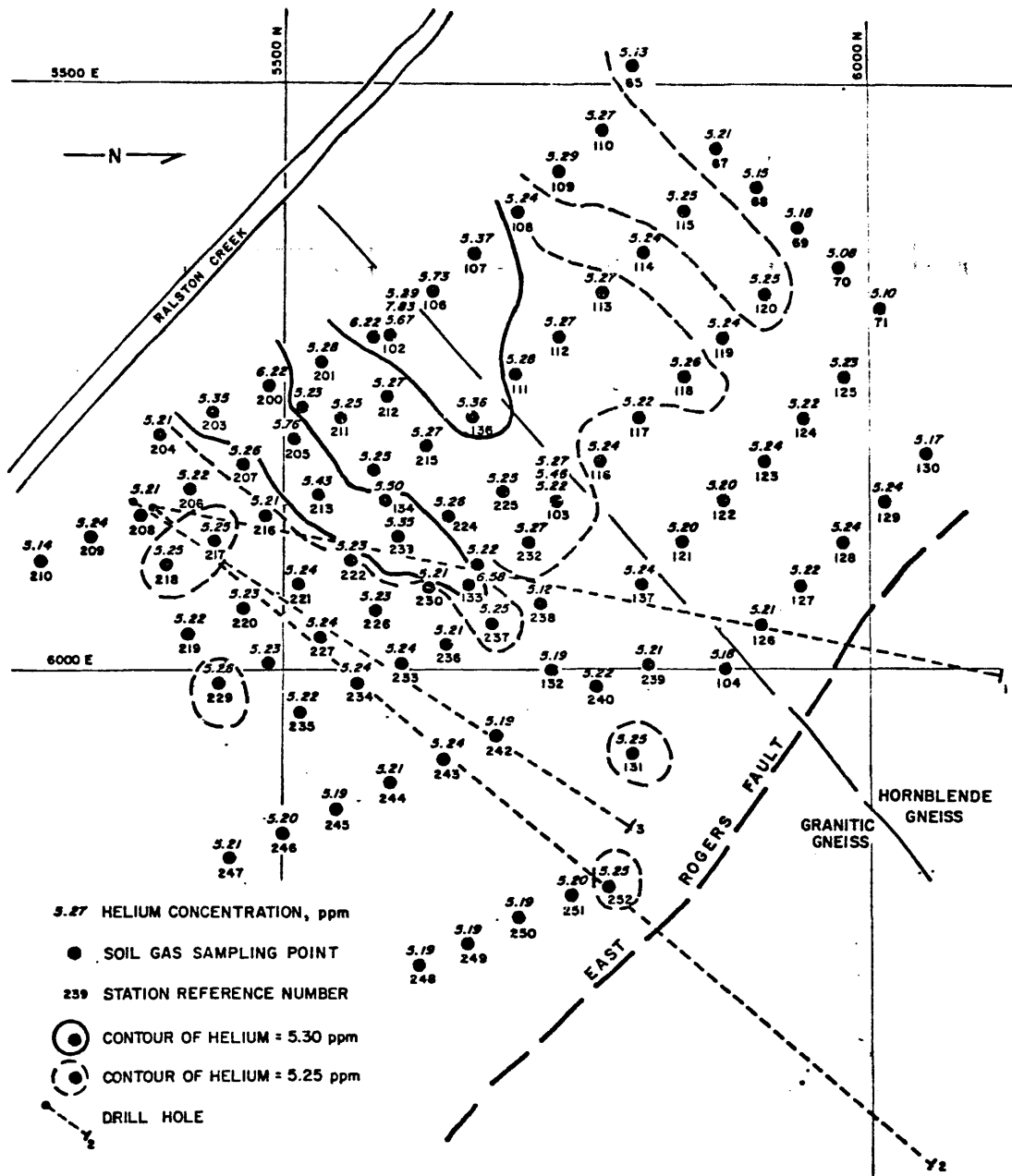


Figure 108. Summary of all helium in soil gas data, Schwartzwalder mine. Geologic data from Young, 1977.

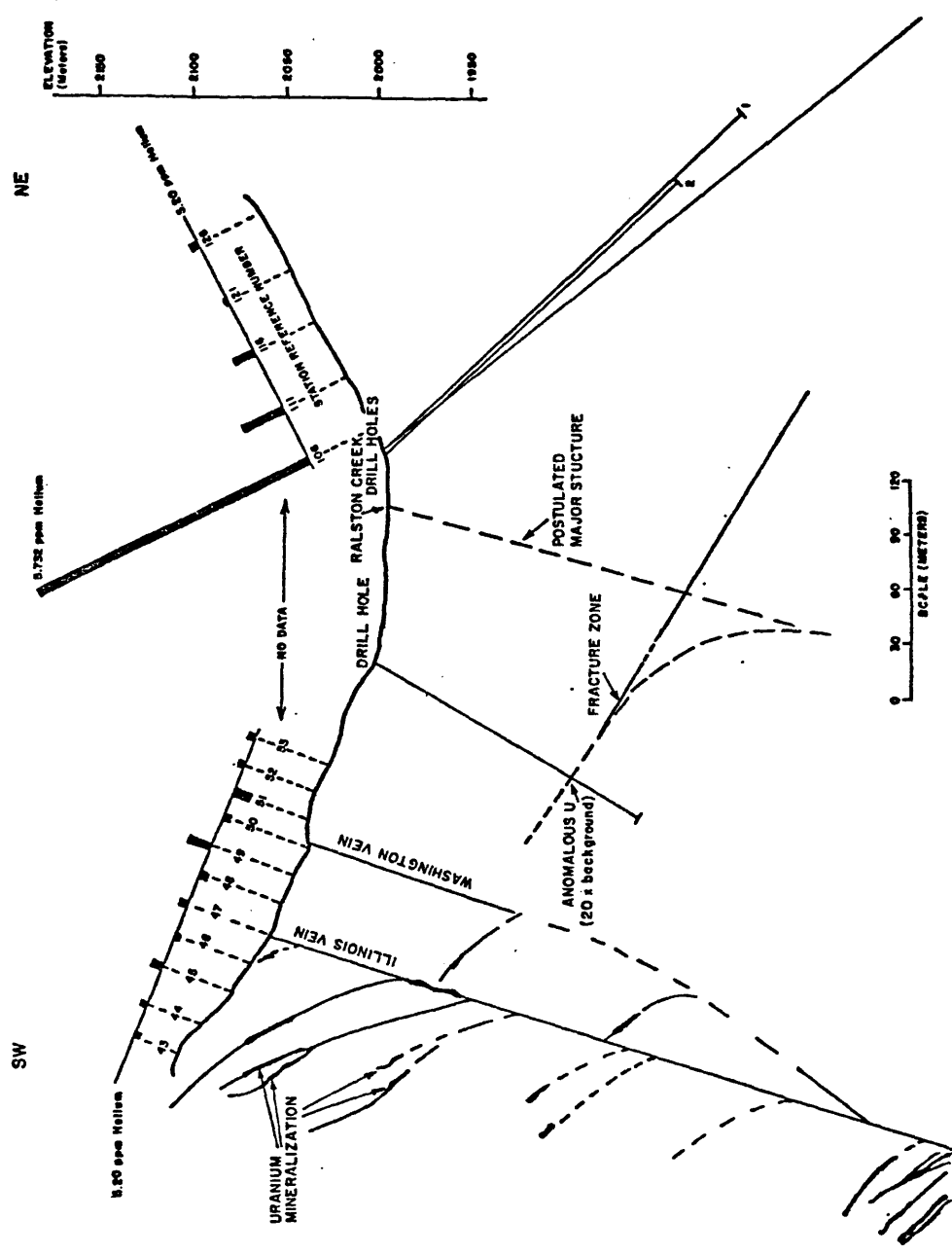


Figure 109. Schematic cross section and helium in soil gas data showing major structures in the vicinity of the Schwartzwalder mine and a postulated structure surfacing at Ralston Creek, which may be the cause of the measured helium anomalies in soil gas. Geologic data from Young, 1977.

survey. Unfortunately no helium measurements were made in the region which is most crucial to this hypothesis because, at the time of measurement, it was considered to be a region which might be badly contaminated by the mining operations which are centered in that area. Three Cotter Corp. core holes (Drill Holes 1, 2, and 3) have been drilled beneath the helium anomaly, as shown in figure 108. These core holes are inclined to the east and intercepted a very minor zone of uranium concentration slightly above background. The holes did not test the existence of the major structure postulated on figure 109 because of their location further to the east. In order to test the existence of the postulated structure, a hole should be drilled in the vicinity of Ralston Creek.

Although the exact source of the anomalous helium in soil gas discovered in this survey is not yet known, the presence of a high amplitude (from 100 to 2580 ppb above background) helium-in-soil-gas anomaly, up to 25 times higher amplitude than any discovered on all of the other soil gas surveys of this research, is extremely important. This data suggests that instantaneous helium-in-soil-gas surveys may be more useful and interpretable in geologic terrane that is highly fractured and faulted in relatively brittle rocks than in sedimentary sequences. The suggestion is that the faults, veins, and fractures represent open channelways for migration of helium from the buried uranium mineralization to the soil, where it can build up to higher, more detectable anomalous levels in the soil gas.

Conversely, the helium anomaly could be a manifestation of a structure as postulated, not because of the presence of uranium ore associated with the structure, but because the structure serves as a vent for deeply buried helium accumulations.

## SUMMARY AND CONCLUSIONS

### Collection and Measurement Techniques

#### Field Mass Spectrometer System

The field instrumentation system consisted of a modified helium leak detector mass spectrometer installed in a 4-wheel drive truck. The mass spectrometer was modified for batch sampling and increased sensitivity by installing five automated shutoff valves in the system and by including a chemical getter pump to keep the system pressure down during the measurement period and to remove all active gases from the sample thereby increasing the system sensitivity by a factor of 100. The inlet manifold provided gas to the sample-defining volume from a sampling syringe inserted into the syringe inlet septum. Two reference gases were provided for frequent calibration of the system sensitivity to helium in soil gas. One was mixed with nearly atmospheric helium concentration while the other was enriched to 46% higher than atmospheric concentration.

All measurements of helium concentration in soil gas, atmosphere, water, or reference gas were made by filling a 20 cm<sup>3</sup> hypodermic syringe with the desired sample and then injecting this sample into the inlet manifold in three increments, obtaining three separate measurements.

#### Soil-Gas Collection

Syringe measurements of soil-gas were made by pushing a probe about 60 cm into the ground. Its lower end, tapered to a point,

had three air inlet holes near the tip. The top end was equipped with a thick surgical rubber septum for inserting the sampling syringe. The first syringe full was discarded to flush out the probe (total internal volume =  $5.6 \text{ cm}^3$ ). The second sample was used for the measurements.

This study has demonstrated that the syringe collection technique yields increased flexibility, greater portability, and more reproducible results than the continuous pumping system.

#### Electronic Radon Alpha Counters (MERAC)

The electronic radon alpha counters only detect alpha particles that are emitted by radon gas which undergoes radioactive decay within a few centimeters of the detector. Alpha particles emitted by solid radioactive nuclei in the soil are not detected since the distance from the detector to the nearest soil exceeds the alpha particle range.

Typical field operational use resulted in 1000 to 10,000 counts per day. The variation from day to day in the counting rate of any one MERAC was minimal.

#### Helium Dissolved in Ground Water

Nalgene bottles were used to collect water from wells and wind-mills. The water is loaded into the quart (0.946 liter) bottle to a standard fill level of 0.85 liter and closed immediately with an air tight cap equipped with a septum. The bottle is stored two to three hours until time of measurement. It is then shaken vigorously for 30 seconds to establish an equilibrium between the helium concentration in the water and in the air above the water. After shaking, it is

allowed to settle for two minutes, whereupon a syringe needle is inserted in the septum to withdraw an air sample which is immediately introduced into the mass spectrometer for helium measurement. Thus, if the concentration of helium in the water is greater than the equilibrium concentration equivalent to the helium concentration in the ambient air, the shaking releases helium into the head space. If the helium concentration in the water is lower, then the shaking causes some of the helium in the head space to dissolve in the water.

#### Gamma-Ray Analysis of Soil Samples

Soil samples were collected by bagging and labeling approximately 1 kg of soil removed by a power auger in drilling holes for the MERAC's. From 130 to 150 gms of sample was subsequently sealed in cans. The gamma-ray analysis is performed about 20 days after sealing the soil in the can to allow the radon gas generated by  $^{226}\text{Ra}$  in the soil to come to secular equilibrium. The gamma rays used to identify uranium are emitted by  $^{214}\text{Bi}$ , one of the decay products in the radon decay chain. This method, in effect, measures the radium in the soil from which the equivalent uranium (eU) is inferred. The thorium (eTh) is measured from the gamma activity of  $^{208}\text{Tl}$  which is in the thorium decay chain.

#### Grid Survey Results

##### Helium in the Atmosphere

The helium concentration in the atmosphere at the surface of the earth varies from minute to minute and from place to place. At



each of the test sites, the atmospheric helium concentration varied generally within the range of 5.16 to 5.29 ppm, although some individual concentrations as low as 5.04 ppm and as high as 5.32 ppm were measured. The instantaneous range was from 60 to 150 ppb at different locations in a field site at the same time. The average helium concentrations of the atmosphere at the ground surface within the different test sites ranged from 5.223 to 5.239 ppm.

At no test site did the variations of the helium concentrations of the atmosphere at the ground surface display a systematic relationship with diurnal or meteorologic changes. This apparent random nature of the variations in the helium concentration of the atmosphere contrasts strikingly with the systematic diurnal variations of the helium concentration in soil gas at the same localities.

Atmospheric helium measurements at all of the test sites show no anomalous helium concentration in the atmosphere at ground level related to buried uranium deposits. These observations of no anomalous atmospheric helium over uranium deposits buried from 6 to 915 meters below the ground surface indicate that atmospheric sampling for helium concentration variations is not a useful technique for uranium exploration.

### Helium, Radon, Uranium, and Thorium in Soil

#### Short-Term Surveys

In almost all cases where the grid-sampling soil-gas surveys were conducted in short time intervals (at four different sites of uranium mineralization buried from 6 to 250 meters deep in the

Powder River Basin, Wyoming), helium in soil gas anomalies were found to occur spatially related to and often directly over the buried uranium deposits. The detailed pattern of the anomalies varied from time to time throughout a single day and from day to day. However, the significant area of anomalous helium in soil gas existed at all times over the subsurface uranium deposit. In some cases, the highest portion of the anomaly existed over the "leading edge" of the buried uranium roll front.

Where surveys were conducted both in the morning and afternoon hours, the amplitude of the helium in soil gas anomalies above background threshold levels was in all cases greater in the afternoon than in the morning. Generally the amplitude of the helium-in-soil-gas anomaly above background threshold was 30-60 ppb in the morning hours and 50-100 ppb in the afternoon hours. The amplitude of the helium anomaly showed no relationship to the depth of the subsurface uranium deposit. Because of the apparent displacement of some of the helium-in-soil-gas anomalies and the different sample spacing at different test sites, no clear relationship between the breadth of the anomalies and the depth of the subsurface uranium mineralization was apparent. In general, however, the broader soil gas anomalies occurred over the more deeply buried uranium deposits.

At one test site (D), cumulative radon-in-soil-gas counts measured with MERAC counters and  $^{214}\text{Bi}$  gamma-ray spectrometric analyses of equivalent uranium (eU) content in the soil were obtained at some of the helium soil gas stations. The generally similar pattern of the MERAC radon-in-soil-gas anomalies to the helium-in-soil-gas anomalies, and the generally dissimilar pattern of the  $^{226}\text{Ra}$  and eU

( $^{214}\text{Bi}$ ) contents in the soil with the helium and radon anomalies suggest that both the anomalous radon and anomalous helium-in-soil-gas at this test site were derived from the radioactive decay of subsurface uranium mineralization (at 140 to 240 meters depth) rather than local generation in the soil.

At another test site (E), the helium-in-soil-gas anomalies correlated reasonably well with the location of subsurface uranium ore. This test site showed a general correlation of anomalous radon concentrations (MERAC counts) with the areas of higher eU and eTh (equivalent thorium) contents of the soil. There was also a lack of correlation of the areas of anomalous helium-in-soil-gas with the areas of high radon, eU, and eTh content. In this case, it appears that the anomalous radon in soil gas was derived from the higher thorium and  $^{226}\text{Ra}$  (the parent of the  $^{214}\text{Bi}$ ) contents in the surface soil, whereas the anomalous helium was derived from the radioactive decay of the subsurface uranium mineralization at a depth of 250 meters. It is, therefore, important to make measurements of the uranium, radium, and thorium contents of the soil in the conduct of helium or radon in soil gas surveys, so that locally generated radon and helium anomalies can be separated from those that are generated from buried uranium deposits.

Laboratory analyses of several soil-gas samples from test site D were conducted for their  $^{222}\text{Rn}$  content and  $^4\text{He}/^{36}\text{Ar}$  and  $^4\text{He}/^{22}\text{Ne}$  ratios. These measurements were not carried out with sufficient sampling densities or with sufficient precision to identify any advantage in these laboratory ratio measurements over the direct helium measurements in the field.

### Long-Term Surveys

In most cases where the grid-sampling, soil-gas surveys were conducted over many hours of a day or several days duration (at test site F, with uranium mineralization buried 915 meters deep in the Grants-Ambrosia Lake area, New Mexico), the pattern of helium-in-soil-gas data seemed to bear very little systematic relationship with the distribution of subsurface uranium deposits.

During the course of these surveys, helium-in-soil-gas measurements were made at reference stations and in a detailed micro-environmental test plot throughout the course of several days. Although the individual soil gas data were scattered over a range from 5.11 to 5.39 ppm, the reference station data showed a general decrease in helium concentration in the soil-gas during the sunlight hours of the day, from an average of 5.27 ppm at 1000 MST to 5.21 ppm at 1600 MST. In the micro-environmental test plot, 37 helium-in-soil-gas readings were taken in a small area (200 meters square) in a single day. Although the individual soil-gas data ranged from 5.20 to 5.27 ppm helium, every single station within the micro-environmental test plot showed a decrease in soil-gas helium concentration from 1100 MST to 1400 MST. The average decrease was 15 ppb in the three-hour period. Thus, the reference station and micro-environmental test data show that diurnal variations of soil gas helium concentrations are important and significantly influence the results and useability of data from samples collected over long time periods (several hours or days in duration). The amplitude of helium-in-soil-gas anomalies discovered over buried uranium deposits in short-time surveys ranged from 30 to 100 ppb and the average variations in daytime background soil gas helium content have been demonstrated to be at least 60 ppb. Therefore,

real helium-in-soil-gas anomalies can be obscured and lost in the high level of background variations on soil-gas surveys conducted over long time periods.

Laboratory analyses for  $^4\text{He}/^{36}\text{Ar}$  and  $^4\text{He}/^{22}\text{Ne}$  ratios were conducted on 25 soil gas samples collected during a short time period from test site E. These samples, which were collected during a short time period from the same stations as were field analysis soil-gas samples over a much longer period of time, show anomalous helium concentrations in a halo above uranium deposits buried as deeply as 600-900 meters, whereas the long-duration, soil-gas survey did not. These data indicate that it is difficult, and possibly unreasonable, to compare helium-in-soil-gas data from samples that were collected over long periods of time in discerning anomalous helium-in-soil-gas concentrations emanating from subsurface uranium deposits. Thus, in order to realistically detect anomalous helium concentrations in soil-gas over subsurface uranium deposits, it is necessary to:

- (a) collect samples over a short period of time, or
- (b) utilize a cumulative collection system whereby the sample represents the helium-in-soil-gas accumulated over a longer period of time, i. e., several days or weeks.

Cumulative radon-in-soil-gas measurements with MERAC counters and eU and eTh spectrometric analyses of soil samples were conducted at scattered locations at test site E. The absence of any significant variations in uranium content in the soil and the existence of a broad radon anomaly, detected during two separate periods of measurement, over the buried uranium deposits indicates that the radon-in-

soil-gas detected by this cumulative radon counting method can be an important technique in detailed exploration programs for uranium deposits, even those buried as deeply as 900 meters.

The MERAC cumulative radon soil-gas data and the helium soil-gas data indicate that there is no apparent effect of preferential helium or radon migration to the ground surface along the faults that offset the uranium deposits at depth. There is some suggestion from the data that the anomalous helium content in soil-gas is offset in the direction of the ground water flow.

#### Summary of Grid Survey Conclusions

These results indicate that:

- (a) The maximum amplitude of helium-in-soil-gas anomalies (above background levels) expected over buried uranium deposits is 0.8 to 1.6 percent in sandstone deposits and two to five percent in faulted igneous-metamorphic terrane.
- (b) The amplitude, breadth, and specific outline of a helium-in-soil-gas anomaly may be related spatially to a subsurface uranium deposit but only in a general way. The exact depth or boundaries of the uranium mineralization will not be defined by the helium-in-soil-gas data, only the general area of mineralization.
- (c) Helium-in-soil-gas surveys have the best chance to show anomalies related to subsurface uranium

deposits if conducted over short time periods during afternoon hours.

- (d) Averaging of data from several surveys on the same site indicates that a cumulative collection system, whereby the sample represents the helium-in-soil-gas accumulated over a time period of several weeks, would significantly enhance the amplitude and the detectability of the helium anomalies over subsurface uranium deposits.
- (e) Atmospheric samples are ineffective in locating subsurface uranium mineralization.

### Regional Profiles

#### Helium-in-Soil-Gas

Regional helium-in-soil-gas traverses were performed in the Powder River Basin, Wyoming, and in the Grants-Gallup-Ambrosia Lake area, New Mexico, in an attempt to determine whether the uranium districts could be detected by a regional helium-in-soil-gas survey. Another purpose of these reconnaissance traverses was to determine if helium was escaping from the upturned outcrops of the host sandstones of the uranium mineralization, although this is unlikely since it would be migrating against the ground water flow. Soil-gas samples were collected over a period of days and irrespective of the time of day by the syringe-probe collection method and analyzed by

the field-based mass spectrometer on 1.6 km sample spacing on long-distance profiles along roads.

The reconnaissance data showed clustering of anomalous helium-in-soil-gas concentrations over a major portion of the southern Powder River Basin and Pumpkin Buttes uranium districts in Wyoming and over most of the area of the Ambrosia Lake "main-trend" uranium deposits. However, other areas of anomalous helium concentration apparently unrelated to uranium districts were also discovered in these regional traverses. There is a slight increase in helium concentration at the outcrop of the Morrison Formation. This is probably not statistically meaningful, however. Since the regional data were collected over a period of several days in each survey, the data reflect changes in meteorologic and other environmental factors as well as helium derived from subsurface uranium deposits. The difficulty in correlating the regional helium-in-soil-gas anomalies with uranium districts and the upturned host sandstones suggest that the interpretability and usefulness of regional soil-gas surveys is limited when conducted in single line traverses. However, the superiority of grid type surveys over single line traverses demonstrated at the specific mineralized sites suggests that regional surveys could be improved by the use of a grid-sampling system with a cumulative collection system.

#### Helium and Uranium in Ground Water

Reconnaissance ground water sampling and analysis for helium content was conducted in the southern portion of the Powder River Basin, Wyoming, and to a lesser extent, in the Grants-Ambrosia Lake area, New Mexico. Upon degassing the helium from the ground-water



samples into air samples, the helium concentration of these air samples from the Powder River Basin ground water ranged from 4.60 to 16.09 ppm. Since the helium concentration of the atmosphere is usually  $5.24 \pm 0.10$  ppm, the degassed samples with significantly higher helium concentration represent ground water of anomalous helium content. A significant cluster of ground water with anomalous helium ranging from 6.00 to 16.09 ppm in the degassed air samples exists to the northeast of the uranium deposits of the southern Powder River Basin offset from the uranium deposits in the direction of ground water flow. The shallow ground water in the immediate area of the uranium deposits generally does not display significantly anomalous helium concentrations (i. e.,  $> 6.0$  ppm). In fact, a large area of lower than atmospheric helium concentration (4.60 - 5.00 ppm) occurs over and offset slightly down the ground water flow direction from some of the uranium deposits. It appears that the large area of anomalous helium concentration in the ground water measurements results from helium emanating from the subsurface uranium ore and its movement vertically down in the stratigraphic sequence in the recharge area and up the stratigraphic sequence to its detection in shallow ground waters in the area of discharge. Thus, the position of anomalous helium concentration in ground water derived from a subsurface uranium deposit or group of deposits is very dependent on the ground water hydrology of the area.

The uranium distribution in ground water in the same area of the southern Powder River Basin, on the other hand, shows a pattern of  $\geq 2$  ppb to the southwest of and up the ground water gradient from the uranium deposits and  $\leq 1$  ppb uranium generally to the north and east of the area of the uranium deposits. The uranium distribution in the

southern Powder River Basin ground water conforms to the model of soluble uranyl dicarbonate, moving in solution in the oxidizing ground water from the southwest to the area of the uranium deposits. There the uranium-bearing water encounters a reducing environment in the sandstones where most of the uranium is precipitated from the ground water. The area of  $\leq 1$  ppm uranium in ground water is the area of the reduced sandstone. Thus, in the southern Powder River Basin, collection of shallow ground water samples and their analysis for uranium and helium concentrations would have been extremely useful in reconnaissance exploration for, and the delineation of, relatively small areas for uranium prospecting and drilling if this type of reconnaissance hydrochemical survey had been conducted prior to uranium discoveries in this area.

A reconnaissance hydrogeochemical survey in the Ambrosia Lake area, which was limited by a scarcity of wells, showed a range of uranium-in-ground-water concentrations from 2 to 980 ppb. Anomalous uranium concentrations ( $>20$  ppb) were confined to ground water samples taken from the Dakota and Morrison Formations in close proximity to uranium deposits. No anomalous uranium in ground water occurred where the uranium deposits were deeply buried and the shallow water wells produced water from stratigraphically much higher sandstones, even from directly over subsurface uranium deposits. Thus, a uranium-in-ground-water survey can be extremely useful in exploration for uranium deposits if water can be sampled from the aquifers that are potential hosts for the uranium mineralization. The utility of uranium-in-ground-water surveys diminishes, however, as the stratigraphic distance from and hydraulic discontinuity with the uraniferous aquifer increases. Thus, as exploration for uranium deposits becomes deeper

and deeper, sampling of ground water from shallow water wells for their uranium concentration becomes less and less useful. Sampling the water from exploration drill holes from several, and possibly all, aquifer horizons that are potential hosts for uranium mineralization, however, can be an important exploration tool. This is effectively a search for a geochemical halo related to an undiscovered uranium deposit. A procedure of water recovery from water-bearing zones in deep exploration drill holes followed by geochemical analysis of the water for uranium, helium, radon, and other constituents, could be an extremely cost-effective technique in exploration for deeply buried uranium deposits. In order to be effective in determining accurately which formation hosts the water tested in this procedure, packer isolation of the aquifers in the drill holes is necessary.

The helium concentrations in the same ground water samples tested for uranium in the Ambrosia Lake area ranged from 4.52 to 44.73 ppm. A striking lack of coincidence occurs between anomalous helium concentrations in ground water and anomalous uranium concentrations of the same water samples. The water samples in the area of the San Mateo uranium deposits, all from sandstones 400 to 1000 meters stratigraphically above the uranium-bearing Morrison sandstones, contain anomalous helium concentrations (from 6.95 to 13.46 ppm) and background levels ( $\leq 2$  ppb) of uranium. The water samples in close proximity geographically and stratigraphically to the Westwater Canyon ore deposits in the Ambrosia Lake area have both anomalous helium (up to 44.74 ppm) and anomalous uranium (63-74 ppb) concentrations. The ground water samples with the highest uranium concentrations (320 - 980 ppb) were obtained from the Morrison and Todilto formations near uranium mineralization and yet have background helium levels

(4.52 - 4.88 ppm). The ground water sample from the Menefee Formation in the area of the Crown Point uranium deposits, which occur stratigraphically approximately 600 - 700 meters deeper than the Menefee Formation, has an anomalous helium concentration (8.82 ppm) but a background uranium level.

The helium data show that helium moves with the ground water as well as through the ground water vertically from subsurface uranium deposits. Thus, anomalous helium concentrations can often be found in ground waters located in stratigraphically higher horizons than the uranium-bearing horizons. This movement of helium toward the atmosphere, independent of the ground-water movement and through rocks relatively impervious to water, permits surveys for helium in ground water to be extremely useful in exploring for uranium deposits at all depths. Hence, sampling of water from shallow wells may be useful in detecting anomalous helium concentrations derived from the radioactive decay of a uranium deposit which is substantially deeper. Thus, helium analysis should be conducted routinely on all ground water samples obtained in a hydrogeochemical exploration survey or encountered in an exploration drilling program.

## RECOMMENDATIONS

The thrust of additional research in the utility of helium-in-soil-gas detection for uranium mineralization should be in the development of a cumulative soil-gas sampling system. Further research in the area of helium-in-ground-water is strongly recommended. Along with helium, analyses should include uranium, radon, and the principal active gases ( $O_2$ ,  $N_2$ ,  $CO_2$ ). The hydrology of the test area must be thoroughly understood to interpret the data. In particular, it is recommended that the multiple aquifer, deep, uranium-deposit area of the southern flank of the San Juan Basin (Grants-Ambrosia Lake area), New Mexico, be used as one such test area. It is further recommended that such helium-in-ground-water research not focus exclusively on shallow water well samples, but also include ground water from uranium-host sandstones that are penetrated in exploration drilling programs. For such ground water samples to be available, it is recommended that cooperation and participation of exploration companies be solicited so that packer isolation of aquifer horizons, particularly the uranium-host aquifers, can be achieved and representative deep ground waters can be sampled. Discounting drilling time, the cost of this program would be approximately \$500.00 per aquifer test. This cost would be offset by the information that is expected to be gained which could aid in uranium exploration in areas where redox boundaries are not discernible.

## LITERATURE CITED

- C. W. Adkisson and G. M. Reimer: "Helium and Radon-Emanation Bibliography-Selected References of Geologic Interest to Uranium Exploration." U.S.G.S. Open File Report, p. 76-860, 1976.
- A. A. Auberts, I. Friedman, T. J. Donovan, E. H. Denton: "Helium Survey, A Possible Technique for Locating Geothermal Reservoirs", Geophysical Research Letters, Vol. 2, p. 209-210, 1975.
- S. H. U. Bowie: "The Status of Uranium Prospecting." Uranium Prospecting Handbook, Eds. S. H. U. Bowie, N. Davis, and D. Ostle London, The Institute of Mining and Metallurgy, p. 1-12, 1972.
- S. H. U. Bowie, T. K. Ball, and D. Ostle: "Geochemical Methods in the Detection of Hidden Uranium Deposits." Geochemical Exploration, Canadian Insti, of Mining and Metallurgy, Special Vol. II, p. 103-111, 1971.
- Chapman, Wood, and Griswold, Inc.: "Geology of Grants Uranium Region", New Mexico Bureau of Mines and Mineral Resources Map (3 sheets), 1973.
- M. O. Childers: "Uranium Occurrences in Upper Cretaceous and Tertiary Strata of Wyoming and Northern Colorado." The Mountain Geologist VII, p. 131-147, 1974.
- W. B. Clark and G. Kugler: "Dissolved Helium in Groundwater: A Possible Method for Uranium and Thorium Prospecting." Economic Geology 68, p. 243-251, 1973.
- W. B. Clark, Z. Top, A. P. Beavan, and S. S. Gandhi: "Dissolved Helium in Lakes: Uranium Prospecting in the Precambrian Terrain of Central Labrador." Economic Geology, Vol. 72, p. 233-242, 1977.

- Cook: in Argon, Helium and the Rare Gases. Inter-science Publishers, p. 175, 1961.
- J. B. Cooper and E. C. John: "Geology and Ground-Water Occurrence in Southeastern McKinley County, New Mexico." in Technical Report #35, State Engineer Office.
- A. R. Dahl and J. L. Hagmaier: "Genesis and Characteristics of the Southern Powder River Basin Uranium Deposits, Wyoming, U. S. A.", in Formation of Uranium Ore Deposits, International Atomic Energy Agency, p. 201-218.
- J. F. Davis: "Uranium Deposits of the Powder River Basin, Wyoming." Wyoming Geological Assoc. Guidebook, Twenty-Second Annual Field Conference, p. 21-29, 1970.
- W. Dyck: "Development of Uranium Exploration Methods Using Radon." Geological Survey of Canada Paper 69-46, 26 p, 1969.
- W. Dyck: "Radon Methods of Prospecting in Canada." Uranium Prospecting Handbook, op. cit. p. 212-243, 1972.
- W. Dyck: "The Use of Helium in Mineral Exploration." Journal of Geochemical Exploration 5, p. 3-20, 1976.
- J. C. Fisher: "Remote Sensing Applied to Exploration for Vein Type Uranium Deposits, Front Range, Colorado." Colorado School of Mines Remote Sensing Report 76-2, 1976.
- E. H. Fleming, A. Ghiorso, and B. B. Cunningham: Phys. Rev. Vol. 88, p. 642, 1952.
- J. E. Gingrich: "Results from a New Uranium Exploration Method." Trans. of Society of Mining Engineers, Vol. 258, p. 61-64, 1975.
- G. R. Goldak: "<sup>4</sup>He Mass Spectrometry in U Exploration (Abstr.)." Society of Mining Engineers 25, p. 47, 1973.
- V. S. Golubev, A. N. Yeremeyev, and I. N. Yanitskiy: "Analysis of some Models of Helium Migration in the Lithosphere," Translated from Geokhimiya No. 7, p. 1067-1076, 1974.

- A. G. Grammakov, V. S. Glebouskaya, and I. M. Khaikovich: "On the Theory of the Helium Method of Prospecting for Deposits of Radioactive Elements." Voprosy Rudnoi Geo Fiziki Gos. Geol. Kom SSSR 5, p. 3-19, 1965.
- A. Grimbert: "Use of Geochemical Techniques in Uranium Prospecting." Uranium Prospecting Handbook, op. cit., p. 110-120, 1972.
- J. L. Hagmaier: "Ground Water Flow, Hydrochemistry, and Uranium Deposition in the Powder River Basin, Wyoming." Univ. of North Dakota, Ph. D. Thesis, 1971.
- P. M. Hurley: "The Helium Age Method and the Distribution and Migration of Helium in Rocks." in Nuclear Geology edit. Henry Faul, John Wiley & Sons, New York, p. 301-329, 1954.
- L. Lovbord: "Assessment of Uranium by Gamma-Ray Spectrometry." Uranium Prospecting Handbook, op. cit., p. 1-12, 1972.
- J. P. Martin and L. E. Bergquist: "Study of the Applicability of the  $^3\text{He}/^4\text{He}$  Ratio for Uranium Prospecting." Final Report MCR-76-567, - MMA Contract with ERDA/BFEC Subcontract 76-006-L (Aug. 1977).
- J. P. Martin, R. H. DeVoto, L. E. Bergquist, and R. H. Mead: "The Potential of Helium as a Guide to Uranium Ore." Electric Power Research Institute EA-813, 177 p., 1978.
- J. M. Miller and W. R. Lasemore: "Instruments Techniques for Uranium Ore Prospecting." Uranium Prospecting Handbook, op. cit., p. 135-148, 1972.
- P. Morrison and J. Pine: "Radiogenic Origin of the Helium Isotopes in Rock." Annals of the New York Academy of Science, Vol. 62, p. 71-92, 1955.
- J. J. Naughton, J. H. Lee, D. Keeling, J. B. Finlayson, and G. Dority: "Helium Flux from the Earth's Mantle as Estimated from Hawaiian Fumarolic Degassing." Science, Vol. 180, p. 55-57, 1973.



- D. Ostle, R. F. Coleman, T. K. Ball: "Neutron Activation Analysis as an Aid to Geochemical Prospecting for Uranium: Uranium Prospecting Handbook, op. cit., p. 95-109, 1972.
- Y. Puibaraud: "Portable Equipment for Uranium Prospecting." Uranium Prospecting Handbook, op. cit., p. 149-156, 1972.
- G. M. Reimer: "Design and Assembly of a Portable Helium Detector for Evaluation as a Uranium Exploration Instrument." USGS Open File Report, 76-398, 1976.
- G. M. Reimer, J. K. Otton: "Helium in Soil Gas and Well Water in the Vicinity of a Uranium Deposit, Weld County, Colorado." USGS Open File Report, 76-699, 1976.
- E. S. Santos: "Relation of Ore Deposits to the Stratigraphy of the Ambrosia Lake Area." in Geology and Technology of the Grants Uranium Region, New Mexico Bureau of Mines and Mineral Resources, Memoir 15, p. 53-59, 1963.
- E. S. Santos and E. Thaden: "Geologic Map of the Ambrosia Lake Quadrangle, McKinley County, New Mexico", U.S. Geological Survey Map GQ-515, 1966.
- W. N. Sharp: "Geology and Uranium Deposits of the Pumpkin Buttes Area of the Powder River Basin, Wyoming." Geological Survey Bulletin 1107-H, 1964.
- W. N. Sharp and A. B. Gibbons: "Geology and Uranium Deposits of the Southern Part of the Powder River Basin, Wyoming." Geological Survey Bulletin 1147-D, 1964.
- I. N. Tolstikhin, B. A. Mamyrin, E. A. Bascov, I. L. Kamensky, G. S. Anufriev, and S. N. Surikov: "He Isotopes in Gases from Hot Springs of the Kuril-Kamchatka Volcanic Region." in Ocherki Sovremennoy geokhimii i analiticheskoy Khimii. Isdvestiya Nauka, Moscow, p. 405-414, 1972.
- K. R. Turekian: in The Origin and Evolution of Atmospheres and Oceans, Eds. P. J. Brancazio and A. G. W. Cameron (Wiley, New York), p. 80, 1964.

E. J. Young: "Geologic, Radiometric, and Mineralogic Maps and Underground Workings of the Schwartzwald Uranium Mine and Area, Jefferson County, Colorado." USGS Open File Report 77-725, 1977.